5-13-2006

Elucidation Of Key Interactions Between In Situ Chemical Oxidation Reagents And Soil Systems

John Michael Harden

ELUCIDATION OF KEY INTERACTIONS BETWEEN IN SITU CHEMICAL OXIDATION REAGENTS AND SOIL SYSTEMS

By

John Michael Harden

A Dissertation
Submitted to the Faculty of
Mississippi State University
in Partial Fulfillment of the Requirements
for the Degree of Doctor of Philosophy
in Chemical Engineering
in the Dave C. Swalm School of Chemical Engineering

Mississippi State, Mississippi

May 2006

ELUCIDATION OF KEY INTERACTIONS BETWEEN IN SITU CHEMICAL OXIDATION REAGENTS AND SOIL SYSTEMS

By

John Michael Harden

Approved:

Mark E. Zappi Adjunct Professor Dave C. Swalm School of Chemical Engineering (Director of Dissertation and Advisor)	Kirk H. Schulz Dean Bagley College of Engineering (Committee Member)
Rafael Hernandez Assistant Professor Dave C. Swalm School of Chemical Engineering (Committee Member)	William Kingery Professor Plant and Soil Sciences (Committee Member)
Clifford E. George Professor and Director of Graduate Studies Dave C. Swalm School of Chemical Engineering (Committee Member)	Roger L. King Associate Dean of Research and Graduate Studies of the Bagley College of Engineering

Name: John Michael Harden

Date of Degree: May 15, 2006

Institution: Mississippi State University

Major Field: Chemical Engineering

Major Professor: Dr. Mark E. Zappi

Title of Study: ELUCIDATION OF KEY INTERACTIONS BETWEEN IN SITU CHEMICAL OXIDATION REAGENTS AND SOIL SYSTEMS

Pages in Study: 486

Candidate for Degree of Doctor of Philosophy

Many soil and aquifer systems in the United States have been subjected to chemical contamination from past industrial and military activities. While many remediation technologies are currently being applied, *in situ* chemical oxidation (ISCO) is one option that is often favored because of its potential for fast remediation times and high user control. This technology involves the direct injection of chemical oxidizers (e.g. hydrogen peroxide, ozone, or permanganate) into targeted contaminant zones within the subsurface, and it has been proven to be amenable to both BTEX compounds and other volatile organic compounds such as chlorinated solvents.

This study had several key objectives. Firstly, multiple soil samples, each containing an elevated level of a targeted chemical constituent, were successfully collected in order to provide a wide range of soil types in order to make important

comparisons and correlations related to ISCO's impacts. Secondly, the impact of common soil constituents on process reagent transport was studied in order to determine which soil constituents would act as primary hindrances for the transport of hydrogen peroxide and ozone into the subsurface. Thirdly, experiments were performed to pinpoint certain personnel safety threats such as excess oxygen and heat generation that might arise during process application. Fourthly, the impact of ISCO process application on soil fabric properties was examined. Soil aerobic microbial populations, soil hydraulic conductivity, soil natural organic matter constituents, and soil adsorptive properties were all shown to be impacted following the application of chemical oxidizers.

DEDICATION

I would like to dedicate this dissertation to my family who has inspired me both personally and professionally to be the absolute best that I can be. This work would never have been possible without the support of my parents, Michael and Sharon; my sister, Rebecca; my grandparents, Nana, Papa, Mamoo, and Papa J; my great-grandmother, Moms; and three of my closest friends, Danny Chapman, Marilyn Lauderdale, and Jeremy Lokits, each of whom will forever be considered "family." Everything that I have and will accomplish in life is because of their Christian love and support.

ACKNOWLEDGMENTS

The Author would like to thank the following committee members whose tireless efforts have made this work possible. Dr. Mark E. Zappi, Advisor and Professor, Dean of Engineering, University of Louisiana at Lafayette; Dr. Rafael Hernandez, Assistant Professor, Dave C. Swalm School of Chemical Engineering, Mississippi State University; Dr. Kirk Schulz, Dean of Engineering, James Worth Bagley College of Engineering, Mississippi State University; Dr. Clifford George, Professor, Dave C. Swalm School of Chemical Engineering, Mississippi State University; Dr. William Kingery, Professor, Department of Plant & Soil Sciences, Mississippi State University. The author would like to extend additional thanks to Dr. W. Todd French, Assistant Research Professor, Dave C. Swalm School of Chemical Engineering, for his scientific and professional guidance. Additional thanks is due to employees of the Environmental Research and Development Center, most notably, Dr. Beth Fleming, Denise MacMillan, and Scott Waisner. The Author also greatly appreciates the laboratory assistance provided by numerous undergraduate researchers who have supported this project. Finally, the author would like to thank the Strategic Environmental Research and Development Program for their financial assistance in supporting this effort.

TABLE OF CONTENTS

CHAPTER Page

CHAPTER Page

CHAPTER Page

CHAPTER Page

LIST OF TABLES

TABLE Page

TABLE Page

TABLE Page

TABLE Page

TABLE Page

LIST OF FIGURES

FIGURE Page

FIGURE Page

FIGURE Page

FIGURE Page

FIGURE Page

FIGURE Page

CHAPTER I

INTRODUCTION

Many soil and aquifer systems in the United States have been subjected to chemical contamination from past industrial and military activities (Hong et al., 1996). A wealth of remediation options is often considered when determining the most efficient mechanism for site cleanup. Remediation techniques fall into one of two categories: *ex situ* and *in situ*. *Ex situ* technologies are invasive procedures in which soil is excavated from the contaminated site, treated in above-ground reactors, and then returned to its natural environment (Acar and Zappi, 1995). While *ex situ* treatments offer a high level of process control, they are often expensive due to the costs of excavation, surface equipment, and contaminated soil handling (Zappi et al., 2000). *In situ* technologies are far less invasive, utilizing the subsurface as the reaction zone. Therefore, there is no requirement to expend capital for excavation procedures or surface treatment system equipment (Nimmer et al., 2000; Chen et al., 2001). *In situ* processes also allow the user to treat contaminated areas without disturbing pre-existing buildings, and they also eliminate the need to handle contaminated soil (Amarante, 2000). Finally, because of greatly reduced site worker exposures, *in situ* technologies are generally considered to be safer than *ex situ* processes (EPA, 2000; ITRC, 2005).

Technology Overview

In situ chemical oxidation (ISCO) is a non-invasive technology that has emerged in recent years as a viable alternative to other treatment methods such as bioremediation and solidification/stabilization. It is becoming increasingly popular for remediating organics in both soil and groundwater environments (Acar and Zappi, 1995; Haselow et al., 2003). *In situ* chemical oxidation is executed by delivering large quantities of chemical oxidants into the subsurface to rapidly degrade organic contaminants (Lowe et al., 2002). A simplistic diagram of a typical *in situ* chemical oxidation application is shown in Figure 1.1. Once the targeted treatment zone is identified, the chosen chemical oxidizer is routed into the subsurface via above-ground pumps. A packer nozzle assembly is fixed at a desired location within the well, and this is used to create a seal within the well to prevent oxidizer solutions from simply rising to the surface. The number of wells and their placement is generally determined by characterization of both the site and the pollutant (Amarante 2000; ARS Technologies, 2005).

Chemical Oxidizer Transport

One of the primary limitations with *in situ* chemical oxidation involves the efficient delivery of process reagents into the subsurface via the process diagram shown in Figure 1.1. In order for chemical oxidizers to react with subsurface contaminants, the oxidizer must physically contact the contaminant in order for a reaction to take place (Amarante, 2000). Two primary concerns exist which must be overcome by practitioners applying an ISCO technology for contaminant remediation.

Firstly, process equipment must be installed which is able to overcome the soil hydraulic conductivity that will restrict flow within the aquifer, a calculation which is usually made based on the application of Darcy's Law (LaGrega et al., 2001; ITRC, 2005). Secondly, natural soil components can limit the efficiency of ISCO due to their scavenging effect on chemical oxidizers. In addition to the desired oxidizer-pollutant reaction, undesired oxidizer-scavenger reactions will take place that will impact the rate at which oxidizers reach targeted contaminants (Amarante, 2000).

Chemical Oxidation Processes

Chemical oxidation may be broken up into two generic categories: primary oxidation and advanced oxidation (Zappi, 1995). In reactions via primary oxidation, the reaction with the specific contaminant relies more on the oxidation via the parent oxidizer (e.g. ozone, hydrogen peroxide, permanganate) rather than via hydroxyl radicals. Ozone, hydrogen peroxide and permanganate have all been historically used in water and wastewater treatment and have recently been applied successfully in ISCO remediation projects (Zappi, 1995; Kuo et al., 1999; Amarante 2000). A second type of oxidation is referred to as advanced oxidation. These are processes that rely primarily on hydroxyl radicals ($OH\cdot$) to oxidize particular contaminants within the subsurface. Examples of advanced oxidation technologies include both Fenton's Reaction and peroxone (Glaze et al., 1989; Hong et al., 1996; Amarante 2000).

Chemical Oxidizer Types

Many different types of chemical oxidizers have been successfully utilized during *in situ* remediation projects. The injection of hydrogen peroxide to promote Fenton's-based chemical reactions has been the most commonly used ISCO application (Watts et al., 1999). Fenton's Reagent oxidation involves the degradation of hydrogen peroxide into hydroxyl radicals in the presence of reduced iron salts (Watts et al., 1999; Zappi et al., 2000). Fenton's Reaction is considered an advanced oxidation process since the hydroxyl radicals are utilized as the principal reaction species (Kakarla et al., 2002). The reaction of hydrogen peroxide and ferrous iron results in the generation of these powerful hydroxyl radicals as reported by Watts et al. (1999):

$$H_2O_2 + Fe^{2+} \rightarrow Fe^{3+} + OH^- + OH\cdot \quad (1)$$

Fenton's Reaction is an extremely popular ISCO candidate because the chemicals are both abundant and relatively inexpensive. Often times, naturally occurring iron minerals within the soil matrix can provide enough ferrous iron to efficiently react with injected hydrogen peroxide (Watts et. al, 1999). Fenton's Reaction also offers the potential for much quicker remediation times as opposed to bioremediation. In the application of Fenton's Reagent at a site in Warren County, NY, overall concentrations of volatile and semi-volatile organic compounds were reduced by as much as 70%, with a required treatment time of less than three months (Violins et al., 2003). These remediation times are much more favorable in comparison to other *in situ* technologies such as bioremediation, which can often require treatment times of a

year or more. Cunningham et al. (2001) utilized a 15-month treatment time in the bioremediation of BTEX-contaminated groundwater, and Frische and Hoper (2003) employed a 17-month bioremediation treatment time of TNT-contaminated soils.

While not as common as the hydrogen peroxide/Fenton's Reagent technologies, ozone can also be used as the oxidizer of choice during ISCO remediation. Ozone (O_3) is sparged into the contaminated area by utilizing an ozone generator and a well (Amarante, 2000). Ozone is a very powerful, unstable oxidant capable of oxidizing many various types of contaminants. Once dissolved into the liquid phase, organic compounds are oxidized by one of two mechanisms, either direct oxidation via ozone or indirect oxidation via free radical intermediates such as hydroxyl radicals (Nimmer et al., 2000). While highly versatile and easily applicable, ozone has several drawbacks that must be considered. Firstly, the purchase and installation of a full-scale ozone generation system is a very costly capital venture (Amarante, 2000). In addition, ozone's relatively fast auto-degradation and relatively low solubility in aqueous solution limit its ability to be transported over long distances through the soil matrix. Often times, pending site conditions, many more treatment wells must be created in order to adequately deliver ozone into the treatment zone (Heynes et al., 1999; Amarante, 2000). In order to enhance the production of hydroxyl radicals from ozone, an ozone-hydrogen peroxide injection has also used in the remediation of contaminated groundwater. This technology, referred to as peroxone, results in the enhanced production of hydroxyl radicals via the reaction of ozone and hydrogen peroxide (Koch et al. 1992; Freese et al, 1999;

Kuo et al., 2000). The complex mechanisms for the formation of hydroxyl radicals during peroxone treatment are illustrated in Chapter II.

Two different types of permanganate compounds are also used with *in situ* chemical oxidation applications. Both potassium permanganate ($KMnO_4$) and sodium permanganate ($NaMnO_4$) have been successfully applied to contaminated soil and groundwater sites (Siegrist et al., 2002). Potassium permanganate has been previously used in the treatment of wastewater and has recently been studied to determine its applicability towards ISCO remediation of organic contamination (Struse et al., 2002). Typical oxidation by-products from oxidation via $KMnO_4$ include carbon dioxide (CO_2), water, potassium (K^+), and manganese dioxide (MnO_2). Because MnO_2 is a naturally occurring compound in soils, its production in oxidation reactions poses no environmental concern. The drawbacks of the utilization of $KMnO_4$ with ISCO are its low water solubility value and its reaction with other naturally occurring soil components such as iron, manganese, and typical organic compounds (Amarante, 2000). While $NaMnO_4$ acts similarly to $KMnO_4$, it does offer the several important advantages. Firstly, higher allowable concentrations in solution are possible due to its increased solubility. This gives the user more control in regards to reaction kinetics within the subsurface. Secondly, because $NaMnO_4$ is available in liquid form, the dusting hazards prevalent in the $KMnO_4$ solid are not of concern (ITRC, 2005). While more costly per pound than $KMnO_4$, the application of $NaMnO_4$ is usually cheaper because of the labor costs saved due to its higher solubility, ease of application, and remediation time (Amarante, 2000).

Pollutants Amenable to Treatment via ISCO

One of the many benefits of *in situ* chemical oxidation is its applicability towards a wide variety of pollutants. In advanced oxidation processes especially, hydroxyl radicals are highly reactive with many contaminants that are persistent within the environment (Watts et al., 2005).

Chlorinated solvents are commonly discharged into the subsurface in the form of dense nonaqueous phase liquids (DNAPLs). USEPA data suggested that two types of chlorinated solvents, perchloroethylene (PCE) and trichloroethylene (TCE), are present in approximately 60% of all Superfund National Priority List sites. The fact that PCE and TCE are suspected carcinogens make them a primary remediation concerns (MacKinnon and Thompson, 2002). Recent findings suggest that both of these compounds can be successfully remediated via chemical oxidation processes. Fenton's Reagent has been observed to be one means of remediating chlorinated solvent contamination. Leung, Watts, and Miller (1992) successfully observed the PCE decomposition pathway in response to treatment via Fenton's Reagent. Past research has also indicated that TCE can be successfully remediated via oxidation by Fenton's Reagent chemistry (Chen et al., 2001; Yang and Liu, 2001; Baciocchi et al., 2004). Much research has also been performed in the realm of the remediation of chlorinated solvents via reaction with permanganate. Both PCE (Conrad et al., 2002; MacKinnon and Thomson, 2002; Li and Schwartz, 2004) and TCE (Schroth et al., 2001; Li and Schwartz, 2004) have been shown to have favorable reaction mechanisms with both $NaMnO_4$ and $KMnO_4$. For chlorinated solvent interaction

with ozone, Craeynest (2003) successfully observed the removal of TCE from waste gases via the peroxone process.

Chemical oxidation technologies have also been successfully applied towards BTEX compounds (benzene, toluene, ethylbenzene, and xylenes) and to petroleum-based pollutants. Multiple oxidation technologies have been commonly used to treat these type compounds. Nimmer et al. (2000) reported at least 95% removal of all BTEX compounds after a one-month treatment via ozone. Laboratory-based experiments have shown benzene to be readily oxidizable via ozone (Kuo and Soong, 1984); additionally, toluene has also been shown to be readily oxidizable by ozone-based chemical oxidation processes (Kuo and Chen, 1996). Various petroleum-based contaminants are also likely candidates for ISCO remediation. In the application of Fenton's Reagent at a site in Warren County, NY, overall concentrations of volatile and semi-volatile organic compounds were reduced by as much as 70% in less than three months (Vitolins et al., 2003). Laboratory-scale experiments have also verified the compatibility of ISCO and petroleum-based contaminants such as n-hexadecane and diesel fuel. Results indicated that Fenton's Reagent offers very rapid reactions with these contaminants in the soil phase; complete mineralization was even possible when enough hydrogen peroxide was added to the system (Chen et al., 1998).

While chlorinated solvents, BTEX compounds, and petroleum-based hydrocarbons are some of the more common contaminants treated by ISCO, many other pollutants have been shown to be treatable by chemical oxidation processes. All of the following contaminants have been shown to be amenable to treatment via

chemical oxidation: polycyclic aromatic hydrocarbons (Trapido, 1999; Saxe et al., 2000; Watts et al., 2002; Kanel et al., 2003; Goi and Trapido, 2004), carbon tetrachloride (Teel and Watts, 2002; Watts et al., 2005), cyanides (Aronstein et al., 1994), nitroaromatics (Zappi, 1995; Kuo et al., 2000; Spanggoord et al., 2000; Trapido et al., 2003), and pentachlorophenol (Ravikumar and Gurol, 1990; Freshour et al., 1996; Watts et al., 1999).

Combination of ISCO with Bioremediation

Recent findings have suggested that chemical oxidation and bioremediation processes can be combined in order to enhance the degradation of certain contaminants. Wang and Zappi (2001) used Fenton's Reagent as a precursor to bioremediation in order to enhance removal efficiencies of petroleum hydrocarbons in both soil slurry and soil column experiments. In Dieng's thesis work at Mississippi State University (2003), research was conducted investigating the coupling of both bioremediation and oxidative remediation technologies for the treatment of polycyclic aromatic hydrocarbons (PAHs). He performed a biotreatment remediation step, a chemical oxidation step, and then a final biotreatment step in the remediation of PAHs. Dieng successfully managed to enhance the bioavailability of PAHs by transforming them into compounds more readily biodegradable, thereby offering significant improvement on PAH remediation.

In Situ **Chemical Oxidation Process Safety**

Many safety issues exist which must be considered by those considering ISCO as a potential remediation tool. Some of the health and safety issues for ISCO include (ITRC, 2005):

- Chemical oxidizers must be handled and stored safely due to high reactivities and corrosivities.
- Dust from permanganate and persulfate is hazardous.
- Uncontrolled exothermic reactions can result from the addition of chemical oxidizers into the subsurface.
- The potential exists for oxidants and/or contaminants to migrate into underground utilities.
- Ozone generation utilizes equipment operating at very high voltages.
- Ozone presence can increase the flammability of many materials.

All of these concerns must be addressed, and a complete health and safety plan must be developed prior to initiation of an ISCO project.

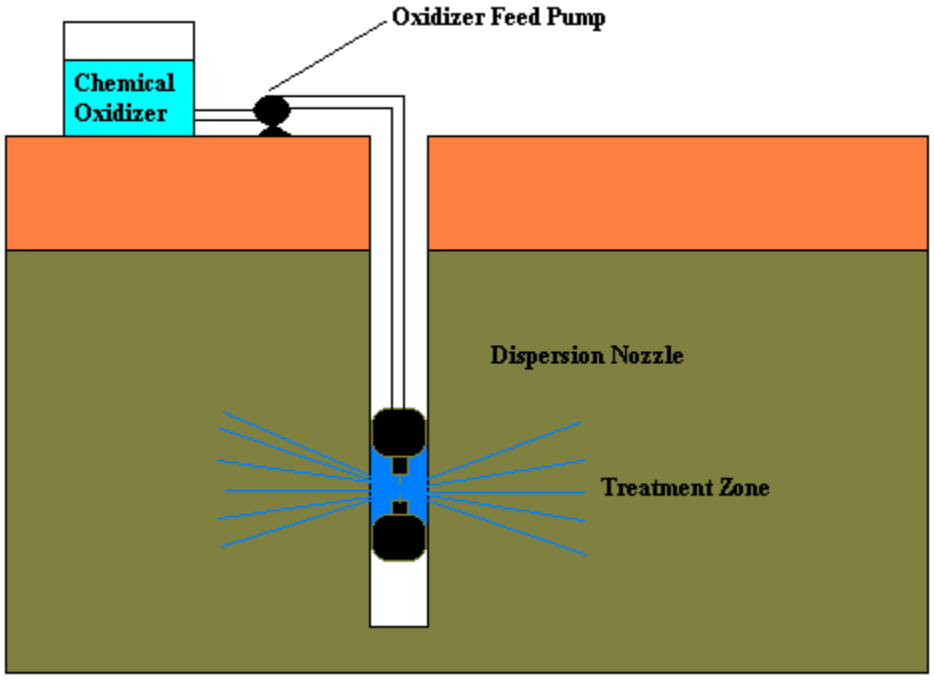

Figure 1.1: Oxidizer Delivery Mechanism for *In Situ* Chemical Oxidation (Source: Adapted, ARS Technologies, 2005)

CHAPTER II

RESEARCH HYPOTHESIS

The hypothesis directing this research focused on addressing the research and development needs relative to the improved understanding of *in situ* chemical oxidation (ISCO). In recent years, *in situ* chemical oxidation has become a viable alternative to other treatment methods such as biotreatment and solidification/stabilization for the remediation of organic contaminants. However, there are many aspects of *in situ* chemical oxidation that have not yet been fully investigated. It is envisioned that this research will offer further understanding of ISCO as it relates to the key mechanisms controlling process performance and economics, inclusive of the design, safety, and other issues related to the application of this technology. It is desired that the research project will provide the experimental data necessary to understand soil-oxidizer-pollutant interactions within a subsurface environment and the key reactions involved in these interactions. This information will be of great value to those interested in researching process limitations and those interested in field application of *in situ* chemical oxidation.

Research Objectives

Secondary objectives have been divided into four distinct categories as to how they relate to this research. The overall objective of this effort was to better elucidate the transport mechanisms that appear to control the application of the technology within greatly different soils.

Objective 1: Collection of Soil Specimens

The first objective required that several different soil samples be collected from sites listed by U.S. Geological Survey (USGS) as having elevated levels of targeted chemical constituents when compared to those levels found within typical soils. The soil types collected included ozonated sand (test control), a high calcium (high pH) specimen, a high iron soil, a soil with an elevated total organic carbon (TOC) level, a biologically stimulated soil, and an "average" soil that contained average levels of common chemical constituents. All of these targeted chemical constituents have been observed to react with chemical oxidizers during treatment of contaminated soil sites. The utilization of multiple soil samples rather than just one standard soil type enabled the research to be applied over a broad spectrum of soil compositions. It is hoped that certain compositional characteristics can be identified as particularly impacting transport.

Objective 2: Impact of Common Soil Constituents on Process Reagent Transport

The second research objective sought to investigate the reaction of both hydrogen peroxide and ozone with the six samples of soil and groundwater that contained various levels of chemical components which are either known or suspected scavengers of chemical oxidizers. Initially, shake-flask experiments were performed to determine the kinetics of the oxidizer-soil reactions using 30% (w/w) slurries. Experiments were also performed to determine the total oxidizer demand of each of the specimens using shake flask systems. Total oxidizer demands refer to the total mass of oxidizer that brings the system to a point in which further oxidizers can be added without any net loss of oxidizer due to reaction with the soil. Additionally, experiments were performed to determine the reaction of both acids and bases with each of the soil types since pH adjustments of the soil are oftentimes preferred prior to ISCO application.

Objective 3: Investigation of Potential Personnel Safety Threats During Process Application

The third research objective sought to explore some of the pertinent safety issues regarding the application of *in situ* chemical oxidation. Because Fenton's Reaction is highly exothermic, it was desired to analyze the temperatures observed in the treatment of 30% (w/w) soil slurries. Additionally, it is known that one of the by-products in the reaction of hydrogen peroxide is oxygen gas. While oxygen is not toxic, increased levels of oxygen gas in a closed system generate flammability concerns. It was desired to monitor the production of oxygen gas upon H_2O_2 and

Fenton's-based reactions within soil slurries to determine some of the safety implications in regards to oxygen's flammability concerns.

Objective 4: Impact of Process Application on Soil Fabric Properties

The fourth research objective sought to investigate the impact of *in situ* chemical oxidation on some basic soil fabric properties. Firstly, the impact of ISCO on soil hydraulic conductivity was investigated using a series of column experiments. Both pre-treatment and post-treatment hydraulic conductivity values were calculated through the use of Darcy's Law. Secondly, the impact of ISCO on soil biomass populations was analyzed due to the fact that many oxidizers are naturally harmful to the health of microorganisms. Heterotrophic plate counts were utilized to quantify bacterial activity both before and after treatment via chemical oxidation. Finally, experiments were performed to determine the impact of ISCO on soil-pollutant adsorption equilibria. 2,4-Dichlorophenol was used as a test adsorbate and the partitioning coefficient (K_d) was calculated both before and after treatments using mass balances to determine the net impact of oxidation on soil adsorption properties.

CHAPTER III

LITERATURE REVIEW

Introduction to *In Situ* Chemical Oxidation

ISCO Technology Overview

In situ processes involve the use of the subsurface as the reaction zone, requiring that process reagents be added into the subsurface in kinetically appropriate quantities to promote targeted treatment reactions. Much research has been performed over the past twenty years on applying *in situ* technologies towards the remediation of many types of organic contaminants. Most of the research attention has focused on applying *in situ* principles towards biotreatment, zero valent iron, electrokinetics, and solvent extraction (Acar and Zappi, 1995). However, limited success has been observed in the *in situ* application of these treatment types towards the remediation of chlorinated solvents, PCB's, some PAH's, and explosives (Zappi, 1995). Over the past ten years, initial research has been performed in the realm of *in situ* chemical oxidation (ISCO) for the purpose of applying chemical oxidizers directly into aquifers for the remediation of organic contaminants via oxidative processes (Amarante, 2000).

While many types of oxidative processes exist, there are several which have been recently used by vendors in a fashion that is both technically and economically

feasible (Amarante, 2000). The technologies that have been developed have been based primarily on four oxidizers: permanganate (MnO_4^-), persulfate ($S_2O_8^{2-}$), hydrogen peroxide (H_2O_2), and ozone (O_3). These technologies are based on the relative oxidation strength of each specific oxidant. Contaminants within soil and groundwater matrices are broken down due to oxidation reactions occurring between the oxidizer and the contaminant (ITRC, 2005). Table 3.1 lists the standard oxidation potentials and relative strengths of common chemical oxidizers. This research only focuses on the applications of ISCO treatments based on hydrogen peroxide and/or ozone.

Chemical Oxidation

The process of chemical oxidation has recently been broken down into two categories, the first of which is labeled primary oxidation. Primary oxidation utilizes parent oxidizers (e.g. hydrogen peroxide or ozone) for the oxidation of specific contaminants. When used as primary oxidizers, the application of either hydrogen peroxide or ozone is referred to peroxidation or ozonation, respectively (Kuo et al., 1991; Zappi, 1995). These primary oxidation technologies have previously been used for water and wastewater treatment (Langlais et al., 1991; Reed et al., 1997). The second category, referred to as advanced oxidation, relies heavily on the hydroxyl radical ($OH^{\bullet}$) as the main reactant for oxidation of targeted contaminants (Glaze and Kang, 1989; Hong et al., 1996). Advanced oxidation processes (AOPs) can be broken up into two subcategories. Most AOPs utilize ultraviolet light photolysis to catalyze the formation of hydroxyl radicals. These processes are commonly referred

to as light AOPs (Gultekin and Ince, 2004). Advanced oxidation processes with the potential to make good candidates for soil remediation are referred to as dark AOPs because they do not use photolysis or light for hydroxyl radical production (Hong et al., 1996; Fleming, 2000).

Multiple reaction products can result when contaminated organics are oxidized. Ideally, complete mineralization of contaminants to water and carbon dioxide is desired for non-chlorinated organics; for the oxidation of chlorinated organics, the ideal end result would include H_2O, CO_2, and an inorganic chloride. However, the oxidation of organic compounds can also result in other products such as aldehydes, carboxylic acids, ketones, and other hydroxylated organics (Adams and Randke, 1992; Trapido, 1994; Zappi, 1995).

Delivery of Oxidants in ISCO Remediation

The delivery of the oxidant is critical because in order to successfully oxidize contaminants, the oxidant must physically contact contaminant molecules so that the oxidation reaction might take place. Two methods exist for the applications of ISCO for remediation purposes. One method involves the injection of oxidizers on one side of the contaminant zone, while performing a simultaneous extraction of groundwater on the other side. This extraction of groundwater creates a negative pressure, causing oxidizers to migrate more rapidly through the zone of treatment. This method is often preferred when the local groundwater is used as a drinking water supply so that the water source might be protected from oxidizer migration (Amarante, 2000).

A second method involves the injection of oxidizers without the use of the simultaneous extraction. The oxidizer of choice is first injected directly into the contaminant. The contaminant is then allowed to migrate through the zone of contamination in either a horizontal or a radial fashion. The pre-existing monitoring wells are then used to monitor both the oxidizer migration and the resulting concentration of pollutants (Amarante, 2000).

Several limitations exist which are problematic in the delivery of oxidants into subsurface systems. Spain et al. (1989) reported on issues associated with the transport of hydrogen peroxide into the subsurface. He found several important factors that impact the transport properties of the oxidant. Firstly, the hydraulic conductivity within the aquifer must be overcome in order for the H_2O_2 to reach targeted reaction zones. Secondly, he found that in addition to H_2O_2 scavengers such as iron, catalase-positive bacterial activity at the point of injection played a key role in promoting wasteful H_2O_2 decomposition. Ozone has also been found to pose problems during ISCO injection due to both its auto-degradative nature and low solubility in the aqueous phase (Ku et al., 1996; ITRC, 2005). Mechanisms controlling these problematic issues are discussed later on in this chapter.

Hydrogen Peroxide and Fenton's Reagent

Introduction to H_2O_2/Fenton's Reaction

In the early 1980's, hydrogen peroxide became a tool in environmental applications in its use to control odors in municipal wastewater treatment facilities.

Following its use against odorous chemicals such as hydrogen sulfide, it became a popular chemical oxidant for industrial remediation operations due to increasing government regulations on hazardous waste disposal. Its non-toxic byproducts (oxygen and water) and its small commercial storage decomposition rate (~1% per year) both led to its industrial popularity (Elizardo, 1991). Rather than using inefficient aeration methods to add oxygen into the subsurface, hydrogen peroxide has been effectively used to enhance bioremediation within aquifer systems. Within these systems, H_2O_2 generally disassociates to produce O_2 and H_2O as shown in the following equation (Zappi et al., 2000):

$$H_2O_2 + H_2O \rightarrow \frac{1}{2}O_2 + 2H_2O \quad (1)$$

However, by itself, hydrogen peroxide is not a good oxidant for most organic contaminants (Ravikumar and Gurol, 1991).

In the 1890's, H.J.H Fenton discovered the fact that the addition of ferrous iron (II) salts greatly enhances the oxidative strength of hydrogen peroxide due to the production of hydroxyl radicals. The reaction of iron-catalyzed H_2O_2 at low pH is now commonly referred to as Fenton's Reaction because of its founder, and the mixture of ferrous iron and hydrogen peroxide is referred to as Fenton's Reagent. The reaction was developed with a hydrogen peroxide concentration of 300 ppm and a pH of less than 5 (ITRC, 2005). The basic hydroxyl radical-producing reaction associated with Fenton's Reaction was reported by Teel et al. (2001) as follows:

$$H_2O_2 + Fe^{2+} \rightarrow OH\bullet + OH^- + Fe^{3+} \quad (2)$$

Because the reaction generates hydroxyl radicals which have a significantly higher oxidative strength than H_2O_2 alone (Table 3.1), Fenton's Reaction becomes a much more effective means of remediating organic pollutants (Ravikumar and Gurol, 1991).

Fenton's Reaction and hydrogen peroxide technologies are also known to be highly exothermic. Large quantities of heat are generated in H_2O_2's reaction with ferrous (II) iron and other natural soil constituents. While the boiling off of natural soil moisture has been observed when very high H_2O_2 concentrations have been used, this exothermic characteristic does offer certain benefits for on-site remediation. When controlled properly, the heat generated can offer the potential to enhance the desorption and dissolution of subsurface NAPLs, making it easier for the chemical oxidizers to contact pollutants (Amarante, 2000; ITRC, 2005).

Modified Fenton's Reaction

Due to various ISCO limitations such as subsurface impurities, Fenton's Reaction in its truest form, involving the use of low concentrations of H_2O_2, is not applicable to a subsurface treatment of organic contaminants. During ISCO treatments, much higher concentrations of H_2O_2 are used, typically ranging from 4% up to 20%. While the reaction stoichiometry is not nearly as efficient as that of traditional Fenton's Reaction, the modified system enhances the desorption of contaminants from the soil matrix and offers the potential for the destruction of contaminants existing as dense nonaqueous phase liquids (DNAPLs) (Teel and Watts, 2002; Watts et al., 2005). The modified Fenton's Reaction system is far more

complex than the case of traditional Fenton's. Fenton's Reagent is not stable under these conditions, and several reactions occur simultaneously, as reported by Chen et al. (2001):

$$Fe^{2+} + H_2O_2 \rightarrow Fe^{3+} + HO^- + HO^\bullet \quad (3)$$

$$Fe^{2+} + HO^\bullet \rightarrow Fe^{3+} + HO^- \quad (4)$$

$$H_2O_2 + HO^\bullet \rightarrow H_2O + HO_2^\bullet \quad (5)$$

$$Fe^{2+} + HO_2^\bullet \rightarrow Fe^{3+} + HO_2^- \leftrightarrow H_2O_2 \quad (6)$$

$$Fe^{3+} + HO_2^\bullet \rightarrow Fe^{2+} + H^+ + O_2 \quad (7)$$

$$Fe^{3+} + H_2O_2 \rightarrow Fe^{2+} + HO_2^\bullet + H^+ \quad (8)$$

In Watts' studies on modified Fenton's Reaction, he observed the following reactions in addition to the basic equation for Fenton's Reaction (Equation 1):

$$H_2O_2 + OH^\bullet \rightarrow HO_2^\bullet + H_2O \quad (9)$$

$$HO_2^\bullet \leftrightarrow H^+ + O_2^{\bullet-} \quad (10)$$

$$HO_2^\bullet + O_2^{\bullet-} \rightarrow HO_2^- + O_2 \quad (11)$$

where $HO_2^\bullet$ is the perhydroxyl radical, $O_2^{\bullet-}$ is the superoxide anion, and HO_2^- is the hydroperoxide anion. In addition to the hydroxyl radicals, the superoxide and hyperoxide anions are both potential reductants in these types of ISCO systems (Watts et al., 1999).

Optimum Conditions for Fenton's Reaction

Fenton's Reaction is optimal at an acidic pH, ranging from 3.0 to 4.0 (Kakarla et al., 2002). If the pH during Fenton's Reaction is less than 5, the solubility of the iron (III) that was produced in Equation 3 is increased. This allows the iron (III) to be more efficiently reconverted to iron (II) via reaction with perhydroxyl radicals as shown in Equation 7. This process allows for the continuation of hydroxyl radical production via Fenton's mechanisms. During the Fenton's process, a side reaction occurs which produces amorphous iron oxide precipitates from the reaction of Fe^{3+} and hydroxide ions, as shown in Equation 12:

$$Fe^{3+} + nOH^{-} \rightarrow \text{amorphous iron oxides} \qquad (12)$$

This undesirable side-reaction occurs more readily at basic pH's. Due to these reasons, ISCO applications based on the use of Fenton's Reaction are far more favorable at acidic pH values (Watts et al., 1999; Kakarla et al., 2002; Teel and Watts, 2002; IRTC, 2005).

The concentration of both ferrous iron and hydrogen peroxide are an important reaction condition. While the optimal case of low H_2O_2 and Fe^{2+} concentrations for standard Fenton's Reaction are not feasible for large-scale remediation of soil and groundwater matrices, the effectiveness of modified Fenton's Reaction, using substantially higher oxidizer doses, does have a dependence on reagent concentrations. Greenberg et al. (1998) performed lab-scale studies on the optimization of Fenton's Reaction in the remediation of contaminated groundwater.

They found that an approximate H_2O_2:Fe^{2+} ratio of 10:1 worked best for their remediation of benzene, toluene, xylenes, and methyl tertiary-butyl ether (MTBE).

Remediation of Pollutants Using Fenton's Reaction

Fenton's Reaction has shown the ability to remediate several different types of pollutants. One variety of pollutant commonly treated by Fenton's Reaction is a group of volatile organic compounds (VOCs) referred to as BTEX compounds (benzene, toluene, ethylbenzene, and xylene). BTEX compounds are common components in gasoline, comprising up to 59% (w/w) of its makeup (Watts et al., 2000). Literature has shown that Fenton's Reaction has been successful in treating BTEX compounds in both groundwater and soil environments. Greenberg et al. (1998) performed an *in situ* Fenton-based remediation project at a site in Union, New Jersey contaminated with BTEX compounds and MTBE. A bench scale study, microcosm study, field pilot study, and full-scale remediation were all conducted during the treatment effort to gauge the effectiveness of remediation via Fenton's Reaction. Following a 98.5% reduction in total VOC concentration during the three-day pilot scale study, a full-scale remediation was implemented using three treatment cycles during a three-month period. Within a year, the site had received regulatory closure after all contaminant levels were reduced to levels that met New Jersey groundwater standards.

Fenton's Reaction has also proven effective in treating another type of VOC referred to as chlorinated solvents, which includes perchloroethylene (PCE) and trichloroethylene (TCE). Kakarla et al. (2002) successfully performed both a

laboratory study and an on-site remediation of chlorinated solvents via Fenton's Reaction. This particular site was located at a former dry-cleaning facility in northeast Florida, and it had cumulative VOC concentrations of up to 3500 ppb. Following the *in situ* treatment via Fenton's Reagent, a 72 percent reduction in total chlorinated solvent contamination was observed following the first injection, and a 90 percent reduction was observed following the second injection event. Watts et al. (1992) analyzed the degradation pathway of PCE via Fenton's Reagent mechanisms. Their results yielded the following mechanism, as shown by Equations 13-16:

$$PCE + OH^{\bullet} \rightarrow DCAC + Cl^{\bullet} \quad (13)$$

$$DCAC + H_2O \rightarrow DCAA + HCl \quad (14)$$

$$DCAA + 2OH^{\bullet} \rightarrow 2HCl + 2CO_2 + HCOOH \quad (15)$$

$$HCOOH + 2OH^{\bullet} \rightarrow 2H_2O + CO_2 \quad (16)$$

where DCAC is dichloroacetyl chloride and DCAA is dichloroacetic acid. Watts also calculated pseudo first-order degradation constants for both the degradation of both PCE and the H_2O_2 during Fenton's Reaction; these values were determined to be 1.65 hr^{-1} and 0.206 hr^{-1}, respectively.

Hydrogen Peroxide and Catalase

Oxidizing agents such as hydrogen peroxide are known to be extremely harmful to certain types of bacteria. Some types of bacteria such as obligate aerobes and facultative anaerobes contain enzymes such as superoxide dismutase and

catalase, which catalyze the destruction of superoxide radicals and H_2O_2. These reactions take place as follows, as reported by Prescott et al. (2001):

$$2O_2^{\bullet} + 2H^+ \xrightarrow{\text{superoxide\_dismutase}} O_2 + H_2O_2 \quad (17)$$

$$2H_2O_2 \xrightarrow{catalase} 2H_2O + O_2 \quad (18)$$

Because strict anaerobes lack both of these protective enzymes, they are rendered far more susceptible to destruction by powerful oxidizers such as hydrogen peroxide (Prescott et al., 2001). Elkins et al. (1999) reported on the protective role that catalase plays in *Pseudomonas aeruginosa* biofilm resistance to H_2O_2. They found that planktonic cells exposed to a dosings of hydrogen peroxide showed a significant decrease in cell viability, whereas the cell viability for the biofilm cells remained near 90%.

There is much literature discussing the role catalase-positive bacteria play on observed H_2O_2 degradation. As previously mentioned, Spain et al. (1989) studied the use of hydrogen peroxide in the aerobic biodegradation of hydrocarbons, finding that catalase played an important role in catalyzing hydrogen peroxide degradation within the subsurface. Zappi et al. (2000) expanded on Spain's work and studied the kinetics of hydrogen peroxide's reaction with equilibrated water samples, soil slurries, and bovine catalase. He found the reaction of H_2O_2 via biotic mechanisms was the primary oxidizer scavenger in his experiments that studied the use of H_2O_2 as an oxygen source for bioremediation efforts within saturated aquifers.

Ozone

Introduction to Ozone

Ozone (O_3), one of the strongest primary oxidants available, has been widely used for treatment and disinfection of drinking water. Ozone is commonly generated by applying an electrical discharge into an oxygen gas stream. The resulting gas stream, containing both oxygen and ozone, can then be transferred to liquid water by bubbling it into solution (Chen et al. 2002). Most commercial ozone generators can produce gas phase ozone with concentrations ranging between 2 and 10 weight percent O_3. During equilibrium with aqueous solution, concentrations of ozone in water generally range between 5 and 30 mg/L, a value that is far greater than that of oxygen (Langlais et al., 1991). During recent years, ozone has proven to be adept at treating complex organic pollutants (Kuo and Song, 1984; Trapido, 1994).

In Situ Ozonation

The use of ozone for *in situ* chemical oxidation poses several design issues different from those posed by Fenton's Reagent. Rather than direct injection of a liquid, *in situ* ozonation often involves the application of a gas into the subsurface. This must be taken into account since the injection of a gas will offer much different subsurface transport properties than the injection of a liquid (Slagle et al., 1990; Nimmer et al., 2000). Choi et al. (2002) investigated the transport characteristics of gas phase ozone in porous media. They found that ozone transport was highly dependent on the moisture content of the soil; as the water content increased in the

soil column tests, the ozone breakthrough time decreased proportionally due to the decreased amount of gas pore volumes within the column. Recently, an alternative ozone application design has been proposed which is more similar to that of a liquid injection. In these applications, ozone is dissolved into liquid water prior to its introduction into the subsurface. The resulting ozonated water is then injected into the subsurface in a liquid form (ITRC, 2005). While the design principles can cause certain challenges, *in situ* ozonation does offer several advantages that are listed below (Nelson and Brown, 1994):

- Ozone gas moves easily through soil when injected properly due to its favorable mass transfer characteristics
- Ozone is roughly 12 times more soluble in water than O_2, making it readily dissolvable in groundwater
- Because ozone is such a powerful oxidizer, oxidation of target chemicals can occur within seconds of contact

Auto-Degradation of Ozone

Another issue with ozone that differs from other oxidizers is its highly auto-degradative nature. Due to its powerful oxidizing potential and high instability, the decomposition mechanism for O_3 is quite complicated (Ku et al., 1996). Throughout literature, there is much disagreement on both the reaction order and reaction rate constant dealing with the auto-decomposition of O_3. Gurol and Singer (1982) summarized the literature findings for O_3 auto-decomposition in water under various reaction conditions; these findings are shown in Table 3.2. As is shown, reaction orders of 1, 3/2, and 2 were all observed dependent on reaction conditions such as pH and temperature. In addition, each of these experimental systems potentially

contained different impurities in water samples and employed various methods for data analysis, leading to the observed differences.

Due to differences in reaction order, many researchers have determined the auto-degradation of ozone based on the calculation of a half-life value in addition to a kinetic rate constant. Kuo et al. (1977) determined a half-life value of approximately 40 minutes for the auto-decomposition of O_3 in deionized water at 25°C and a pH of approximately 5.3. Kong et al. (2003) performed similar experiments in their experiments on ozone kinetics and diesel decomposition by ozonation in groundwater. In determining the auto-decomposition of O_3 in their experiments, they observed a second order reaction rate constant that varied dependent on the initial O_3 concentration, but a relatively constant half-life of 37.5 minutes, which was consistent with the findings of Kuo et al.

Reaction of Ozone with Organics

Two different types of organic oxidation via ozone are noted in the literature. The first type involves the direct reaction of the organic molecule with ozone. This reaction involves an ozone molecule's attack on the unsaturated carbon-carbon bonds located within an organic molecule. This reaction is summarized as follows (Qui et al, 1999):

$$O_3 + R\text{-}C{=}C\text{-}R \rightarrow R\text{-}C\text{-}O\text{-}C\text{-}R + O_2 \qquad (19)$$

A second type of oxidation via ozonation also exists that is based on the reactions of organics with hydroxyl radicals formed during the ozonation process. When ozone is added into environments with neutral to basic pH values, hydroxyl radicals are

formed from ozone's side reaction with hydroxide ions. This chain-initiating reaction that generated hydroxyl radicals was documented by Staehelin and Hoigne (1982) and is summarized in the following equations:

$$O_3 + OH^- \rightarrow HO_2^- + O_2 \quad (20)$$

$$O_3 + HO_2^- \rightarrow OH^\bullet + {}^\bullet O_2^- + O_2 \quad (21)$$

$$O_3 + {}^\bullet O_2^- \rightarrow {}^\bullet O_3^- + O_2 \quad (22)$$

$${}^\bullet O_3^- + H_2O \rightarrow OH^\bullet + OH^- + O_2 \quad (23)$$

These hydroxyl radicals derived from ozone-based reactions can then be reacted with various organic molecules through chain-propogating reactions as summarized in the following equations (ITRC, 2005):

$$OH^\bullet + R\text{-}H \rightarrow R^\bullet + OH^- \quad (24)$$

$$R^\bullet + O_3 + H_2O \rightarrow R\text{-}OH + O_2 + OH^\bullet \quad (25)$$

Ozone Scavengers

In addition to the previously outlined reaction of ozone with both organic pollutants and hydroxide ions, many types of naturally occurring soil constituents have shown to be significant scavengers of ozone molecules in both soil and groundwater environments. These scavengers will provide a further ozone demand on these systems than that which is exerted by the targeted organic contaminant. Sotello et al. (1989) performed experiments to determine the impact of suspected scavengers on ozone decomposition in aqueous solution. They observed radical scavenging effects and destabilization of ozone both in high pH conditions and in

environments containing significant quantities of chloride, sulfate, phosphate, and carbonate ions. This scavenging effect was reported to be caused by the initiation of a chain-terminating step that was strongly dependent on the reactivity of the ionic salt with hydroxyl radicals. These termination steps were observed to be first order and proved to destabilize ozone in solution.

Ozone has also been shown to react with natural organic matter (NOM) present in soil and groundwater environments. The rates of reaction are highly dependent on both carbon bonding and the functional group content. Both ozone and hydroxyl radicals have proven to react with NOM to produce organics that typically have a lower molecular weight and more polarity than the parent organic compound. Generally, the by-products from NOM ozonation include ketones, carboxylic acids, and aldehydes (Chandrakanth and Amy, 1996; Westerhoff et al., 1999; Jung and Choi, 2003; Sohi et al, 2005).

Native microbial populations within soil matrices also have the potential to exert an ozone demand during chemical oxidation. Whiteside and Hassan (1987) performed experiments to determine ozone's induction and inactivation of the catalase and superoxide dismutase enzymes in E. coli. Results showed that ozone showed an increase in enzyme activity in bacterial cultures that were exposed to ozone. This result led to both the inhibition of growth and a decrease in cell viability in these cultures.

Kinetics of Ozone Degradation in Soil and Groundwater

Due to its application in ISCO remediation efforts, initial work has been done investigating the reaction kinetics of ozone in both contaminated soil and groundwater systems. Multiple types of kinetic studies have been used in these analyses. Kuo and Chen (1996) performed kinetic studies on the ozonation of toluene in aqueous solution. They monitored the liquid phase concentration of ozone in a stopped-flow water circulation system with accompanying spectrophotometer. They determined that the rate constants were first order with respect to ozone, having a value of 4.86 s^{-1} at a pH of 10.0 and a value of 10.73 s^{-1} at a pH of 11.0. Lim et al. (2002) investigated ozone decomposition kinetics in soil slurries using similar principles. They utilized gas-tight batch reactors by mixing ozone-containing feed water and specified soil slurries into the reactor. Liquid samples were continually sampled and monitored using a UV-detection system in order to calculate first order rate constants for ozone's decay. Rather than using traditional kinetic modeling, Zappi (1995) monitored ozone degradation and ozone demand in semi-batch systems by developing a term known as an ozone utilization rate (OZUR) term for his studies in the reaction of ozone with TNT contaminated aqueous solutions. Ozone was continuously applied to a fixed mass of solution and both off-gas and liquid phase concentrations of ozone were continuously monitored. He was then able to successfully calculate a differential (flux) mass input expression based on a steady state mass balance of ozone for the semi-batch reactor.

Peroxone

Introduction to Peroxone

The reaction of ozone with hydrogen peroxide to form hydroxyl radicals is an advanced oxidation process commonly referred to as peroxone. This reaction results in increased generation of powerful hydroxyl radicals as compared to those generated solely through ozonation (Glaze and Kang, 1989; Kuo et al., 2000). This technology has long been used for the *ex situ* treatment of contaminated water (Freese et al., 1999). During the past few years, research has been conducted to determine effective ways of implementing the peroxone technology for ISCO remediation of organic contaminants (Fleming, 2000; Wang et al., 2001). The optimization of ISCO via peroxone is of important consequence since it is considered to be one of the most aggressive technology types due to the significantly higher yields of hydroxyl radicals as compared even to other AOPs such as Fenton's Reaction. Results in laboratory scale experiments utilizing peroxone have shown that it can be far more effective than both ozone and Fenton's Reaction in the remediation of petroleum-based pollutants (Hoigne and Bader, 1983; Hong et al., 1996; Wang et al., 2001).

Peroxone Reaction Mechanisms

Langlais et al. (1991) discussed the reaction mechanisms associated with the reaction of ozone with hydrogen peroxide. The general reaction is summarized as shown in the following equation:

$$2O_3 + H_2O_2 \rightarrow 2OH^{\bullet} + 3O_2 \qquad (26)$$

However, the complete mechanism for this is far more dynamic than one simple reaction. Both Langlais et al. (1991) and Kuo et al. (1999) discussed the complete mechanism for the peroxone reaction. This reaction mechanism is summarized in the following equations:

$$H_2O_2 + H_2O \rightarrow HO_2^- + H_3O^+ \quad (27)$$

$$O_3 + HO_2^- \rightarrow OH^\bullet + O_2^{-\bullet} + O_2 \quad (28)$$

$$O_2^- + H^+ \leftrightarrow HO_2^\bullet \quad (29)$$

$$O_3^- + O_2^{-\bullet} \rightarrow O_3^{-\bullet} + O_2 \quad (30)$$

$$O_3^- + H^+ \leftrightarrow HO_3^\bullet \quad (31)$$

$$HO_3^\bullet \rightarrow OH^\bullet + O_2 \quad (32)$$

Additional Hydroxyl Radical Scavengers

While many hydroxyl radical scavengers such as hydroxide ions and carbonates were previously discussed in regards to scavengers of ozone, one non-native hydroxyl radical scavenger has the potential to play a significant role in oxidation via peroxone. Kuo et al. (2000) observed that hydrogen peroxide acted as an important scavenger of hydroxyl radicals in the remediation of 2,4,6-trinitrotoluene. While the H_2O_2 reaction rates with hydroxyl radicals were generally slower than that of ozone, the two reaction rates became much more similar when excess hydrogen peroxide was present. Under the condition where very high H_2O_2 concentrations were used, H_2O_2 acted as a hydroxyl radical scavenger and actually adversely affected the reaction rates of TNT in aqueous solution. Kuo quantified that

the optimum peroxone ratio was approximately one mole of hydrogen peroxide per mole of ozone used in the treatment.

Soil Hydraulic Conductivity

Darcy's Law

In the mid-nineteenth century, Henry Darcy performed experiments in order to better understand the flow of liquid through porous media. By flowing water through sand columns, he discovered that the observed flow rate was proportional to both the hydraulic head differential and the cross-sectional are of flow; he also found that the flow rate was inversely proportional to the length of the column of sand. This led him to the development of Darcy's Law, as shown in the following equation:

$$Q = k * i * A \tag{33}$$

where q is the volumetric flow rate, i is the hydraulic gradient, and A is the cross-sectional area of the flow measured perpendicular to the flow direction. He found that a constant of proportionality, k, related these terms together, and it is referred to as either hydraulic conductivity or permeability. Darcy's Law has since become the basis for much of environmental engineers' understanding of the flow of groundwater in aquifers (LaGrega et al., 2001).

Measurement of Soil Hydraulic Conductivity

Darcy's Law can be used to measure the hydraulic conductivity value for soil by using a device known as a permeameter. Two basic types of permeameters exist for measuring soil permeability in the laboratory. The first type, known as a rigid

wall permeameter, can be created by using PVC pipe as the main body which houses the soil sample for testing. Laboratory permeameters are usually either of the up-flow or down-flow variety. In up-flow permeameters, the liquid flows against the force of gravity, while in down-flow permeameters, the liquid flow with gravity. For permeameters of the down-flow design, either a constant-head or falling-head setup may be utilized (Daniel, 1989; Noll, 2003). A second type of permeameter is referred to as a rigid wall permeameter. Daniel and Choi (1999) discussed the use of flexible wall permeameters in their hydraulic conductivity evaluations of vertical barrier walls. These flexible wall permeameter tests are performed by molding a test specimen in a cylinder and then transferring the specimen to the permeameter. The permeability is then measured in a flexible-wall cell. The major advantage of flexible wall permeameters is its wide acceptance rate in industry due to its enhanced control over the degree of saturation. The main disadvantages of flexible wall permeameters include both the difficulty in creating/molding test specimens and the complex and expensive equipment that is required.

Typical Values for Soil Hydraulic Conductivity

Soil hydraulic conductivity is extremely important in the flow of groundwater in aquifers. Due to vast differences in physical and chemical properties among different types of soils, hydraulic conductivities can differ in the range of many orders of magnitude. An environment of pure gravel will have a hydraulic conductivity of approximately $1*10^{5}$ cm/s while an environment made up entirely of clay can have a hydraulic conductivity as low as $1*10^{-9}$ cm/s. Table 3.3 lists the typical ranges of

hydraulic conductivity values for various types of soils. These values can provide engineers with a good initial assessment of expected hydraulic conductivity values when dealing with groundwater flow. However, it should be also noted that most soil environments are highly complex and non-homogenous. Therefore, hydraulic conductivity, and thus groundwater flow, will not be constant throughout the aquifer (LaGrega et al., 2001; van der Kamp, 2001).

Soil hydraulic conductivities can also vary due to both natural and unnatural events that take place within the soil matrix. Blume et al. (2002) observed permeability changes in layered sediments due to particle release. In their experiments, soil columns were subjected to a highly saline $NaNO_3$ solution followed by fresh doses of distilled water that caused the release of fine sediment particles into the course soil matrix. Results indicated that soil permeability was irreversibly decreased by up to 20% of its initial value due to the release of fine layer sediments and subsequent clogging of column pore space. Additionally, certain field applications of ISCO have shown preliminary results indicating that transport properties within the soil matrix change as a result of the application of chemical oxidizers. Insoluble by-products (e.g. amorphous iron oxides) can be formed during reaction with oxidizers such as H_2O_2 and hydroxyl radicals, and they have the potentially to alter the soil hydraulic conductivity and other soil transport properties (Amarante, 2000).

Soil Adsorption

Adsorption Theory

Adsorption is the process whereby one component migrates from one phase to another phase across some known boundary. For the adsorption of organics onto soil particles, the process normally occurs at the soil surface. Four distinct surface phenomena typically take place during the adsorption process: bulk fluid transport, film transport, intraparticle transport, and physical attachment. Chemical affinity, van der Waal's forces, electrical attraction, and hydrophobic properties of organics are all driving forces that control adsorption of organics in soils. Table 3.4 lists some of the factors known to influence adsorption. The solubility, molecular structure, molecular weight, polarity, and hydrocarbon saturation all play a role in how readily organics adsorb onto soil particles (LaGrega et al., 2001).

Freundlich Isotherms

For liquid/solid adsorption data, the final amount of contaminant adsorbed per mass of soil (q) can be plotted versus the final concentration of the contaminant in the bulk liquid (C) to generate an adsorption isotherm. While several isotherm models exist in literature, the Freundlich isotherm is very popular for the adsorption of contaminants in soil. It is an empirical model in the form of the following equation:

$$q = K * C^{1/n} \tag{34}$$

where K is the Freundlich adsorption coefficient and n is the Freundlich exponent (Carmo et al., 2000; LaGrega et al., 2001). This Freundlich model has been modified

in some literature to let n equal 1.0 in all cases. This linear isotherm model allows for the direct comparison of the adsorption partitioning coefficients calculated for different experimental conditions. The resulting modified Freundlich isotherm is given by the following equation (Thibodeaux, 1979):

$$q = K_d * C \quad (35)$$

where K_d is the partitioning coefficient for the adsorption of the organic onto the soil particle. The Freundlich isotherm model has been successfully used to model the adsorption of PCE, TCE, naphthalene, phenanthrene, 2,4,6-trinitrotoluene, copper, zinc, and 2,4-dichlorophenol (Carmo et al., 2000; Mesquita et al., 2002; Subramani, 2002; Kobayashi et al., 2004; Hwang et al., 2005).

2,4-Dichlorophenol as an Adsorbent

Chlorophenols are a type of organic chemical commonly used in pulp and paper facilities. They have been known to contaminate wastewaters and aquifers and are mobile within the groundwater due to their water solubility. 2,4-Dichlorophenol (2,4-DCP) has been shown in the literature to be a good adsorbent candidate for adsorption isotherm experiments, and its chemical structure is shown in Figure 3.1. Physical and chemical properties for 2,4-DCP are shown in Table 3.5 (LaGrega et al., 2001; Subramani, 2002). Subramani (2002) performed experiments to determine the 2,4-DCP adsorptive capacities and adsorption isotherms for kenaf, peat moss, and peanut hulls. Subramani successfully applied the Freundlich isotherm model to 2,4-DCP adsorption data, generating R^2 values of no less than 0.9 for each of his tested adsorbents.

Potential Impact of ISCO on Soil Adsorption

As discussed previously in the literature review, various oxidizers have the potential to react with existing NOM within the soil matrix, potentially impacting soil-pollutant adsorption equilibria in the subsurface environment. Karickhoff (1984) researched the mechanisms surrounding organic pollutant sorption in aquatic systems since these mechanisms can affect both transport and kinetics of pollutants. They also observed that sorption processes within soils were highly dependent on the sorptive sites provided by natural organic matter, and that organic matter was the primary sorbing constituent in sediments and soils. Kawahara et al. (1995) performed basic experiments on this subject in his observations on PAH release from soils during treatment with Fenton's Reagent. They performed lab-scale tests using 30% H_2O_2 and 8.84 mM $FeSO_4$ in treating samples from an Ohio wood-treating site. In addition to analyzing for PAH treatment, preliminary experiments were performed to determine the extractability of the PAHs from the soil post-treatment. Out of the fourteen different types of PAHs tested, twelve showed significant increases, ranging from 13% to 56%, in extractability from soil following one hour of contact time with the Fenton's Reagent mixture. The authors proposed that these initial results might enhance soil remediation by promoting the increased transport of PAH contamination from the soil matrix to the liquid phase containing Fenton's Reagent.

Table 3.1: Thermodynamic Oxidation Potentials of Common Oxidizers (Siegrest et al., 2001; Hernandez et al., 2002)

Chemical Species	**Standard Oxidation Potential (Volts)**	**Relative Oxidation Strength (Chlorine = 1.0)**
Hydroxyl radical ($OH^{-\bullet}$)	2.8	2.0
Sulfate radical ($SO_4^{-\bullet}$)	2.5	1.8
Ozone (O_3)	2.1	1.5
Sodium persulfate (NaS_2O_8)	2.0	1.5
Hydrogen peroxide (H_2O_2)	1.8	1.3
Permanganate ($NaMnO_4$ or $KMnO_4$)	1.7	1.2
Chlorine	1.4	1.0
Oxygen	1.2	0.9
Superoxide ion ($O^{-\bullet}$)	-2.4	-1.8

Table 3.2: Summary of the Auto-decomposition Kinetics of Ozone in Water (Gurol and Singer, 1982)

pH	Temperature (°C)	Reaction Order
2-4	0	2
5.3-8	0	2
Acidic	-	3/2
Basic	-	1
1-2.8	0-27	1
7.6-10.4	1.2-19.8	1
0-6.8	25	3/2
8-10	25	2
5.4-8.5	5-25	3/2
10-13	25	1
9.6-11.9	25	1
6	10-50	3/2-2
8	10-20	1
2-4	30-60	2
0.22-1.9	5-40	1 or 2
9	20	1
8.5-13.5	18-27	1
0.5-10.0	3.5-60	1
2.1-10.2	25	3/2
Acidic	25	1-2
Basic	25	1

Table 3.3: Typical Ranges of Hydraulic Conductivity for Various Soil Types (LaGrega et al., 2001)

Soil Type	**Hydraulic Conductivity (cm/s)**
Clean gravel	$1*10^{5}$ to 1.0
Clean sand or sand + gravel mixtures	1.0 to $1*10^{-3}$
Fine sands and silts	$1*10^{-2}$ to $1*10^{-6}$
Silty clay and clay	$1*10^{-5}$ to $1*10^{-9}$

Table 3.4: Factors Affecting Adsorption of Organics (LaGrega et al., 2001)

Factor	**Effect**
Solubility	Less soluble compounds adsorb more readily than more soluble compounds
Molecular structure	Branch-chain organics are more easily adsorbed than straight chain organics
Molecular weight	Larger molecules are generally more readily adsorbed than smaller molecules
Polarity	Less polar organic molecules are generally more easily adsorbed than polar organics
Hydrocarbon saturation	Unsaturated organics are adsorbed more easily than saturated organics

Table 3.5: Chemical and Physical Properties of 2,4-Dichlorophenol (LaGrega et al., 2001)

Property	**Value**
Molecular Weight	163 g/mol
Boiling Point	240 °C
Melting Point	88.7 °C
Vapor Pressure	$5.90*10^{-2}$ mm Hg
Water Solubility	$4.50*10^{3}$ mg/L @ 25 °C
K_{OC}	$3.80*10^{2}$ mL/g
Log K_{OW}	2.90

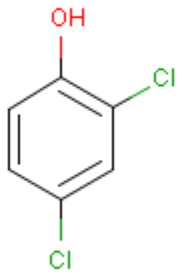

Figure 3.1: Chemical Structure of 2,4-Dichlorophenol (Subramani, 2002)

CHAPTER IV

METHODS AND MATERIALS

Introduction

Due to an overwhelming abundance of many different method types, Chapter IV serves as an abbreviated procedural section outlaying certain key methods, materials, and analytical procedures used throughout this research project. For ease of reading, specific procedures for each experiment are located within each results chapter in which the procedures apply.

Soil Collection

Soil Collection

Because different soil environments offer varying responses to *in situ* chemical oxidation, a wide range of soil samples were selected for use during the research project. Six soil samples, each having a dominant geological characteristic, were selected based on analysis of U.S. Geological Survey databases. Standard playground sand was purchased from Wal-Mart for use as a control in experiments. The first soil selected was one that had constituent levels that were relatively average when compared to the composition of most U.S. soils. Other soil samples collected included specimens with

high iron content, high content of total organic carbon (TOC), a specimen with a high initial pH, and a biologically stimulated soil with elevated levels of microbial populations. Additional test soil samples were collected from the Mississippi State Department of Plant and Soil Sciences to broaden the overall database in selected experiments.

The playground sand was ozonated in the laboratory to remove any trace organic that might influence test results. A 30% (w/w) slurry of sand and DI-water was added to a 20-liter reactor. The sand was ozonated for three hours per day over a period of three days at a concentration of 5.5 wt. % O_3 in the gas phase.

The five real soil samples were collected from their native environment using shovels and five gallon buckets. As soil samples were collected, the top foot layer of soil (O-horizon) was removed prior to soil collection since most all sub-surface contamination occurs below this layer. Following collection, the soil samples were transported to the laboratory, and allowed to air-dry for one week in plastic swimming pools purchased from Wal-Mart. All soils were then sieved using a No. 4 sieve in order to generate a clean, uniform soil consistency, free of rock, sticks, and various detritus. Following the sieving procedure, soils were stored in 5-gallon buckets at room temperature; samples for experiments were withdrawn as needed.

The biologically stimulated soil was created in the laboratory using the average soil collected from Warren County, MS. NDS, Inc. bioreactors were utilized in creating the average soil. A diagram and photograph of the bioreactor setup is shown in Figures 4.1 and 4.2 respectively. A method was derived to add appropriate nutrients to the soil in

order to enhance the growth of native bacteria populations within the soil. An initial nutrient solution was made using the nutrient quantities listed in Table 4.1 and using DI-water as the solvent. This solution was autoclaved at 121 degrees Celsius for 15 minutes and allowed to cool to room temperature. Then, 3500 g of nutrient solution was combined with 1500 g dry average soil within the bioreactor. The soil slurry was stirred at 300 rpm for 31 days. Weekly nutrient supplements were added to the bioreactor to re-spike the slurry with necessary nutrients. The amount of nutrients spiked were of a quantity such that that the added recharges corresponded to the values listed in Table 4.1. Following the 31-day microbial stimulation, the soil slurry was drained and centrifuged at 2000 rpm for 30 minutes. The nutrient solution was decanted and discarded; the remaining soil was air-dried for one week. Following the air-drying procedure, the biologically stimulated soil was treated in a similar manner to the other soil types and was used in selected experiments in which bacterial populations were expected to play an important role in the outcome.

Groundwater Simulation

For some experiments, it was desired to test solely site groundwater in addition to experiments on the soil phase. Because pre-existing wells did not exist at the soil sampling locations, a method to create a simulated groundwater was developed in the laboratory. 30% (w/w) soil slurries were created by adding 120 grams of dry soil with distilled water such that the total water content was 280 grams in 1,000-mL Erlenmeyer flasks. Soil slurries were allowed to shake for two weeks on an orbital shaker table (Bigger Bill Thermolyne model). This acclimation period allowed for soluble soil

constituents to partition into the liquid phase, allowing for a more accurate simulation of true aquifer conditions. Following the equilibration period, the soil slurries were centrifuged at 2000 rpm for 30 minutes, and the supernatant was filtered using 0.45-micron filters (Millipore, AP25, 47mm) and a vacuum pump filtration apparatus. The soil was discarded, and all the liquid that passed through the soil filter was stored in a refrigerator at 2 degrees Celsius prior to use as the equilibrated water in experiments.

Oxidizer Generation

Solution Preparations

Several solutions were commonly used during many stages of *in situ* chemical oxidation research. Firstly, solutions of ferrous iron were generated in order to equilibrate Fe^{2+} within the soil for initiation of Fenton's Reaction. Iron (II) sulfate heptahydrate (Sigma Aldrich, CAS 7782-63-0) was used to generate the Fe^{2+} solution. The properties of iron (II) sulfate heptahydrate can be seen in Table 4.2. Since the molecular weight of Fe^{2+} is 55.85 g/mol, basic stoichiometry indicated that 4.98 grams of $FeSO_4 \bullet 7H_2O$ be added per every gram of Fe^{2+} required in solution. Solutions were created by adding the appropriate quantity of $FeSO_4 \bullet 7H_2O$ to a 1-liter volumetric flask. The solution was then heated on a hot/stir plate for 5 minutes and 90 degrees Celsius in order to fully ionize the ferrous sulfate into ferrous ions. Following the heating procedure, the ferrous iron solution was allowed to cool to room temperature prior to experimental use.

Solutions of hydrogen peroxide were also utilized often for oxidative treatment. Hydrogen peroxide solutions of both 3.0 weight percent and 30.0 weight percent were purchased from Sigma Aldrich (CAS 7722-84-1). The properties of hydrogen peroxide can be seen in Table 4.2. Various hydrogen peroxide stock solutions were made over the course of experimentation. The 3.0 wt. % H_2O_2 stock was used in creating stock solutions in which the desired concentration was less than 3 wt. %, while the 30.0 wt. % H_2O_2 stock was used if the desired solution concentration was between 3 weight percent and 30 weight percent.

Ozone Generation

Ozone was generated using a laboratory-scale ozone generator manufactured by Ozonology, Inc. (Evanston, IL). This unit had an interior Airsep Corporation oxygen generator (Model AS-12) with capabilities of producing a concentrated stream at 90 volume percent (+/- 5%) pure oxygen. Ozone was generated via a process whereby high purity oxygen was passed through an electrically charged corona discharge tube within the machine. The amount of ozone produced was directly based on the amount of voltage applied to this corona. The voltage could be varied from 0 kV where only oxygen was emitted, up to 10.5 kV where concentrations of ozone could reach upwards of 6 percent by weight. The generator was equipped with four independent ozone-producing cells such that multiple ozone and oxygen streams could be run simultaneously. The total gas flow through each cell could also be controlled independently; gas flow could vary between 0 and 24 standard cubic feet per hour (scfh). The amount of gas flow through each cell was controlled by rotameters with the ability to regulate volumetric flow of

oxygen to the corona. For all experiments, a flow rate of 2 scfh of the ozone/oxygen mixture was utilized, and the concentration of ozone was controlled by adjusting the primary voltage applied to the coronas.

Analytical Methods

Soil and Equilibrated Water Characterization

Both the physical and chemical characteristics of each soil type were analyzed such that the results from experiments might be explained based on the differences in soil properties. Soil samples from each soil were shipped to the Continental Analytical Services, Inc. in Salina, Kansas for characterization. Analysis of the metals content within different soil types was performed using EPA Method 6010B. Moisture contents were determined in order that all experiments might be performed on a dry weight of soil basis. Initially 5.00 grams of moist soil was weighed in an aluminum dish and dried in a laboratory oven at 105 degrees Celsius for 12 hours. The mass of the dry soil was recorded immediately after the drying period had completed. Analyses of equilibrated water samples were performed by the Mississippi State Chemical Laboratory to determine each sample's various chemical constituents.

Analysis of Hydrogen Peroxide

Hydrogen peroxide was measured in the liquid phase using an RQflex reflectometer (EM Science) and accompanying Reflectoquant hydrogen peroxide test strips (EM Science, Catalog #16974-1). These test strips contain two organic redox indicators that react in the presence of H_2O_2. Oxygen from the decomposition of

peroxide converts the indicators into a blue-tinted oxidation product during a 15-second reaction period. Initially, test strips are dipped into peroxide solution for five seconds and removed. The second five-second period involves a light shaking of the test strip to remove any moisture prior to analysis; the third and final five-second period involves the transport of the test strip into the testing area of the reflectometer. The two reaction indicators on the strips allow for the generation of replicate analyses per sample. The reflectometer's double optic system measures the peroxide concentration based on light reflected from the indicator zones. Barcode-controlled software within the unit calculates the mean of the two measurements. The H_2O_2 indicator test strips have a range from a lower limit 0.2 mg/L to an upper limit of 20 mg/L. For test solutions with concentrations higher than 20 mg/L, 1:10 serial dilutions were made by adding 1-mL of H_2O_2 solution to 9-mL of distilled water.

Analysis of Ozone

Ozone was measured in the gas phase using a Model HC ozone monitor (PCI Ozone & Control Systems, Inc.). The monitor contains a UV absorption ozone photometer within a protective cabinet casing. The sampling system consists of a sample pump, ozone scrubber, solenoid valve, and a sample chamber. The solenoid valve enables the system to alternate between the flow of an ozone-containing gas sample stream and an oxygen stream to the detector. The concentration of ozone is calculated by a Beer's Law ratio comparing the intensity of the UV light traversing the ozone stream to the intensity of the UV light traversing the oxygen stream.

Ozone was measured in the liquid phase of samples using a CHEMetrics ozone test kit (Catalog #K-7402). This procedure uses a colorimetric test method using the DDPD methodology derived by CHEMetrics, Inc. The ozone-containing liquid sample was treated with an excess of potassium iodide, and the ozone oxidizes the iodide to iodine. The iodine then oxidized the DDPD, a methyl-substituted form of DPD (N,N-diethyl-p-phenylenediamine) to form a purple-tinted species that is proportional to the ozone concentration. A 25-mL volumetric sample cylinder was included in the test kit to allow for various quantities of ozone-containing solution and distilled water (for dilution purposes) to be mixed. Once 25-mL of liquid was in the cylinder, 5 drops of the A-744 activator solution (potassium iodide) was added. The solution was briefly stirred for five seconds to mix the sample contents, and the mixture was allowed to sit for one minute. The CHEMet ampoule (Catalog #R-7402), initially containing DDPD solution, was inserted into the sampling cylinder, and the tip of the ampoule was snapped by pressing the ampoule against the side of the cylinder. The ampoule was then filled with the solution ozone-containing solution. The contents of the ampoule were mixed by inverting it several times, and color development was allowed to occur for one minute. Either the C-7401 comparator (0.05 to 0.6 ppm O_3) or the C-7402 comparator (0.6 to 2.0 ppm) was used to physically observe the ozone concentration.

Analysis of pH

The pH of both soil slurries and solutions were monitored using a Denver Instrument brand pH/mV meter (UltraBasic Model) equipped with a Denver Instrument pH probe. Three point calibrations were performed using Fisher certified buffer solutions of pH 4, 7, and 10.

Analysis of Oxygen, Nitrogen, Carbon Dioxide, and Methane

Gas samples were analyzed for oxygen, nitrogen, and methane using an Agilent 6890N Gas Chromatograph (GC) with a thermal conductivity detector (TCD, Agilent model # G1563A). A volume of 100 µL was injected in to the GC using a 200 µL glass syringe. Two columns were used simultaneously within the GC unit. A Supelco 80/100 Porapak column was used to separate methane, carbon dioxide, and an oxygen/nitrogen composite stream. The column was made of stainless steel and had a length of 6 feet and an inner diameter of 1/8 inch. The peaks corresponding to methane and carbon dioxide were detected at approximately 1.1 minutes and 1.5 minutes respectively. Oxygen and nitrogen were separated using a Supelco 45/60 stainless steel column with a 5A mole sieve; this column had a length of 10 feet and an inner diameter of 1/8". The peaks corresponding to oxygen and nitrogen were detected at approximately 3.3 minutes and 3.8 minutes respectively. Standard curves were created and stored within the GC software by injecting fixed amounts (10, 50, and 100 µL) of pure gas and plotting the net responses. The operating parameters of the GC are located in Table 4.3.

Analysis of 2,4-Dichlorophenol

2,4-Dichlorophenol (2,4-DCP) was analyzed using a Hewlett Packard Series 1100 high performance liquid chromatography (HPLC) unit by following EPA Method 604. A QuatPump (Model G1311A) was used to pump both the carrier fluid and methanol (system rinsing) through the HPLC system. A Symmetry C_8 Waters column (3.9 mm x 150 mm) was used in conjunction with an HP (Model 1100) diode array detector to analyze for 2,4-DCP. A mobile phase of 1% acetic acid in distilled water and 1% acetic acid in acetonitrile was used with gradient flow. An HP automatic liquid sampler (Model G1313A) was used to withdraw sample from HPLC sample vials and inject 40 µL of sample into the HPLC system. A ten-point calibration curve was created within the HPLC software by diluting standards from a 500 mg/L stock solution of 2,4-DCP in distilled water. The method was routinely checked by injecting known standards to ensure the calibration curve remained accurate. Operating parameters of the HPLC are located in Table 4.4.

Table 4.1: Nutrient Addition for Biologically Stimulated Soil

Nutrient	**Initial Nutrient Solution (mg/L)**	**Weekly Recharge (mg/L)**
Ammonium nitrate	200	50
Sodium phosphate	100	25
Glucose	2,000	500
Sodium acetate	1,000	250

Table 4.2: Properties of Iron (II) Sulfate Heptahydrate and Hydrogen Peroxide

Chemical/Property	**Iron (II) sulfate heptahydrate**	**Hydrogen peroxide**
Chemical Formula	$FeSO_4 \bullet 7H_2O$	H_2O_2
CAS	7782-63-0	7722-84-1
Formula Weight	278.02	34.02

Table 4.3: GC Operating Conditions for Gas Analysis

Oven Temperature	initially at 200°C for 3 minutes ramped to 150°C at 25°C per minute
Front inlet temperature	200°C
Front detector temperature	250°C
Heater temperature	250°C
Reference flow	20 mL/min
Helium make-up flow	5 mL/min
Column flow	20 mL/min
Total flow	21.2 mL/min

Table 4.4: HPLC Operating Parameters for 2,4-DCP Analysis

Control	
Flow	1.200 mL/min
Stoptime	30.00 min
Posttime	5.00 min
Solvents	
Solvent A	30.0% (1% Acetic Acid/Acetonitrile)
Solvent B	70.0% (1% Acetic Acid/DI-water)
Pump Pressure Limits	
Minimum pressure	0 bar
Maximum pressure	400 bar
Spectrum	
Store spectra	All
Range from	190 nm
Range to	400 nm
Range step	2.00 nm
Threshold	1.00 mAU
Slit	4 nm
Injection	
Injection Mode	Standard
Injector volume	40.0 µL
Autosampler Auxillary	
Draw-speed	200 µL/min
Eject-speed	200 µL/min

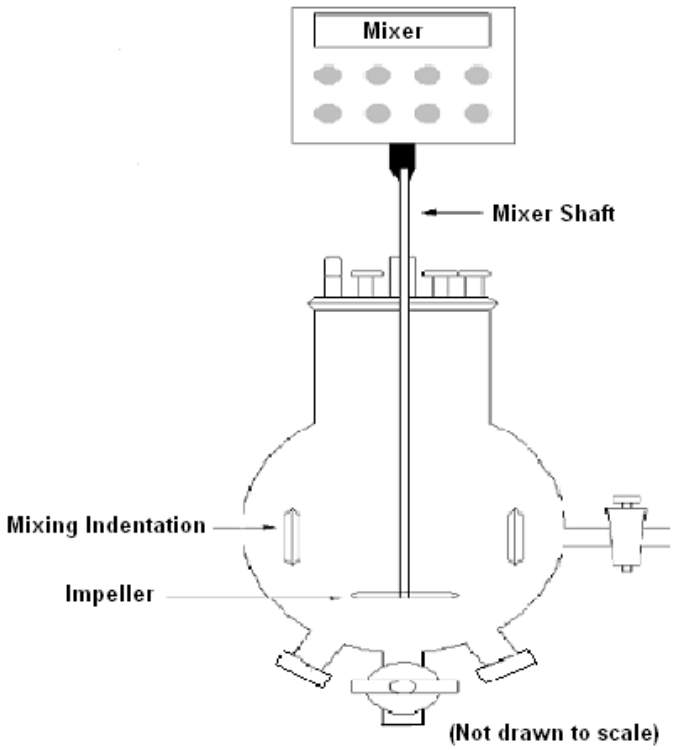

Figure 4.1. Schematic Drawing of Bioreactor Setup (Dieng, 2003)

Figure 4.2. Photograph of the Bioreactor Setup

CHAPTER V

IMPACT OF SOIL CONSTITUENTS ON HYDROGEN PEROXIDE FATE

Background

One of the primary keys in the success of any *in situ* chemical oxidation (ISCO) projects is the ability of the design engineer to effectively introduce oxidizers at appropriate concentrations and rates into the targeted treatment zones (Amarante, 2000; Chen et al., 2001). Several factors believed to control the introduction of oxidizers into the soil matrix include biomass populations, organic matter, iron, calcium, and pH (Spain et al., 1989; Yuteri and Gurol, 1989; Tyre et al., 1991; Bartoli et al., 1992; Koch et al., 1992; Fleming, 2000; Zappi et al., 2000). These factors limit ISCO applications in that their natural presence in the soil matrix results in a scavenging effect on oxidizers and radicals. Instead of all oxidation reactions occurring with targeted contaminants, some oxidizers are lost due to reaction with these scavengers (Staehelin and Hoigne, 1982; Glaze et al., 1992; Amarante, 2000).

Objective

Because multiple potential oxidizer scavengers are naturally occurring in soils, it was desired to evaluate the impact of common soil constituents on the

stability of hydrogen peroxide (H_2O_2), a chemical oxidizer commonly used with ISCO. To accomplish this task, a wide range of soil samples was selected for use during the research project. Six soil samples, each having a targeted dominant geological characteristic suspected to be an oxidizer scavenger, were identified and collected based on analysis of U.S. Geological Survey databases (U.S. Geological Survey, 2002). This database search enabled us to located and collect soil specimens which included a filter sand control, a high iron content specimen, a high organic carbon content specimen, a high calcium (i.e. high pH) content specimen, a biologically stimulated specimen, and an "average" soil. The definitions of "high" and "average" were based on the average values of U.S. soils listed by Dragun and Chiasson (1991). By collecting a variety of soil samples, it would enable distinct comparisons and correlations to be made between the fate of hydrogen peroxide and the characteristics that make up soil samples. It was desired to determine both H_2O_2 kinetics and total H_2O_2 demands for both soil and equilibrated water samples and to correlate their values to evaluate relationships with these suspected oxidizer scavengers.

Methods and Materials

Kinetics of Hydrogen Peroxide Degradation

The reaction kinetics of hydrogen peroxide degradation within the equilibrated water phase was studied under batch conditions. A 50 mL sample of the appropriate equilibrated water was added to a 250-mL Erlenmeyer flask. The flask

was placed on a Thermolyne Bigger Bill series orbital shaker and shaken at 150 rpm throughout the duration of the experiment. Initially, the equilibrated water sample was dosed with a quantity of 3% (w/w) H_2O_2 stock solution such that the initial concentration of H_2O_2 within the equilibrated water was approximately 20 mg/L. The concentration of hydrogen peroxide was monitored with respect to time by performing hydrogen peroxide analyses at five-minute intervals. In addition to the normal equilibrated water samples, the same procedure was performed on similar equilibrated water samples that were autoclaved for 15 minutes at 121°C prior to any application of H_2O_2. Experiments were run in triplicate for each equilibrated water type.

The reaction kinetics of hydrogen peroxide degradation within the soil phase was studied under batch conditions. A 30 gram sample of dry soil was added to a 250-mL Erlenmeyer flask. The flask was placed on a Thermolyne Bigger Bill series orbital shaker and shaken at 150 rpm throughout the duration of the experiment. 20-mg/L H_2O_2 solution was added to the flask at time zero such that 70 grams of total liquid was present in the slurry, thereby creating a 30% (w/w) soil slurry. Samples were taken from the flask by extracting approximately 2-mL of sample using a 250 mL plastic luer-lok syringe and filtering the slurry through a 0.45 micron inline filter (Osmonics, Inc.; Cameo 30N Syringe Filter; Nylon; 30mm). The resulting filtrate was then analyzed to determine its H_2O_2 concentration. Samples were taken at approximately two minute intervals during the kinetic determination experiments. In addition to the normal soil samples, the same procedure was performed on similar soil

samples that were autoclaved for 45 minutes at 121°C prior to any application of hydrogen peroxide. Experiments were run in triplicate for each soil type.

Total Hydrogen Peroxide Demand

The total hydrogen peroxide demand of the equilibrated water phase was studied under batch conditions. A 50-mL sample of equilibrated water was added to a 250-mL Erlenmeyer flask, and the sample was initially spiked with a volume of 3.0% (w/w) hydrogen peroxide stock solution such that the initial concentration of H_2O_2 within the equilibrated water was 1,000 mg/L. The flask was capped using a rubber stopper, and it was continuously shaken at 150 rpm on the orbital shaker unit throughout the experiment. Routine monitoring of the hydrogen peroxide concentration was performed, and additional 1-mL additions of 3.0% (w/w) H_2O_2 stock solution were made if the hydrogen peroxide concentration in the sample fell below 100 mg/L. The total hydrogen peroxide demand was assumed to have been reached if the concentration maintained a constant value over the course of a 24-hour period. Experiments were performed in duplicate.

The total hydrogen peroxide demand of the soil phase was studied under batch conditions. A 2.0 gram sample of dry soil was added to a 1,000-mL Erlenmeyer flask, and the sample was initially spiked with 50-mL of a 100,000 mg/L H_2O_2 solution. The flask was capped using a rubber stopper, and it was continuously shaken at 150 rpm on the orbital shaker unit throughout the experiment. Routine monitoring of the hydrogen peroxide concentration was performed, and additional 50-mL additions of 30% (w/w) stock H_2O_2 solution were made once the sample

concentration fell below 1,000 mg/L. The total hydrogen peroxide demand was assumed to have been reached if the H_2O_2 concentration maintained a constant value over the course of a 24-hour period. Experiments were performed in duplicate.

Results and Discussion

Characterization

Analysis of Soil

The soil physical characterization data are shown in Table 5.1. Soils were analyzed for percent sand, percent silt, percent clay, percent solids, and aerobic biological activity via total aerobic heterotrophic plate counts. The Ozonated Sand test control, as suspected, was dominated by an extremely high percent sand value. The Average Soil and Biologically Stimulated Soil were characterized as having a relatively high percent silt and biological activity. Upon completion of the microbial stimulation process for the Biologically Stimulated Soil, the aerobic bacterial populations increased by approximately one order of magnitude, from $1.1*10^7$ cfu/g to $1.6*10^8$ cfu/g, according to standard plate count agar testing. The High pH Soil, High Iron Soil, and High TOC Soil each had percent sand values of approximately 50%.

The soil chemical characterization data are shown in Table 5.2. Chemical components making up the Ozonated Sand were very low and non-detectable; the test control had a pH of 6.6. The Average Soil and Biologically Stimulated Soil were dominated by their high iron and total organic carbon (TOC) levels. The High pH

Soil was dominated by its high level of calcium, and it had an extremely large pH value of 9.8. The High Iron Soil and High TOC Soil were dominated by their high iron and high TOC concentrations, respectively. All in all, these soil specimens appear to provide the targeted range and separations in terms of the dominant characteristics.

Analysis of Equilibrated Water

The equilibrated water characterization data are shown in Table 5.3. The equilibrated water derived from the Ozonated Sand displayed minimal values of most all constituents, and it had a pH of 6.85. The equilibrated water created from the Average Soil appeared to have relatively average levels of most chemical constituents and had a pH of 5.83. The High pH equilibrated water sample had relatively high levels of sodium, chloride ions, and sulfate ions; it also had the highest pH value (8.24). The High TOC equilibrated water, as expected, contained a high concentration of total organic carbon (110.1 mg/L) and a low pH value (4.51). The equilibrated water derived from the Biologically Stimulated Soil maintained levels similar to that of the Average equilibrated water.

Hydrogen Peroxide Reaction Kinetics

Equilibrated Water Phase

Equilibrated water was reacted with hydrogen peroxide in order to determine rate order kinetics in the liquid phase, and thereby, expected groundwater reactivity. The H_2O_2 concentration versus time data was obtained from the equilibrated water

experiments. This data was successfully fitted to first-order kinetics via Equation 1. A typical H_2O_2 degradation plot is shown in Figure 5.1 as a means of illustrating typical plots generated. The first order rate constants were determined by calculating the graph's slope using Equation 1 as follows:

$$\ln\left(\frac{[H_2O_2]}{[H_2O_2]_0}\right) = -k_{peroxide} * t \quad (1)$$

where,

$[H_2O_2]$ = Concentration of hydrogen peroxide at any time, mg/L

$[H_2O_2]_0$ = Initial concentration of hydrogen peroxide, mg/L

k = first order rate constant, mg/(L*min)

t = time, minutes

The averages of the calculated R^2 values for each equilibrated water type are given in Table 5.4. These high R^2 values are indicative of good data fits to the first-order degradation model.

Rate constants calculated for both the autoclaved and non-autoclaved equilibrated water samples using average run values are shown in Figure 5.2. As expected, equilibrated water created from the Ozonated Sand control and distilled water displayed negligible reaction with hydrogen peroxide. The highest rate of hydrogen peroxide degradation (non-autoclaved) was observed in the High pH equilibrated water. pH is a known influence on the fate of oxidizers within soil and groundwater matrices. Watts et al. (1999) observed that hydroxyl radical production rates were greater at higher pH values than at acidic pH values. An increased

hydroxyl radical production rate corresponded with an increased degradation of H_2O_2 within the soil matrix. Glaze et al. (1992) also found that an increased pH corresponded to faster oxidizer degradation rates in their modeling of advanced oxidation processes. The Average equilibrated water, High Iron equilibrated water, High TOC equilibrated water, and equilibrated water from the Biologically Stimulated Soil all displayed similar non-autoclaved H_2O_2 degradation constants of 0.005, 0.005, 0.006, and 0.005 min^{-1} respectively.

Similar experiments were also performed on equilibrated water that was autoclaved prior to the application of hydrogen peroxide. Oxidizing agents such as hydrogen peroxide are known to be extremely harmful to certain types of bacteria. Some types of bacteria such as obligate aerobes and facultative anaerobes contain enzymes such as catalase, which catalyze the destruction of H_2O_2. This reaction takes place as follows (Prescott et al. 2001):

$$2H_2O_2 \xrightarrow{catalase} 2H_2O + O_2$$

Autoclaves are designed to subject samples to temperatures and pressures that sterilize microbial populations, thereby eliminating these catalase-producing aerobes. The calculated equilibrated water rate constants indicated that autoclaving had no significant impact on hydrogen peroxide's reaction within the Ozonated Sand, High Iron, and High TOC equilibrated water samples. However, in the equilibrated water samples with the high initial microbial levels (Average Soil, High pH Soil, and Biologically Stimulated Soil), bacteria levels were a key factor in H_2O_2 degradation rates. Following the elimination of microbial populations via autoclaving, the

equilibrated water rate constants were reduced by 80% in the Average equilibrated water sample and by 60% in the Biologically Stimulated equilibrated water. These results agreed with Zappi's results that examined H_2O_2's use as an oxygen source for bioremediation (Zappi et al., 2000).

For practitioners using ISCO to remediate a contaminated groundwater environment, evidence indicates that both a high pH value and a high level of microbial populations have the potential to significantly enhance non-pollutant related degradation of hydrogen peroxide within the subsurface. The scavenging of chemical oxidizers by these factors will play a key role in determining the rate at which H_2O_2 must be added to the targeted treatment zone.

Soil Phase

The reaction of hydrogen peroxide reaction and the 30% (w/w) soil slurries was also studied to investigate the relative H_2O_2 degradation kinetics and ascertain the reactivity of the various soil constituents. The averaged degradation versus time graph for H_2O_2 decay data for each specimen are shown in Figure 5.3 for non-autoclaved conditions and Figure 5.4 for autoclaved conditions.

The data for each soil type, both for non-autoclaved and autoclaved samples, were successfully fitted to First Order Kinetics via Equation 1. The average R^2 values for the three triplicate test runs of each soil type are shown in Table 5.5, and these values indicate that the First Order Model was appropriate due to all soil types having an R^2 value of at least 0.9. A sample plot showing the linear first-order relationship in one of the soil test runs is shown in Figure 5.5. First-order rate

constants were determined by calculating the slope of the line in the first-order kinetic plots, and results were averaged for triplicate experiments. Rate constants for both non-autoclaved and autoclaved soil slurries are shown in Figure 5.6.

Ozonated Sand test controls showed no signs of detectable H_2O_2 degradation over the recorded time period. For the biologically active samples, the High Iron Soil displayed the highest rate constant value at approximately 0.9 min^{-1}; for the autoclaved samples, the High Iron Soil also displayed the highest rate constant value at approximately 0.7 min^{-1}. The higher H_2O_2 reaction rates within the High Iron Soil were most likely due to the additional Fenton's Reaction mechanism whereby hydrogen peroxide reacted with naturally occurring ferrous iron (Fe^{2+}) in addition to other typical soil constituents (Watts et al., 1999). Non-autoclaved experiments involving Average Soil, High pH Soil, and High TOC Soil resulted in similar H_2O_2 first-order rate constants.

As also seen in Figure 5.6, autoclaved soil experiments indicated that microbial populations within soil samples played a significant role in hydrogen peroxide degradation rates in some, but not with all of the various soil types. The first order rate constants for the Ozonated Sand, High pH Soil, High Fe Soil, and High TOC Soil were not significantly affected by the autoclaving procedure, most likely due to lower initial levels of aerobic microbial activity as compared to the other two soil samples. However, both the Average Soil and the Biologically Stimulated Soil showed significant reductions in their respective first order rate constants due to the elimination of native bacteria. These H_2O_2 losses were a function of the

degradation of the catalase enzyme via the native microorganisms already present in soil samples (Prescott et al., 2001). In the Biologically Stimulated Soil, the first-order H_2O_2 rate constant was reduced by more than 80% following the elimination of native bacteria.

It was desired to explore the functionality of hydrogen peroxide rate constants as compared to H_2O_2-scavenging soil components. Figure 5.7 shows the first-order H_2O_2 rate constant measurements as a function of both Iron and TOC level. Figure 5.8 shows those same H_2O_2 rate constants as a function of initial microbial levels within the soil. The combination of these figures indicates that H_2O_2 degradation within the soil matrix is occurring at all levels within these three constituents. Iron, TOC, and total microbial populations all appear to offer scavenging challenges for ISCO design engineers. However, results from these experiments and literature (Zappi et al., 2000) clearly show that elevated levels of microbial populations will significantly impact H_2O_2 degradation rates within the soil matrix. Additionally, it was anticipated that soil particle size has the potential play a role in H_2O_2 degradation. Figure 5.9 compares the autoclaved first order soil slurry phase H_2O_2 rate constant versus the clay content in the Average, High pH, High Iron, and Biologically Stimulated Soils. The comparison indicates a positive correlation ($R^2 = 0.77$), suggesting that smaller particle sizes have the potential to increase the observed H_2O_2 rate constant. Decreased soil particle size corresponds to an increased total surface area of soil exposed to H_2O_2 within the slurry, thereby providing more available reactive sites than in soils with relatively low clay contents.

From analysis of these trends and the first order H_2O_2 degradation constants given in Figure 5.6, the data indicates that iron, bacterial populations, and soil particle size, rather than TOC or pH, appear to be the dominating scavengers of H_2O_2 within the soil matrix. The first order rate constants are significantly higher in the High Fe Soil and the Biologically Stimulated Soil than in the remainder of the tested soil types. The large scavenging effect in the Biologically Stimulated Soil is most likely due to the catalase enzyme present in bacteria such as obligate aerobes and facultative anaerobes. This enzyme enhances the conversion of H_2O_2 into H_2O and O_2 (Prescott et al., 2001). The scavenging effect of the High Fe Soil is most likely due to the significant impact of Fenton's Reaction due to the abundance of naturally occurring iron minerals within the soil. Watts et al. (1999) observed that soils containing iron minerals such as hematite and magnetite enhanced the catalysis of hydrogen peroxide via the initiation of Fenton-like oxidation. However, the scavenging effect due to these reactions could potentially be beneficial to ISCO practitioners since Fenton's Reaction yields useful hydroxyl radicals as its product rather than simply H_2O and O_2. Experimental results and literature indicate that soil microbial populations will tend to present the most significant challenge to ISCO practitioners.

Hydrogen Peroxide Total Demands

Equilibrated Water Phase

Equilibrated water total hydrogen peroxide demand experiments were run using 50 mL of equilibrated water as the basis. Following the completion of the

experiment, the total hydrogen peroxide demand of the equilibrated water was calculated by using Equation 2 as shown below:

$$Demand = \frac{M_A - M_B}{V} \quad (2)$$

where,

Demand = Total H_2O_2 Demand of the equilibrated water, mg/L

M_A = Total mass of H_2O_2 added to the equilibrated water, mg

M_B = Final total mass of H_2O_2 remaining in the equilibrated water, mg

V = Volume of equilibrated water, L

The total equilibrated water H_2O_2 demand data are shown in Figure 5.10. The Ozonated Sand control showed a slight H_2O_2 demand of approximately 5 mg/L. For the five other equilibrated water samples, the High TOC equilibrated water had a significantly higher hydrogen peroxide demand (760 mg/L) than any other sample; the equilibrated water sample derived from the Average Soil had a significantly lower H_2O_2 demand than the any other non-control equilibrated water type.

These results indicated that TOC content appeared to be a contributing factor in the total H_2O_2 demand of equilibrated water samples. Figure 5.11 compares the equilibrated water TOC values with their respective total H_2O_2 demands for equilibrated water. While the total H_2O_2 demand for most equilibrated water samples are not significantly different, the data point for the High TOC soil is significantly greater than the other equilibrated water types. The reasoning for TOC's importance in comparison to other minerals such as iron, calcium, and manganese most likely deals with the amount of TOC solubilized in the equilibrated water as compared with

other known oxidizer scavengers. Figure 5.12 presents the data comparing the concentrations of suspected oxidizer scavengers in equilibrated water samples. The total organic carbon levels clearly dominate the chemical composition of the equilibrated water, thereby causing it to be a significant factor in observed total H_2O_2 demands.

Soil Phase

Soil total hydrogen peroxide demand experiments were run using 2 grams of dry soil as the basis. Following the completion of the experiment, the total hydrogen peroxide demand of the equilibrated water was calculated by using Equation 3 as detailed below:

$$Demand = \frac{M_C - M_D}{M_S} \tag{3}$$

where,

Demand = Total H_2O_2 Demand of the soil, lbs H_2O_2/lb dry soil

M_C = Total mass of H_2O_2 added to the soil slurry, lbs H_2O_2

M_D = Final total mass of H_2O_2 remaining in the soil slurry, lbs H_2O_2

M_S = Mass of dry soil, lbs

The total soil H_2O_2 demand data for all of these soils are shown in Figure 5.13. The High Iron Soil and the Biologically Stimulated Soil had the highest total H_2O_2 demands at 21 and 23 lbs H_2O_2/lb dry soil respectively. It was also observed that the biological stimulation of the Average Soil had a large impact on the total hydrogen peroxide demand of the soil samples. The demand increased from 14 lbs

H_2O_2/lb dry soil for the Average Soil to 23 lbs H_2O_2/lb dry soil following the microbial enhancement.

While different soil constituent levels all had an important impact on total hydrogen peroxide demands within different soils, data indicated that the bacterial populations within the soil samples had a significant impact on H_2O_2 demand. Figure 5.14 compares the order of magnitude of bacterial populations within each soil type to its corresponding total H_2O_2 demand. As was the trend observed with the H_2O_2 soil degradation rates, increased bacterial populations resulted in an increased hydrogen peroxide demand in the soil. Figure 5.15 compares both of the H_2O_2 fate (rate and total demand) data sets with the order of magnitude of bacterial populations and shows a very similar trend between both the H_2O_2 rate constant and H_2O_2 total demand correlations. This plot gives further evidence to the notion that soil aerobic bacteria populations are playing a key role in H_2O_2 fate within the soil matrix.

Additionally, it was observed that the total H_2O_2 demand for the High TOC Soil displayed the lowest value among non-control soil types, while the equilibrated water derived from the High TOC soil displayed the highest value among non-control equilibrated water types. Analysis of the chemical characterization data of equilibrated water samples (Table 5.3) indicated that TOC had a far greater potential to solubilize within the aqueous phase as compared to other suspected H_2O_2 scavengers such as calcium and iron; this caused TOC to play a much more significant role in H_2O_2 fate within equilibrated water samples as opposed to soil samples. In soil slurry experiments, H_2O_2 had universal access to all scavengers

contained within soil slurries without regards to the restrictions of the two-week equilibration period used to create the aqueous samples.

Equilibrated Water /Soil H_2O_2 Demand Correlation

One of the key objectives of the H_2O_2 total demand experiments was to test the hypothesis that the total hydrogen peroxide demand of a soil could be estimated given information regarding the total demand of the associated groundwater. For sites with pre-existing sampling wells, this would enable ISCO users to estimate a total amount of hydrogen peroxide required without having to perform any type of soil excavation. In order to better assess this hypothesis, five additional soil samples were acquired from the Mississippi State University Department of Plant and Soil Sciences. H_2O_2 demand experiments for both equilibrated water and soil samples were performed to gain five additional data points for comparison. Figure 5.16 shows the soil and equilibrated water correlation comparing all of the calculated total equilibrated water H_2O_2 demands (converted to lbs H_2O_2/lb of equilibrated water) with their corresponding total soil H_2O_2 demands. The data indicates a fairly consistent relationship suggesting that an increase in total hydrogen peroxide demand for the equilibrated water corresponds with an increased total H_2O_2 demand for the corresponding soil.

Upon reviewing the data, the High TOC Soil was the obvious outlier in this correlation. This was most likely due to a combination of two reasons. Firstly, as was previously discussed, TOC appeared to solubilize more readily into the equilibrated water samples than other suspected H_2O_2 scavengers (Figure 5.12). This

result was also observed in equilibrated water samples tested by Zappi et al. (2000), and it led to a significantly higher H_2O_2 demand for the High TOC equilibrated water. Secondly, the High TOC Soil had limited amounts of aerobic biological activity as indicated by plate counts of aerobic heterotrophs. Because most anaerobic bacteria lack the catalase enzyme that readily impacts H_2O_2 degradation (Prescott et al., 2001), the dramatically reduced bacterial populations caused the total H_2O_2 demand of the High TOC Soil to be unnaturally low. The combination of these two simultaneous effects on the High TOC Soil and its corresponding equilibrated water led to its outlier status. If the outlying data from the High TOC Soil is removed from the graph, the correlation in Figure 5.17 results. While it's not an exact linear relationship, the correlation shows a great deal of promise in regards to the prediction of soil hydrogen peroxide demands from groundwater H_2O_2 demands. The correlation has an R^2 value of 0.6, and it indicates that the total soil H_2O_2 demand (lbs H_2O_2/lb dry soil) can be reasonably estimated by multiplying the total equilibrated water H_2O_2 demand (lbs H_2O_2/lb equilibrated water) by a factor of 38,809.

Table 5.1: Physical Characterization of Experimental Soils

Soil Type	**Location**	**% Sand**	**% Silt**	**% Clay**	**% Solids**	**Total heterotrophic aerobes (cfu/g dry soil)**
Ozonated Sand	Wal-Mart	96	4	0	99	ND
Average Soil	Warren County, MS	8	76	16	88	$1.12*10^7$
High pH Soil	Crot, AZ	48	24	28	97	$5.23*10^6$
High Iron Soil	Monroe County, TN	51	21	28	93	$4.10*10^6$
High TOC Soil	Greene County, MS	53	35	12	85	ND
Biologically Stimulated Soil	Warren County, MS	0.5	85	14	87	$1.57*10^8$

*ND indicates non-detected

Table 5.2: Chemical Characterization of Experimental Soils

Soil Type	Calcium (mg/kg)	Iron (mg/kg)	Manganese (mg/kg)	Potassium (mg/kg)	Zinc (mg/kg)	TOC (mg/kg)	pH
Ozonated Sand	~ 0	~ 0	~ 0	~ 0	~ 0	~ 0	6.6
Average Soil	2,170	15,600	645	17	48	15,832	6.1
High pH Soil	20,300	9,840	201	2,700	29	3,800	9.8
High Iron Soil	410	30,100	826	900	23	2,712	5.5
High TOC Soil	171	140	9	53	7	19,660	4
Biologically Stimulated Soils	1,951	6,800	74	145	9	14,408	5.8

Table 5.3: Characterization Data for Equilibrated Water Samples

Analyte	Ozonated Sand	Average	High pH	High Fe	High TOC	Biologically Stimulated
Sodium (mg/L)	1.5	2.9	410	1.3	1.4	1.3
Potassium (mg/L)	3.8	4.8	2.6	2.0	6.8	3.2
Magnesium (mg/L)	0.12	4.2	0.45	0.40	3.0	4.7
Calcium (mg/L)	0.68	16	5.5	2.9	7.8	18
Chloride (mg/L)	3.7	4.7	34	2.3	1.7	1.5
Nitrate (mg/L)	0.20	40	64	2.9	78	27
Sulfate (mg/L)	0.41	3.1	390	4.1	4.9	2.9
Iron (mg/L)	0.04	0.05	0.13	0.19	<0.01	0.19
Manganese (mg/L)	<0.01	<0.01	0.40	<0.01	0.34	0.03
Phosphorus (mg/L)	<0.1	0.29	1.8	<0.1	<0.1	<0.1
TOC (mg/L)	28.2	81.3	65.7	61	110.1	75.5
Alkalinity (mg/L of $CaCO_3$)	<10	16	550	<10	<10	18
pH	6.85	5.83	8.24	6.86	4.51	5.65

Table 5.4: R^2 Values for H_2O_2 Degradation in Equilibrated Water Based on First-Order Reaction Kinetics

Equilibrated Water Type	**Average R^2**
Ozonated Sand – No Autoclave	0.179
Ozonated Sand – With Autoclave	0.233
Average – No Autoclave	0.851
Average – With Autoclave	0.669
High pH – No Autoclave	0.979
High pH – With Autoclave	0.878
High Fe – No Autoclave	0.907
High Fe – With Autoclave	0.869
High TOC – No Autoclave	0.973
High TOC – With Autoclave	0.978
Biologically Stimulated – No Autoclave	0.873
Biologically Stimulated – With Autoclave	0.958

Table 5.5: R^2 Values for H_2O_2 Degradation in Soil Based on First-Order Reaction Kinetics

Equilibrated Water Type	**Average R^2**
Ozonated Sand Soil – No Autoclave	0.065
Ozonated Sand Soil – With Autoclave	0.255
Average Soil – No Autoclave	0.997
Average Soil – With Autoclave	0.973
High pH Soil – No Autoclave	0.967
High pH Soil – With Autoclave	0.923
High Fe Soil – No Autoclave	0.994
High Fe Soil – With Autoclave	0.954
High TOC Soil – No Autoclave	0.950
High TOC Soil – With Autoclave	0.946
Biologically Stimulated Soil – No Autoclave	0.982
Biologically Stimulated Soil – With Autoclave	0.971

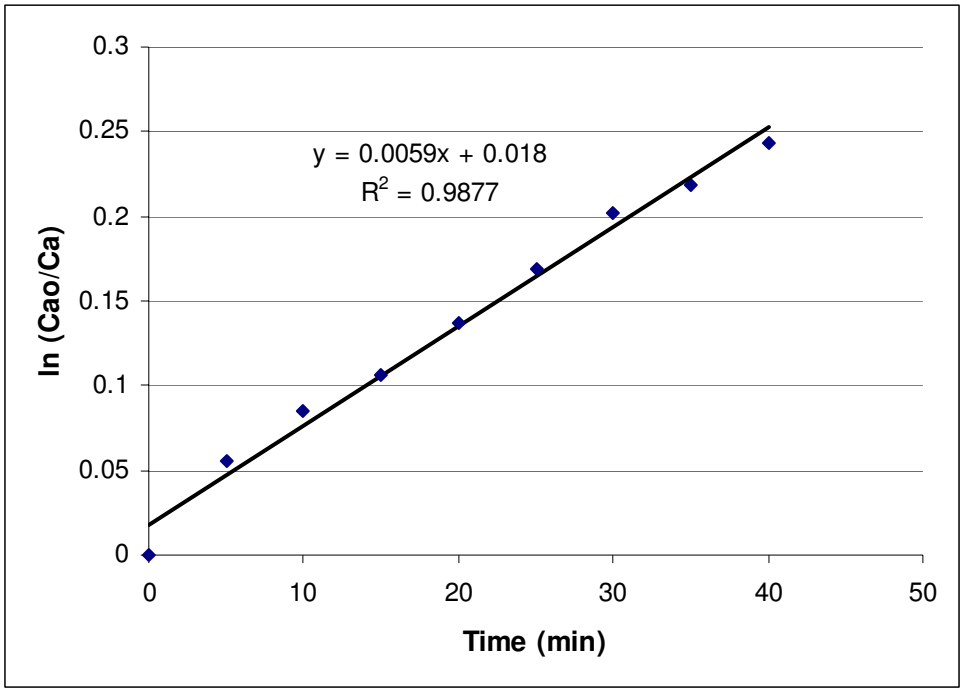

Figure 5.1: H_2O_2 Reaction within Non-Autoclaved High TOC Equilibrated Water (Run 1)

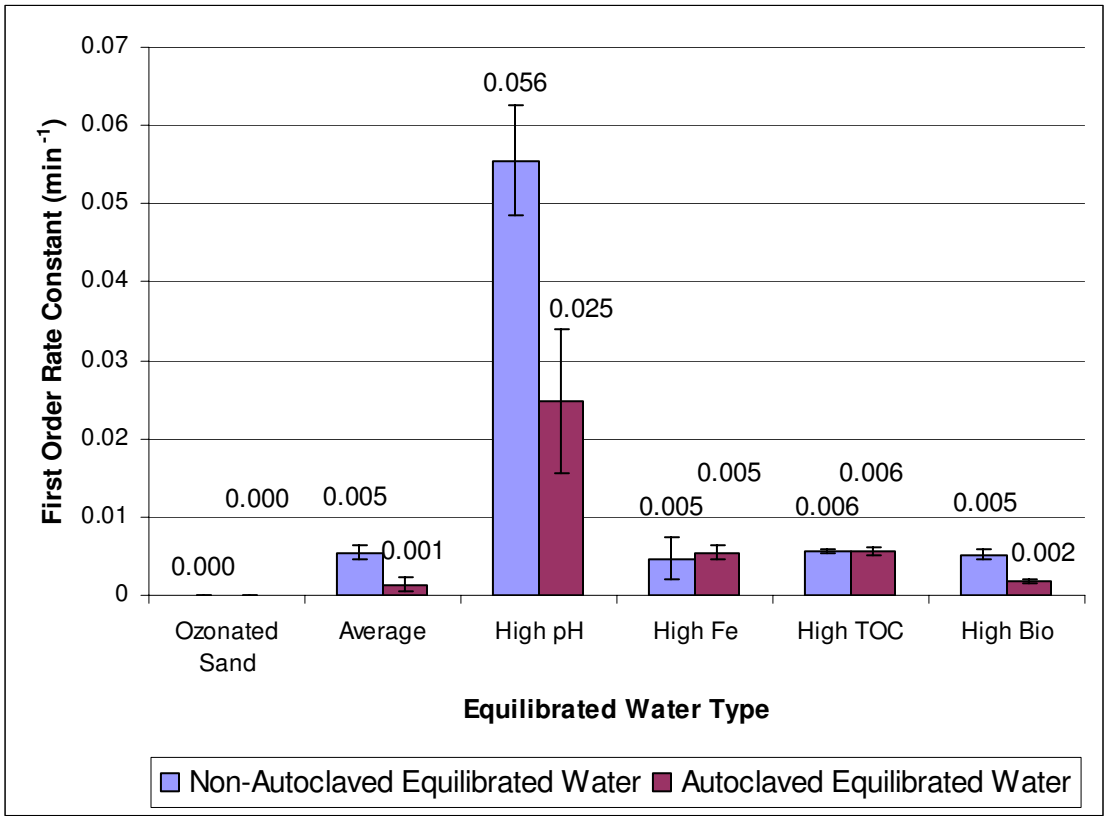

Figure 5.2: First-Order H_2O_2 Rate Constants within Equilibrated Water, $[H_2O_2]_0$ = 20 mg/L

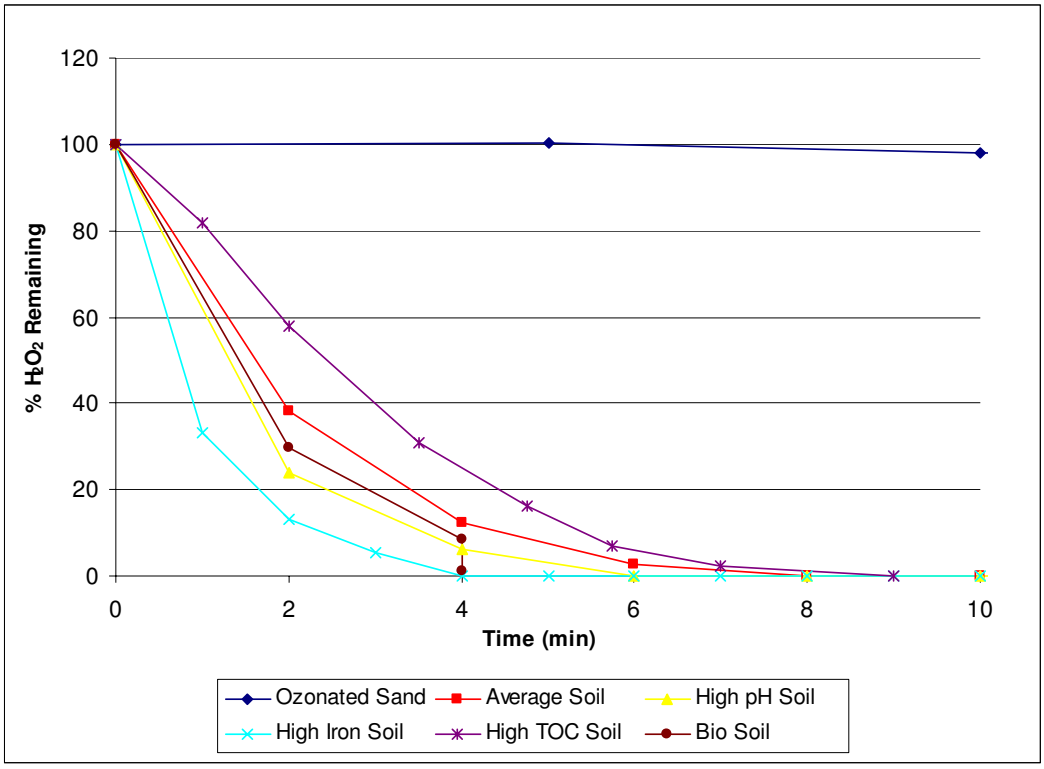

Figure 5.3: Degradation of H_2O_2 within Non-Autoclaved 30% Soil Slurries

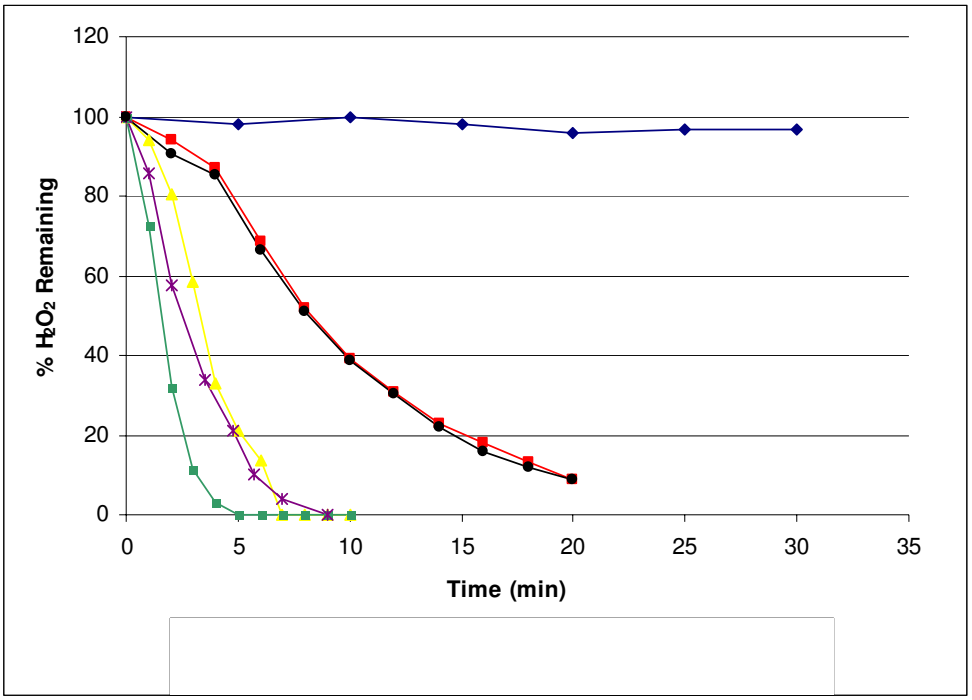

Figure 5.4: Degradation of H_2O_2 within Autoclaved 30% Soil Slurries

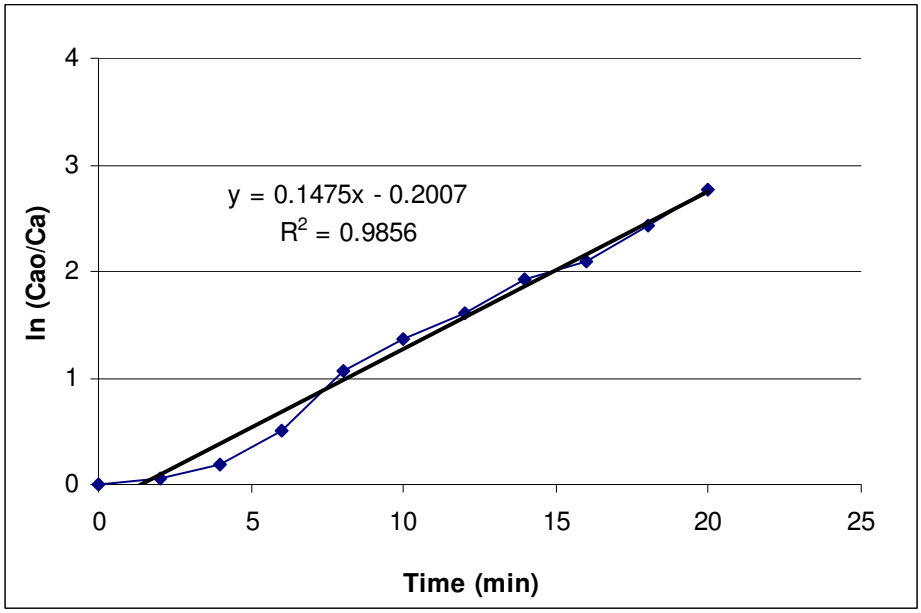

Figure 5.5: H_2O_2 Reaction within Autoclaved Average Soil (Run 2)

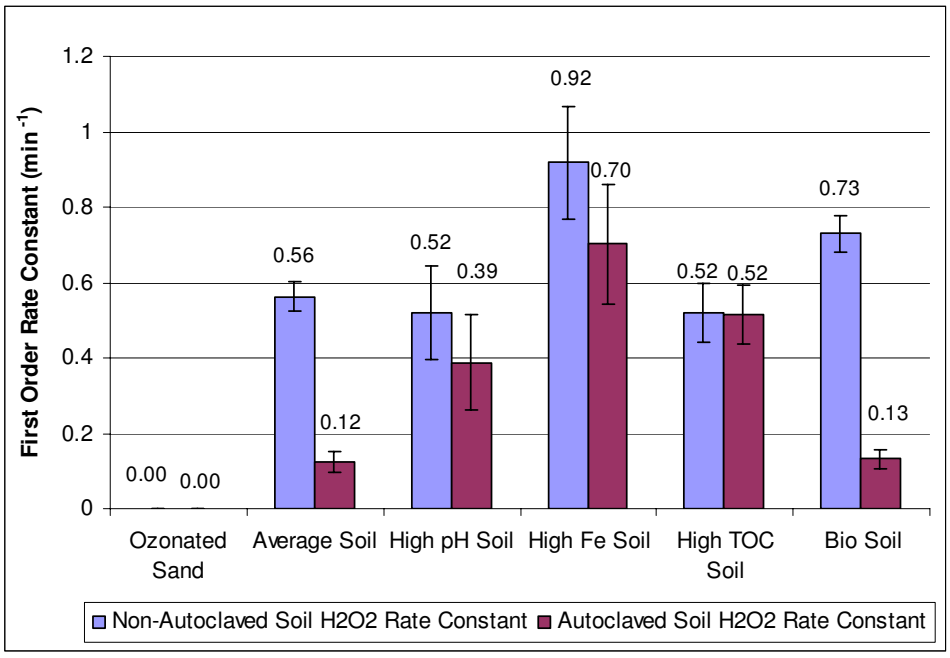

Figure 5.6: First-Order H_2O_2 Rate Constants within 30% Soil Slurries, $[H_2O_2]_0$ = 20 mg/L

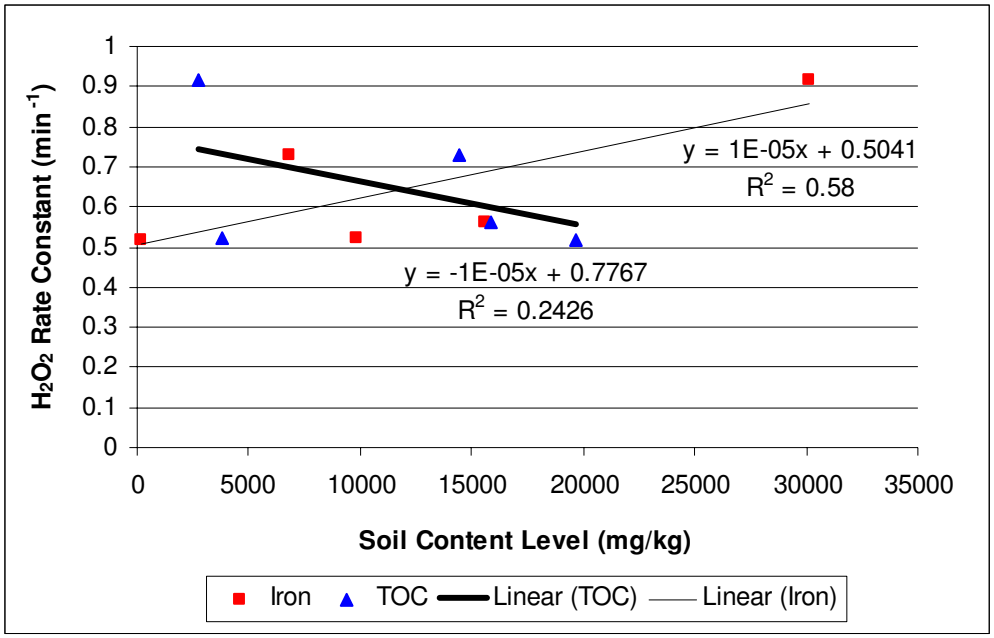

Figure 5.7: First Order H_2O_2 Rate Constant vs. Soil Iron and TOC Content

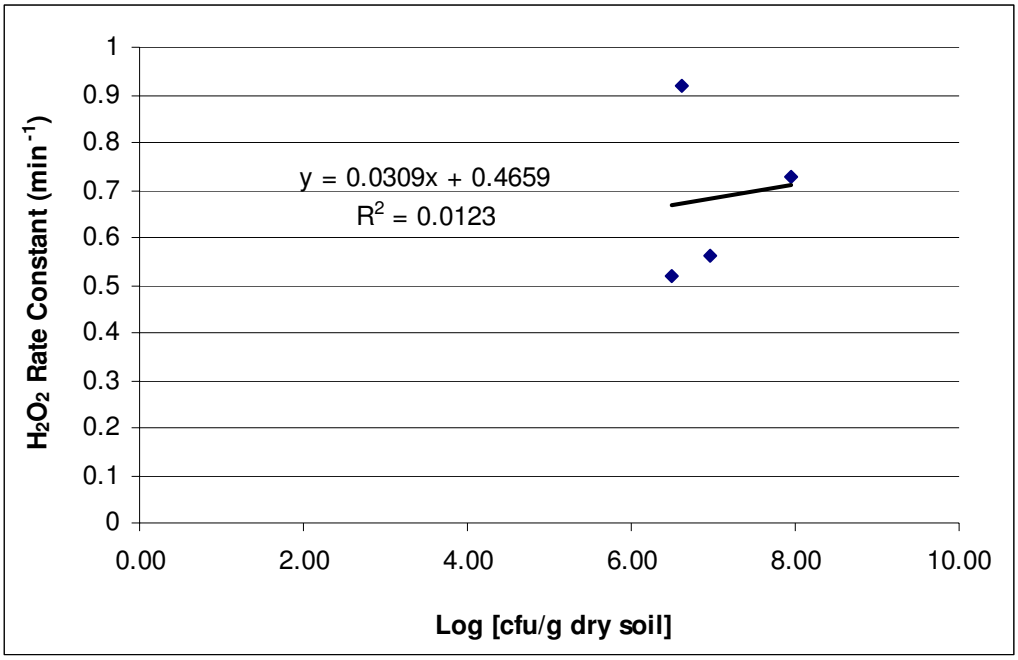

Figure 5.8: First Order H_2O_2 Rate Constant vs. Initial Soil Microbial Populations

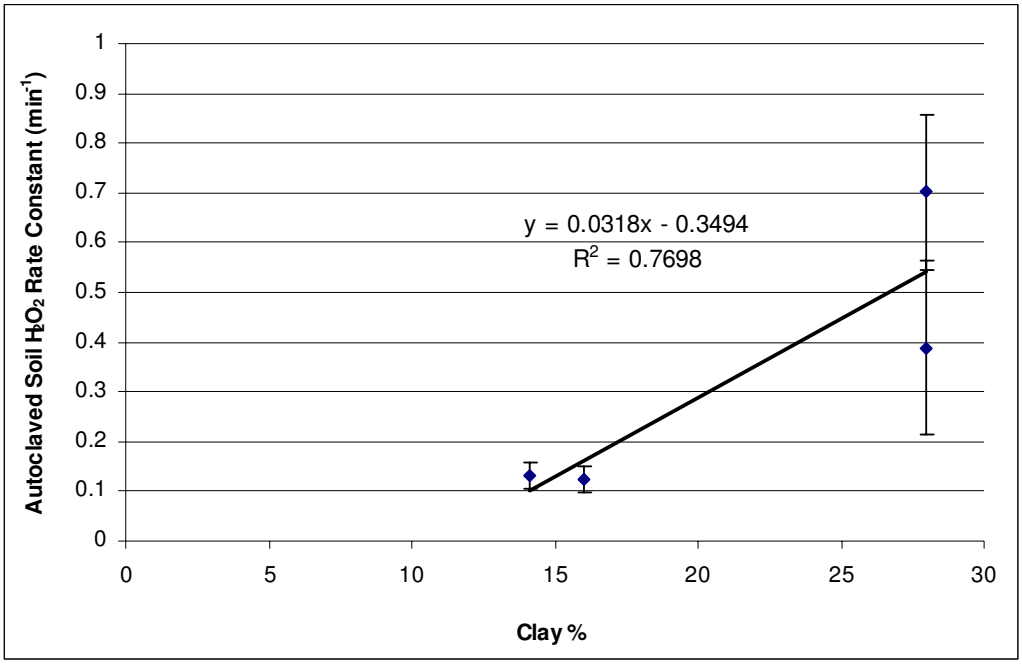

Figure 5.9: Autoclaved First Order H_2O_2 Rate Constant vs. Soil Clay Content

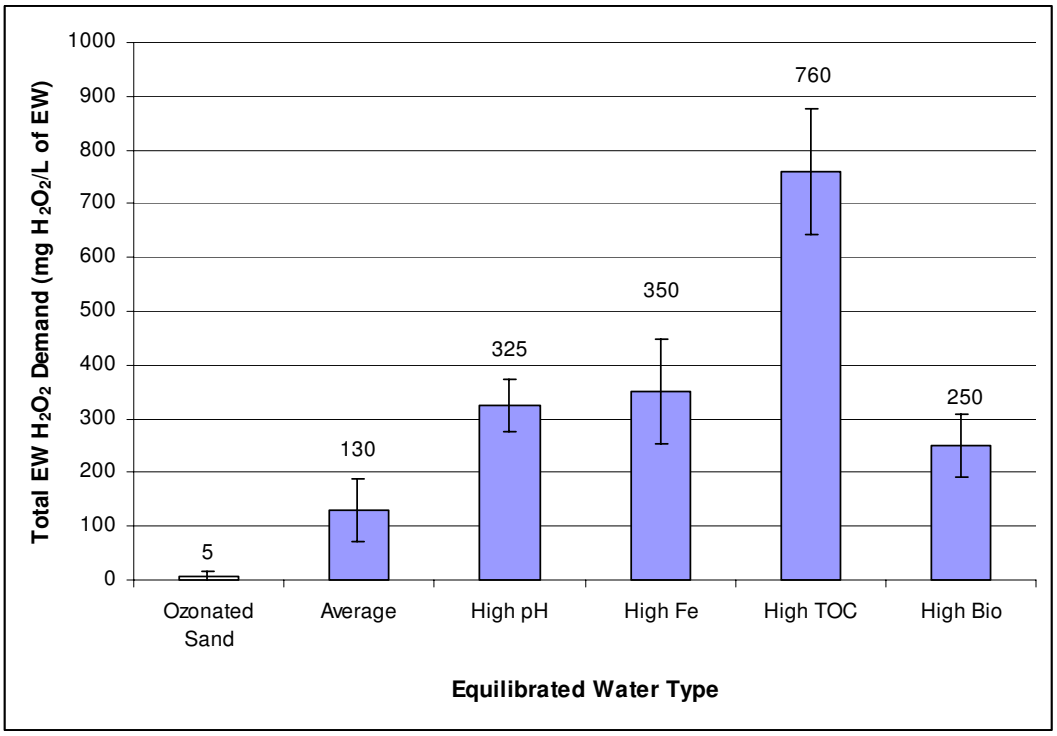

Figure 5.10: Total H_2O_2 Demands for Equilibrated Water

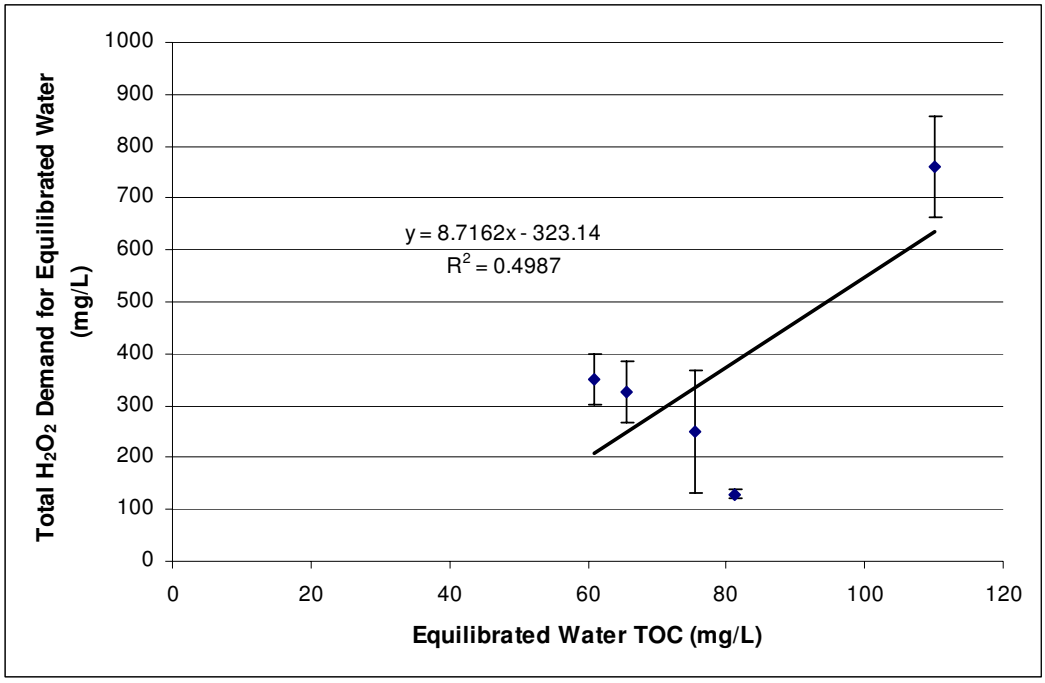

Figure 5.11: Total Equilibrated Water H_2O_2 Demand vs. Equilibrated Water TOC Content

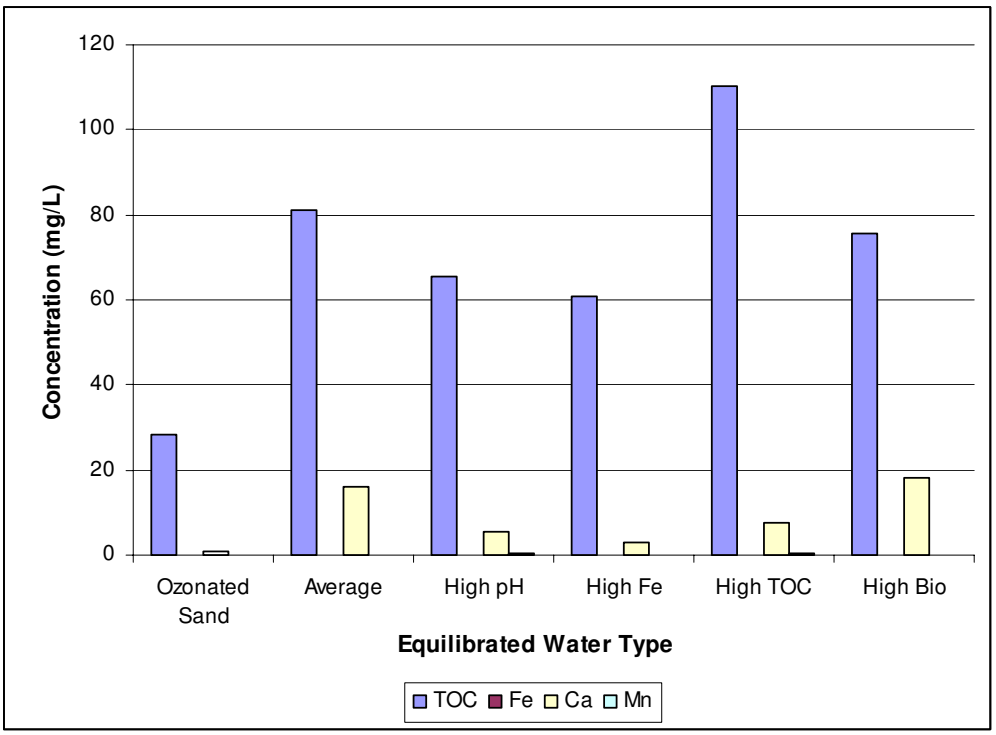

Figure 5.12: Concentrations of Suspected Oxidizer Scavengers within Equilibrated Water Samples

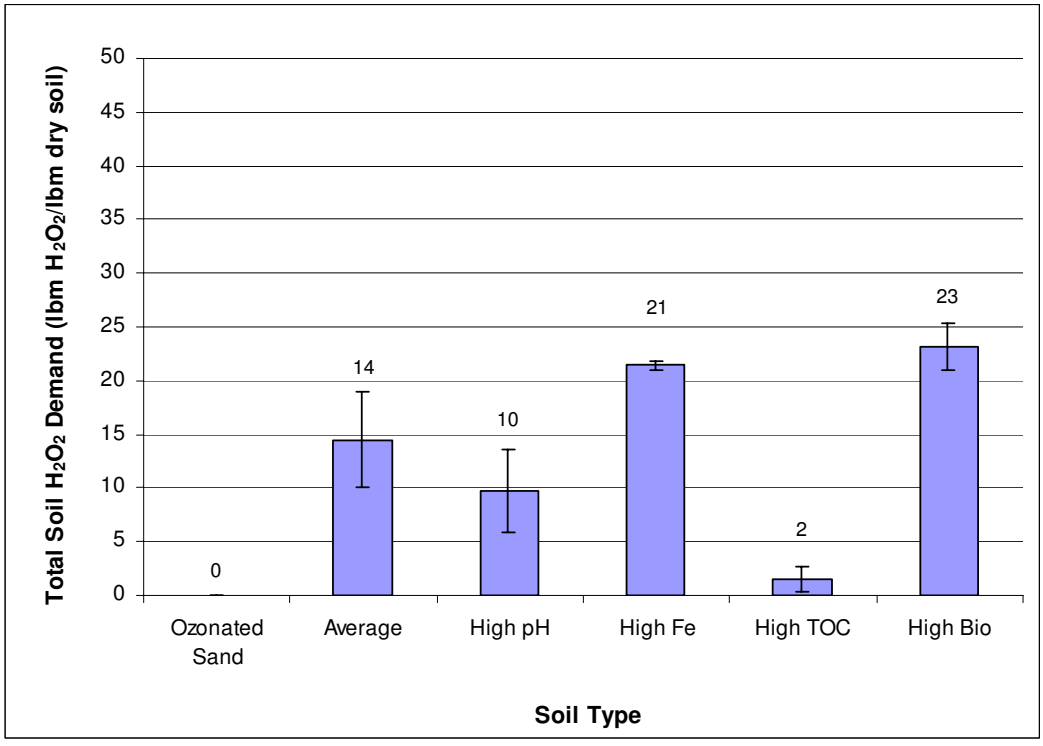

Figure 5.13: Total H_2O_2 Demands for Soil

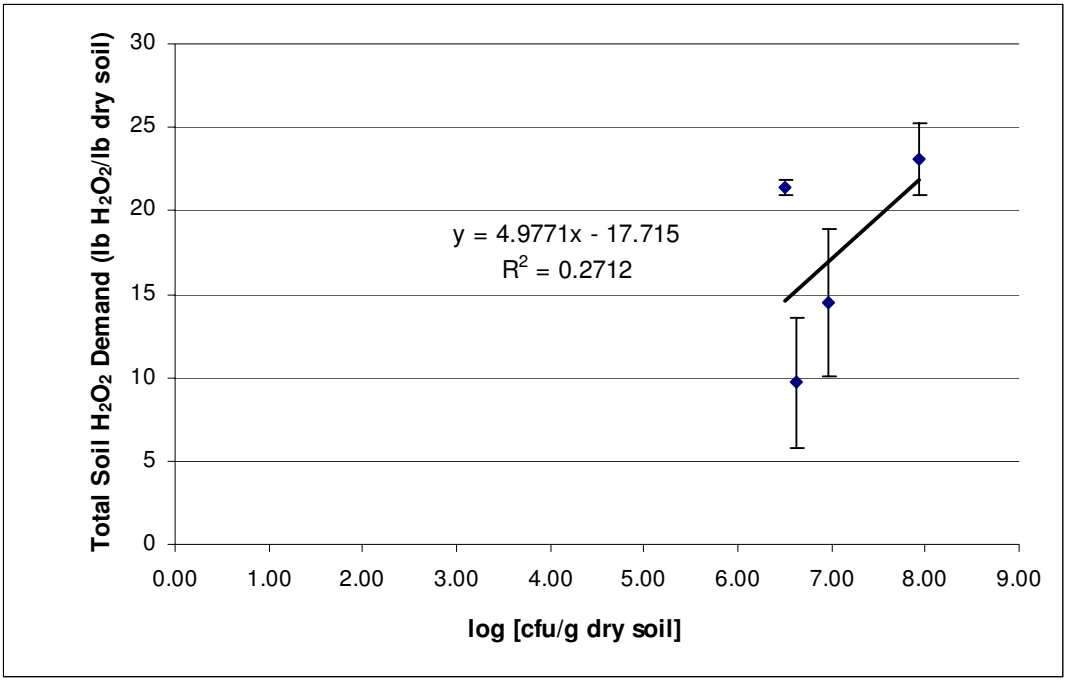

Figure 5.14: Total Soil H_2O_2 Demand vs. Soil Bacterial Populations

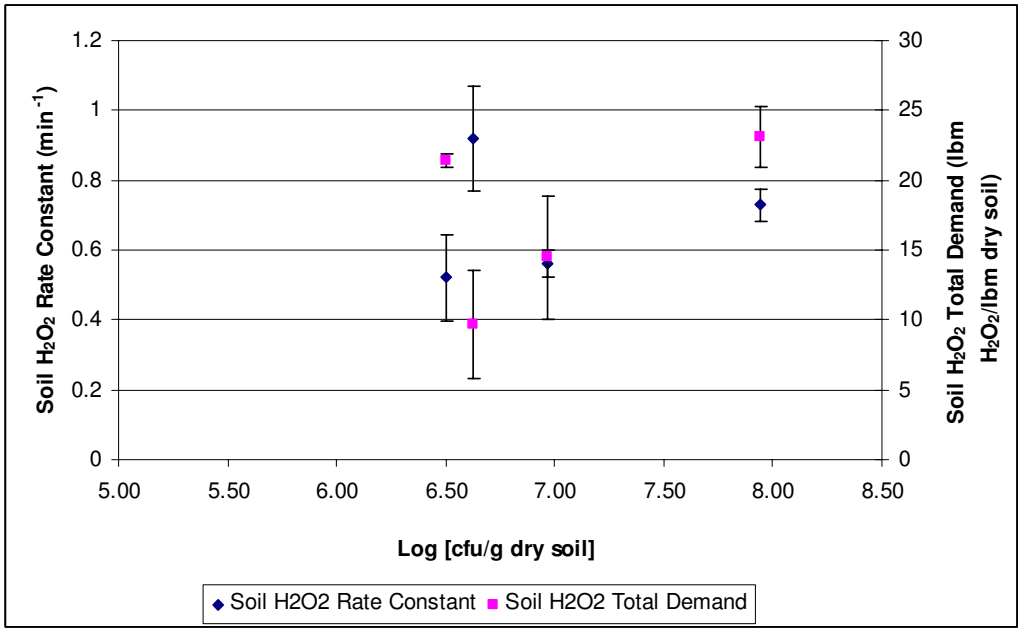

Figure 5.15: H_2O_2 Fate vs. Soil Bacterial Populations

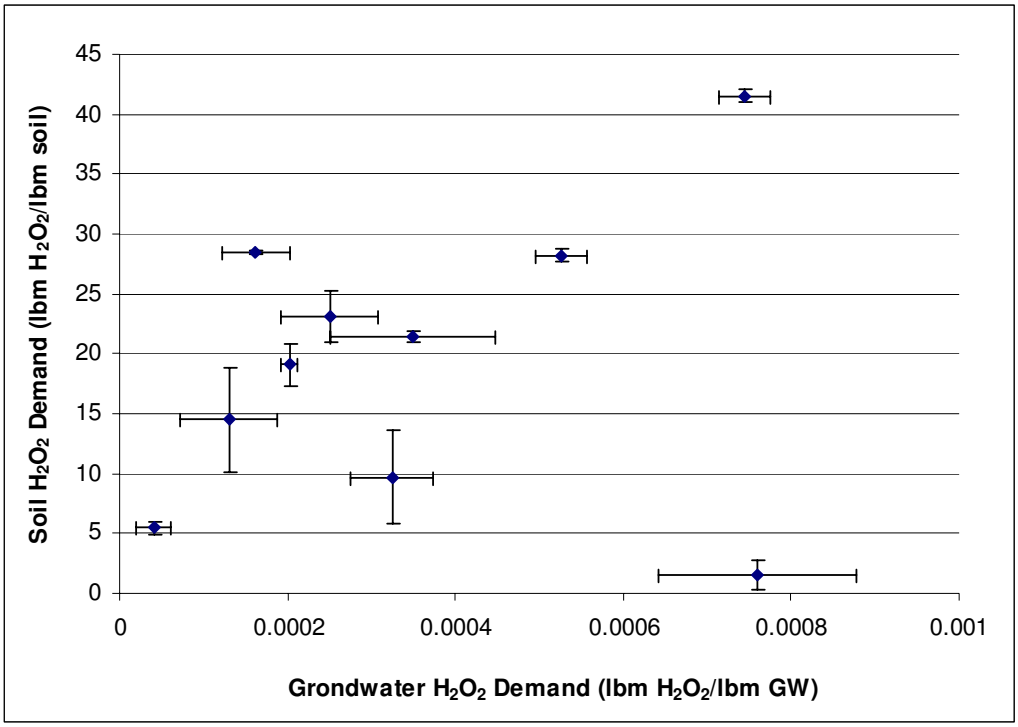

Figure 5.16: Total H_2O_2 Demand Soil/Equilibrated Water Correlation (All Soils)

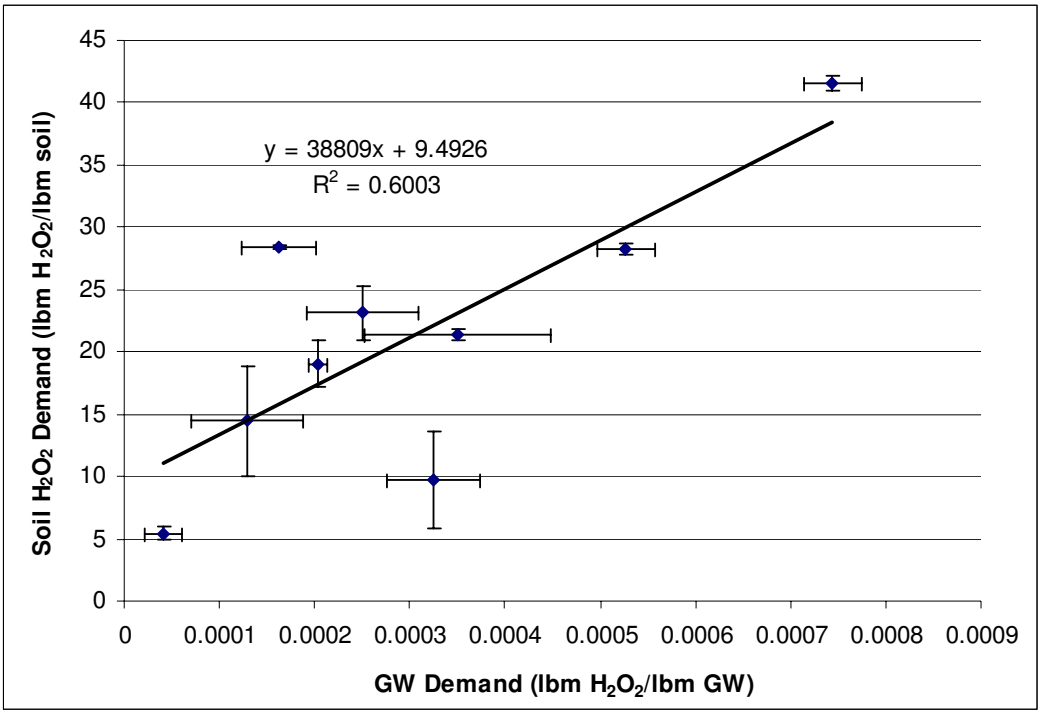

Figure 5.17: Total H_2O_2 Demand Soil/Equilibrated Water Correlation (All Soils Except High TOC)

CHAPTER VI

IMPACT OF SOIL CONSTITUENTS ON OZONE

Background

One of the primary keys in the success of *in situ* chemical oxidation (ISCO) projects is the ability of the practitioner to effectively introduce oxidizers at appropriate concentrations and rates into the targeted treatment zones (Amarante, 2000; 074, Chen et al., 2001). Several factors known to control the introduction of oxidizers into the soil matrix include biomass populations, organic matter, iron, calcium, and pH (Spain et al., 1989; Yuteri and Gurol, 1989; Tyre et al., 1991; Bartoli et al., 1992; 136, Koch et al., 1992; Fleming, 2000; 001, Zappi et al., 2000). These factors limit ISCO applications in that their natural presence in the soil matrix results in a scavenging effect on oxidizers and radicals. Instead of all oxidation reactions occurring with targeted contaminants, some oxidizers are lost due to reaction with these scavengers (Staehelin and Hoigne, 1982; Glaze et al., 1992; Amarante, 2000).

Objective

Because multiple oxidizer scavengers are naturally occurring in soils, it was desired to evaluate the impact of common soil constituents on the stability of ozone

(O_3), a chemical oxidizer commonly used with ISCO. To accomplish this task, a wide range of soil samples was selected for use during the research project. Six soil samples, each having a targeted dominant geological characteristic, were selected based on analysis of U.S. Geological Survey databases (U.S. Geological Survey, 2002). Collected soil specimens included a filter sand control, a high iron content specimen, a high organic carbon content specimen, a high calcium (i.e. high pH) content specimen, a biologically stimulated specimen, and an "average" soil. The definitions of "high" and "average" were based on the average values of U.S. soils listed by Dragun and Chiasson (1991). It was desired to determine both O_3 kinetics and total O_3 demands for both soil and equilibrated water samples and to correlate their values to evaluate relationships with these suspected oxidizer scavengers.

Methods and Materials

Kinetics of Ozone Degradation

The reaction kinetics of ozone degradation within the equilibrated water phase was studied under semi-batch conditions due to the low solubility of ozone. Initially, the ozone generator was adjusted such that the initial gas phase ozone concentration was 3.0% (w/w) O_3. The operating conditions for the ozone generator during the ozone kinetic experiments for equilibrated water can be seen in Table 6.1. After the appropriate set point had been reached, 100-mL of equilibrated water was added to a 500-mL Erlenmeyer flask, and ozone was continuously applied to the system. The process flow diagram for the application of ozone to the equilibrated water phase is

shown in Figure 6.2. The ozone concentration of the exit gas was recorded at ten minute intervals by reading the output of the ozone monitor. Additionally, a small sample of liquid was extracted every ten minutes and analyzed to determine the liquid phase concentration of ozone within the sample. Ozone degradation was allowed to reach a steady-state condition in which the concentration of O_3 in the exit gas remained constant (+/- 0.1 %). Experiments were performed in triplicate.

The reaction kinetics of ozone degradation within the soil phase was also studied under semi-batch conditions. Initially, the ozone generator was adjusted such that the initial gas phase ozone concentration was 3.0% (w/w) O_3. The operating conditions for the ozone generator during the ozone kinetic experiments for soil are shown in Table 6.1. After the appropriate set point had been reached, a 1,000-mL Erlenmeyer flask, containing a 30% (w/w) soil slurry (120 g soil & 280 g DI-H_2O) that had been equilibrated for 24-hours, was added to the system as shown in the process flow diagram for soil slurries (Figure 6.2). The ozone concentration of the exit gas was recorded at ten minute intervals by reading the output of the ozone monitor. Ozone degradation was allowed to reach a steady-state condition in which the concentration of O_3 in the exit gas remained constant (+/- 0.1 %). Experiments were performed in triplicate.

Total Ozone Demand

The total demand of ozone degradation within the equilibrated water phase was determined using semi-batch conditions due to the low solubility of ozone. Initially, the ozone generator was adjusted such that the initial gas phase ozone

concentration was 3.0% (w/w) O_3. The operating conditions for the ozone generator during the ozone demand experiments for equilibrated water can be seen in Table 6.1. After the appropriate set point had been reached, 100-mL of equilibrated water was added to a 500-mL Erlenmeyer flask, and ozone was continuously applied to the system. The process flow diagram for the application of ozone to the equilibrated water phase is shown in Figure 6.1. The ozone concentration of the exit gas was recorded at ten minute intervals by reading the output of the ozone monitor. Additionally, a small sample of liquid was extracted every ten minutes and analyzed to determine the liquid phase concentration of ozone within the sample. Distilled water was utilized as the test control, and the ozone degradation due to these test runs was assumed to be solely due to the autodegradative nature of ozone. Ozonation runs for soil slurries were allowed to continue until the concentration of ozone in the exit gas reached the conditions equivalent to that of the test control. Experiments were performed in duplicate.

The total demand of ozone degradation within the soil phase was also determined under semi-batch conditions. Initially, the ozone generator was adjusted such that the initial gas phase ozone concentration was 3.0% (w/w) O_3. The operating conditions for the ozone generator during the ozone kinetic experiments for soil are shown in Table 6.1. After the appropriate set point had been reached, a 1,000-mL Erlenmeyer flask, containing a 30% (w/w) soil slurry (120 g soil & 280 g DI-H_2O) that had been equilibrated for 24-hours, was added to the system as shown in the process flow diagram for soil slurries (Figure 6.2). The ozone concentration of the

exit gas was recorded at ten minute intervals by reading the output of the ozone monitor. Additionally, a small sample of liquid was extracted every ten minutes and analyzed to determine the liquid phase concentration of ozone within the sample. The ozonated playground sand was utilized as the test control, and the ozone degradation due to these test runs was assumed to be solely due to the autodegradative nature of ozone. Ozonation runs for soil slurries were allowed to continue until the concentration of ozone in the exit gas reached the conditions equivalent to that of the test control. Experiments were performed in duplicate.

Results and Discussion

Ozone Reaction Kinetics

Equilibrated Water Phase

Steady-state ozone profiles for both liquid and gas phase ozone concentrations were obtained for each experimental run. A sample profile for one ozone equilibrated water test run is shown in Figure 6.3 as an example of the data which were typically observed. Both the gas phase and liquid phase concentrations usually reached steady state values ($\Delta[O_3] < 0.1\%$ for any given 5 minute interval) approximately 20 minutes into each test run.

Rather than utilizing standard batch-phase kinetics, mass balances were performed on equilibrated water samples to generate ozone utilization rates (OZUR's) for each sample. Zappi (1995) used this same approach when he defined the OZUR

as a differential mass flux input expression for ozone degradation. Experiments were performed using a basis of 100 mL of equilibrated water. OZUR's were calculated using standard mass balances, defined in the following series of equations (Equations 1-5) as reported by Zappi (1995):

$$\dot{M}_{OzoneGas,in} = [O_3]_{gas,in} * \dot{V} * Z \quad (1)$$

$$\dot{M}_{OzoneGas,out} = [O_3]_{gas,SS} * \dot{V} * Z \quad (2)$$

$$\dot{M}_{OzoneLiquid,SS} = [O_3]_{liquid,SS} * \dot{V} \quad (3)$$

$$\dot{M}_{OzoneLost} = \dot{M}_{OzoneGas,in} - \dot{M}_{OzoneGas,out} - \dot{M}_{OzoneLiquid,SS} \quad (4)$$

$$OZUR_{EW} = \frac{\dot{M}_{OzoneLost}}{V_{EW}} \quad (5)$$

where,

$\dot{M}_{OzoneGas,in}$ = O_3 mass flow rate into reactor, mg O_3/min

$[O_3]_{gas,in}$ = Input gas phase O_3 conc. = 3 wt. % O_3 (constant)

$\dot{V}$ = Volumetric flow rate of total gas = 0.94 L/min (2 scfh, constant)

Z = O_3 conc. conversion factor = 12.15 (mg O_3/L)/(% wt. O_3), constant

$\dot{M}_{OzoneGas,out}$ = Outlet gas flowrate of O_3 at steady state, mg O_3/min

$[O_3]_{gas,SS}$ = Steady state conc. of O_3 in outlet, wt. % O_3

$\dot{M}_{OzoneLiquid,SS}$ = O_3 mass flow rate into the liquid phase, mg/min

$[O_3]_{liquid,SS}$ = steady state conc. of O_3 in equilibrated water, mg O_3/L

$\dot{M}_{OzoneLost}$ = Mass flow rate of O_3 lost, mg O_3/min

V_{EW} = Volume of equilibrated water sample = 100 mL

$OZUR_{EW}$ = Ozone utilization rate for equilibrated water, mg O_3/(L*min)

This system of equations represents the mass balance procedure utilized to calculate the OZUR's for equilibrated water samples. Rather than just choosing one arbitrary data point to act as the steady state concentrations of ozone off-gas and liquid phase ozone, the $[O_3]_{gas,SS}$ and $[O_3]_{liquid,SS}$ terms were determined by averaging ozone concentration output data recordings taken between 40 and 60 minutes after reaction initiation.

Results for all the ozone utilization rates for equilibrated water samples are shown in Figure 6.4. The OZUR for the Ozonated Sand water test control was determined to be 8 mg O_3/(min*L of EW). This degradation was primarily due to the autodegradative nature of ozone as previously mentioned. Because ozone is unstable in air at concentrations produced by the ozone generator, ozone degradation will occur even without the presence a reactive liquid species (Ku et al., 1996). Ozone utilization rates for other equilibrated water samples had increased ozone utilization rates due to reactive species within samples. Of the equilibrated water samples tested, the High pH equilibrated water displayed the greatest reactivity with ozone with an OZUR value of 89 mg O_3/(min*L of equilibrated water), significantly greater than any other equilibrated water type. Results from all other equilibrated water types, excluding the experimental control, displayed OZUR differences that were statistically insignificant according to 95% confidence intervals. Due to this result, it

is hypothesized that the increased pH of the equilibrated water sample (~8.2) was playing the most significant role in the increased ozone degradation. Elovitz et al. (2000) observed the effects of pH on ozone degradation in their studies on hydroxyl radical/ozone ratios during oxidation via O_3. They observed an increased reaction of ozone with dissolved organic matter at higher pH values (~9) when compared to lower pH values (~6). This result was attributed to the hydroxide-initiated O_3 decomposition reactions discussed by Staehelin and Hoigne (1982) in their findings on the topic. They observed the degradation of O_3 via the following proposed mechanism:

$$O_3 + OH^- \rightarrow HO_2^- + O_2$$

The increased level of hydroxide ions shifted the kinetics of reaction in favor of the products.

Soil Phase

Steady-state ozone profiles for off-gas ozone concentrations were obtained for each experimental run. A sample profile for one ozone soil test run is shown in Figure 6.5. The gas phase ozone concentration usually reached reacting steady state values approximately 20 minutes into each test run and remained at this level until depletion of soil reactivity began to occur.

Liquid phase concentrations were unable to be recorded for the soil phase due to the dark color of the slurry hindering the colorimetric test technique. Therefore, it was assumed that any ozone within the liquid phase immediately reacted with the soil slurry, and that the liquid phase concentration of ozone was approximately zero. This

is a good assumption based on the low OZUR levels reported with the equilibrated water samples. As was performed in the equilibrated water ozonation experiments, ozone reaction kinetics were analyzed based on calculated ozone utilization rates (OZUR's). OZUR's were calculated using a mass balance approach using Equations 1, 2, 6, and 7:

$$\dot{M}_{OzoneLost} = \dot{M}_{OzoneGas,in} - \dot{M}_{OzoneGas,out} \quad (6)$$

$$OZUR_{Soil} = \frac{\dot{M}_{OzoneLost}}{M_{Soil}} \quad (7)$$

where,

M_{Soil} = Mass of dry soil = 0.120 kg

$OZUR_{Soil}$ = Ozone utilization rate for soil, kg O_3/(min*kg dry soil)

These equations represent the mass balance procedure utilized to calculate the OZUR's for 30% (w/w) soil slurry samples. Rather than just choosing one arbitrary data point to act as the steady state concentrations of ozone off-gas, the $[O_3]_{gas,SS}$ term was determined by averaging ozone off-gas concentration output data recorded between 40 and 60 minutes after reaction initiation.

The calculated ozone utilization rates for the 30% (w/w) soil slurries are shown in Figure 6.6. As was observed in the equilibrated water phase, ozone degradation was observed within the Ozonated Sand test control due to the autodegradation of ozone; the value was calculated to be 14 kg O_3/(min*kg dry soil). The High pH Soil displayed an OZUR of 142 kg O_3/(min*kg dry soil), a value that

was significantly higher than those observed for all other soil types; the High Fe Soil displayed an OZUR of 32 kg O_3/(min*kg dry soil), a value that was significantly lower than those observed for all other non-control soils. Figure 6.7 shows the correlation between the soil TOC and Fe contents and the associated soil OZUR. These results indicate reaction at all levels between ozone and these particular suspected scavengers. Figure 6.8 shows the correlation between soil bacterial populations and soil OZUR's, suggesting that bacterial populations had a no significant effect on ozone degradation in comparison to other constituents. These results are consistent with the previously discussed literature indicating that each of these constituents plays some role in the enhancement of ozone degradation.

Figures 6.9 and 6.10 displayed correlations suggesting that both the pH and calcium content appeared to have the most significant effect on observed ozone utilization rates for soil samples. The rationale for pH effects on ozone degradation deals with the scavenging nature of hydroxide ions and was previously discussed for the kinetics of ozone degradation in equilibrated water (Staehelin and Hoigne, 1982). Figure 6.10 indicated a consistent trend suggesting that an increased soil calcium content resulted in an increased ozone utilization rate for soils. Figure 6.11 is a second plot of the soil calcium content versus the soil ozone utilization rate; it eliminates the High pH Soil data point that is an outlier due to its extraordinarily high levels of calcium. The high dependence of ozone degradation based on calcium can be based on two ideas. Firstly, calcium ions have themselves been shown to act as an ozone scavenger during limited experiments on soils. Chandrakanth and Amy (1996)

observed that during ozonation of oxalic acid, significantly greater ozone destabilization was observed in the presence of calcium. Secondly, in addition to calcium ions, it is highly probable that much of the calcium content in the High pH Soil was actually in the form of calcium carbonate ($CaCO_3$). Calcium carbonate, often used as lime in efforts to raise soil pH levels, is a common constituent among highly basic soils (Conyers et al., 2000). The carbonate ions offer another means for ozone to react. Acero and von Gunten (2000) reported on the influence of carbonate on oxidation processes involving ozone. They found that both carbonate and bicarbonate acted as important promoters for the decomposition of ozone in oxidation reactions.

For ISCO applications on sites with either high calcium/carbonate levels or high pH values, practitioners can expect accelerated rates of ozone decomposition due to naturally occurring ozone scavengers located within the soil matrix. Successful treatment via ozone-based technologies will probably require either an initial site pH adjustment or an application of ozone at a faster rate than would normally be considered.

Ozone Total Demands

Equilibrated Water Phase

Equilibrated water total demand experiments were run using 100 mL of equilibrated water from each specimen as the basis. For example, the data necessary to estimate the total ozone demand for equilibrated water samples was obtained from

the same equilibrated water data used to calculate the ozone utilization rates for equilibrated water. The data from one of the High pH equilibrated water experimental runs (Figure 6.3) indicates that this particular sample reached its total ozone demand at approximately 300 minutes. Total ozone demands and accompanying total net ozone demands, which factored out O_3 losses due to autodegradation, were then estimated by using Equations 8-10 as shown below:

$$O_3\ Demand_{EW} = OZUR_{EW} * t \quad (8)$$

$$O_3\ Losses = OZUR_{Sand\ EW} * t \quad (9)$$

$$O_3\ Net\ Demand_{EW} = O_3\ Demand_{EW} - O_3\ Losses \quad (10)$$

where,

$O_3\ Demand_{EW}$ = Total ozone demand of the equilibrated water, mg O_3/L

$OZUR_{EW}$ = Ozone utilization rate for equilibrated water, mg O_3/(L*min)

t = time required to reach control conditions, minutes

O_3 Losses = Total ozone losses due to autodegradation, mg O_3/L of EW

$OZUR_{Sand\ EW}$ = O_3 utilization rate for sand equilibrated water, mg O_3/(L*min)

$O_3\ Net\ Demand_{EW}$ = Total net O_3 demand for equilibrated water, mg O_3/L

As mentioned previously, the value of t was determined from analysis of the equilibrated water off-gas O_3 concentration profiles. The value was chosen based on the time required for the experimental conditions to reach the baseline data calculated from the Ozonated Sand/DI-water controls.

The total ozone demand data ($O_3\ Demand_{EW}$, Equation 8), without the subtraction of O_3 autodegradation losses, are shown in Figure 6.12. As was the case

with the ozone utilization rates for equilibrated water, the High pH equilibrated water exhibited the greatest total ozone demand ($2.6*10^4$ mg O_3/L of EW). The Average, Biologically Stimulated, and High Iron equilibrated water samples all exhibited total ozone demands of approximately $1*10^4$ mg O_3/L of EW, while the High TOC equilibrated water exhibited a slightly higher ozone demand of $1.6*10^4$ mg O_3/L of EW.

The total net ozone demand data (O_3 Net $Demand_{EW}$, Equation 10), inclusive of the subtraction of O_3 autodegradation losses, are shown in Figure 6.13. While a visual comparison of Figures 6.12 and 6.13 indicate that O_3 autodegradation losses were fairly insignificant in comparison to the O_3 losses due to natural soil constituents, both values were reported as a benefit to ISCO practitioners. It should be mentioned that the potential error in these data are prone to increase due to the additional error associated with the autodegradation rates experimentally determined from Ozonated Sand controls. Because two values, each with their own error, were added/subtracted, these errors become additive as well. Therefore, both values and plots have been included for the benefit of ISCO practitioners.

As was the case with the ozone utilization rates for equilibrated water, the High pH sample had significantly larger total ozone demands than all other equilibrated water types due to the scavenging nature of hydroxide ions (Staehelin and Hoigne, 1982). A groundwater environment with a high pH value will offer challenges towards ISCO remediation via ozone.

Soil Phase

Soil total ozone demand experiments were run using 30% (w/w) soil slurries and 120 grams of dry soil as the basis. The data necessary to estimate the total ozone demand for equilibrated water samples were obtained from the same equilibrated water data used to calculate the ozone utilization rates for soil. The data from one of the High pH Soil slurry experimental runs (Figure 6.5) indicate that this particular sample reached its total ozone demand at approximately 700 minutes. Total ozone demands and accompanying total net ozone demands, which factored out O_3 losses due to autodegradation, were then estimated by using Equations 11-13 as shown below:

$$O_3\ Demand_{Soil} = OZUR_{Soil} * t \quad (11)$$

$$O_3\ Losses = OZUR_{Sand} * t \quad (12)$$

$$O_3\ Net\ Demand_{Soil} = O_3\ Demand_{Soil} - O_3\ Losses \quad (13)$$

where,

$O_3\ Demand_{Soil}$ = Total ozone demand of the dry soil, kg O_3/kg of dry soil

$OZUR_{Soil}$ = Ozone utilization rate for dry soil, kg O_3/(min*kg dry soil)

t = time required to reach control conditions, minutes

O_3 Losses = Total ozone losses due to autodegradation, kg O_3/kg dry soil

$OZUR_{Sand}$ = Ozone utilization rate for sand control, kg O_3/(min* kg dry soil)

$O_3\ Net\ Demand_{Soil}$ = Total net O_3 demand for soil, kg O_3/kg dry soil

As mentioned previously, the value of t was determined from analysis of the soil slurry off-gas ozone concentration profiles. The value was chosen based on the time

required for the experimental conditions to reach that of the Ozonated Sand/DI-water slurry controls.

As was done with the total ozone demand of the equilibrated water, two different ozone demands were calculated, one of which included the autodegradation of O_3 (Equation 11) and another that removed O_3 degradation from the calculated demand value (Equation 13). The ozone total demand data still containing O_3 autodegradation are reported in Figure 6.14, and the ozone net total demand data, having removed O_3 losses due to autodegradation, are shown in Figure 6.15. A comparison of the two graphs indicated that ozone losses in oxidizer demand calculations due to the autodegradation of ozone were insignificant in comparison to losses due to oxidizer scavengers naturally occurring within soil samples. For calculated values of total net O_3 demand, the Ozonated Sand test control exhibited a total ozone demand of approximately $9.8*10^0$ kg O_3/kg soil. The Average Soil and Biologically Stimulated Soil exhibited similar total ozone demands of $2.5*10^4$ and $2.6*10^4$ kg O_3/kg dry soil respectively, indicating that bacterial populations were not a dominating reactant with ozone. The High Iron Soil and High TOC Soil exhibited similar total ozone demands of $6.9*10^3$ and $8.4*10^3$ kg O_3/kg dry soil respectively.

It was desired to determine the functionality of the total net ozone demand based on certain soil characteristics. Figure 6.16 compares the iron and TOC levels within soil samples to the total net ozone demand for its respective soil. Those correlations proved to be inconclusive in determining a consistent pattern. Figure 6.17 compares the initial level of microbial populations with total net ozone demand,

and as was the case for soil OZUR's, bacteria appeared to have no significant effect as compared to other soil constituents. As was observed in the ozone utilization rate data for the soil phase, Figure 6.18, which excluded the Ozonated Sand control data point, and Figure 6.19 showed strong trends indicating that soil pH and soil calcium content both played significant roles in determining to what extent ozone was consumed by natural soil constituents. The rationale behind these findings was previously discussed in the soil OZUR section. To develop a better trend for the relationship with soil calcium content, Figure 6.20 was developed from Figure 6.19 by removing the High pH Soil data point that did not fit with the linear profile of other data points. In an effort to guide ISCO practitioners in estimating expected total net ozone demands that can be expected among soil sites, predictive equations (R^2>0.90) for both dependence on soil pH (Equation 14) and soil calcium content (Equation 15) were developed from experimental data relationships:

$$\text{Soil } O_3 \text{ Demand} = 16{,}950 * \text{pH} - 72{,}636 \quad (14)$$

$$\text{Soil } O_3 \text{ Demand} = 9.933 * [\text{Ca}] + 5{,}025 \quad (15)$$

where,

Soil O_3 demand = total net O_3 demand for soil, kg O_3/kg dry soil

pH = Initial soil pH

[Ca] = Initial level of calcium in soil, mg/kg

ISCO practitioners must be aware of soil pH and soil calcium content prior to initiating an ISCO remediation project using ozone-based technologies, since these

two soil characteristics play a significant role in ozone degradation within the soil matrix.

Equilibrated Water/Soil O_3 Demand Correlation

As was done for the H_2O_2 total demands in Chapter V, it was desired to test the hypothesis that the total net ozone demand of a soil could be estimated given information regarding the total net ozone demand of the associated groundwater. For sites with pre-existing sampling wells, this would enable ISCO users to estimate a total amount of ozone required without having to perform any type of soil excavation. Figure 6.21 shows the correlation between total net ozone demands for equilibrated water and the total net ozone demands for soil samples. The data indicates a fairly consistent relationship (R^2=0.72) suggesting that an increase in total ozone demand for the equilibrated water corresponds with an increased total ozone demand for the corresponding soil. This relationship has the potential to provide ISCO users with another tool in estimating the total net ozone demand of the soil site, in addition to the predictive equations based on soil pH and soil calcium content.

Table 6.1: Operating Conditions for the Ozone Generator During Kinetics & Total Demand Experiments

Operating Condition	**Value**
Voltage Setting	78%
Primary Voltage	90 AC Volts
Flow Rate	2 SCFH
Initial O_3 Conc.	3.00 % (w/w)

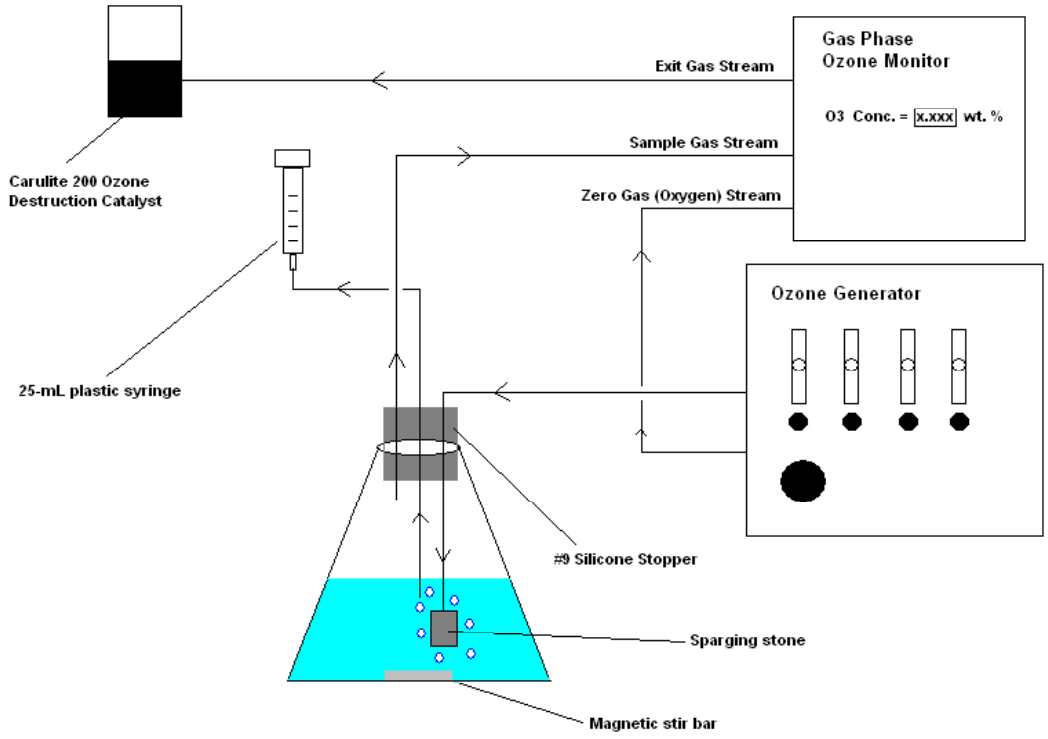

Figure 6.1: Groundwater Ozonation PFD

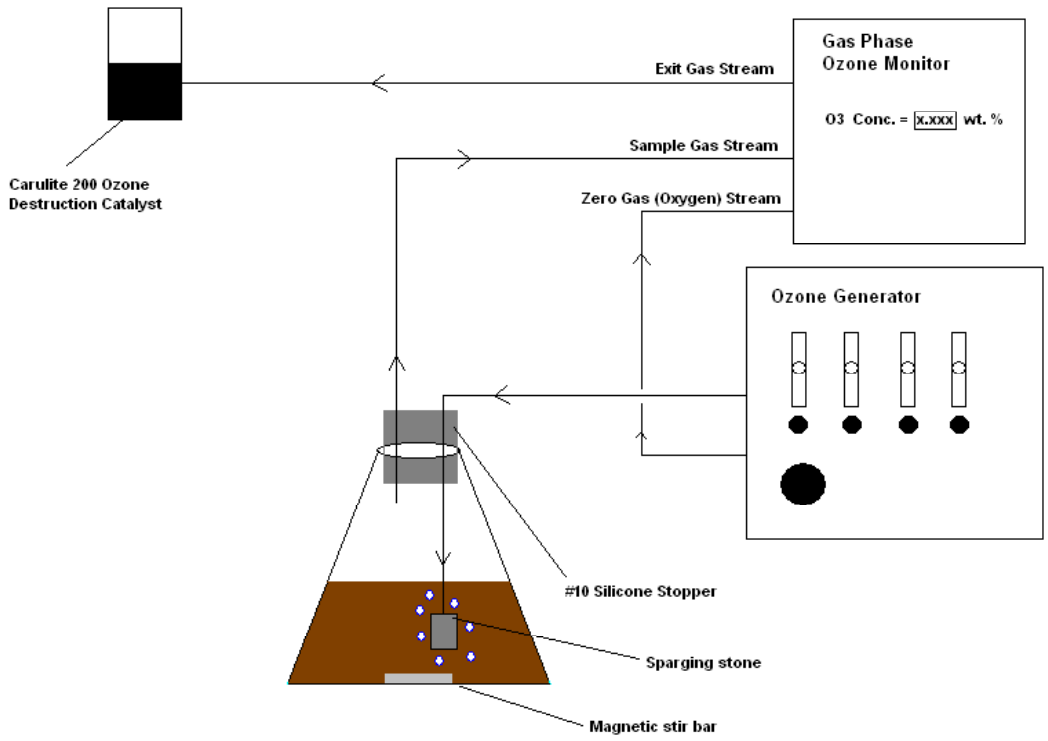

Figure 6.2: Soil Slurry Ozonation PFD

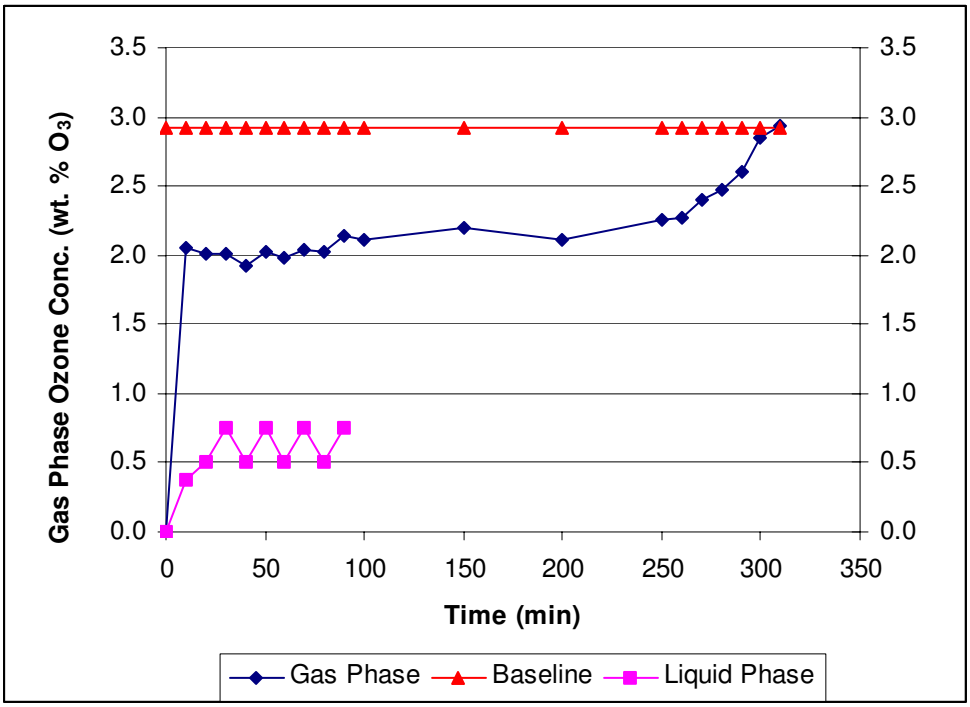

Figure 6.3: Sample Profile for Reactivity of Ozone with Equilibrated Water (High pH Equilibrated Water – Run 3)

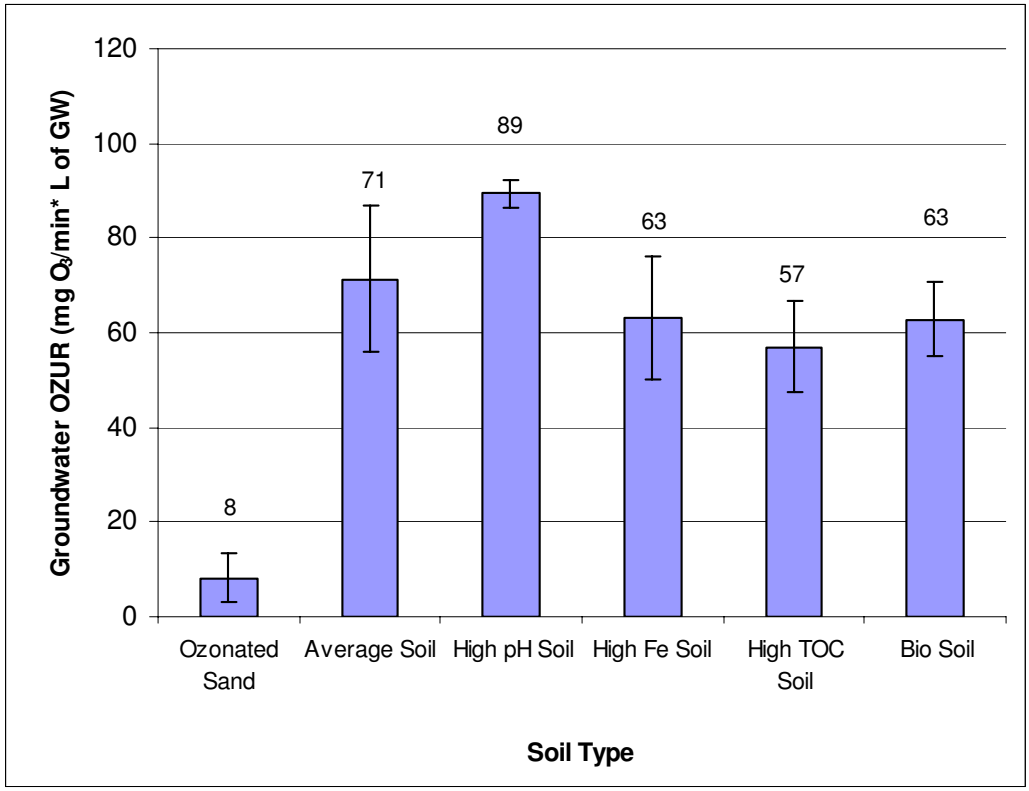

Figure 6.4: Equilibrated Water Ozone Utilization Rates

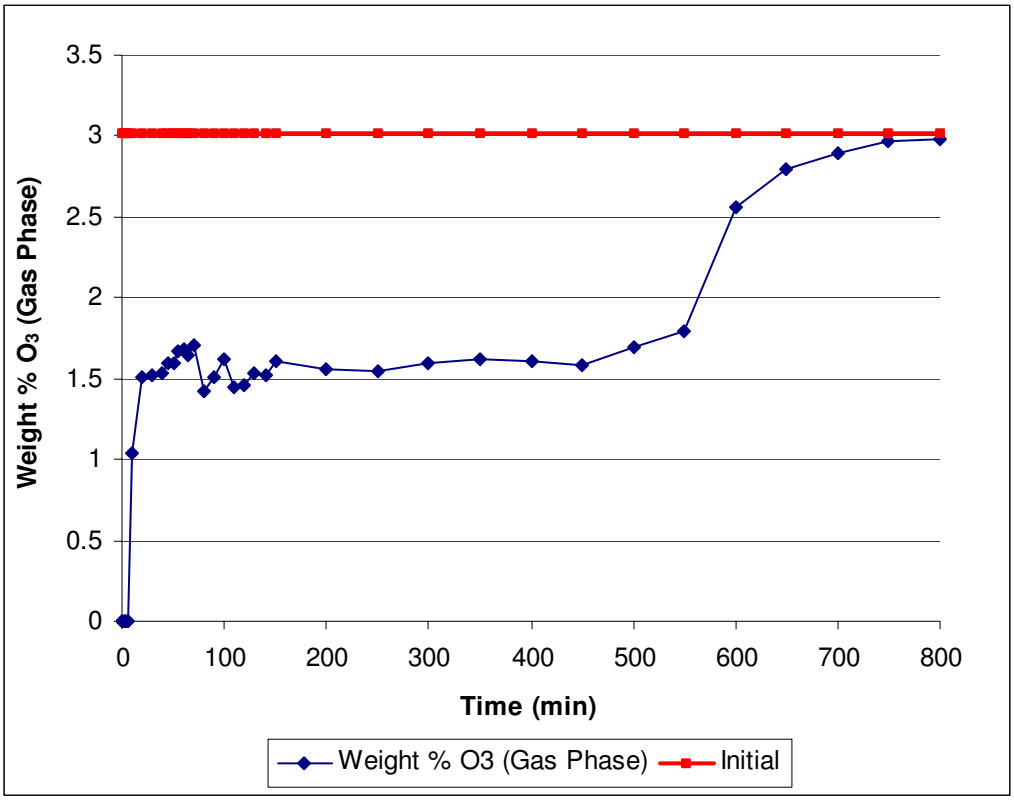

Figure 6.5: Sample Profile for Reactivity of Ozone with 30% Soil Slurries (High pH Soil – Run 1)

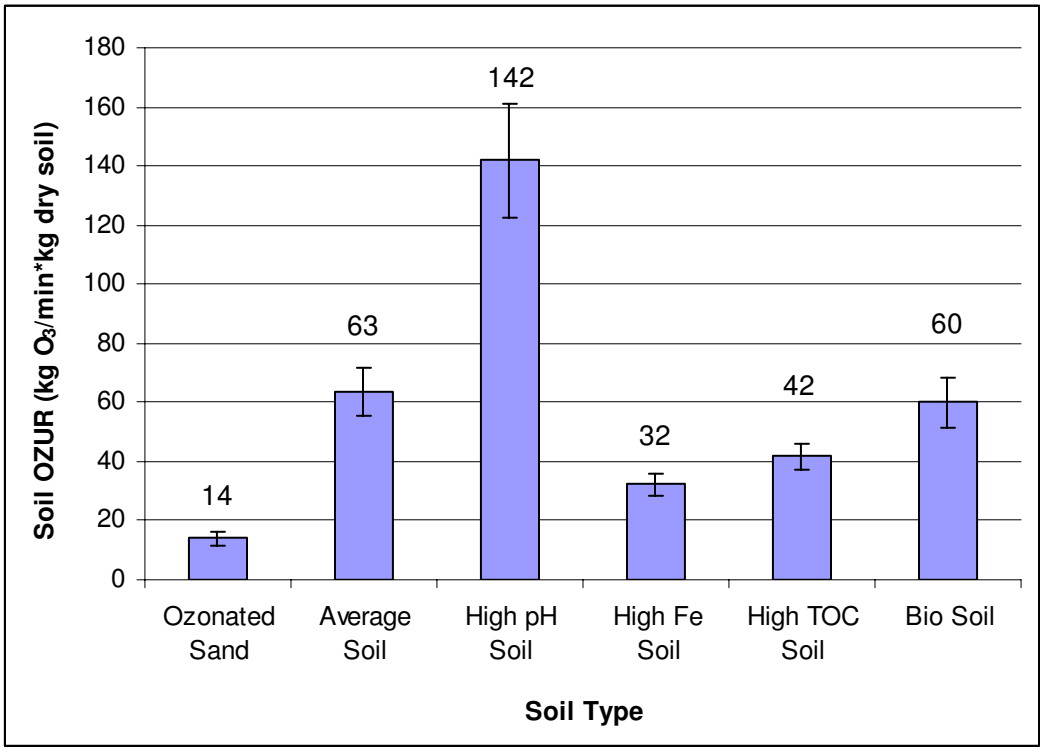

Figure 6.6: Soil Ozone Utilization Rates

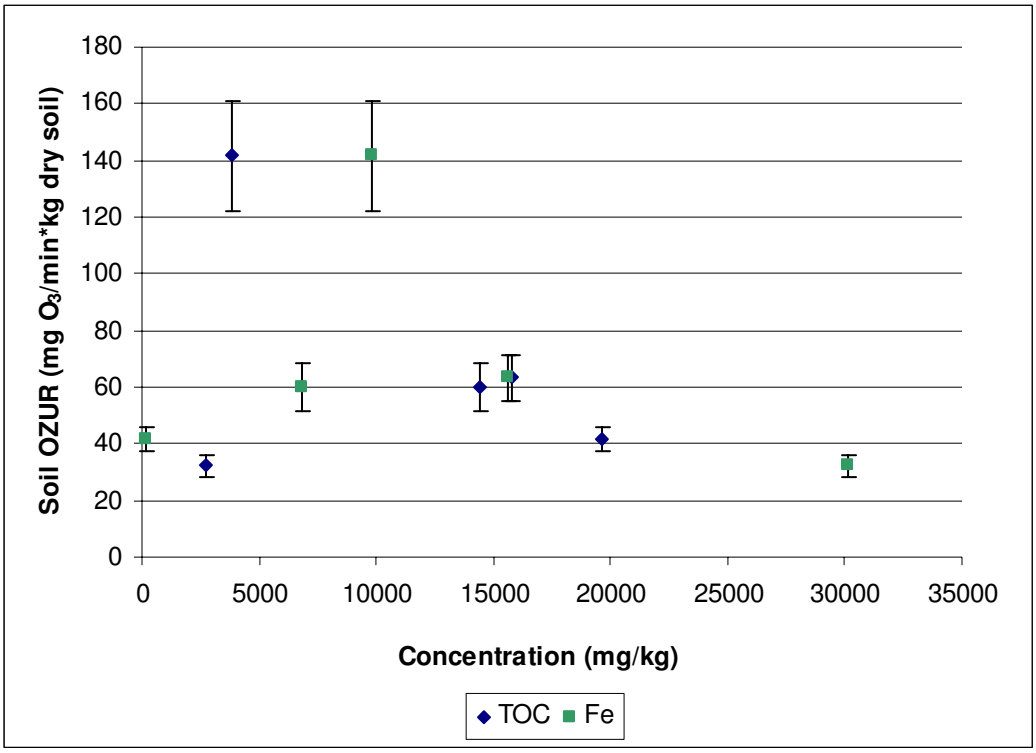

Figure 6.7: Soil Ozone Utilization Rates vs. Soil TOC and Fe Content

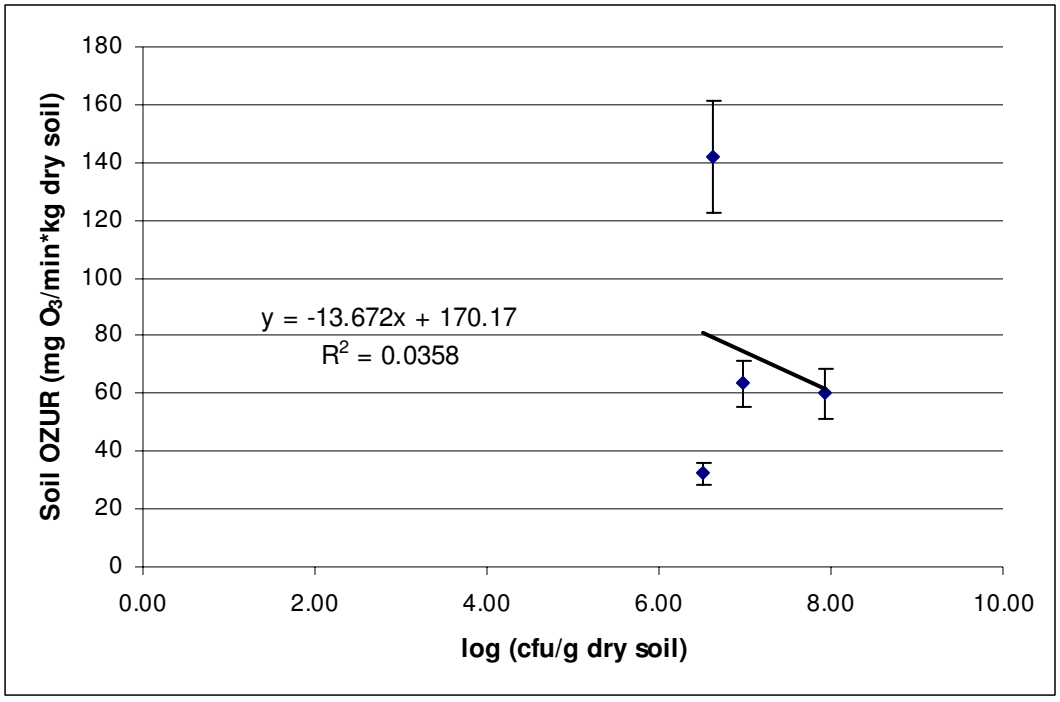

Figure 6.8: Soil Ozone Utilization Rates vs. Soil Microbial Populations

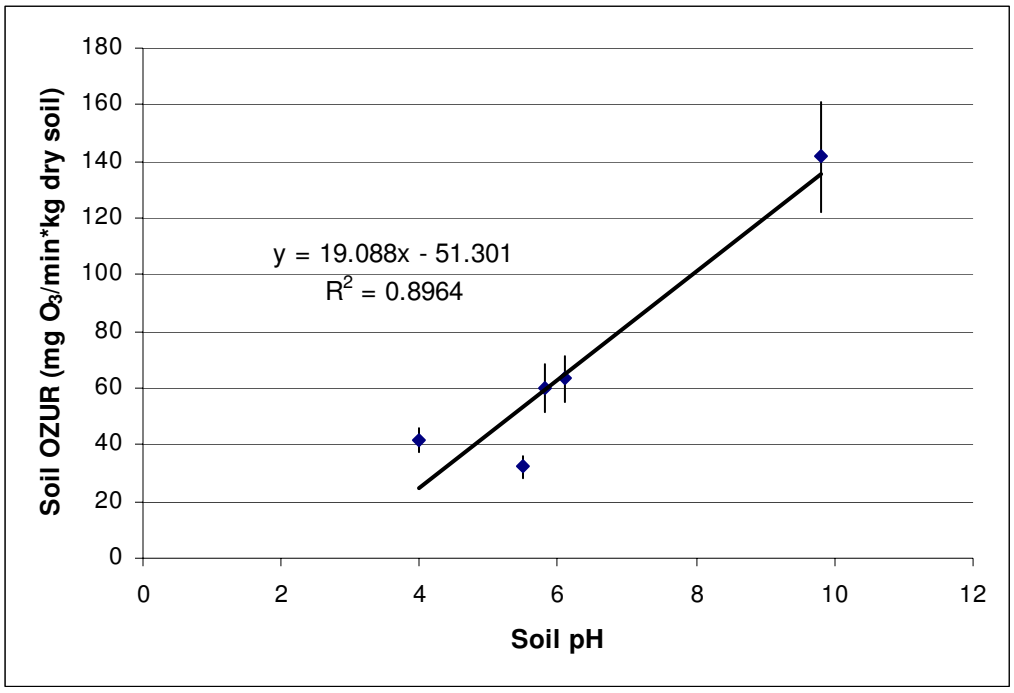

Figure 6.9: Soil Ozone Utilization Rates vs. Soil pH

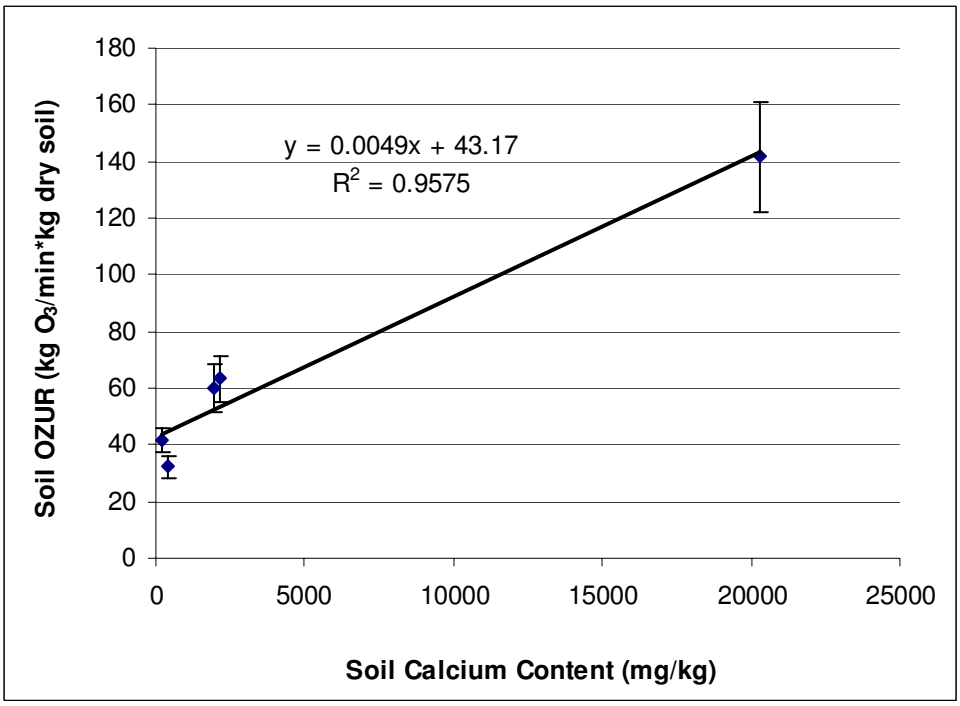

Figure 6.10: Soil Ozone Utilization Rates vs. Soil Calcium Content for All Soils

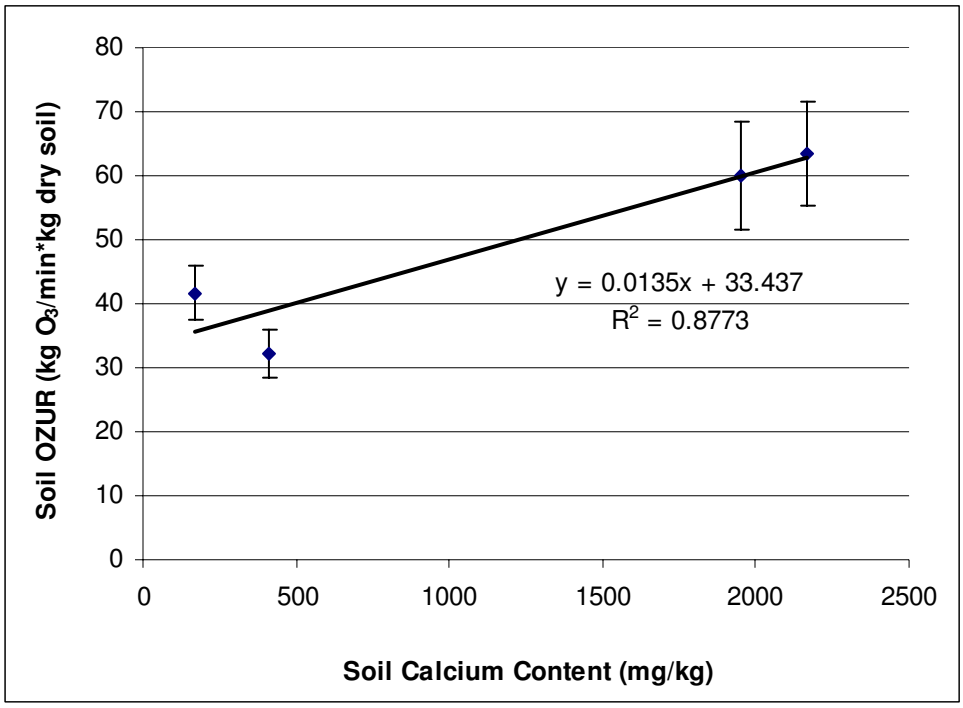

Figure 6.11: Soil Ozone Utilization Rates vs. Soil Calcium Content for All Soils Excluding the High pH Soil

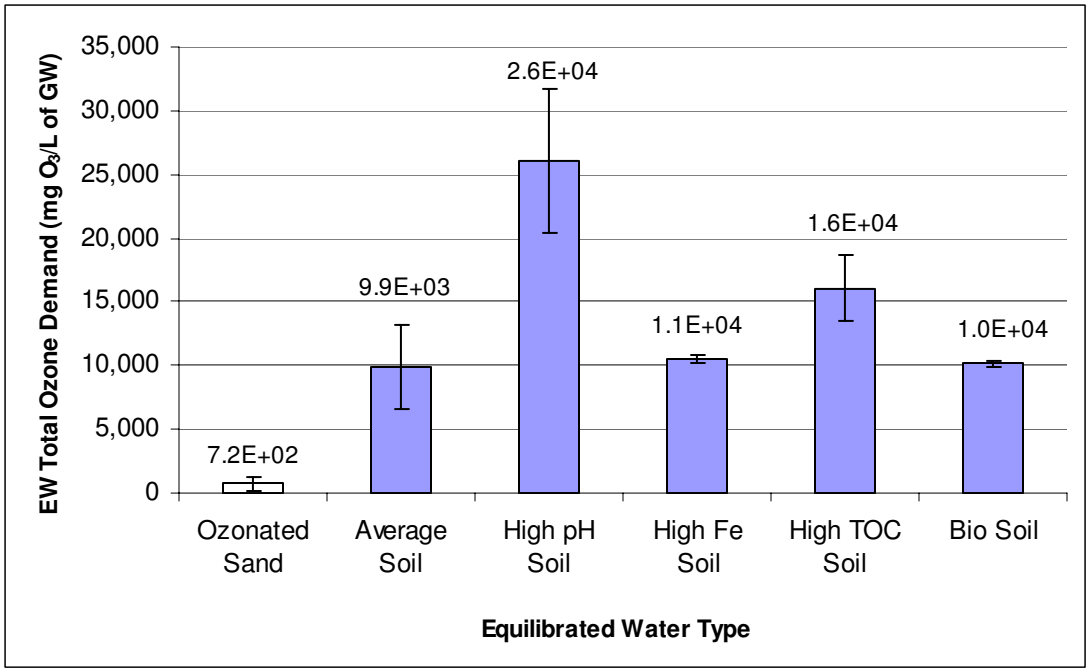

Figure 6.12: Total Ozone Demands for Equilibrated Water, Inclusive of O_3 Autodegradation Losses

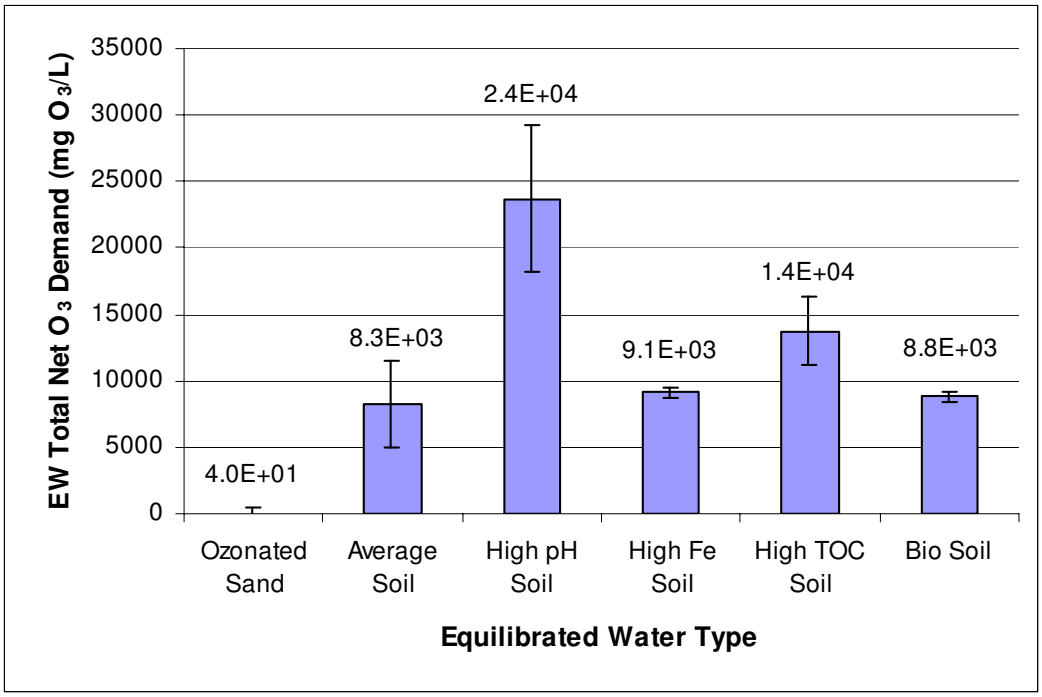

Figure 6.13: Total Ozone Demands for Equilibrated Water, Exclusive of O_3 Autodegradation Losses

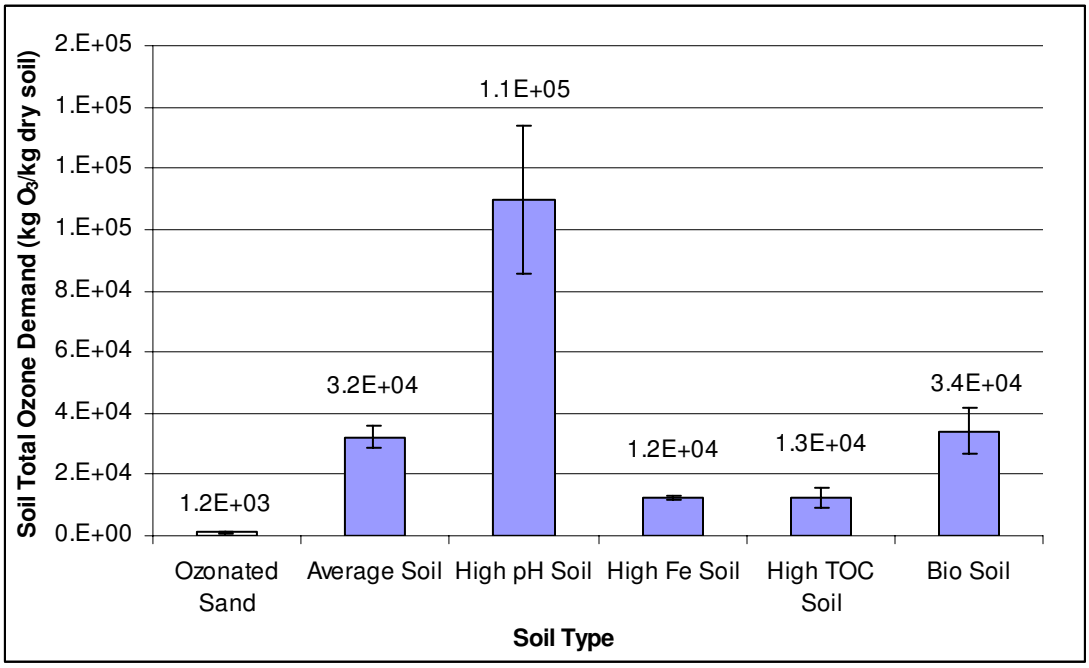

Figure 6.14: Total Ozone Demands for Soil, Inclusive of O_3 Autodegradation Losses

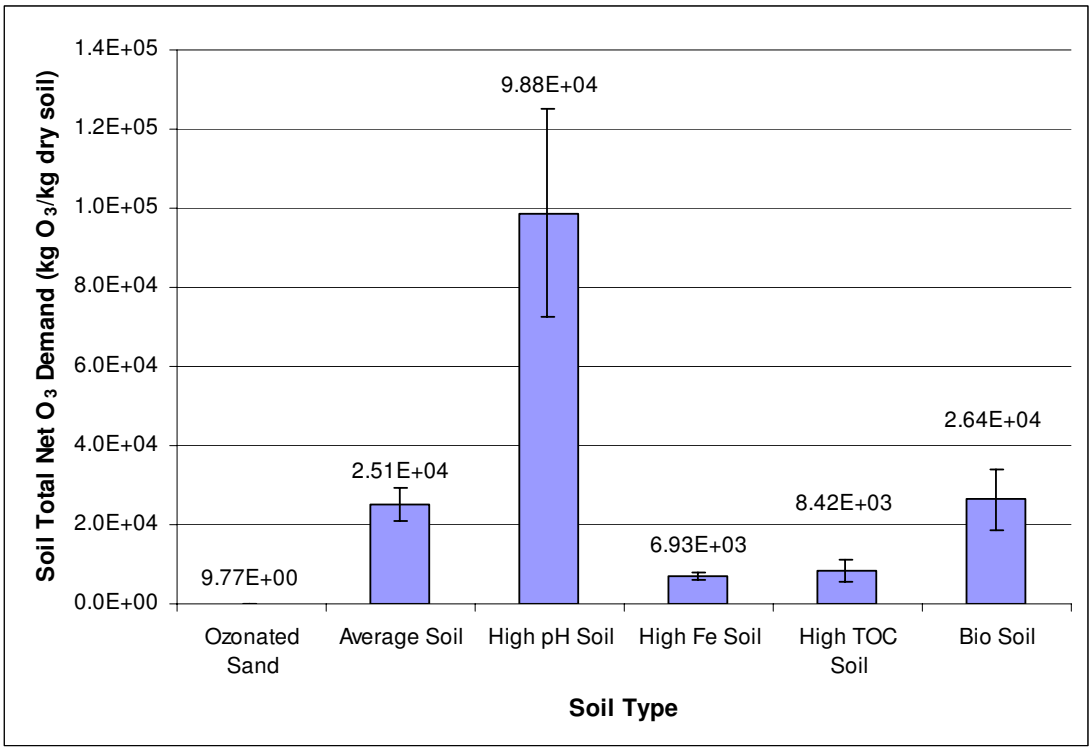

Figure 6.15: Total Ozone Demands for Soil, Exclusive of O_3 Autodegradation Losses

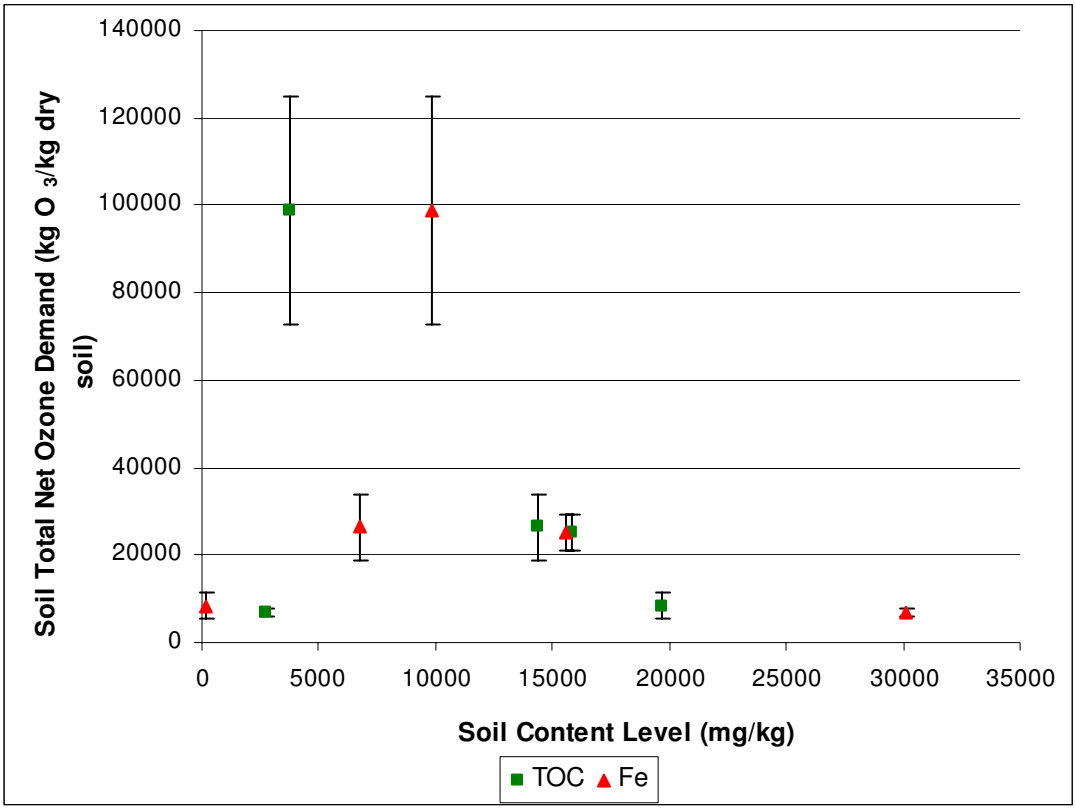

Figure 6.16: Soil Total Net Ozone Demand vs. Soil Iron and TOC Content

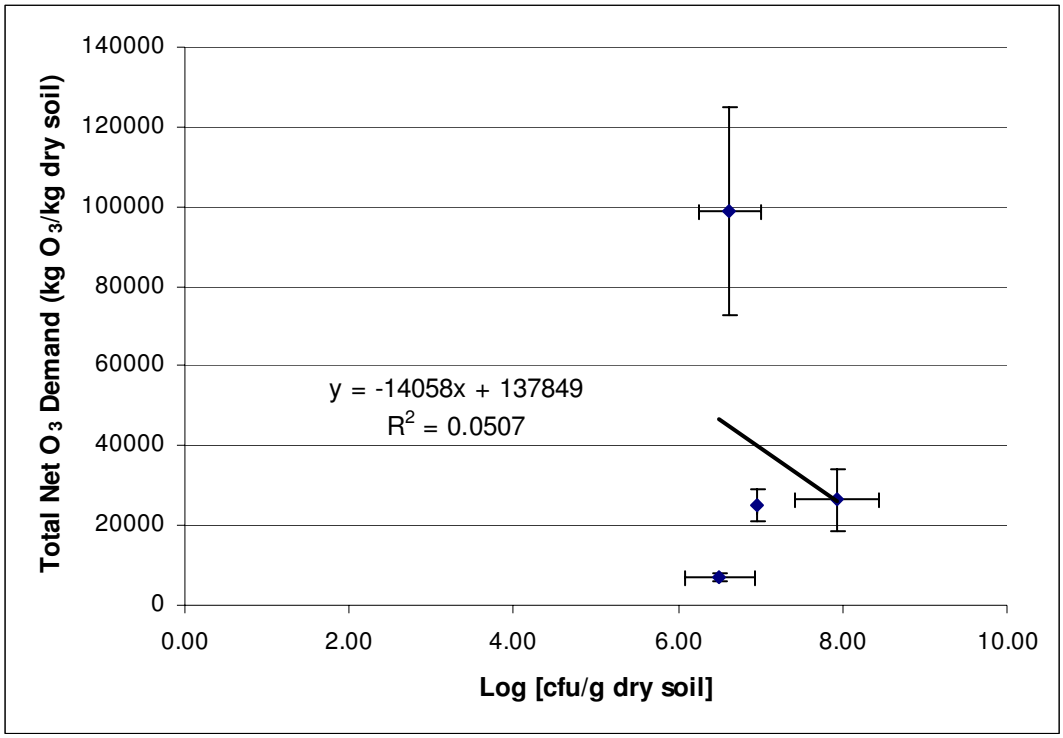

Figure 6.17: Soil Total Net Ozone Demand vs. Soil Microbial Populations

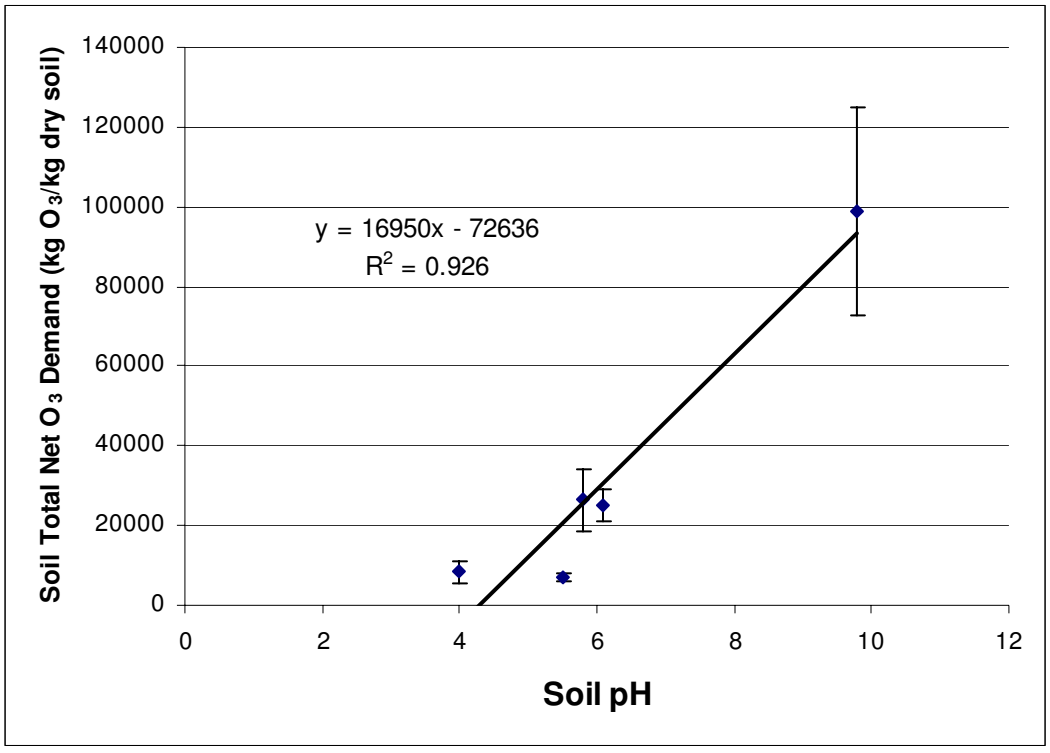

Figure 6.18: Soil Total Net Ozone Demand vs. Soil pH

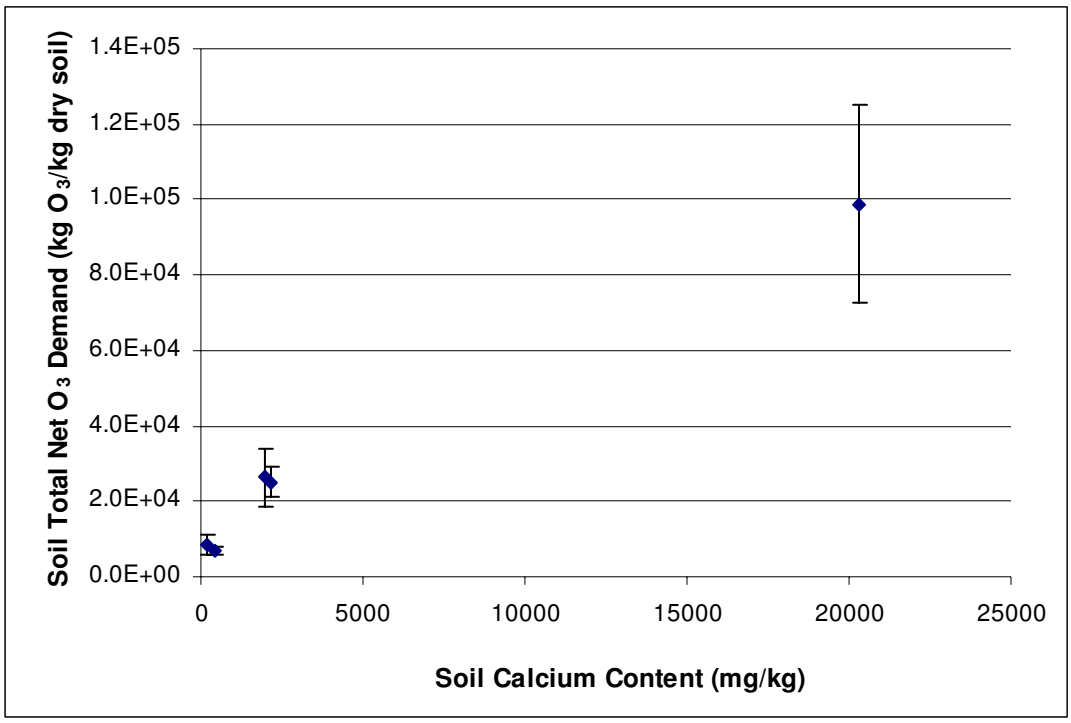

Figure 6.19: Soil Total Net Ozone Demand vs. Soil Calcium Content

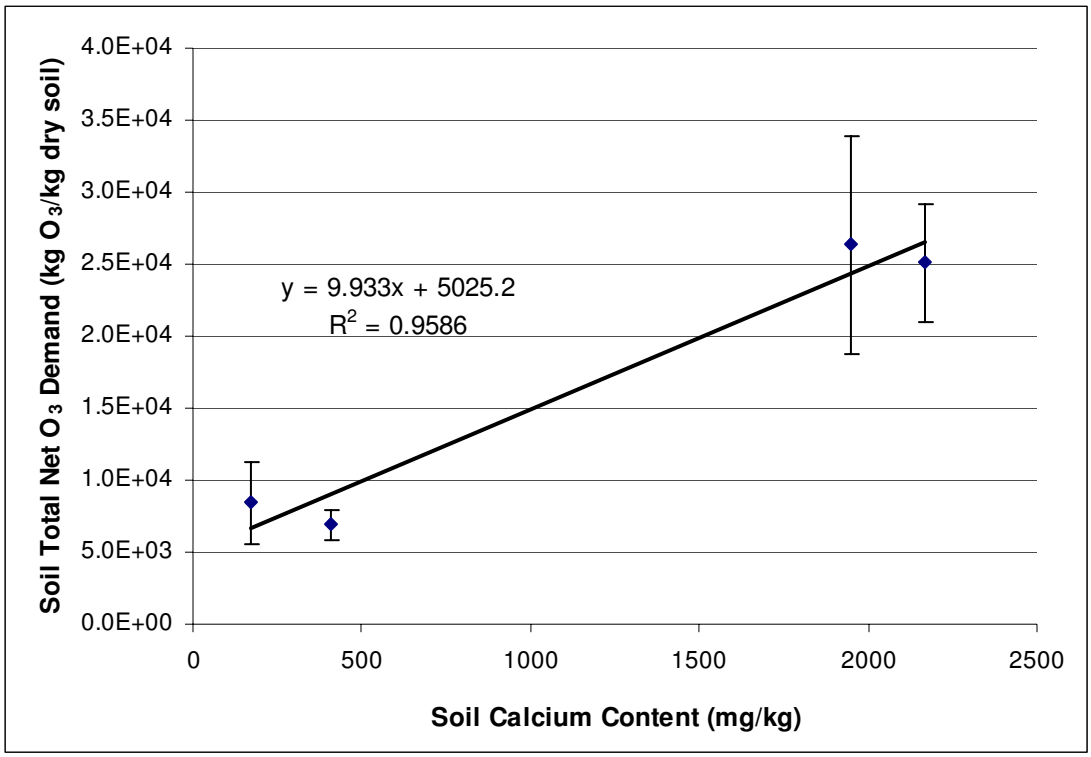

Figure 6.20: Soil Total Net Ozone Demand vs. Soil Calcium Content for All Soils Excluding the High pH Soil

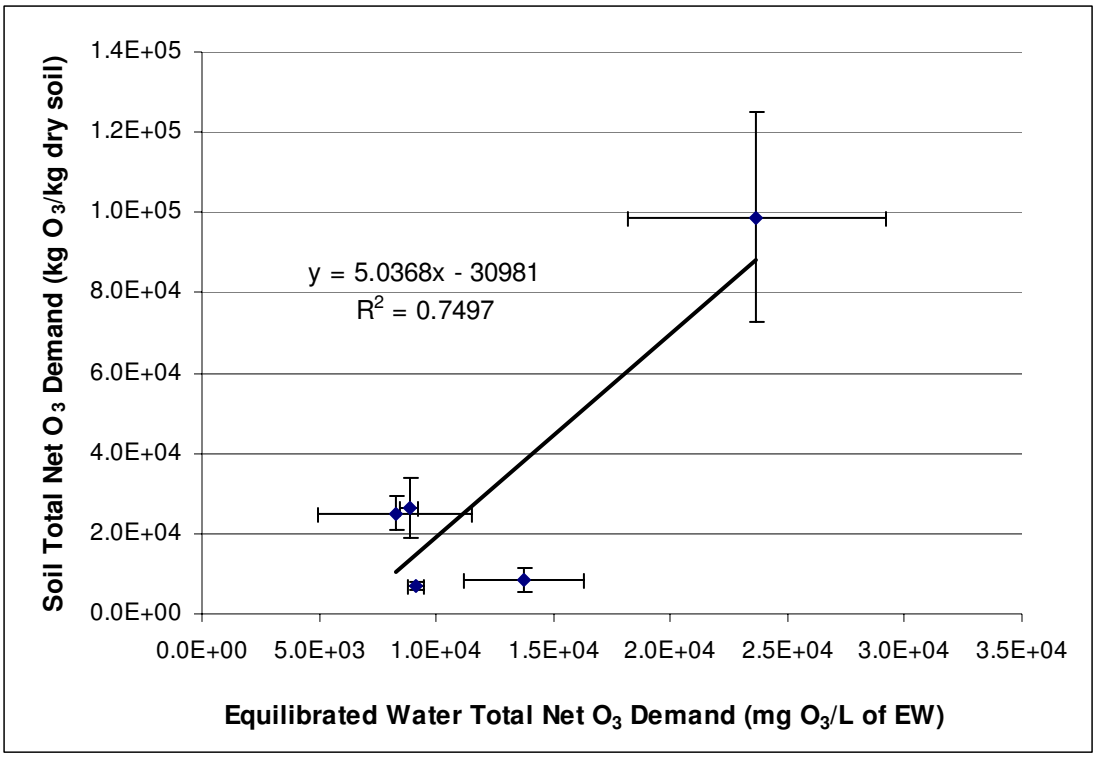

Figure 6.21: Total O_3 Demand Soil/Equilibrated Water Correlation (All Soils)

CHAPTER VII

IMPACT OF SOIL CONSTITUENTS ON ACIDS AND BASES

Background

During some ISCO processes, it is advantageous to either raise or lower the natural pH of the soil in an effort to optimize certain oxidation reactions. For Fenton's Reaction chemistry, Watts et al. (1990) reported that a pH value between 3 and 4 is optimal for the generation of free hydroxyl radicals. The Fenton's Reagent mechanism is as follows (Kakarla et al., 2002):

$$H_2O_2 + Fe^{2+} \rightarrow OH\bullet + OH^- + Fe^{3+}$$

Fenton's Reaction is enhanced at a low pH because of the increased solubility of iron at low pH values. The solubilized iron (III) can then be reconverted to iron (II) via reaction with the perhydroxyl radical. This newly reformed iron (II) allows for the continuance of hydroxyl radical production (Watts et al., 1990; ITRC, 2005). Watts et al. (1990) reported on the rate constant for the conversion of Fe^{3+} back into Fe^{2+} at reduced pH values. While the conversion is highly dependent on the pH conditions, the rate constant generally ranges from $2*10^4$ to $1*10^6$ L/mole*sec. These values indicate that significant rate enhancement in the orders of magnitude range can be obtained through pH reductions of soil environments.

While Fenton's Reagent becomes enhanced at a low pH, advanced oxidation using ozone/hydrogen peroxide (i.e. peroxone) is optimal at higher pH values. Kuo and Chen (1996) performed experiments studying the oxidation of toluene by ozone-hydrogen peroxide mixtures at variable pH values. Kuo observed that the oxidation reactions were slow in highly acidic environments, whereas those same reactions became much faster in highly alkaline solutions. Kuo proposed that in acidic solutions with a pH of 3.0, the ozonation processes were controlled by the direct oxidation of ozone molecules, thereby resulting in slower reaction rates. When solutions were buffered with sodium hydroxide to a pH of 10 or more, the formation of powerful hydroxyl radicals became dominant in determining contaminant oxidation rates. Qui et al. (2002) studied the ozonation of six dichlorophenol isomers at variable pH values, analyzing DCP conversion in both their molecular and ionic forms. They found that ozonation rates of DCP isomers increased significantly as the concentration of hydroxyl ions (i.e. pH) increased in aqueous solutions.

In order to address these ISCO optimization concerns, several candidate acid/base buffering reagents were chosen based on a review of literature. These buffering reagents could then be applied to soil environments in order to generate conditions more optimal for ISCO performance. Both the Interstate Technology & Regulatory Council In Situ Chemical Oxidation Team (2005) and the U.S. Navy (2002) commented on the successful application of phosphoric acid (H_3PO_4) for buffering soil pH to levels conducive for efficient Fenton's chemistry. Having been cited in several instances of literature, phosphoric acid was chosen as the candidate

acid reagent for the soil buffering kinetic experiments. Literature also indicated that potassium and sodium phosphates are commonly used with hydrogen peroxide-based ISCO technologies to stabilize H_2O_2 decomposition within contaminated aquifers (Kakarla and Watts, 1997). To increase soil pH, Wang and Zappi (2001) successfully used sodium hydroxide to increase the pH of soil slurries to basic levels. Therefore, sodium hydroxide was chosen as the candidate reagent for high pH buffering.

Objective

While many practitioners have assumed that pH adjustments in soil is not feasible due to buffering capacity concerns, it is proposed that addition of acids or bases into the soil matrix can in fact sustain soil pH values at a desired level optimal for ISCO performance. Because of the potential need for soil pH buffering information, the response of soils to the application of acids and bases was studied to generate preliminary data that may potentially be used to guide *in situ* chemical oxidation (ISCO) practitioners with soil pH adjustments for a given range of soil types. Information was desired that would quantify both the rate of the pH buffering reactions within experimental soils and the total amount of candidate reagents required to maintain soil pH values at desired levels.

Materials and Methods

Acid/Base Neutralization Capacity

Experiments were performed in duplicate on the Average, High pH, High Iron, and High TOC Soils to determine soil buffering and acid/base neutralization profiles. Initially, 150 grams of each soil sample was crushed using a mortar and pestle. The sample was then dried at 60°C in a drying oven for one month. The crushed dry soil was then passed through an ASTM No. 100 sieve (150 μm), and the soil that passed was utilized as the test soil in the experiment. Eleven 50 mL polypropylene centrifuge tubes with round bottoms and leak proof screw closures were used and labeled from 0 to 10. 5.00 grams of the ground soil sample were added to each tube. Two 50 mL burets were used to measure out the appropriate amounts of distilled water and 0.5 M H_3PO_4 for each tube as indicated in Table 7.1. Each polypropylene tube was then sealed and manually shaken until contents appeared mixed. The tubes were then placed in a rotary extractor and allowed to tumble for 48-hours at room temperature. Following the tumbling period, the tubes were centrifuged at 2000 rpm for 15 minutes. Following the centrifugation, the pH of the supernatant was recorded to generate the pH change due to the addition of the acid. The procedure was repeated for the application of a base, where 0.25 M NaOH was substituted for the phosphoric acid; Table 7.2 shows the centrifuge tube experiment matrix used with the base.

Soil Buffering Kinetics

Experiments were performed in duplicate to determine the buffering kinetics of 30% (w/w) soil slurries. These slurries were created by adding 30 grams of dried soil and 70 grams of distilled water. The slurries were then mixed on an orbital shaker at 150 rpm for 2 weeks to allow for equilibration between the soil and liquid phases. Following the equilibration period, the initial pH of the soil slurry was recorded.

To determine the soil buffering kinetics at a reduced pH, a stock solution of 85% o-phosphoric acid (H_3PO_4, Fisher Chemicals, CAS 7664-38-2) was used to create a 0.1 M solution of H_3PO_4. A quantity of 0.1 M H_3PO_4 was then added to the soil slurry such that the slurry pH was reduced to 3.0. Slurries were shaken at 150 rpm on the orbital shaker throughout the experiment. The pH of the soil slurry was then recorded with respect to time over the course of approximately one week.

To determine the soil buffering kinetics at an increased pH, a stock bottle of sodium hydroxide (NaOH, Fisher Chemicals, CAS 1310-73-2) was used to create a 0.1 M solution of NaOH. A quantity of 0.1 M NaOH was then added to the soil slurry such that the slurry pH was increased to 10.0. Slurries were shaken at 150 rpm on the orbital shaker throughout the experiment. The pH of the soil slurry was then recorded with respect to time over the course of approximately one week.

Total Acid/Base Demands

Experiments were performed in duplicate to determine the total amount of acid or base required to stabilize the pH of a soil slurry at a desired pH. Soil slurries (30% by weight) were created by adding 30 grams of dried soil and 70 grams of distilled water. The slurries were mixed on an orbital shaker at 150 rpm for 2 weeks to allow for equilibration between the soil and liquid phases. Following the equilibration period, the initial pH of the soil slurry was recorded.

To determine the total demand of acid, a stock solution of 85% o-phosphoric acid (H_3PO_4, Fisher Chemicals, CAS 7664-38-2) was used to create a 1.0 M solution of H_3PO_4. A quantity of 1.0 M H_3PO_4 was then added to the soil slurry such that the slurry pH was reduced to 3.0. Slurries were shaken at 150 rpm on the orbital shaker throughout the experiment. As the recorded pH increased above 3.1, additional quantities of 1.0 M H_3PO_4 were added to reduce the pH to 3.0. This process was repeated until the pH of the slurry was stable at a value of 3.0 for at least 24-hours.

To determine the total demand of base, a stock bottle of sodium hydroxide (NaOH, Fisher Chemicals, CAS 1310-73-2) was used to create a 1.0 M solution of NaOH. A quantity of 1.0 M NaOH was then added to the soil slurry such that the slurry pH was increased to 10.0. Slurries were shaken at 150 rpm on the orbital shaker throughout the experiment. As the recorded pH decreased below 9.9, additional quantities of 1.0 M NaOH were added to increase the pH to 10.0. This process was repeated until the pH of the slurry was stable at a value of 10.0 for at least 24-hours.

Results and Discussion

Acid/Base Neutralization Capacities

The data shown in Figure 7.1 are the resulting acid/neutralization capacity plots as it relates to the soil buffering profiles. The data clearly indicate that the addition of certain quantities of acid or base were successful at stabilizing soil pH at values conducive to the application of both Fenton's Reagent and peroxone technologies. For additions of acid, the Average, High Fe, and High TOC soils all behaved in a similar fashion; due to its initial pH of approximately 9.8, the High pH Soil offered the most resistance to soil pH reduction via acid dosing. Likewise, for the addition of sodium hydroxide, the High TOC Soil's extremely low pH (~4.0) made it significantly more resistant to user-controlled increases in soil pH. While this particular data set showed promising initial results, the collected data did not provide enough experimental data to thoroughly investigate pertinent questions as it related to soil pH buffering during ISCO such as how much or how fast acid and base reagents should be added into soil systems. Therefore, further experiments exploring in-depth buffering kinetics and necessary acid/base additions were explored and as such will be discussed in the subsequent sections.

Phosphoric Acid Buffering Kinetics

30% (w/w) soil slurries were spiked with phosphoric acid such that the pH of the soil slurry was stabilized at 3.0 for at least 30 seconds. The pH reading of the soil slurry was then monitored over time to generate necessary data to assess soil

buffering kinetics. After obtaining the data, pH values were converted to H_3O^+ concentrations via Equation 1 as shown below:

$$[H_3O^+] = 1{,}000 * 10^{-pH} \quad (1)$$

where,

$[H_3O^+]$ = hydronium ion concentration at any time, mmol/L

pH = pH of the soil slurry at time, t

Once $[H_3O^+]$ was calculated, the resulting concentrations were fitted to multiple kinetic order profiles and analyzed for appropriate curve fittings. Equation 2 represents a zero-order kinetic model for H_3PO_4 soil buffering:

$$[H_3O^+] = -k_{buffering,0} * t \quad (2)$$

where,

$k_{buffering,0}$ = zero order rate constant for H_3PO_4 soil buffering, mmol/(L*min)

t = time, minutes

Equation 3 represents a first-order kinetic model for H_3PO_4 soil buffering:

$$\ln\left(\frac{[H_3O^+]}{[H_3O^+]_0}\right) = -k_{buffering,1} * t \quad (3)$$

where,

$[H_3O^+]_0$ = initial concentration of hydronium ion, mmol/L

$k_{buffering,1}$ = first order rate constant for H_3PO_4 soil buffering, min^{-1}

Equation 4 represents a second-order kinetic model for H_3PO_4 soil buffering:

$$\frac{1}{[H_3O^+]} - \frac{1}{[H_3O^+]_0} = -k_{buffering,2} * t \quad (4)$$

where,

$k_{buffering,2}$ = second order rate constant for H_3PO_4 soil buffering, L/(mmol*min)

The results for zero order and first order H_3PO_4 buffering are shown in Tables 7.3 and 7.4 respectively. After analyzing the H_3PO_4 buffering data, the degradation of hydronium ion did not appear to follow either zero or first order kinetics due to calculated R^2 values being significantly less than 0.85 for fitted kinetic equations. However, the soil buffering kinetics data were successfully fitted to second order kinetics, each having an R^2 value of 0.9 or greater. A typical second order kinetic plot for H_3O^+ degradation, highlighting both actual and predicted data, is shown in Figure 7.2. Table 7.5 shows the calculated second order kinetic buffering constants, accompanying 95% confidence intervals, and average R^2 values. All R^2 values were greater than 0.90 except for the ozonated sand runs. This deviation was due to the fact that hydronium ion concentrations showed minimal degradation when contacted with ozonated sand slurries. And while insignificant chemical reactions are not modeled well via higher order kinetics, these second order rate constants were calculated for ozonated sand to serve as a basis of comparison among other soil types.

Figure 7.3 displays the calculated second order kinetic H_3PO_4 buffering constants with accompanying 95% confidence intervals as previously described. The extremely low second order kinetic rate constant for the ozonated sand indicated very little degradation potential with respect to hydronium ions. The data clearly indicated that the High pH Soil, with an initial pH of 9.8, displayed the fastest rate of hydronium ion degradation within 30% (w/w) soil slurries. The High TOC Soil,

having a very low initial pH (4.0), displayed the slowest kinetic buffering constant for hydronium ion degradation.

Figure 7.4 displays the correlation comparing the calculated H_3PO_4 kinetic buffering constants with the initial pH of the soil. As was expected, the data clearly shows an evident trend that as the initial pH of the soil slurry increases, the H_3PO_4 kinetic buffering constant increases. By definition, soils with higher pH values have a greater concentration of hydroxide ions (OH^-). Acid/base reaction chemistry is based on the net ionic reaction as reported by Kotz and Treichel (1996):

$$H_3O^+_{(aq)} + OH^-_{(aq)} \leftrightarrow H_2O_{(l)}$$

As the concentration of available hydroxide ions available for reaction with the phosphoric acid increases, the reaction will shift to the right, thereby increasing the pH buffering constant observed within soil slurries. For ISCO users seeking to acidify a soil site for use with the Fenton's Reaction technology, one can expect variable soil buffering rates with most of the dependency coming from the initial pH of the soil. Soils with high initial pH values will offer more challenges in regards to pH adjustments because the rate of pH increase following acidification will be significantly faster. ISCO practitioners working with this soil type will therefore have less time to apply ISCO before the adjusted soil buffers back to a pH that is no longer optimal for chemical oxidation.

Total H_3PO_4 Demands

Experiments were performed to determine the amount of phosphoric acid required to maintain the pH of a 30% (w/w) soil slurry at 3.0 for a period of 24-hours. As available hydroxide ions were consumed by added hydronium ions, the soil slurries became less and less resistant to the buffering of additional hydronium ions. Equation 5 was used to calculate the total H_3PO_4 demand for each soil type as shown below:

$$H_3PO_4 \text{ Demand} = \frac{M_A}{M_S} \tag{5}$$

where,

H_3PO_4 Demand = total H_3PO_4 demand for pH=3.0, lb H_3PO_4/lb dry soil

M_A = total mass of H_3PO_4 added, lb H_3PO_4

M_S = total mass of dry soil present in the soil slurry, lb dry soil

The data for the calculated H_3PO_4 total demands necessary to maintain a pH of 3.0 are shown in Figure 7.5.

The ozonated sand control displayed a significantly smaller H_3PO_4 demand than other soils due to its lack of chemical constituents that were available to act as buffers. Louzao et al. (1990) reported that within soils, several mechanisms can be responsible for the consumption of hydronium ions. These mechanisms include reactions with $CaCO_3$, silicate, cation exchange, aluminum, and iron. Because Ozonated Sand slurries lacked the constituents necessary to promote buffering mechanisms, the smallest total H_3PO_4 demand was observed for the sand control.

The High pH Soil, due to its high concentrations of hydroxide ions initially present (pH = 9.8), displayed the greatest H_3PO_4 demand, while the High TOC Soil, due to is natural acidity, displayed the smallest H_3PO_4 demand.

Figure 7.6 shows data comparing the initial soil pH to the observed total H_3PO_4 demand necessary to equilibrate the slurry at a pH of 3.0. The data clearly indicates that as the initial pH of the soil increases, the total H_3PO_4 demand increases exponentially. These results were expected due to the nature of pH and how it relates to the net ionic reaction as previously described. As the pH increases, the concentration of hydroxide ions present increases exponentially due to the logarithmic nature of the pH scale as shown in Equation 6:

$$pH = \log_{10}(H_3O^+) = 14 - \log_{10}(OH^-) \quad (6)$$

Therefore, since the concentration of available hydroxide ions is increasing exponentially, it is reasonable to expect based on the stoichiometry of the net ionic equation that the total H_3PO_4 demand would increase exponentially as well.

For ISCO users seeking to reduce the soil pH to levels optimal for Fenton's Reaction performance, the total acid demand will vary among different contaminated sites. A measurement of the initial soil pH appears to be the best way in determining the amount of acid required to maintain a desired stable pH within the soil matrix. From the regression results of these data (R^2=0.8835) in Figure 7.6, the total H_3PO_4 demand can be predicted using Equation 7 as shown below:

$$H_3PO_4 \text{ Demand} = 0.0004 * (\text{Initial Soil pH})^{2.3374} \quad (7)$$

This total H_3PO_4 demand predictor has the potential to be extremely helpful to ISCO practitioners for applying remediation technologies in which pH has an important impact in oxidation mechanisms.

Sodium Hydroxide Buffering Kinetics

30% (w/w) soil slurries were spiked with sodium hydroxide such that the pH of the soil slurry stabilized at 10.0 for at least 30 seconds. The pH reading of the soil slurry was then monitored over time to generate data necessary to perform soil buffering kinetic analyses. After obtaining the data, the pH values were converted to hydroxide ion (OH^-) concentrations via Equation 8 as shown below:

$$[OH^-] = 1{,}000 * 10^{-(14 - pH)} \quad (8)$$

where,

$[OH^-]$ = hydroxide ion concentration at any time, mmol/L

pH = pH of the soil slurry at time, t

Once $[OH^-]$ data was calculated, the resulting concentrations were fitted to multiple kinetic order profiles and analyzed for appropriate curve fittings similar to the procedure performed for H_3PO_4. However, degradation rates of hydroxide ions were plotted rather than for hydronium ions. Equation 9 represents a zero-order kinetic model for NaOH soil buffering:

$$[OH^-] = -k_{buffering,0} * t \quad (9)$$

where,

$k_{buffering,0}$ = zero order rate constant for NaOH soil buffering, mmol/(L*min)

t = time, minutes

Equation 10 represents a first-order kinetic model for NaOH soil buffering:

$$\ln\left(\frac{[OH^-]}{[OH^-]_0}\right) = -k_{buffering,1} * t \quad (10)$$

where,

$[OH^-]_0$ = initial concentration of hydroxide ion, mmol/L

$k_{buffering,1}$ = first order rate constant for NaOH soil buffering, min^{-1}

Equation 11 represents a second-order kinetic model for soil buffering:

$$\frac{1}{[OH^-]} - \frac{1}{[OH^-]_0} = -k_{buffering,2} * t \quad (11)$$

where,

$k_{buffering,2}$ = second order rate constant for NaOH soil buffering, L/(mmol*min)

The results for zero order and first order NaOH buffering are shown in Tables 7.6 and 7.7 respectively. After analyzing the NaOH buffering data, the degradation of hydroxide ion did not appear to follow either zero or first order kinetics due to calculated R^2 values being significantly less than 0.85 for most all fitted kinetic equations in these cases. However, the soil buffering kinetics data were successfully fitted to second order kinetics, each having an R^2 value of 0.85 or greater. A typical second order kinetic plot for OH^- degradation, highlighting both actual and predicted data, is shown in Figure 7.7. Table 7.8 shows the calculated second order kinetic buffering constants and accompanying 95% confidence intervals and average R^2 values. All R^2 values were greater than 0.85 except for the ozonated sand runs. The rationale for the poor fits of ozonated sand kinetic profiles was already discussed in the H_3PO_4 buffering kinetics section.

Second order kinetic NaOH buffering constants with accompanying 95% confidence intervals are shown in Figure 7.8. The extremely low second order kinetic rate constant for the ozonated sand indicated very little degradation potential with respect to hydroxide ions. The High pH Soil had the highest initial pH value, and it subsequently displayed the lowest NaOH soil buffering constant (0.01 L/mmol*min) for all soils other than the Ozonated Sand test control. The High TOC Soil had the lowest initial pH, and it subsequently displayed the highest NaOH soil buffering constant (0.12 L/mmol*min). As was expected due to the nature of acid/base chemistry, the NaOH buffering kinetics data appeared in a fashion that was inverse of the H_3PO_4 buffering kinetics data. The High pH Soil had the highest H_3PO_4 kinetic buffering constant, but it had the lowest NaOH kinetic buffering constant.

Figure 7.9 shows the comparison between the initial soil pH and the NaOH soil buffering kinetic constant. The graph appears to be simply an inverse of the same graph for H_3PO_4 (Figure 7.4). As the initial soil pH increases, the calculated second order kinetic buffering constant for the application of NaOH decreases in a relatively linear manner. This again is due to simple kinetic reaction equilibrium as it relates to the net ionic reaction (Kotz and Treichel, 1996) as shown below:

$$H_3O^+_{(aq)} + OH^-_{(aq)} \leftrightarrow H_2O_{(l)}$$

As was discussed in the H_3PO_4 buffering kinetics section, the decreased concentration of available hydronium ions offer less reactant for the added hydroxide ions from the NaOH solution. This shifts the reaction towards the left, thereby decreasing the kinetic rate constant.

These results agreed with findings by Matula and Pechova (2002) in regards to a simplified approach to liming in soils. They used calcium carbonate ($CaCO_3$) additions in order to alter pH. When the lime is added to a moist soil, Ca^{2+} ions result, and they exchange with naturally occurring H^+ ions located within soil colloidal complexes. The H^+ ions release and react with OH^- ions via the net ionic reaction (Shawarbi, 1952). Matula and Pechova (2002) subsequently found that the liming rate necessary to for desired soil pH adjustments was highly functional on the initial pH of the soil. More acidic soils required a faster rate of lime addition due to the more rapid buffering response rate when subjected to a base. While these experiments utilized NaOH rather than a more traditional lime application, the basic stoichiometric principles in fact remain the same.

Therefore, for ISCO users seeking to raise the pH of the soil for treatment via peroxone technologies, one can expect the initial soil pH to play a key factor in how a soil's buffering response will behave. A soil with a lower initial pH will display much more of a buffering potential upon the application of sodium hydroxide necessary to raise the soil's pH.

Total NaOH Demands

Experiments were performed to determine the amount of sodium hydroxide required to maintain the pH of a 30% (w/w) soil slurry at 10.0 for a period of at least 24-hours. As available hydronium ions were consumed by added hydroxide ions, the soil slurries became less and less resistant to the buffering of additional hydroxide ions. Equation 12 was used to calculate the total NaOH demand for each soil type.

$$\text{NaOH Demand} = \frac{M_B}{M_S} \quad (12)$$

where,

NaOH Demand = total NaOH demand for pH=10.0, lb NaOH/lb dry soil

M_B = total mass of NaOH added, lb NaOH

M_S = total mass of dry soil present in the soil slurry, lb dry soil

The data for the calculated NaOH total demands necessary to maintain a pH of 10.0 are shown in Figure 7.10. Discounting the Ozonated Sand test control, the High pH Soil displayed the lowest value for total NaOH demand (0.0032 lb NaOH/lb dry soil); the High TOC Soil displayed the greatest total NaOH demand value (0.0166 lb NaOH/lb dry soil). These results were hypothesized to be a primary function of the initial pH of the soil.

Figure 7.11 shows data comparing the initial soil pH to the observed total NaOH demand necessary to equilibrate the slurry at a pH of 10.0. The data clearly indicates that as the initial pH of the soil increases, the total NaOH demand decreases. The predictive equation (R^2=0.7228) for the total NaOH demand as a function of the soil's initial pH is given in Equation 13 as shown below:

$$\text{NaOH Demand} = -0.0156*(\text{Initial Soil pH}) + 0.1588 \quad (13)$$

However, in addition to a correlation with the initial pH, Magdoff and Bartlett (1985) observed correlations giving mechanistic insights into the pH buffering of a variety of acidic Vermont soils. They concluded that the presence of organic matter and its accompanying functional group association/dissociation was the dominating factor in

the degree of pH buffering observed. Figure 7.12 shows current data comparing soil TOC levels with the calculated total NaOH demands. These results indicate a strong correlation (R^2=0.8968) between the total NaOH demand observed and the initial level of total organic carbon within the soil. The predictive equation based on this correlation is given in Equation 14 as shown below:

$$\text{NaOH Demand} = 7*10^{-7} * (\text{TOC}) + 0.001 \quad (14)$$

where,

TOC = total organic carbon level in the soil, (mg TOC/kg dry soil)

Because total base demands will vary among various contaminated soil sites, these total NaOH demand predictors have the potential to be extremely helpful to ISCO practitioners when applying remediation technologies in which an increase in soil pH offers a beneficial impact on oxidation mechanisms (e.g. peroxone). A measurement of the initial soil pH and the initial soil TOC appear to be the best means in determining the amount of base required to stabilize the soil pH at a value of 10.0.

Summary

The soil buffering results, both for H_3PO_4 and NaOH data, were successfully fitted to second order reaction kinetics for all soil types ($R^2 > 0.85$). Results indicated that the soil buffering rates observed were highly dependent upon the initial pH of the soil samples. The total acid and base demands for H_3PO_4 and NaOH respectively were also successfully calculated using standard mass balances. As expected, an increased initial soil pH resulted in both an increased total H_3PO_4 demand and a decreased total NaOH demand.

For users of ISCO technologies, the initial soil pH will obviously play a critical role in determining if and how chemical oxidation is applied within the subsurface. Because Fenton's Reaction is optimal at low pH values and peroxone is optimal at high pH values, a site pH determination might prove beneficial in determining which type of technology to suggest. For soils with naturally high pH values, peroxone might be a much more appropriate choice than Fenton's Reagent; and for soils with naturally low pH values, Fenton's Reaction might be a much more appropriate choice. This would prevent large quantities of acid or base from needing to be purchased and delivered into the subsurface prior to oxidative treatment. However, the user should not make this decision based on pH readings alone. A full site evaluation of both pollutants and naturally occurring constituents should be performed, and all pertinent data should be analyzed to determine the most optimal remediation technology.

Table 7.1: Acid Neutralization Experimental Matrix

Centrifuge Tube #	**Amount of DI-Water (mL)**	**Amount of 0.5 M H_3PO_4 (mL)**
0	30.0	0.0
1	29.0	1.0
2	28.0	2.0
3	27.0	3.0
4	26.0	4.0
5	25.0	5.0
6	24.0	6.0
7	23.0	7.0
8	22.0	8.0
9	21.0	9.0
10	20.0	10.0

Table 7.2: Base Neutralization Experimental Matrix

Centrifuge Tube #	**Amount of DI-Water (mL)**	**Amount of 0.25 M NaOH (mL)**
0	30.0	0.0
1	29.0	1.0
2	28.0	2.0
3	27.0	3.0
4	26.0	4.0
5	25.0	5.0
6	24.0	6.0
7	23.0	7.0
8	22.0	8.0
9	21.0	9.0
10	20.0	10.0

Table 7.3: H_3PO_4 Soil Buffering Kinetic Constants Data and R^2 Values for Zero-Order Kinetics

Soil	**Reaction Order**	**H_3PO_4 kinetic buffering rate constant, k (mmol/L*min)**	**95% C.I. (mmol/L*min)**	**Average R^2 for Zero Order Kinetic Fit**
Ozonated Sand	Zero	0.00002	$9.8*10^{-5}$	0.06845
Average Soil	Zero	0.0002	0	0.56575
High pH Soil	Zero	0.00015	$9.8*10^{-5}$	0.40385
High Fe Soil	Zero	0.000095	$9.8*10^{-6}$	0.49685
High TOC Soil	Zero	0.0002	0	0.6507

Table 7.4: H_3PO_4 Soil Buffering Kinetic Constants Data and R^2 Values for First-Order Kinetics

Soil	**Reaction Order**	**H_3PO_4 kinetic buffering rate constant, k (min^{-1})**	**95% C.I. (min^{-1})**	**Average R^2 for First Order Kinetic Fit**
Ozonated Sand	1st	-0.000025	0.00011	0.0703
Average Soil	1st	0.0007	0	0.79995
High pH Soil	1st	0.00085	0.00049	0.74375
High Fe Soil	1st	0.0005	0	0.8137
High TOC Soil	1st	0.00045	$9.8*10^{-5}$	0.79215

Table 7.5: H_3PO_4 Soil Buffering Kinetic Constants Data and R^2 Values for Second-Order Kinetics

Soil	**Reaction Order**	**H_3PO_4 kinetic buffering rate constant, k (L/mmol*min)**	**95% C.I. (L/mmol*min)**	**Average R^2 for Second Order Kinetic Fit**
Ozonated Sand	2^{nd}	0.000035	0.000127	0.07205
Average Soil	2^{nd}	0.00395	0.00049	0.94925
High pH Soil	2^{nd}	0.01415	0.0048	0.9729
High Fe Soil	2^{nd}	0.007	0.00098	0.9722
High TOC Soil	2^{nd}	0.0013	0.0002	0.90535

Table 7.6: NaOH Soil Buffering Kinetic Constants Data and R^2 Values for Zero-Order Kinetics

Soil	**Reaction Order**	**NaOH kinetic buffering rate constant, k (mmol/L*min)**	**95% C.I. (mmol/L*min)**	**Average R^2 for Zero Order Kinetic Fit**
Ozonated Sand	Zero	$6.5*10^{-6}$	$6.9*10^{-6}$	0.47865
Average Soil	Zero	$1.5*10^{-5}$	$9.8*10^{-6}$	0.6009
High pH Soil	Zero	$1.0*10^{-5}$	0	0.67705
High Fe Soil	Zero	$1.4*10^{-5}$	$1.2*10^{-5}$	0.3633
High TOC Soil	Zero	$8.0*10^{-6}$	$3.9*10^{-6}$	0.29155

Table 7.7: NaOH Soil Buffering Kinetic Constants Data and R^2 Values for First-Order Kinetics

Soil	**Reaction Order**	**NaOH kinetic buffering rate constant, k (min^{-1})**	**95% C.I. (min^{-1})**	**Average R^2 for First Order Kinetic Fit**
Ozonated Sand	1^{st}	$7*10^{-5}$	$5.9*10^{-5}$	0.4663
Average Soil	1^{st}	$7.5*10^{-4}$	$9.8*10^{-5}$	0.8615
High pH Soil	1^{st}	$3.0*10^{-4}$	0	0.8056
High Fe Soil	1^{st}	$6.0*10^{-4}$	$5.9*10^{-4}$	0.64685
High TOC Soil	1^{st}	$6.0*10^{-4}$	$2.0*10^{-4}$	0.70915

.

Table 7.8: NaOH Soil Buffering Kinetic Constants Data and R^2 Values for Second-Order Kinetics

Soil	**Reaction Order**	**NaOH kinetic buffering rate constant, k (L/mmol*min)**	**95% C.I. (L/mmol*min)**	**Average R^2 for Second Order Kinetic Fit**
Ozonated Sand	2^{nd}	0.00075	0.000686	0.4988
Average Soil	2^{nd}	0.0931	0.0521	0.8864
High pH Soil	2^{nd}	0.0122	0.00235	0.9038
High Fe Soil	2^{nd}	0.03865	0.0211	0.850
High TOC Soil	2^{nd}	0.11765	0.00578	0.97135

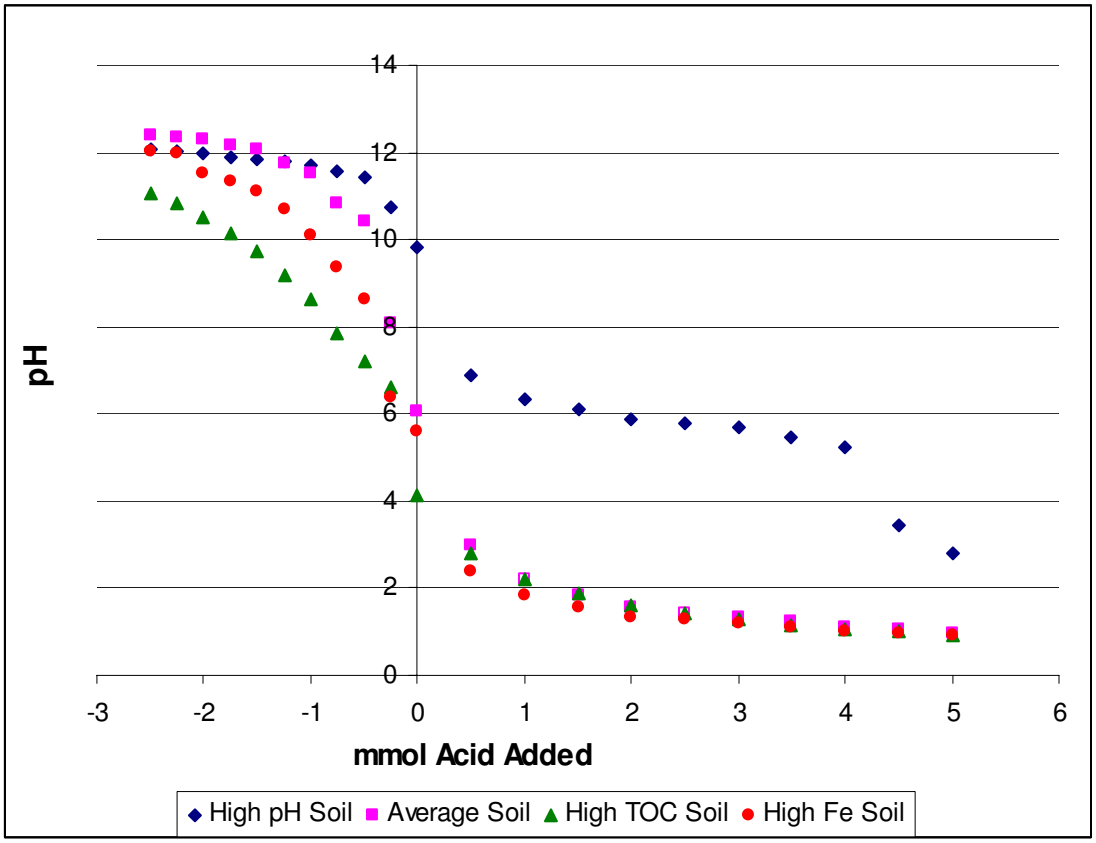

Figure 7.1: Acid/Base Neutralization Capacity of Experimental Soils,
Note: A negative acid addition indicates a positive addition of base

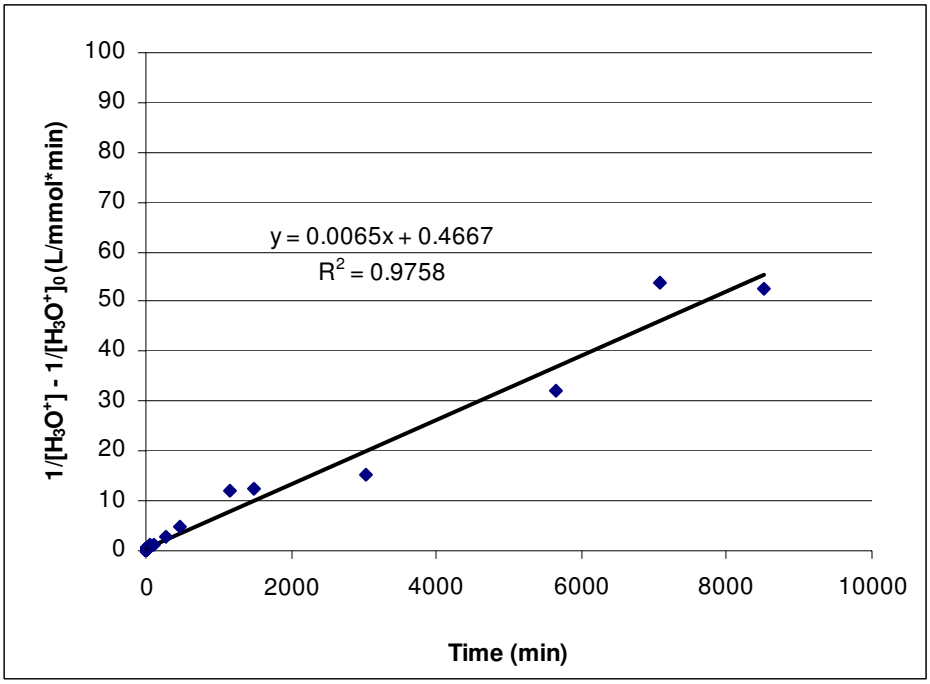

Figure 7.2: A typical second order kinetic plot for H_3PO_4 Buffering (High Fe Soil, Run 2)

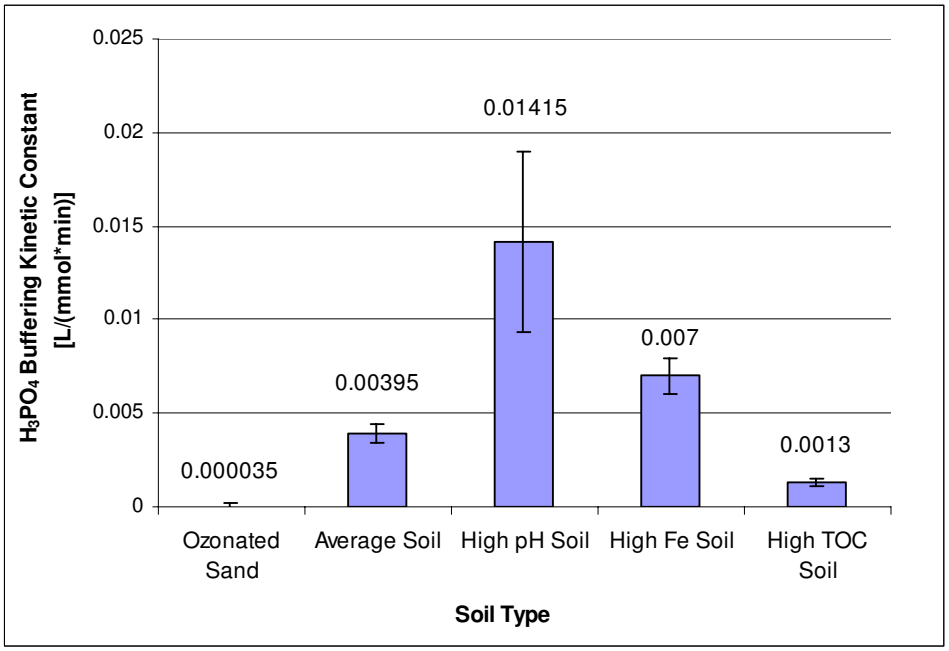

Figure 7.3: H_3PO_4 Buffering Kinetic Constants

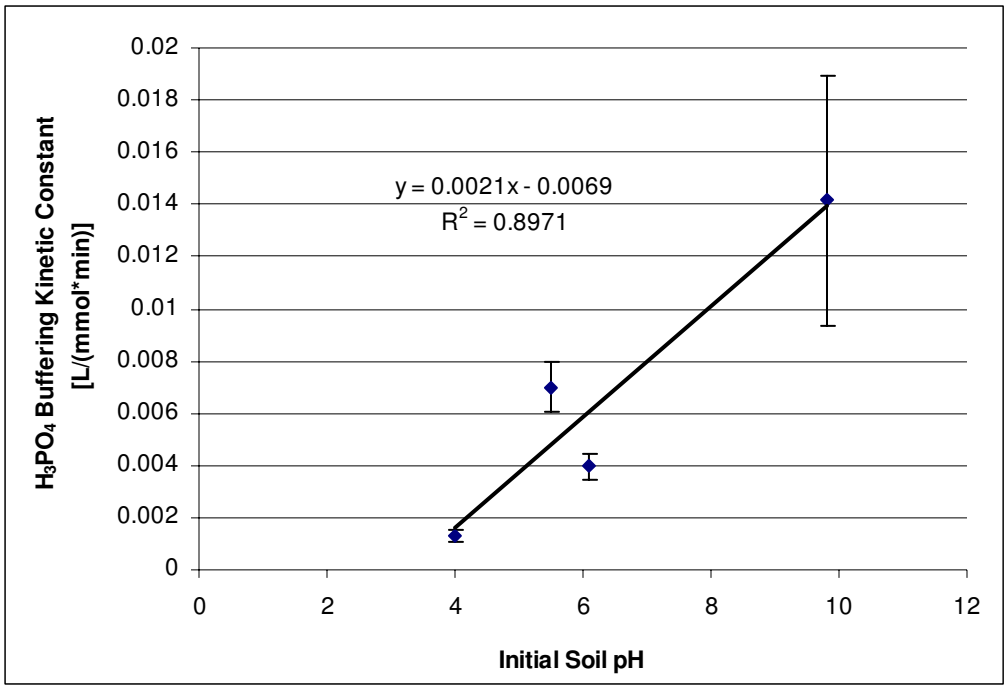

Figure 7.4: H_3PO_4 Buffering Kinetic Constants vs. Initial Soil pH

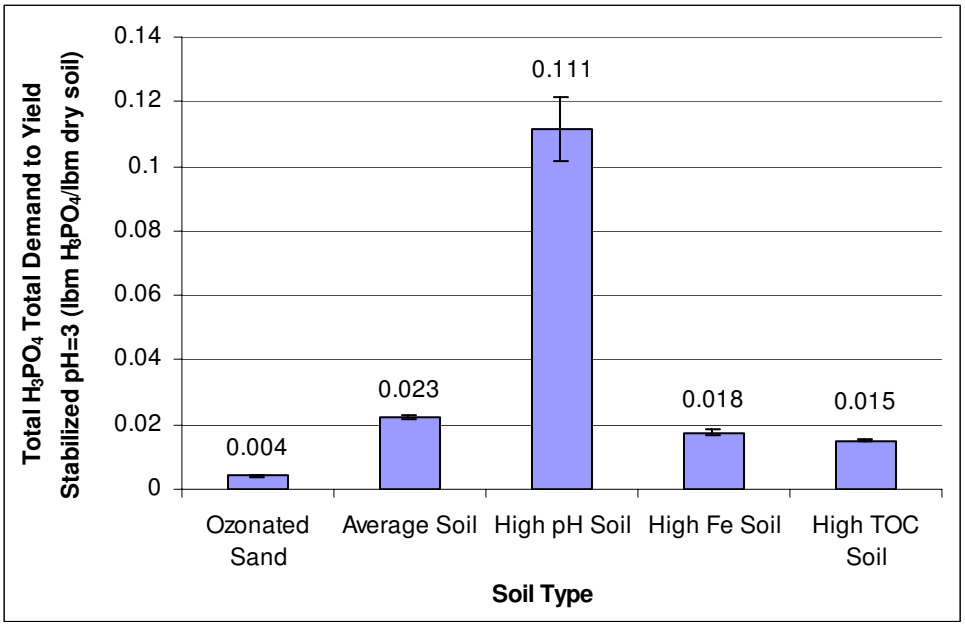

Figure 7.5: H_3PO_4 Total Demands

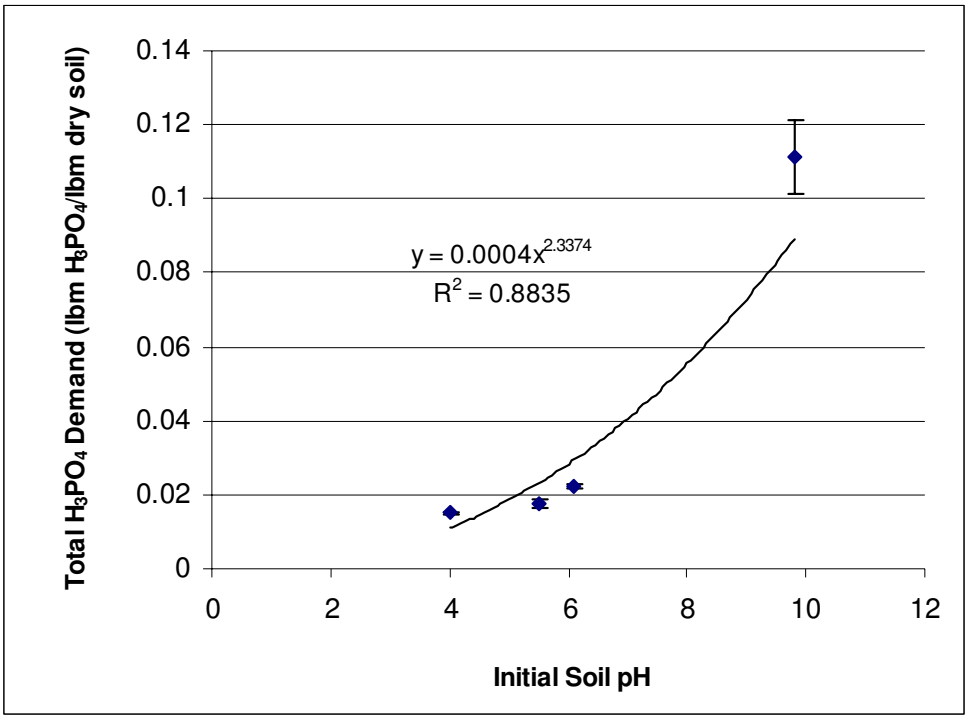

Figure 7.6: H_3PO_4 Total Demands vs. Initial Soil pH

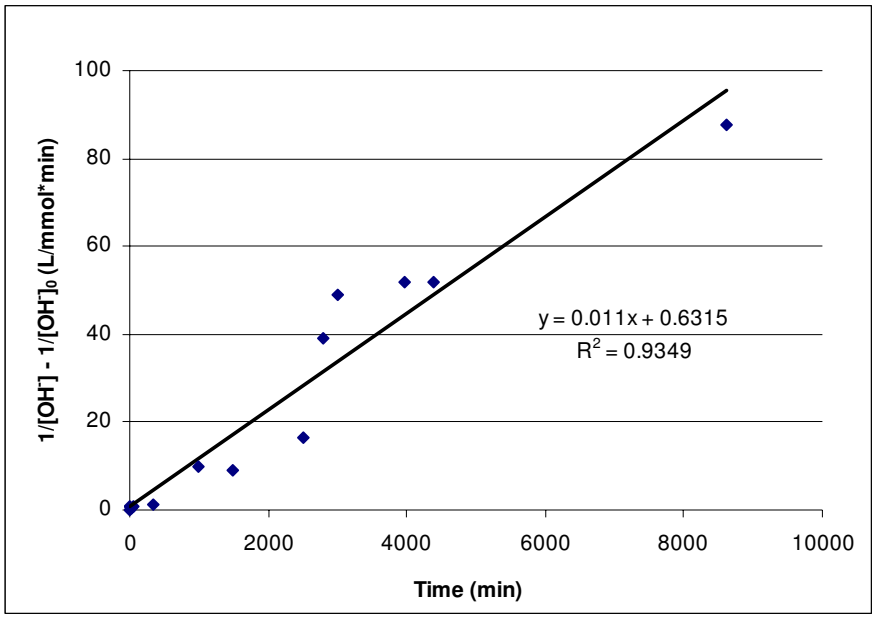

Figure 7.7: A typical second order kinetic plot for NaOH Buffering (High pH Soil, Run 1)

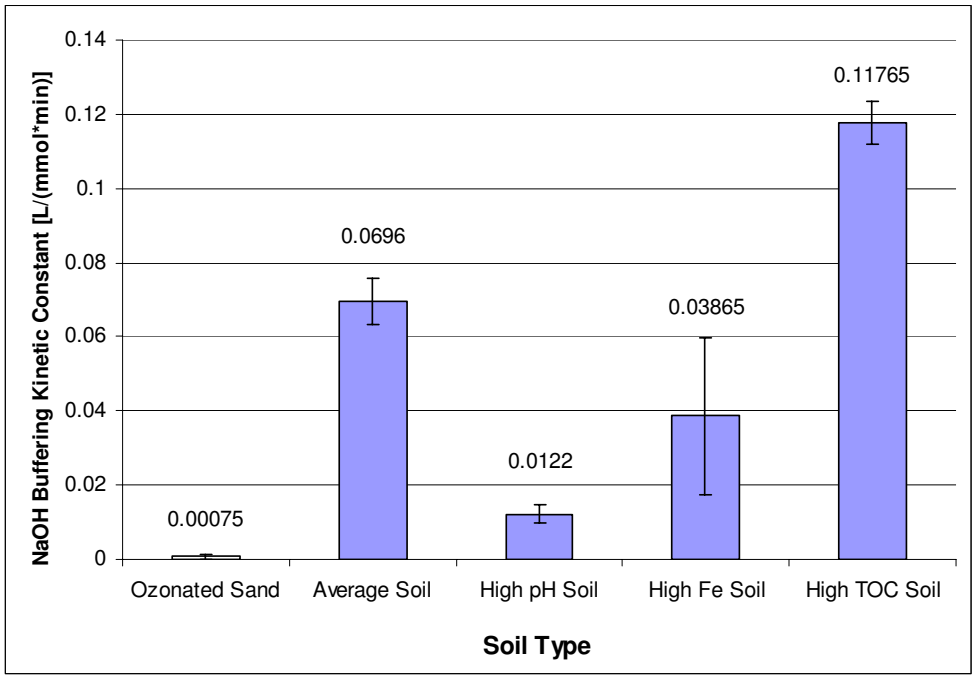

Figure 7.8: NaOH Buffering Kinetic Constants

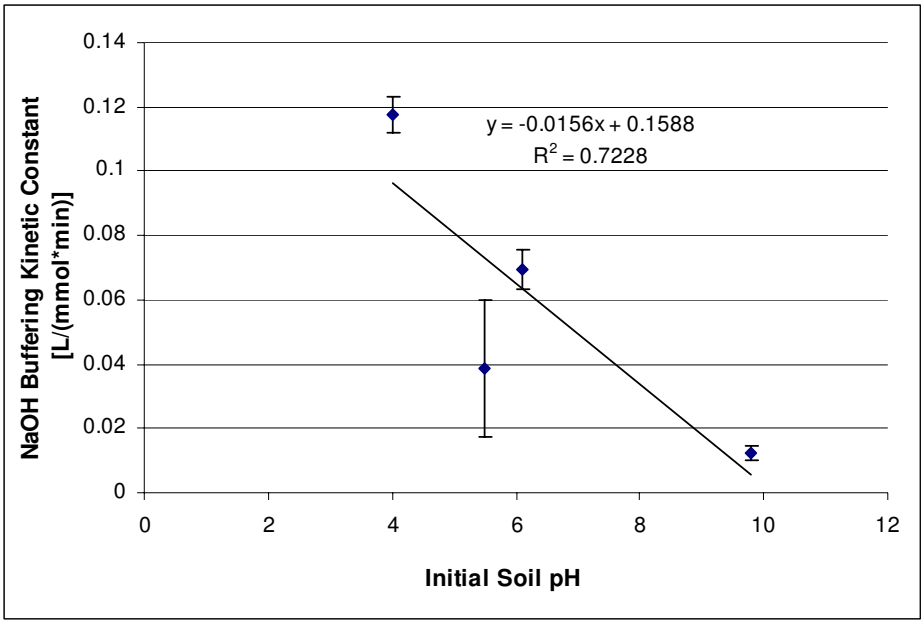

Figure 7.9: NaOH Buffering Kinetic Constants vs. Initial Soil pH

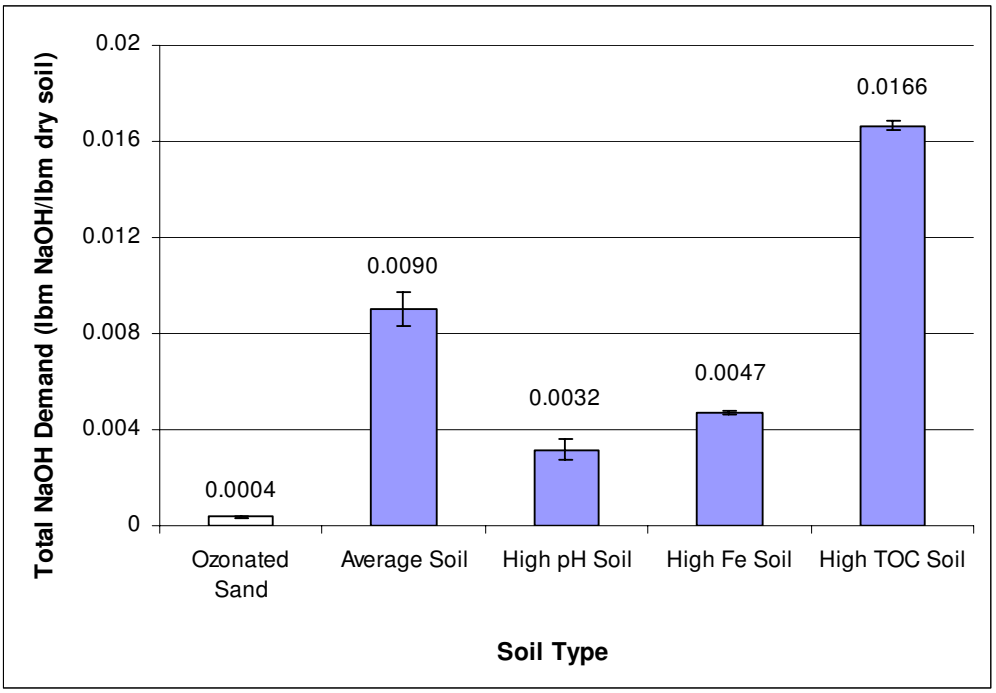

Figure 7.10: NaOH Total Demands

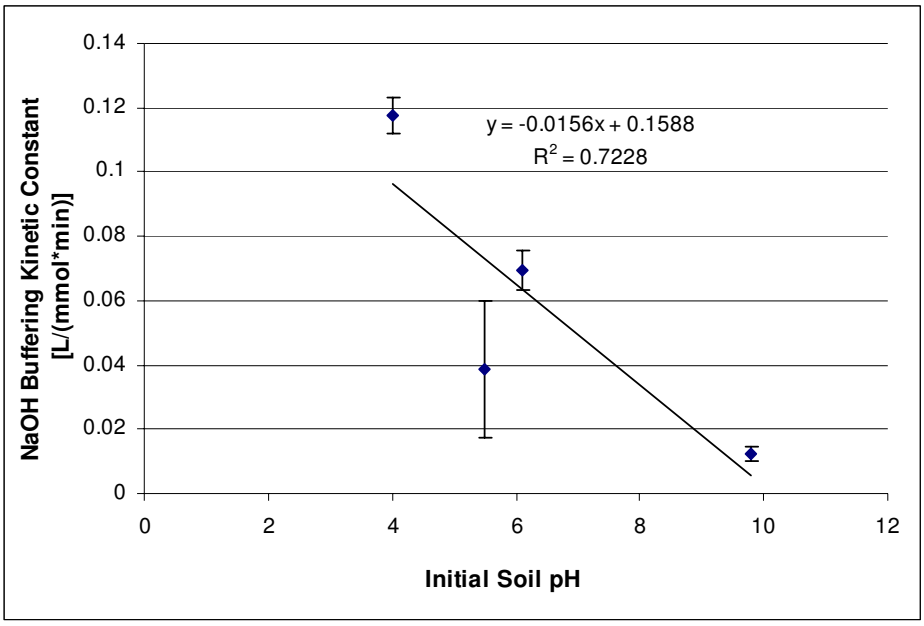

Figure 7.11: NaOH Total Demands vs. Initial Soil pH

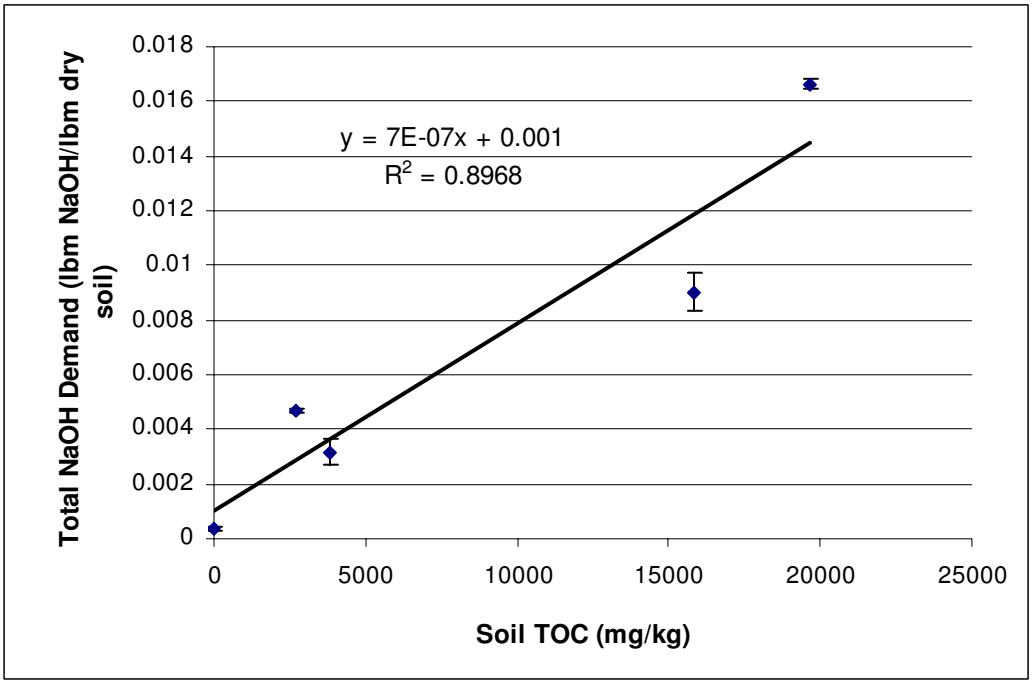

Figure 7.12: NaOH Total Demands vs. Soil TOC

CHAPTER VIII

IMPACT OF SOIL CONSTITUENTS ON SOIL TEMPERATURE AND O_2 PRODUCTION

Background

The use of ISCO technologies based on hydrogen peroxide (H_2O_2) has certain results that practitioners must be aware of when treating contaminated soil sites. Firstly, H_2O_2-based reactions such as Fenton's Reaction are known to be highly exothermic. In cases in which H_2O_2 is added in concentrations of 10% or greater, the reaction has the potential to boil water out of the soil (Amarante, 2000). The potential for temperature changes within subsurface environments poses both potential advantages and disadvantages as it relates to ISCO. A rise in temperature can be advantageous to remediation efforts since the heat generated from Fenton's Reaction can enhance the desorption and dissolution of nonaqueous phase liquids (NAPLs), thereby improving remediation efficiency when properly controlled (ITRC, 2005). However, several negative impacts on increased temperatures also exist. Heister et al. (2004) reported on hydrogen peroxide's potential for thermal decomposition. At high temperatures, H_2O_2 can degrade more rapidly than at ambient conditions, leading to altered kinetic responses within the subsurface. Additionally, high temperatures also pose the risk of harming native microorganisms

within soil environments. Kaleli and Islam (1996) performed experiments to determine the impact of temperature on the growth of wastewater bacteria and found that at temperatures greater than 60 °C, bacteria began to die off due to the denaturing of enzymes.

A second property of H_2O_2 is that it can degrade into oxygen and water via the catalase enzyme, as shown in the following equation (Prescott et al., 2001):

$$2H_2O_2 \xrightarrow{catalase} 2H_2O + O_2$$

Zappi et al. (2000) used hydrogen peroxide as a bioremediation enhancer by utilizing the resulting oxygen to stimulate appropriate biological activity. However, the production of oxygen in this reaction can cause risks to ISCO practitioners due to the potential for oxygen to build up in a confined space without the proper means to quickly exit the subsurface environment. While oxygen deficient environments (<19.5% O_2) pose hazardous risks related to breathing issues, oxygen enriched environments also pose serious safety risks. When the oxygen content in a confined space exceeds 23.5%, considerable explosion risks arise; this environment causes substances to combust much more vigorously than at atmospheric conditions (DOE, 1998).

Objective

Because of these previously discussed issues, it was desired to investigate both the temperature change and the oxygen production due to the application of ISCO technologies based on hydrogen peroxide. To determine the role that the

particular soil type played on observed results, experiments were performed on a wide variety of soil samples collected including an Ozonated Sand control, Average Soil, High pH Soil, High Iron Soil, High TOC Soil, and Biologically Stimulated Soil. It was desired that the generated data would help ISCO practitioners assess potential effects and risks associated with these two properties associated with H_2O_2 degradation.

Methods and Materials

Fenton's Reaction Temperature Profiles

Experiments were performed in duplicate to determine the temperature rise in soil slurries due to the exothermic nature of Fenton's Reaction. Two different 30% (w/w) slurry ratios were tested in duplicate to determine the impact of the total soil mass on recorded temperatures. 30 grams of dry soil and 59.5 g of 5,883 mg/L Fe^{2+} solution were added to a 500-mL Erlenmeyer flask and mixed on an orbital shaker at 150 rpm. Soil slurries were allowed to equilibrate for 24 hours. The flasks were then dosed with 10.5 mL of 30% (w/w) H_2O_2 stock solution, and the temperature readings were continuously recorded with respect to time by using a Fisherbrand 76mm Immersion thermometer. For experiments on the second slurry ratio, 120 grams of dry soil and 280 g of 5,000 mg/L Fe^{2+} solution were added to a 1,000 mL Erlenmeyer flask and mixed on an orbital shaker at 150 rpm. Soil slurries were allowed to equilibrate for 24 hours. The flasks were then dosed with 50 mL of 30% (w/w) H_2O_2

stock solution, and the temperature readings were continuously recorded with respect to time by using the same thermometer.

Oxygen Production from the Reaction of Hydrogen Peroxide

Experiments were performed in triplicate to determine the amount of oxygen produced with respect to the amount of hydrogen peroxide added to native soils. Experiments were performed in 500-mL Kimax batch reactors (round, flat-bottom) which were constructed by Ace Glass (Vineland, NJ). The diagram of the batch reactor is shown in Figure 8.1. The reactors were constructed such that they had three threaded necks. The first neck (#15 sized threads) was used for loading soil and liquid samples into the reactor. Following loadings, this neck was sealed with a solid threaded male PTFE plug sealed with an o-ring. The second neck (#15 sized threads) was used to enable pressure readings. An Ashcroft Test Pressure Gauge was affixed to the second neck to enable the monitoring of total gas production within the reactor. The Ashcroft Test Pressure Gauge (Case Type 1084) was constructed out of 316 Stainless Steel and allowed for recorded pressure readings between 0 and 15 psig (+/- 0.5%). The pressure gauges were attached to the reactor using a PTFE adapter and an accompanying Swagelok connection (#15 Ace Threads x ¼" NPT female). The third neck enabled multiple gas samples to be made throughout the experiments. This center neck (#7 Ace Threads) was fitted with an adapter consisting of a threaded bushing with a 1.5 mm bored cavity and a 1.5 mm glass capillary tube. These were affixed to the reactor via a nylon bushing (#7 Ace Threads) with a 7.5 mm cavity in the center. This portion of the reactor was sealed via a rubber o-ring, and an 11 mm

septa (Agilent) was placed between the bushing and the capillary tube to enable multiple gas samplings. Teflon tape was applied to all fittings to prevent leaking, and batch reactors were leak tested via application of N_2 at a pressure of 10 psig.

Experiments were performed in triplicate on four different ISCO treatment applications. Three different H_2O_2 concentrations (10,000 mg/L, 50,000 mg/L, and 100,000 mg/L) and one Fenton's Reagent application (5,000 mg/L Fe^{2+} + 50,000 mg/L H_2O_2) were selected as test treatments. Initially 15 grams of dry soil was added to the batch reactor. For H_2O_2 treatments, oxidation was initiated by adding 35 grams of the appropriate H_2O_2 solution. For treatment via Fenton's Reaction, oxidation was initiated by adding 29.75 g of 5,883 mg/L Fe^{2+} followed by a 5.25 g addition of 30% (w/w) H_2O_2 stock solution. Immediately following the application of hydrogen peroxide, the PTFE plug was used to seal the reactor, and the time was recorded as time zero of the reaction. Reactor pressures were recorded with respect to time. As reactor pressures approached 15 psig (maximum recordable level of the Ashcroft gauge), a 100 µL gas sample was extracted using a 200 µL gas sampling syringe. This sample was analyzed for oxygen concentration using the Agilent 6890N Gas Chromatograph (TCD). The pressure was quickly released from the reactor, reduced to 0 psig, and the reactor was quickly re-sealed. This process was repeated as necessary for a 24-hour reaction period. At the end of the period, a final gas sample was extracted and analyzed for O_2 concentration.

Results and Discussion

Temperature Response due to H_2O_2/Fenton's Reaction

Figure 8.2 shows the maximum observed temperatures for each soil type during experimental runs. For runs using 30 grams of initial soil, maximum temperatures ranged from 37°C in the Ozonated Sand controls to as high as 56°C in the Biologically Stimulated Soil. However, when the size of the slurry was increased by a factor of four, much higher temperatures were observed in soil slurries. In those experiments, the Ozonated Sand control showed a similar temperature increase as was observed in the smaller scale experiments, reaching a value of approximately 45°C. But temperature increases in all other soil types proved to be of a much larger scale. The High TOC soil showed the greatest resistance to temperature change, having only reached a maximum temperature of 49°C. This was expected due to the extremely low quantities of naturally occurring iron within the soil. However, the temperatures in the other soil slurries all increased to over 70°C. The temperatures in the slurries containing Average Soil (92°C) and Biologically Stimulated Soil (97°C) each reached peak temperatures in excess of 90°C.

Data from these experiments indicated that the application of H_2O_2-based ISCO technologies have the potential to severely impact the immediate temperatures within soil environments. With temperatures approaching the boiling point of water in some soils, ISCO practitioners must be aware of the following potential side effects due to the severe temperature increases:

- Pros of Increased Temperatures:
  - Increased remediation efficiency due to the desorption and dissolution of NAPL contamination from the soil matrix

- Cons of Increased Temperatures:
  - Increased mobility of NAPL contamination as it desorbs from the soil matrix
  - Increased degradation rates of H_2O_2 in the subsurface due to thermal decomposition
  - Decreased viability of native microorganisms present in the subsurface

Oxygen Production from Hydrogen Peroxide

Oxygen Production Data Analysis

It was desired to determine the ratio of oxygen produced to the amount of hydrogen peroxide added into the batch reactor to analyze the potential for oxygen buildup in subsurface environments. Equations 1-6 represent the series of equations used to calculate the O_2/H_2O_2 mass ratio values for each experiment.

$$n_{total,initial} = \frac{P_{total,initial} * V}{R * T} \quad (1)$$

$$n_{oxygen,initial} = x_{oxygen,initial} * n_{total,initial} \quad (2)$$

$$n_{total,final} = \frac{P_{total,final} * V}{R * T} \quad (3)$$

$$n_{oxygen,final} = x_{oxygen,final} * n_{total,final} \quad (4)$$

$$m_{oxygen,produced} = (n_{oxygen,final} - n_{oxygen,initial}) * MW_{oxygen} \quad (5)$$

$$O_2 / H_2O_2 Ratio = \frac{m_{oxygen,produced}}{m_{peroxide}} \quad (6)$$

where,

$n_{total,initial}$ = initial total moles of gas, mol

$P_{total,initial}$ = initial pressure within reactor (atmospheric), psia

V = volume of headspace within the reactor, mL

R = Universal gas constant, (mL*psia)/(mol*K)

T = Temperature, K

$n_{oxygen,initial}$ = initial total moles of oxygen gas, moles

$x_{oxygen,initial}$ = initial volume (or mole) fraction of oxygen

$n_{total,final}$ = final total moles of gas, mol

$P_{total,final}$ = final pressure within reactor, psia

$n_{oxygen,final}$ = final total moles of oxygen gas, moles

$x_{oxygen,final}$ = final volume (or mole) fraction of oxygen

MW_{oxygen} = molecular weight of O_2 gas, g/mol

$m_{oxygen,produced}$ = net mass of oxygen produced, g O_2/g H_2O_2

$m_{peroxide}$ = mass of peroxide added to the reactor, g H_2O_2

O_2/H_2O_2 Ratio = mass ratio of O_2 produced to H_2O_2 added, g O_2/gH_2O_2

In order to determine the net production of oxygen, it was first required to calculate the initial mass of oxygen present within the reactor. The Ideal Gas Law (Equation 1) was applied to the initial reactor system to determine the moles of total gas present prior to the addition of H_2O_2. Because mole fractions are equivalent to volume

fractions, Equation 2 was used to determine the initial moles of oxygen gas present prior to the addition of H_2O_2. Once the reaction was completed, the Ideal Gas Law (Equation 3) was again used to calculate the moles of total gas post-reaction. Equation 4 was then used to calculate the final moles of oxygen present following the completion of the reaction. The net mass of oxygen produced was calculated using Equation 5, and the mass ratio of oxygen produced to peroxide added was calculated using Equation 6. While the units in Equation 6 work out to grams of O_2 produced per gram of H_2O_2 added, this value is equivalent to any ratio of identical mass (e.g. g/g, kg/kg, lbm/lbm, etc.).

Oxygen Production Results

Results for the O_2 produced to H_2O_2 added mass ratios are presented in Figure 8.3. For Ozonated Sand test controls, minimal quantities of oxygen were produced during reaction with 10,000, 50,000, and 100,000 mg/L H_2O_2. However, during the Ozonated Sand test control experimental run using Fenton's Reagent (5,000 mg/L Fe^{2+} and 50,000 mg/L H_2O_2), approximately 0.4 pounds O_2 were produced per pound of H_2O_2 added to the reactor system. This result was consistent with all of the other soil types treated with this particular application of modified Fenton's Reagent. The average mass ratio values ranged from 0.407 lbm O_2/lbm H_2O_2 (Ozonated Sand) to 0.447 lbm O_2/lbm H_2O_2 (High Iron Soil). However, because all of the 95% confidence intervals overlapped, the different soil types showed no significant difference in total oxygen production using this particular application of Fenton's Reagent.

For most soil types, treatments via 50,000 and 100,000 mg/L H_2O_2 offered similar results to that of the Fenton's Reaction treatment. Excluding the Ozonated Sand test control, all soil types tested using an initial H_2O_2 concentration of 50,000 mg/L yielded mass ratios varying between 0.387 lbm O_2/lbm H_2O_2 (Average Soil) and 0.424 lbm O_2/lbm H_2O_2 (High Iron Soil). Due to calculated 95% confidence intervals for this treatment, no significant difference between soil types was observed. For treatment via 100,000 mg/L H_2O_2, significant differences were observed among some soil types. While mass ratios of the Average Soil, High Iron Soil, and Biologically Stimulated Soil were all approximately 0.4 lbm O_2/lbm H_2O_2, results for both the High pH Soil (0.3 lbm O_2/lbm H_2O_2) and High TOC Soil (0.2 lbm O_2/lbm H_2O_2) were significantly less than the values observed in the Average Soil, High Iron Soil, and Biologically Stimulated Soil. This was primarily due to the fact that the total soil hydrogen peroxide demands for these soil types were significantly less. The 100,000 mg/L application of hydrogen peroxide was enough to approach the total H_2O_2 demand of the soil, thereby leaving much of the H_2O_2 unreacted in the batch reactor.

For treatment via 10,000 mg/L H_2O_2, data indicated oxygen/peroxide mass ratios significantly lower than that of other treatments. Excluding the minimal mass ratio of the Ozonated Sand control, values for test soils ranged from 0.217 lbm O_2/lbm H_2O_2 in the High pH Soil to 0.242 lbm O_2/lbm H_2O_2 in the Biologically Stimulated Soil. Values for the 95% confidence intervals indicated that the differences among the different soil types for a 10,000 mg/L H_2O_2 application were

not significant. However, the differences in the mass ratios between the 10,000 mg/L H_2O_2 treatment and other treatments were in fact significant. This phenomena can be explained by the modified Fenton's Reaction mechanism as discussed in Chapter III. At higher concentration of H_2O_2, much of the hydrogen peroxide can be scavenged to produce perhydroxyl radicals, which can further result in O_2-producing irreversible reactions. The 10,000 mg/L application of H_2O_2 is much closer to optimum Fenton's Reaction conditions in which these scavenging radical reactions are limited, thereby limiting oxygen production (Watts et al., 1999; Chen et al., 2001).

Figure 8.4 presents the data listing the final O_2 volume percents observed in the 500-mL batch reactors at the completion of experimental runs. For the Ozonated Sand test control experiments, oxygen levels remained consistent with that of atmospheric conditions in the three experiments in which only H_2O_2 was added (10,000 mg/L, 50,000 mg/L, and 100,000 mg/L). However when ferrous (II) iron was added to the Ozonated Sand along with H_2O_2, the final O_2 concentration was approximately 70% (v/v). The final O_2 volume concentration was also roughly 70% for Fenton's Reagent application to the five other test soils (Average Soil, High pH Soil, High Iron Soil, High TOC Soil, and Biologically Stimulated Soil). For additions of 10,000 mg/L H_2O_2 to non-control test soils, the final observed O_2 concentration by volume was observed to be roughly 30%. For additions of solely 50,000 mg/L H_2O_2 to non-control test soils, the reactors performed very similarly to the Fenton's Reagent applications based on 50,000 mg/L H_2O_2, producing final O_2 volume concentrations of approximately 70%. When 100,000 mg/L H_2O_2 was added to the

batch reactors, final oxygen volume percents of approximately 90% were observed in the Average Soil, High pH Soil, High Iron Soil, and Biologically Stimulated Soil.

In all cases involving non-control experimental soils, the final observed oxygen concentrations observed were greater than the 23.5% (v/v) level at which flammability and explosion is severely enhanced. For application of 100,000 mg/L H_2O_2, a level consistent with common ISCO applications, oxygen levels reached values of almost 90% (v/v), considerably higher than the threshold normally conducive for a safe environment. These results indicate that ISCO practitioners must be very careful when dealing with hydrogen peroxide application into the subsurface. If the resulting oxygen is not properly released into the atmosphere, it can potentially linger in the subsurface and be subject to a serious explosion if accidentally ignited.

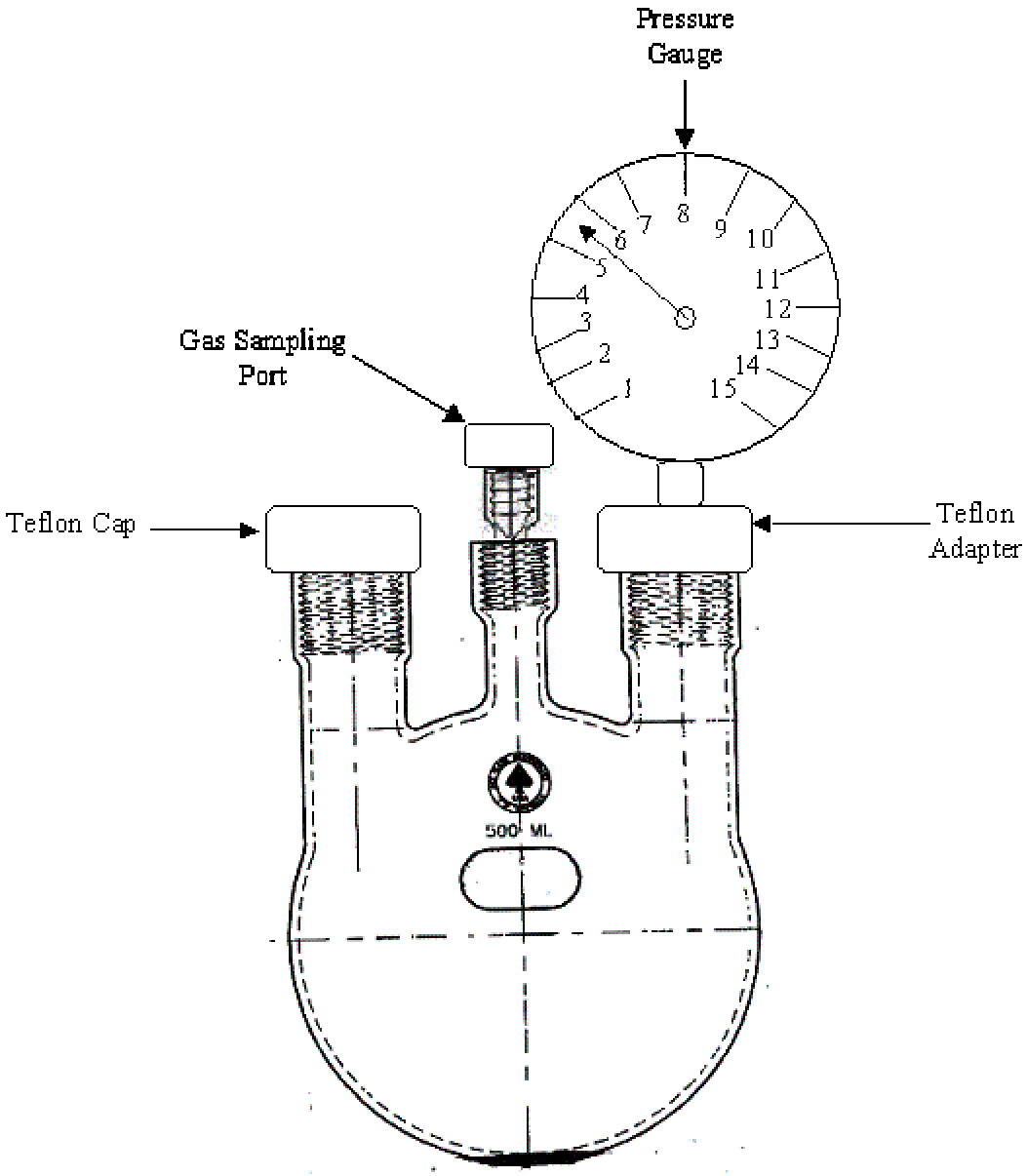

Figure 8.1: Diagram of O_2 Production Batch Reactor System (Taconi, 2004)

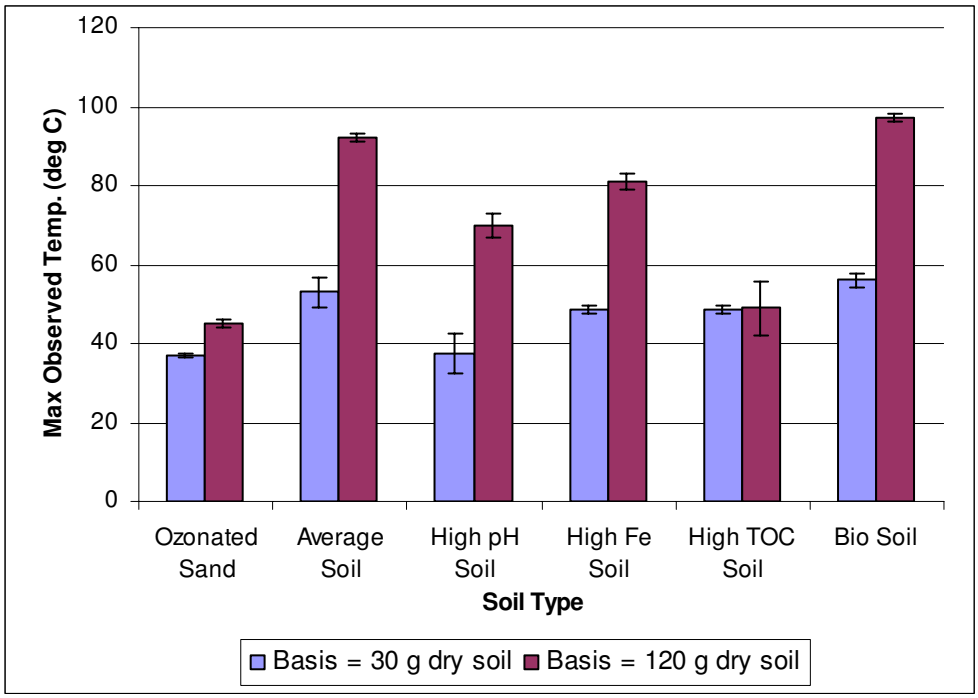

Figure 8.2: Maximum Observed Temperatures in Fenton's Reaction Experiments

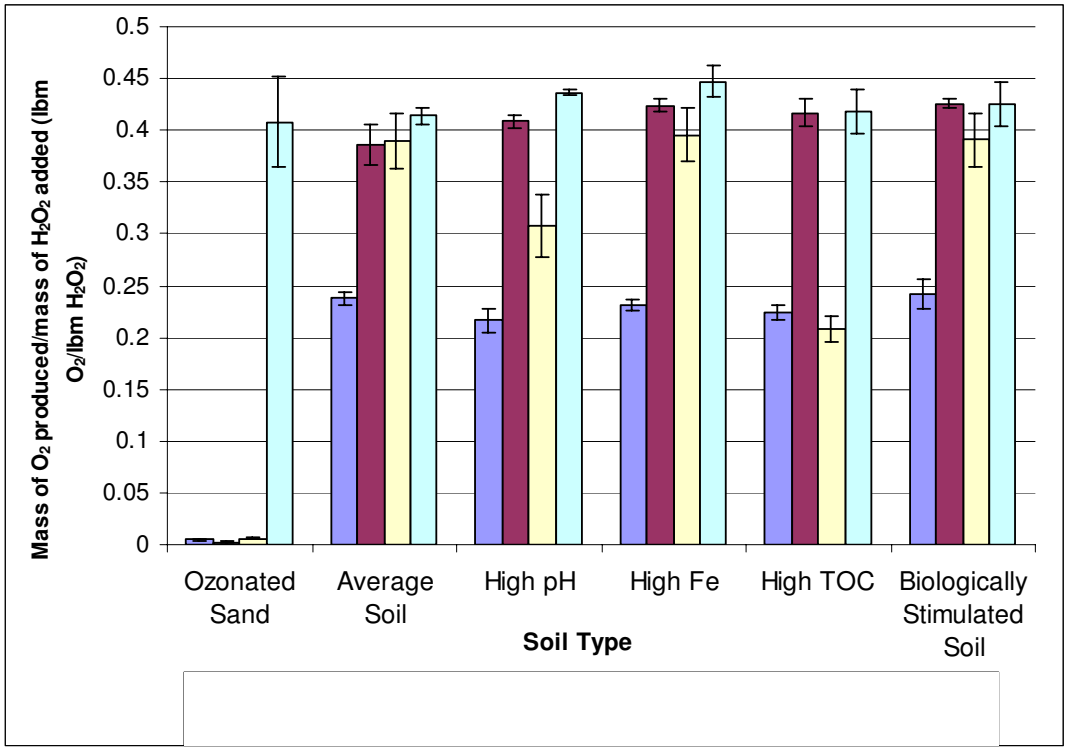

Figure 8.3: Ratio of Oxygen Produced to Hydrogen Peroxide Added for Multiple Soil Treatments

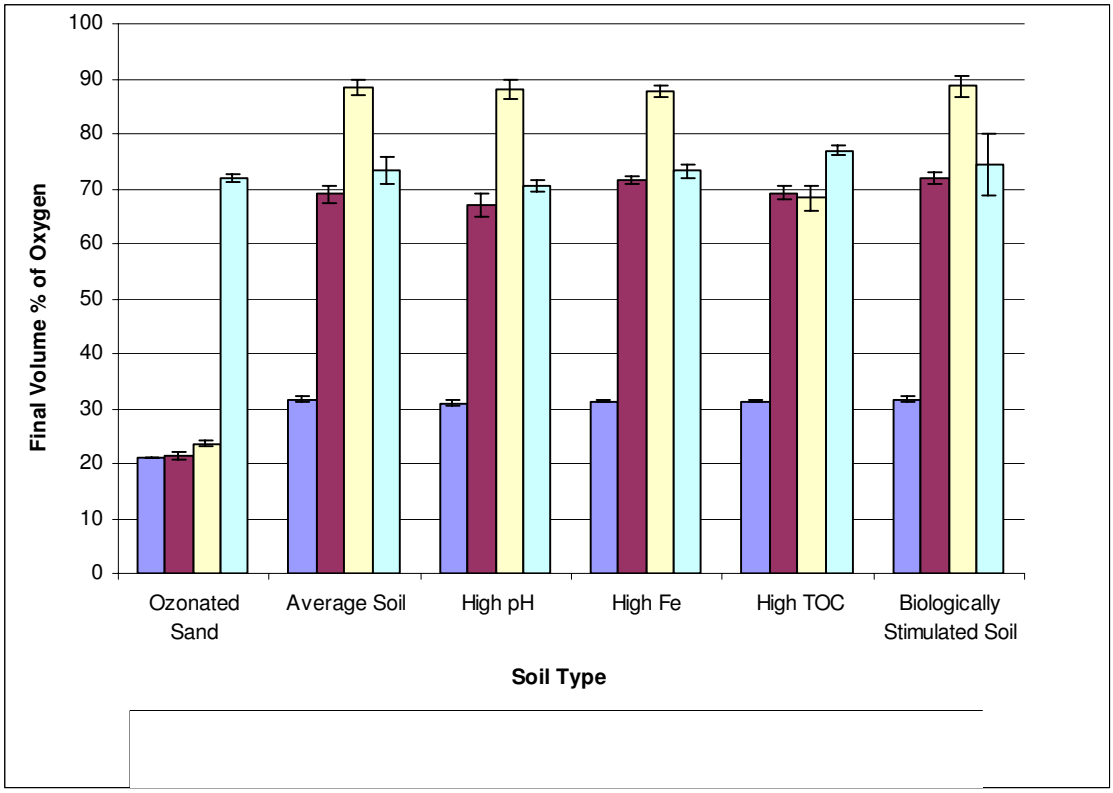

Figure 8.4: Maximum Volume Percents of Oxygen Obtained during H_2O_2 Batch Reactor Experiments

CHAPTER IX

KINETIC MODELING OF HYDROGEN PEROXIDE FATE WITHIN SOILS

Background

Reaction of hydrogen peroxide with various soil types was modeled via first order kinetics by Zappi's investigations into H_2O_2's use an a bioremediation oxygen source (Zappi et al., 2000). More detailed analysis of the reaction of H_2O_2 with additional soil types was performed in Chapter V following first order kinetic mechanisms as proposed by Fogler (1999). However, other kinetic fate models exist which can offer more realistic and accurate forecasts than simple first order kinetics.

The Langmuir-Hinshelwood Model can be used to model heterogeneous mechanisms based on the principles of Langmuir adsorption. This model utilizes a multi-step sequence of diffusion, adsorption/desorption, and reaction steps, each having its own particular reaction rate law. Hernandez (2002) successfully applied a Langmuir-Hinshelwood kinetic model towards the reaction of TNT with zero-valent iron and zinc. Additionally, the Langmuir-Hinshelwood Model was successfully utilized to describe dechlorination kinetics in the abiotic reduction of chlorinated solvents. This particular model was preferred in these experiments because it enabled

the inclusion of the decreasing reductive capacity of soil minerals within the kinetic model (Lee and Batchelor, 2002).

Objective

To investigate a potentially more powerful tool in the prediction of H_2O_2 degradation data, the use of the Langmuir-Hinshelwood Model was proposed as a potential modeling tool for the degradation of hydrogen peroxide in the Average Soil. This approach would factor not only the reaction of H_2O_2 with the soil surface, but it would also factor the Langmuir principles of adsorption and desorption (Fogler, 1999).

Methods and Materials

The reaction kinetics of hydrogen peroxide degradation within the Average Soil was studied under batch conditions using four different initial starting concentrations of H_2O_2 (20, 100, 1,000 and 10,000 mg/L). A 30 gram sample of dry Average Soil was added to a 250-mL Erlenmeyer flask. The flask was placed on a Thermolyne Bigger Bill series orbital shaker and shaken at 150 rpm throughout the duration of the experiment. 70 grams of the appropriate H_2O_2 solution was added to the flask at Time Zero to create a 30% (w/w) soil slurry. Samples were taken from the flask by extracting approximately 2-mL of sample using a 250 mL plastic luer-lok syringe and filtering the slurry through a 0.45-micron inline filter (Osmonics, Inc.; Cameo 30N Syringe Filter; Nylon; 30mm). The resulting filtrate was then analyzed to determine its H_2O_2 concentration. Samples were taken at approximately two to

three minute intervals during the experiments. In addition to the experiments at 150 rpm, the tests utilizing 20 mg/L and 10,000 mg/L H_2O_2 were repeated for a shaker speed setting of 250 rpm in order to determine if diffusion effects of H_2O_2 had any bearing on observed degradation rates. Experiments were run in duplicate for each initial H_2O_2 concentration.

Results and Discussion

Proposed Mechanism

The reaction of hydrogen peroxide (H_2O_2) with soil is a reaction that is catalyzed by the catalase enzyme as reported by Prescott, Harley, and Klein (2001).

$$2H_2O_2 \xrightarrow{catalase} 2H_2O_2 + O_2 \quad (1)$$

In addition to the H_2O_2 kinetic determinations made in Chapter V, it was proposed that hydrogen peroxide degradation can be better modeled based on more advanced kinetic evaluation which included steps consistent with Fogler's proposals for heterogeneous reactions. While traditional kinetic determinations such as those made in Chapter V assume a complete homogeneity of a reacting system, evaluations such as the Langmuir-Hinshelwood Model can be more akin to heterogeneous systems such as soil slurries due to its inclusion of a multi-step and multi-functional mechanism (Fogler, 1999). Figure 9.1 displays a visual diagram of the proposed Langmuir-Hinshelwood Model, a proposal that includes the following steps:

1. Diffusion of H_2O_2 from the bulk water to the soil surface

2. Adsorption of H_2O_2 onto the soil surface
3. Reaction of H_2O_2 at the soil surface
4. Desorption of reaction product from the soil surface
5. Diffusion of the reaction product from the soil surface into the bulk slurry

A shaker table setting of 150 rpm was selected to ensure that diffusion would not be the limiting factor when determining the parameters of the hydrogen peroxide degradation. Figure 9.2 shows the data used to justify the assumption that diffusion was not a limiting factor. For two different initial H_2O_2 doses, 20 mg/L and 10,000 mg/L, the calculated H_2O_2 degradation rates showed no significant deviation when subjected to the increased shaker speed setting of 250 rpm as compared to 150 rpm. This finding eliminates Steps 1 and 5 from consideration in a proposed mechanism. A mechanism for hydrogen peroxide decay was then developed using Steps 2, 3, and 4 as proposed. Step 2 represents the adsorption of a molecule of hydrogen peroxide onto a vacant reactive site (S) located on the surface of a soil particle, and it is represented by Equation 2:

$$H_2O_2 + S \longleftrightarrow H_2O_2 \bullet S \qquad (2)$$

where,

S = a vacant reactive site on the soil surface

H_2O_2•S = a reactive site linked with H_2O_2

Data in Chapter V regarding hydrogen peroxide kinetics indicated that the reaction rates of hydrogen peroxide in the soil phase were far greater than reaction rates of hydrogen peroxide in the groundwater phase. Therefore, it was assumed that the

majority of the hydrogen peroxide degradation occurred on the soil phase and that reaction with the bulk liquid was negligible. Thus, this overall system does appear to be actually a heterogeneous system.

Step 3 (Equation 3) represents the reaction of hydrogen peroxide at the surface of the soil.

$$H_2O_2 \bullet S \rightarrow H_2O \bullet S + \tfrac{1}{2}O_2 \qquad (3)$$

where,

$H_2O \bullet S$ = a reactive site linked with H_2O

O_2 = the oxygen gas produced in the reaction

This equation was derived from the reaction stoichiometry as reported in Equation 1.

The final step (Equation 4) considered in the development of a reactive model for H_2O_2 was the desorption of water from the soil surface.

$$H_2O \bullet S \longleftrightarrow H_2O + S \qquad (4)$$

The step assumes that vacant sites previously reacted will again be available for reaction. Therefore, this mechanism does not consider the effect of the reduction in available soil sites as the total peroxide demand for the soil is approached. Reaction rates for hydrogen peroxide degradation will decrease as available soil reactive sites become the limiting factor in the model.

Rate Law Development

Equation 5 represents the net rate of H_2O_2 disappearance from the soil slurry. It was derived from Equation 2 by factoring both the rate of adsorption and the rate of desorption of hydrogen peroxide from the soil surface. This net rate is as follows:

$$-r_A = k_A\left(C_{H_2O_2} * C_v - \frac{C_{H_2O_2 \bullet S}}{K_{H_2O_2}}\right) \quad (5)$$

where,

$-r_A$ = net rate of H_2O_2 adsorption onto soil surface, mg H_2O_2/(g soil * min)

k_A = rate constant for adsorption of H_2O_2 on surface, L/(mol active site*min)

C_{H2O2} =concentration of H_2O_2 in the bulk liquid, mg H_2O_2/L

C_V = concentration of vacant sites, mol active sites/g of dry soil

$C_{H2O2 \bullet S}$ =concentration of H_2O_2 adsorbed on soil surface, mg H_2O_2/g dry soil

K_{H2O2} = adsorption equilibrium constant for H_2O_2, L/mol active sites

Equation 6 shown below represents the equation derived from Equation 3 for the reaction of hydrogen peroxide at the soil surface. Because the reaction is irreversible only the one term in the equation exists. The net surface reaction rate is as follows:

$$-r_S = k_S * C_{H_2O_2 \bullet S} \quad (6)$$

where,

r_S = rate of H_2O_2 reaction at the soil surface, m H_2O_2/(g soil * min)

k_S = rate constant for reaction of H_2O_2 at soil surface, min^{-1}

Equation 7 shown below represents the equation for the desorption of liquid water from the soil surface. It was derived from Equation 4 by factoring both the desorption of liquid water from the soil surface and the re-adsorption of liquid water onto the soil surface. This net rate is described as follows:

$$-r_D = k_D * \left(C_{H_2O \bullet S} - K_{H_2O} * C_{H_2O} * C_V\right) \quad (7)$$

where,

r_D = net rate of H_2O desorption from soil surface, mg H_2O/(g soil * min)

k_D = rate constant for desorption of H_2O from surface, L/mol active site*min

K_{H2O} = adsorption equilibrium constant for H_2O, L/mol active sites

C_{H2O} = Concentration of H_2O in the soil slurry, mg/L

C_V = concentration of vacant sites, mol active sites/g of dry soil

A site balance was performed in order to determine the concentration of the vacant soil sites. The concentration of total sites, both occupied and vacant, is shown below:

$$C_t = C_V + C_{H_2O_2 \bullet S} + C_{H_2O \bullet S} \quad (8)$$

where,

C_t = concentration of total sites, mol active sites/g of dry soil

Steady State Approximation

The steady-state approximation was applied to the reaction intermediates (H_2O_2•S and H_2O•S) in order to derive the final kinetic model. This method is based on the assumption that intermediates within the reaction are consumed as quickly as

they are generated, and thus their concentrations remain constant during the course of the reaction. The net production rate of H_2O_2•S from Equations 2-4 is given by the following equation:

$$\text{Production rate of } H_2O_2\bullet S = k_A * C_{H_2O_2} * C_V \tag{9}$$

The net consumption rate of H_2O_2•S from Equations 2-4 is given by the following equation:

$$\text{Consumption rate of } H_2O_2\bullet S = \frac{C_{H_2O_2\bullet S}}{K_{H_2O_2}} + k_S * C_{H_2O_2\bullet S} \tag{10}$$

By applying the steady state approximation in which the production rate of H_2O_2•S is equal to the consumption rate of H_2O_2•S, the following equation for the concentration of H_2O_2•S results:

$$C_{H_2O_2\bullet S} = \frac{k_A * C_{H_2O_2} * C_V}{\frac{1}{K_{H_2O_2}} + k_S} \tag{11}$$

The net production rate of H_2O•S from Equations 2-4 is given by the following equation:

$$\text{Production rate of } H_2O\bullet S = k_S * C_{H_2O_2\bullet S} + \frac{C_{H_2O} * C_V}{K_{H_2O}} \tag{12}$$

The net consumption rate of H_2O_2•S from Equations 2-4 is given by the following equation:

$$\text{Consumption rate of } H_2O\bullet S = k_D * C_{H_2O\bullet S} \tag{13}$$

By applying the steady state approximation in which the production rate of H_2O•S is equal to the consumption rate of H_2O•S, the following equation for the concentration of H_2O•S results:

$$C_{H_2O\bullet S} = \frac{k_S * C_{H_2O_2\bullet S}}{k_D} + \frac{C_{H_2O} * C_V}{k_D * K_{H_2O}} \tag{14}$$

After plugging in the result of Equation 11 into Equation 14, the following equation for the concentration of H_2O•S results:

$$C_{H_2O\bullet S} = \frac{k_S * k_A * C_{H_2O_2} * C_V}{k_D * \left(\frac{1}{K_{H_2O_2}} + k_S \right)} + \frac{C_{H_2O} * C_V}{k_D * K_{H_2O}} \tag{15}$$

Having obtained concentrations of each intermediate, the total site balance to solve for the concentration of vacant sites. Equations 11 and 15 can be substituted into Equation 8 to yield the following equation for the concentration of vacant sites:

$$C_V = \frac{C_t}{1 + \left(\frac{k_S * k_A * C_{H_2O_2}}{k_D * \left(\frac{1}{K_{H_2O_2}} + k_S \right)} \right) + \left(\frac{k_A * C_{H_2O_2}}{k_S + \left(\frac{1}{K_{H_2O_2}} \right)} \right) + \left(\frac{C_{H_2O}}{k_D * K_{H_2O}} \right)} \tag{16}$$

This equation can be simplified by defining two empirical model constants as follows:

$$K_1 = \frac{k_A}{k_D * \left(\frac{1}{K_{H_2O_2}} + k_S \right)} * \left(k_S + k_D \right) \tag{17}$$

$$K_2 = \frac{1}{k_D * K_{H_2O}} \tag{18}$$

where,

K_1 = Langmuir empirical constant for H_2O_2 term

K_2 = Langmuir empirical constant for H_2O term

Equations 15-18 can be combined with the rate equation for the reaction of hydrogen peroxide at the soil's surface (Equation 6) to yield the following kinetic equation based on the Langmuir-Hinshelwood Kinetic Model:

$$-r'_{H_2O_2} = \frac{k_S * k_A * C_{H_2O_2}}{\frac{1}{K_{H_2O_2}} + k_S} * \frac{C_t}{1 + K_1 * C_{H_2O_2} + K_2 * C_{H_2O}} \tag{19}$$

The overall rate constant, k_1, can be defined by the following equation:

$$k_1 = \frac{k_S * k_A * C_t}{\left(\frac{1}{K_{H_2O_2}} + k_S\right)} \tag{20}$$

Therefore, the definition for the loss of H_2O_2 based on the steady-state approximation of the Langmuir-Hinshelwood Kinetic Model results, as shown below:

$$-r'_{H_2O_2} = k_1 * \frac{C_{H_2O_2}}{1 + (K_1 * C_{H_2O_2}) + (K_2 * C_{H_2O})} \tag{21}$$

Since the adsorption and desorption of water from the available soil sites is suspected to have little impact in comparison to the hydrogen peroxide, it is assumed that the K_2 term is negligible in this reaction mechanism and that the final definition for the loss

of H_2O_2 based on the steady-state approximation of the Langmuir-Hinshelwood Kinetic Model becomes:

$$-r'_{H_2O_2} = k_1 * \frac{C_{H_2O_2}}{1+(K_1 * C_{H_2O_2})} \quad (22)$$

The benefit of this model as compared to the simple first order kinetic model is that it includes the K_1 empirical constant, which is a function of the K_{H2O2} term that factors the adsorption of H_2O_2 onto the soil surface.

Application of the Proposed Kinetic Model

Hydrogen peroxide rates determined for batch experiments utilizing initial H_2O_2 concentrations of 20, 100, 1,000, and 10,000 mg/L were used in the kinetic model application. These values used in the kinetic model are given in Table 9.1. Polymath 5.1 was then used to fit these data to the kinetic model (Equation 22).

Final Results and Discussion of the Proposed Kinetic Model

The regression data determined for k_1 and K_1 are shown in Table 9.2. The values determined for k_1 (0.1029 min^{-1}) and K_1 ($3.853*10^{-5}$ L/mol active sites) indicate that k_1 is the dominant term whereas K_1 appears to be insignificant in the overall model. Since K_1 approaches zero in the Polymath 5.1 regression results, the model in essence simplifies to a generic first order kinetic model. A basic analysis of these results indicates that while the Langmuir-Hinshelwood model is definitely applicable to the degradation of H_2O_2 in soil slurries, it appears to offer no new information or modeling ability with regards to the system involving hydrogen

peroxide's degradation within soil slurries as compared to the a simple first order kinetic response. However, some evidence towards the model's applicability was obtained by further analysis of the model and its associated data.

Figure 9.3 shows a comparison between the actual hydrogen peroxide degradation rates observed in batch experiments and the hydrogen peroxide degradation rates predicted by the model for the four tested data points. While the overall R^2 value for the Langmuir-Hinshelwood Model is very high (0.99), the plot does indicate some noticeable deviations between the model and experimental results as the initial concentration of H_2O_2 decreases to values less than 1,000 mg/L. Figure 9.4 shows a second comparison of the observed H_2O_2 degradation rates and the H_2O_2 degradation rates as predicted by the Langmuir-Hinshelwood Model. This plot further shows that the chosen model is far more accurate for higher H_2O_2 concentrations as opposed to the H_2O_2 concentrations that are 100 mg/L or less.

The data suggests that the Langmuir-Hinshelwood empirical constant (K_1) is relatively insignificant at H_2O_2 concentrations 1,000 mg/L or greater. It is possible that the deviation observed at the lower concentrations may indicate more dependence on H_2O_2 adsorption. One potential explanation for this observation deals with the availability of reactive sites on the soil surface. A soil particle will only have a fixed number of available reactive sites in which H_2O_2 molecules can adsorb. For conditions in which H_2O_2 is in excess and the available soil sites are limiting (i.e. high concentrations of H_2O_2), a steady state appears to be reached in that as soon as one H_2O_2 molecule adsorbs and reacts at a soil site, an additional molecule is ready

and available for reaction upon the completion of the first molecule's reaction. However, as the H_2O_2 concentration is reduced, there must be a point corresponding to a certain H_2O_2 level in which the number of available reactive soil sites is actually greater than the number of H_2O_2 molecules present (Fogler, 1999). It is suspected that this transition to the condition in which the H_2O_2 molecules become the limiting reagent in the reaction is causing the observed deviations in the Langmuir-Hinshelwood Model. Similar results in the Langmuir-Hinshelwood Model were observed by Hogmin et al. (2005) in their modeling investigations into photocatalytic oxidation of gas phase-formaldehyde over titanium dioxide. Their kinetic analyses showed that for low concentrations of formaldehyde, the calculated reaction coefficient was lower and the half-life was longer as compared to formaldehyde at a higher initial concentration.

Summary of the Proposed Kinetic Model

The Langmuir-Hinshelwood Model offered promising results in its ability to predict H_2O_2 degradation rates at multiple concentrations of H_2O_2. The model had more accuracy at the higher levels of H_2O_2 than at low levels of H_2O_2, possibly due to the differences in whether the soil reactive sites or the H_2O_2 was the limiting reagent during the reaction of hydrogen peroxide. Due to the fact that concentrations of H_2O_2 typically applied in remediation via *in situ* chemical oxidation are at levels of between 4% and 20%, preliminary results of this model indicate that the Langmuir-Hinshelwood Model could be accurately applied to ISCO applications using hydrogen peroxide (ITRC, 2005).

Table 9.1: H_2O_2 Rate Data Used in Langmuir-Hinshelwood Kinetic Model

$[H_2O_2]_0$ (mg/L)	**$-r_{H2O2}$ (mg/L*min)**
20	11.387
100	45.34
1,000	103.25
10,000	1674

Table 9.2: Regression Analysis of H_2O_2 Rate Data Using Langmuir-Hinshelwood Approach

Variable	**Value**
k_1	0.1029 min^{-1}
K_1	$3.853*10^{-5}$ L/mol active sites
R^2	0.9993

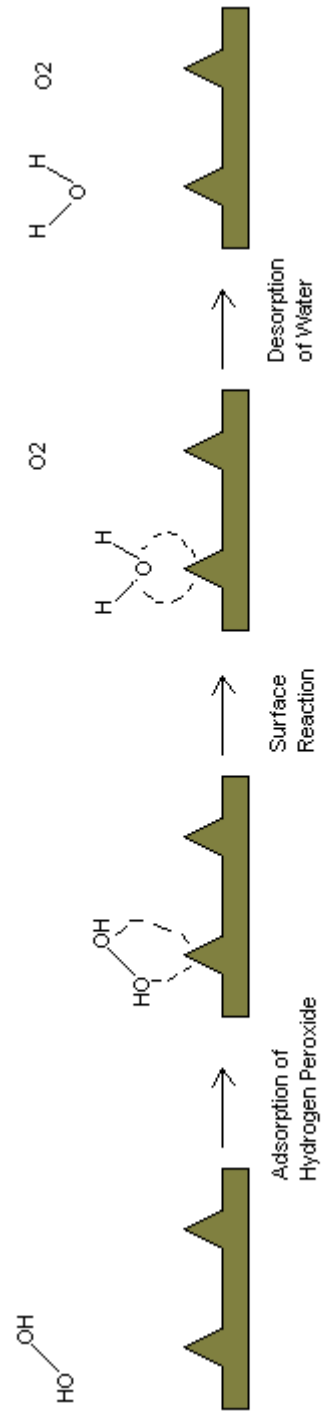

Figure 9.1: Diagram of Proposed Langmuir-Hinshelwood Model

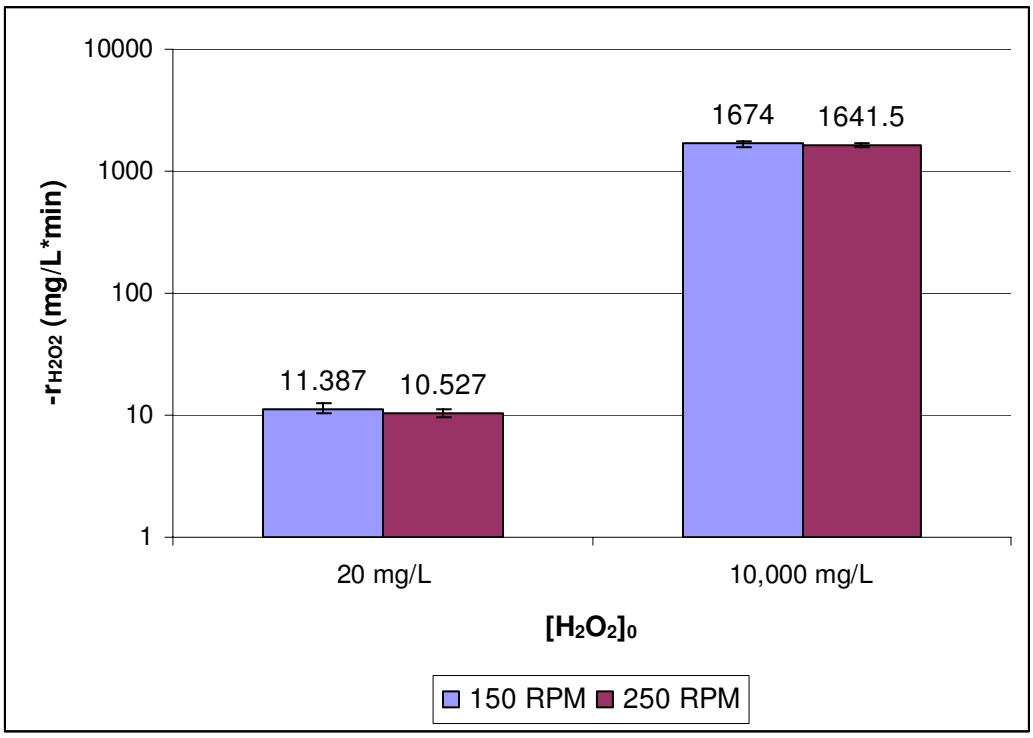

Figure 9.2: Analysis of Diffusion Effects in H_2O_2 Degradation Modeling

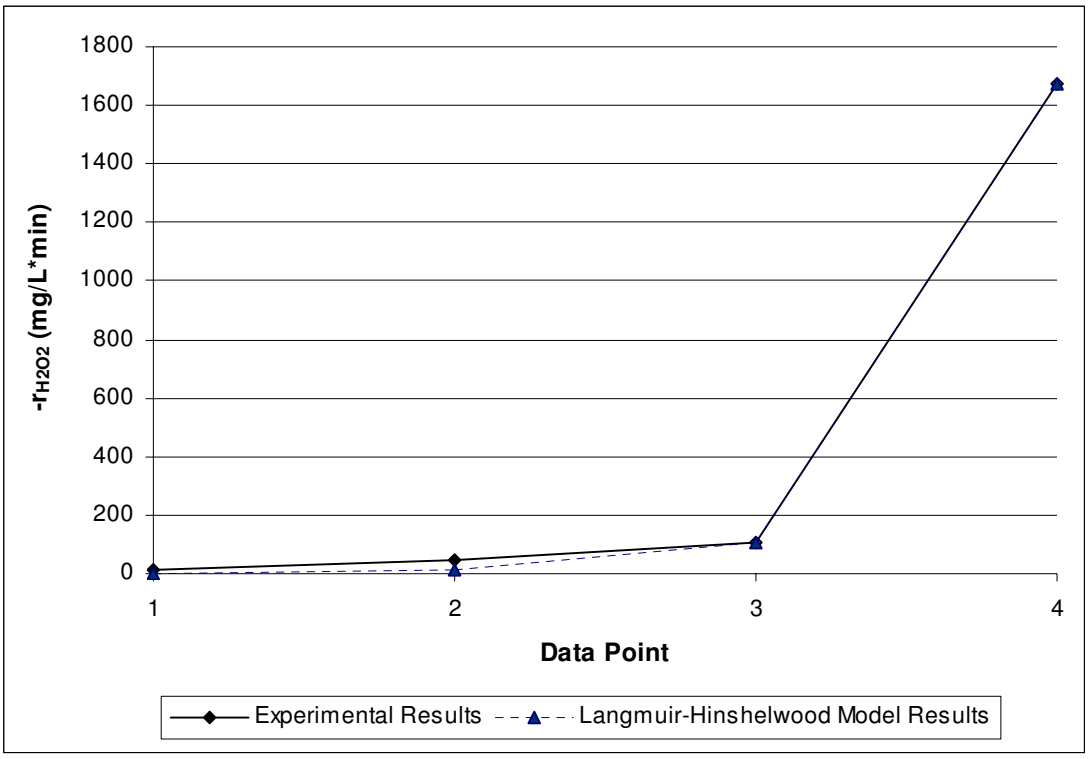

Figure 9.3: Data Point Comparison of the H_2O_2 Degradation Experimental and Model Results; Data Points 1, 2, 3, & 4 correspond to $[H_2O_2]_0$ = 20, 100, 1,000, and 10,000 mg/L H_2O_2 respectively

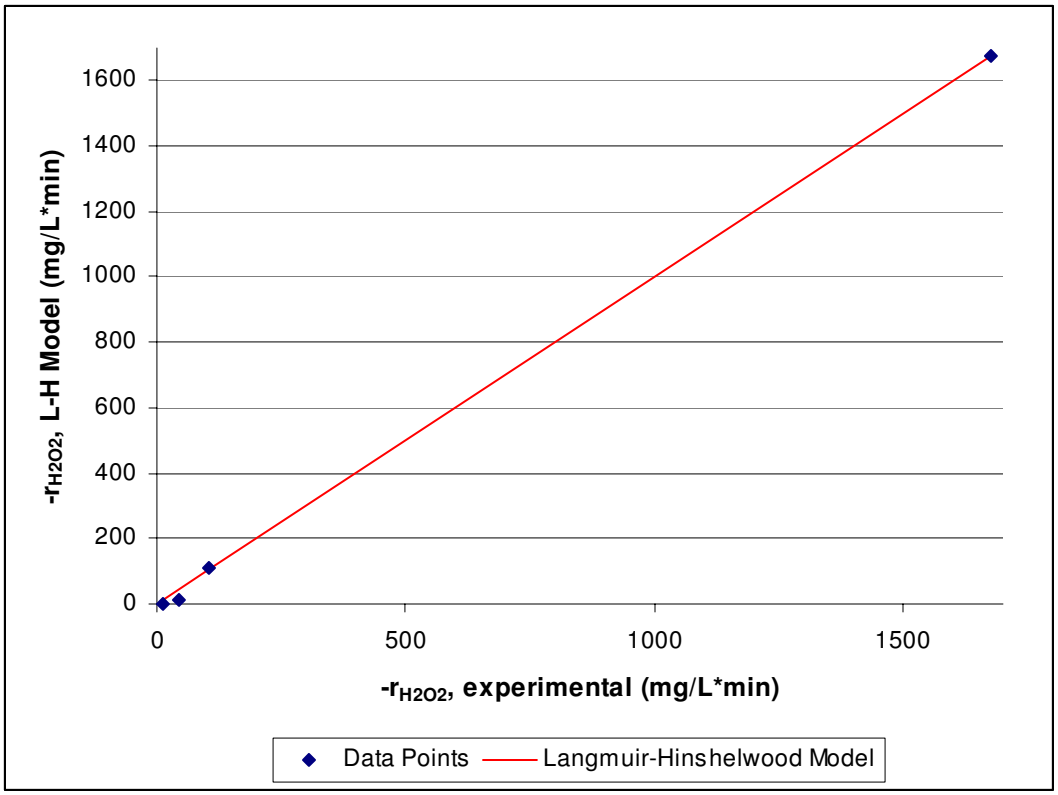

Figure 9.4: Deviation of the Langmuir-Hinshelwood Model from Observed Experimental Results

CHAPTER X

IMPACT OF *IN SITU* CHEMICAL OXIDATION ON AEROBIC SOIL MICROBIAL POPULATIONS

Background

Oxidizing agents such as hydrogen peroxide are known to be extremely harmful to certain types of bacteria. Some types of bacteria such as obligate aerobes and facultative anaerobes contain enzymes such as superoxide dismutase and catalase, which catalyze the destruction of superoxide radicals and H_2O_2. These reactions take place as follows (Prescott et al. 2001):

$$2O_2^{\bullet} + 2H^+ \xrightarrow{\text{superoxide\_dismutase}} O_2 + H_2O_2$$

$$2H_2O_2 \xrightarrow{catalase} 2H_2O + O_2$$

Because strict anaerobes lack both of these protective enzymes, they are rendered far more susceptible to destruction by powerful oxidizers such as hydrogen peroxide (Prescott et al., 2001). Elkins et al. (1999) reported on the protective role that catalase plays in *Pseudomonas aeruginosa* biofilm resistance to H_2O_2. They found that planktonic cells exposed to dosings of hydrogen peroxide showed a significant decrease in cell viability, whereas the cell viability for the biofilm cells remained near 90%.

In Dieng's thesis work at Mississippi State University (2003), research was conducted investigating the coupling of both bioremediation and oxidative remediation technologies for the treatment of polycyclic aromatic hydrocarbons (PAHs). He performed a biotreatment remediation step, a chemical oxidation step, and then a final biotreatment step in the remediation of PAHs. The objective of his research was to enhance the bioavailability of PAHs by transforming the PAHs into compounds that were more readily biodegradable. Results showed significantly improved remediation of PAH compounds by combining bioremediation and chemical oxidation technologies.

Objective

Because of the potential benefits of coupling bioremediation and *in situ* chemical oxidation (ISCO) technologies, it was desired to determine the impact of ISCO on the health of native aerobic microbial populations within the soil matrix. Therefore, a set of experiments was proposed utilizing standard plate counts on both treated and non-treated soil samples in order to determine the effects of chemical oxidation on soil aerobes.

Methods and Materials

Soil Treatments

Several batch treatment strategies were selected for evaluation of impact to microbial populations within different soil matrices. These included treatment using

distilled water, ferrous iron, hydrogen peroxide, Fenton's Reagent, ozone, or peroxone. A listing of all treatments evaluated is shown in Table 10.1. All treatments were performed in duplicate and tested for impact to aerobic microbial populations.

All treatments were performed in 30% (w/w) soil slurries. These slurries were created by adding 120 grams of soil (dry basis) to a 1,000-mL Erlenmeyer flask and adding enough solution such that the total mass of liquid was 280 grams. For the pre-treatment (initial) runs, distilled water was utilized as the liquid solution in the soil slurry creation. The soil/DI-water slurries were allowed to shake for 24-hours on a Bigger Bill Thermolyne orbital shaker at 150 rpm. Following a 24-hour equilibration, slurries were sampled for microbial analysis.

For treatment via hydrogen peroxide, a stock solution of 100,000 mg/L H_2O_2 was used as the applied solution in order to generate the 30% (w/w) soil slurry. The slurry was allowed to shake for 24-hours at 150 rpm in order to allow the hydrogen peroxide to react with both the native bacteria and natural components within the soil. Following a 24-hour reaction period, slurries were sampled for microbial analyses.

For treatment via Fenton's Reaction, a stock solution of 5,000 mg/L Fe^{2+} solution was utilized as the liquid solution when creating the 30% (w/w) slurries. The soil/ferrous iron slurries were then allowed to shake for 24-hours at 150 rpm to allow the ferrous iron to diffuse into soil pores and reach equilibrium. Following this shake period, a dose of 30% (w/w) stock H_2O_2 was added to the soil slurry such that the initial concentration of hydrogen peroxide corresponded to an initial level of

100,000 mg/L H_2O_2. Following a 24-hour reaction period with the hydrogen peroxide, slurries were sampled for microbial analyses.

For treatment via ozone, a stock solution of DI-water was utilized as the liquid solution when creating the soil slurries. The Ozonology, Inc. ozone generator was used to continuously apply ozone to the soil slurry via a gas sparge stone at an O_3 concentration of 3% (gas phase) for 3 hours at a flow rate of 2 SCFH. A stir plate and accompanying stir bar were used on the #5 setting to ensure ample mixing of the slurry. The peroxone treatment was performed in the exact same fashion as the ozone treatment. However, following the first 10 minutes of ozone application, 30% (w/w) H_2O_2 was injected into the reactor such that the initial hydrogen peroxide concentration reached the desired 1,000 mg/L concentration. Ozone was continually applied over the final 170 minutes of the treatment process, yielding a total ozone treatment time of 3 hours. Following the treatment via ozone or peroxone, soil slurries were allowed to shake at 150 rpm for 21-hours and then sampled for microbial analysis.

Additionally, due to the issues concerning the exothermic nature of Fenton's Reaction, a hot plate treatment of the High Iron Soil was performed in order to determine the impact temperature had on native soil bacteria without the presence of oxidizers. Treatment of this particular soil type was performed by heating the 30% (w/w) soil slurry to 80 °C. After stabilizing the slurry temperature at 80 °C for five minutes, the soil slurry was then taken off of the hot plate and allowed to cool to room temperature prior to sampling.

Creation of Agar Plates

Difco Plate Count Agar was used as the medium for viewing growth of microbial populations. The agar powder was purchased pre-made from Fisher Scientific (Ref. # 247910), however the approximate formulation can be viewed in Table 10.2. A 23.5 g/L solution of the agar was created by adding by adding 70.5 grams of the agar powder and diluting it with distilled water to a total volume of 3.0 liters. The agar solution was then stirred and heated on a Corning Stirrer/Hot Plate until the solution reached boiling and had maintained boiling for approximately one minute and all the powder had clearly dissolved into solution. The agar solution was then transferred into 250-mL Wheaton storage bottles. The bottles were capped (but not fully sealed), and the agar bottles were autoclaved at 121 degrees Celsius for 15 minutes to eliminate any residual bacteria that might be present. Following the autoclave, the bottles were removed from the incubator and allowed to cool for 15 minutes. Prior to the pouring of the plates, the mouths of the bottles were flamed over a Bunsen burner to reduce the possibility of contamination. The agar was then poured into standard, pre-sterilized petri dishes (100 x 15mm) such that the agar solution fully covered the bottom of the plate. Plates were then covered with their lids and allowed to solidify for two hours. Plates were then stacked and stored in a refrigerator until needed for experimental use.

Creation of Dilution Tubes

Dilution tubes were created by using a 0.85% (w/w) solution of sodium chloride (Sigma Aldrich, CAS 7647-14-5) in distilled water. Following the creation of the dilute salt solution, the pH was adjusted to 7.0 by adding (drop-wise) a 0.125 M solution of potassium hydroxide. 9-mL of the pH-adjusted NaCl solution were added to 10-mL Pyrex test tubes; these tubes were then autoclaved at 121 degrees Celsius for 15 minutes, capped, and allowed to cool to room temperature prior to use.

Slurry Sampling and Dilutions

Following the treatment of the soil slurries via the appropriate oxidizer applications, 1 mL of the 30% (w/w) soil slurry was removed using a 10-mL sterilized pipette and applied to the first dilution tube that contained 9-mL of the NaCl solution. This tube (the 10^{-1}dilution) was shaken using a Fisher Vortex (Genie 2 model) for 10 seconds on the maximum #8 setting. One milliliter of the 10^{-1} dilution was withdrawn using a 1-mL pre-sterilized plastic pipette and added to a fresh dilution tube. This newly created dilution tube became the 10^{-2} dilution. This newly created tube was then vortex mixed, and 1 mL of the 10^{-2} dilution was added to a fresh tube to create the 10^{-3} dilution. This process of serial dilutions was repeated until a 10^{-6} dilution tube was acquired. For each of the duplicate treatments, 3 sets of dilutions and corresponding plates (A-C) were created due to the high degree of randomness in bacterial populations. So for each oxidative treatment, the plate sets included multiple dilutions of a 1A, 1B, 1C, 2A, 2B, and 2C samplings. During the entire process of creating the dilutions, the Bunsen burner was utilized to flame the

mouths of test tubes immediately after opening and prior to re-sealing the caps. Also, when test tubes were opened, they were maintained at a 45-degree angle rather than upright. These steps enabled the prevention of any unnecessary contamination from non-native bacteria.

Spreading of Samples onto Agar Plates

0.1-mL of liquid from the appropriate dilution was added to the center of the agar plate using a 1-mL plastic pipette. During this transfer an extra dilution factor was added due to the amount of liquid added (0.1-mL instead of 1-mL). Therefore, adding 0.1 mL of the 10^{-2} dilution to a plate yields a plate with a dilution factor of 10^{-3}. After each plate had the appropriate dilutions added, the liquid was spread over the entire plate using sterilized hockey stick style petri dish spreaders. Following the spreading of the plates, the tops were applied; plates were then flipped over and transferred to the Fisher Scientific Isotemp Incubator (Model 304) and incubated for 72 hours at 35°C. Once the incubation was complete, the plates were observed, and the number of individual bacterial colonies was counted. Only plates containing between 30 and 300 individual colonies were considered statistically valid bacterial counts (Prescott et al., 2001).

Results and Discussion

Data Analysis

Once the appropriate plate count numbers and dilution factors were determined for each specific soil and treatment type, Equation 1 was used to determine the number of colony forming units per milliliter of soil slurry:

$$CFU_V = N * D \quad (1)$$

where,

CFU_V = colony forming units per milliliter of soil slurry, cfu/mL

N = number of individual colonies observed

D = dilution factor of observed plate

The data calculated for CFU_V's were then converted to a standard basis of colony forming units per gram of dry soil by using Equation 2:

$$CFU_M = CFU_V * \frac{V_L}{M_S} \quad (2)$$

where,

CFU_M = colony forming units per gram of dry soil, cfu/g

CFU_V = colony forming units per milliliter of soil slurry, cfu/mL

V_L = volume of liquid in soil slurry, mL

M_S = mass of dry soil in soil slurry, g

Impact of ISCO on Aerobic Populations

Results for experiments performed on the Average Soil, High pH Soil, High Fe Soil, and Biologically Stimulated Soil are shown in Figures 10.1, 10.2, 10.3, and 10.4, respectively. Results were plotted to compare the base-ten logarithmic of the aerobic heterotrophic plate count populations observed (cfu/g) with the individual soil/treatment type. Data for the microbial populations within the High TOC soil were not included since plate count experiments did not yield plates that contained more than 30 colonies, even at the zero-order dilution factor. It was concluded that due to the lack of observed aerobic populations and the relatively low pH (~4.0) of the soil, most all of the microbial populations contained within the High TOC Soil were of the anaerobic variety. Anaerobic bacteria are common producers of organic acids in soil environments, and this process can often lower the pH of soil environments (Montville et al., 1985; Prescott et al., 2001). Another potential reason for the low levels of aerobic populations dealt with the low initial pH of the soil sample caused by the large quantities of organic acid. While there exist certain types of extremophiles able to survive in low pH environments, most aerobes are not compatible with thriving in low pH environments. Acidic conditions are commonly known to denature and destroy macromolecules and speed up the molecular breakdown rates of various microorganisms (Prescott et al., 2001; Messerli et al., 2005).

Data for all of the soil types tested showed similar results regarding the effects of each generic treatment type. The impact of simple additions of ferrous (II) iron

solution displayed insignificant impact towards soil microbial populations in all of the soil types. Treatment via 100,000 mg/L H_2O_2 significantly reduced the order of magnitude of bacterial populations in all four soil types. Similarly, treatment via the Fenton's Reaction treatment strategy produced significant reductions in the number of bacterial populations observed within soil samples. Application of a gas stream of ozone at a concentration of 3% resulted in significant decreases in bacteria levels in all soil types. Treatment via the peroxone treatment strategy showed significant reductions in microbial populations for every soil type except for the High pH Soil.

In order to better compare which ISCO treatments were most detrimental to microbial populations, the net difference in magnitude orders was calculated using Equation 3:

$$\Delta[\log(\text{cfu/g})] = M_i - M_f \quad (3)$$

where,

$\Delta[\log(\text{cfu/g})]$ = Net decrease in avg. order of magnitude of microbial populations

M_i = Avg. order of magnitude of initial microbial populations

M_f = Avg. order of magnitude of post-treatment microbial populations

Figure 10.5 shows $\Delta[\log(\text{cfu/g})]$ for all of the oxidative treatment strategies (H_2O_2, Fenton's Reaction, O_3, and peroxone) tested in these experiments. The ISCO treatment that appeared to be the most aggressive towards the health of native bacteria was the Fenton's Reaction treatment strategy. Microbial populations during these treatments were reduced by approximately four orders of magnitude in the

Average, High pH, and Biologically Stimulated Soils and by over six order of magnitude in the High Iron Soil. Treatment via 100,000 mg/L H_2O_2 reduced bacterial populations in the Average Soil by approximately three and half orders of magnitude, in the High pH Soil by approximately two orders of magnitude, in the High Fe Soil by approximately three orders of magnitude, and in the Biologically Stimulated Soil by approximately four and half orders of magnitude. For treatments based on ozone, the data indicated that the threat of ISCO to bacteria was greater during treatments via peroxone as opposed to treatments in which only ozone was applied.

Several important trends were observed during these experimental sets. Firstly, two treatments were based on the application of 100,000 mg/L H_2O_2, one treatment that utilized H_2O_2 only and another that used manually added ferrous (II) iron to catalyze Fenton's Reaction. When comparing these two treatments among different soil types, the reduction in aerobic microbial populations due to Fenton's Reaction was significantly greater than that of H_2O_2-only for both the High pH Soil and the High Iron Soil; for the Average Soil and Biologically Stimulated Soil, both the 100,000 mg/L H_2O_2 treatment and the Fenton's Reaction treatment displayed similar impacts on soil aerobes. In the High Fe soil, oxidation via Fenton's Reaction (5,000 mg/L Fe^{2+}/100,000 mg/L H_2O_2) reduced all traces of significant bacterial populations. Figure 10.6 correlates the H_2O_2 kinetic rate constant for each soil type with the change in microbial populations (Δlog[cfu/g]) observed for the two hydrogen peroxide-based treatments. An evident correlation exists (R^2=0.83) suggesting that as a soil type's reaction with H_2O_2 became more aggressive, a more detrimental impact

on soil aerobic populations results. These Fenton's Reaction versus H_2O_2-only observations can be based on a key principle reported on in literature. Prescott et al. (2001) reported that powerful oxidizers are a significant threat to certain types of bacteria that lack enzyme-based defense mechanisms. Reactions such as Fenton's Reaction and peroxone rely heavily on the production of powerful, highly reactive hydroxyl radicals that drive reaction mechanisms. Hydroxyl radicals have a significantly greater oxidative potential than ozone or hydrogen peroxide alone (Glaze et al., 1992; Siegrest et al., 2001). Therefore, it stands to reason that these more powerful oxidizers will potentially cause greater harm to bacteria within the soil matrix than primary oxidants.

A second trend noticed within the experimental data was that technologies that utilizing hydrogen peroxide tended to cause a more substantial reduction in microbial populations than did technologies based solely on ozone. A review of the literature does indicate that O_3 is in fact hazardous to the health of bacteria. Whiteside and Hassan (1987) performed research that examined the induction and inactivation of catalase and superoxide dismutase of *Escherichia coli* by ozone. Firstly, they observed both an inhibition of *E. coli* growth and a decrease in cell viability after exposure to O_3. Secondly, the authors found that *E. coli* significantly increased the activities of catalase and superoxide dismutase by factors as high as 1,160% and 400% respectively. These data seemed to verify the results from ISCO experiments suggesting that ozone was in fact detrimental to the health of native bacteria. One primary reason for this difference could be due to the highly different

solubilities of H_2O_2 and O_3. While H_2O_2 is often applied at concentrations at up to 50%, O_3 is far less soluble in water than H_2O_2. The maximum solubility of ozone at atmospheric pressure and room temperature is generally observed to be approximately 20 ppm. While ozone has been more commonly used in water treatment than hydrogen peroxide, treatment of soils can be much more problematic, and it is reasonable to expect that the impact of low O_3 solubility on the reaction efficiency within soil environments will be compounded exponentially as compared to the aqueous phase (Heynes et al., 1999; Amarante, 2000; ITRC, 2005). It is therefore hypothesized that the relatively low solubility of ozone in the soil slurries was the primary cause of the limited impact of ozone applications to soil microbial populations.

Temperature's Impact on Soil Aerobic Populations

In addition to the impact of oxidizers on the population of aerobes within soil environments, an additional variable also plays a role in the observed detriment of microbial viability. This variable is based on the known thermodynamics of Fenton's Reaction. Fenton's Reaction is an extremely exothermic process that has even been known to boil off soil moisture during ISCO applications (Amarante, 2000). These results were also seen in the observations in Chapter VIII during the Fenton's Reaction temperature experiments. Figure 10.7 displays the temperatures observed during Fenton's Reaction treatments in microbial impact experiments. Temperatures reached as high as 97°C in the Biologically Stimulated Soil and reached temperatures higher than 80°C in both the Average Soil and High Fe Soil. An additional

experiment was performed on the High Iron Soil to isolate the impact that the increased temperature had on the health of aerobic microorganisms. The result of this experiment is included in Figure 10.3 and shows that the increase in temperature from ambient conditions to 80°C had a significant impact on soil microbial populations. This temperature change reduced bacterial populations by approximately three orders of magnitude, even without the addition of chemical oxidizers. High temperatures are known to be lethal to many microorganisms because the conditions denature enzymes, proteins, and transport carriers. Most microorganisms fall into the category of mesophiles, whose conditions for healthy growth occur between 20 and 45°C (Prescott et al., 2001). Kaleli and Islam (1997) observed these same results in experiments on wastewater bacteria. As experimental temperatures were raised to 60 and 80°C, bacteria actively died off due to protein denaturing and the inability of microorganisms to perform metabolic processes outside the bounds of the cell. Because of both the experimental observations comparing temperature-only and Fenton's Reaction impact to microbial populations and a review of pertinent literature, it is apparent that both the increased temperature and the oxidizer application are having an additive impact on the health of aerobes within the soil matrix.

Summary

Results clearly indicated that treatment of different soil types by ISCO processes had a significant detrimental impact on aerobic soil bacteria populations

due to both the reaction with oxidizers and the effects of increased temperature due to the exothermic nature of reactions. Microbial reductions were observed to decrease by as many as six orders of magnitude in some ISCO treatments. These observations are of great importance of ISCO practitioners such as Dieng (2003) who seek to couple chemical oxidation with biotreatment. While a chemical oxidation treatment cycle could theoretically follow a biotreatment cycle without problems, observed results in these experiments suggest that the reverse case might not be nearly as effective. Fenton's Reaction was clearly shown to have a detrimental impact on native bacteria within the soil matrix. If a remediation treatment strategy called for an initial treatment via an ISCO technology and a follow-up treatment strategy involving bioremediation, this scenario would most likely prove to be infeasible. Generally, native bacteria are stimulated during bioremediation to enhance the biodegradation of contaminants. If aerobic bacterial populations were detrimentally impacted by prior ISCO applications, the bioremediation step in the treatment strategy would be much more difficult to successfully execute.

Table 10.1: Experimental Matrix for Impact of ISCO on Biomass Populations

Treatment	**$[Fe^{2+}]_{initial}$ (mg/L)**	**$[H_2O_2]_{initial}$ (mg/L)**	**$[O_3]_{applied}$ (wt. %)**
Initial	0	0	0
Ferrous Iron	5,000	0	0
Hydrogen Peroxide	0	100,000	0
Fenton's Reaction	5,000	100,000	0
Ozone	0	0	3%
Peroxone	0	1,000	3%

Table 10.2: Difco Plate Count Agar Composition

Component	**Concentration in Agar Solution (g/L)**
Pancreatic digest of Casein	5.0
Yeast Extract	2.5
Dextrose	1.0
Agar	15.0
Total Concentration of Difco PCA	*23.5*

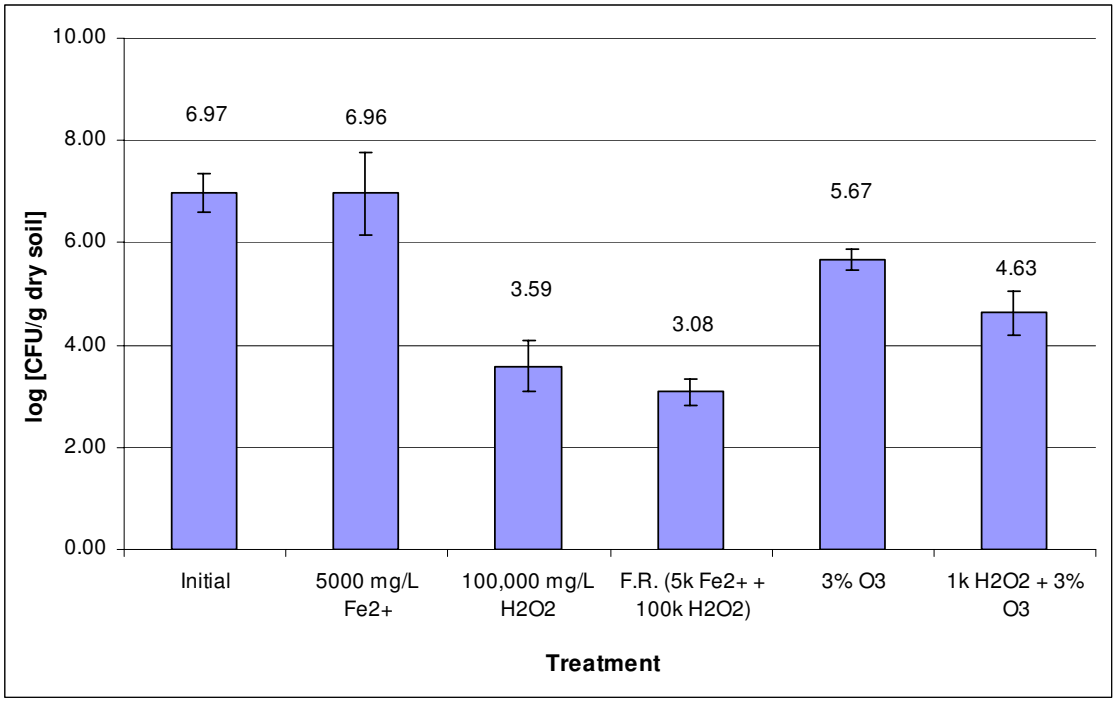

Figure 10.1: Impact of ISCO on Aerobic Microbial Populations in Average Soil

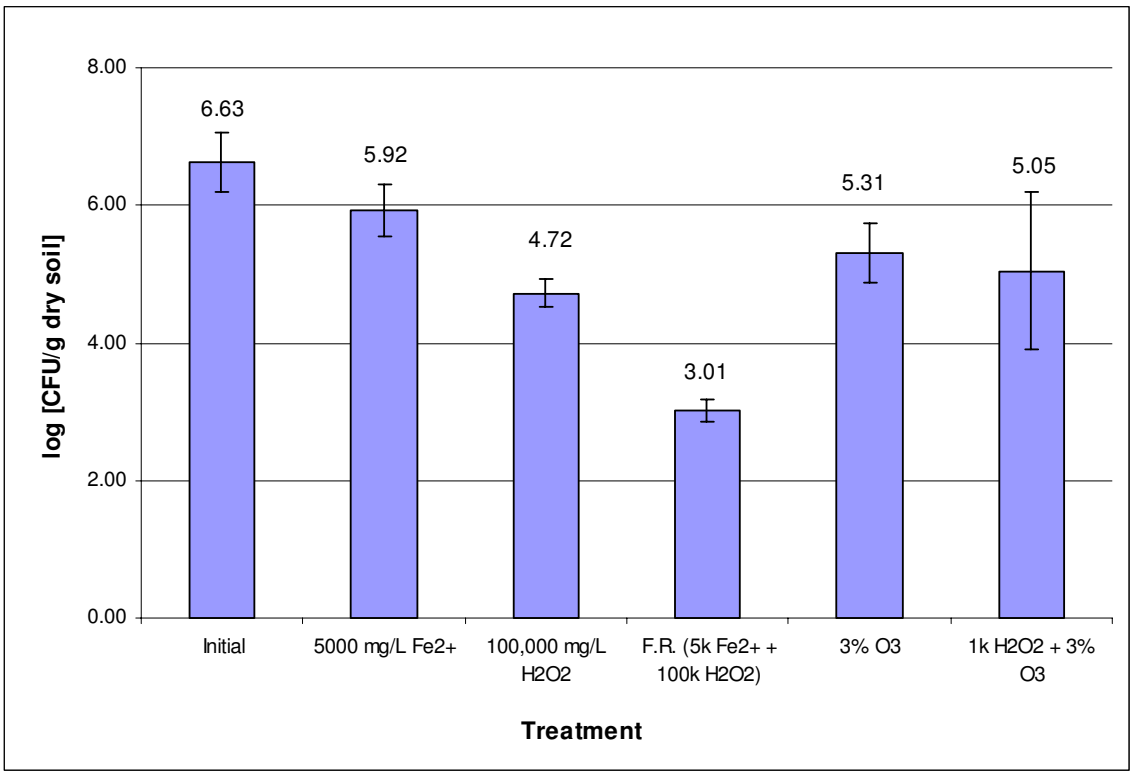

Figure 10.2: Impact of ISCO on Aerobic Microbial Populations in High pH Soil

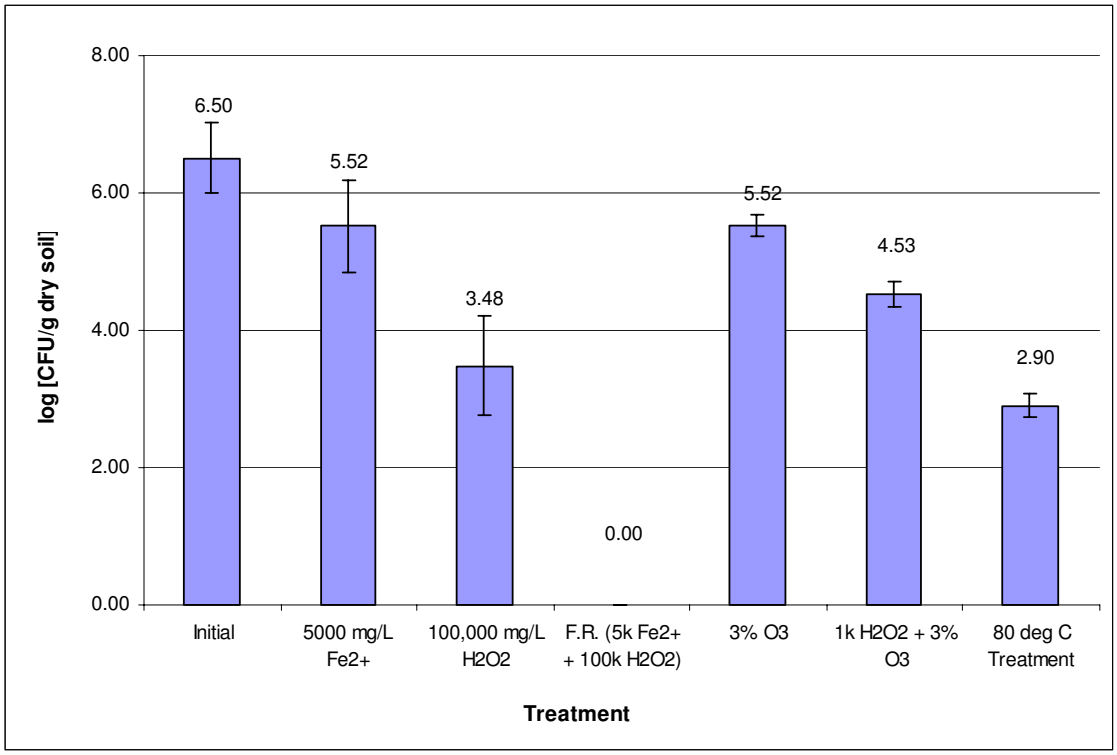

Figure 10.3: Impact of ISCO on Aerobic Microbial Populations in High Fe Soil

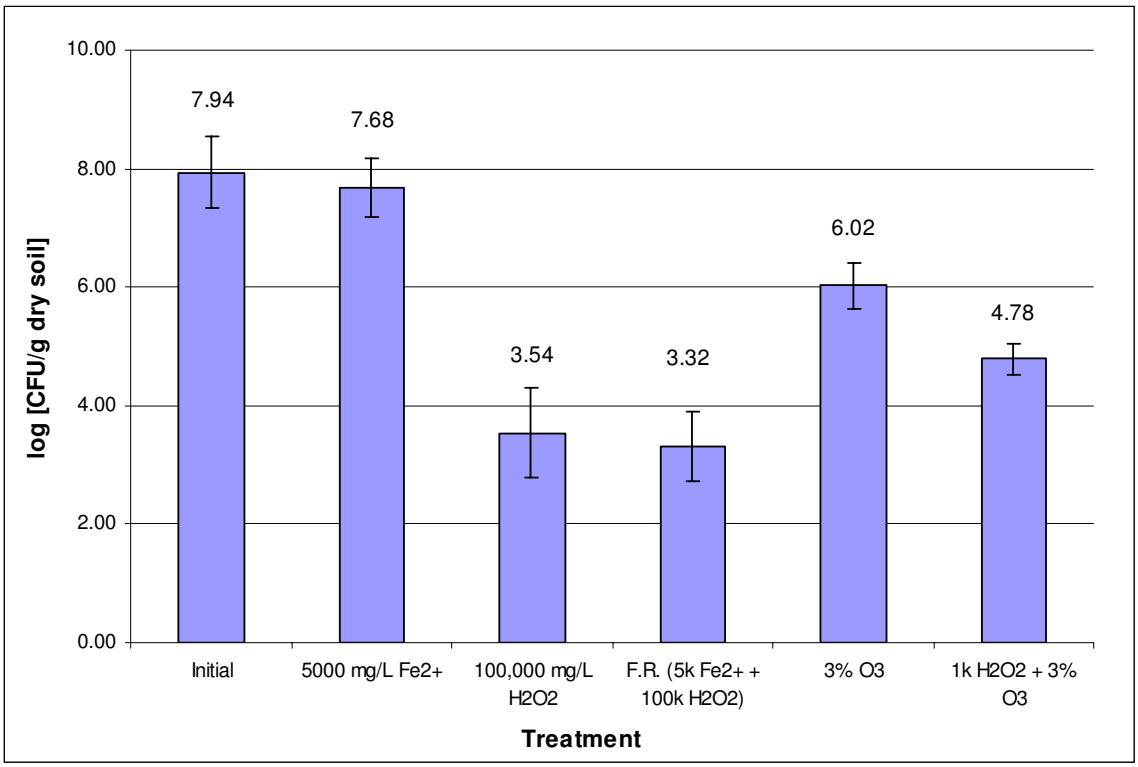

Figure 10.4: Impact of ISCO on Aerobic Microbial Populations in Biologically Stimulated Soil

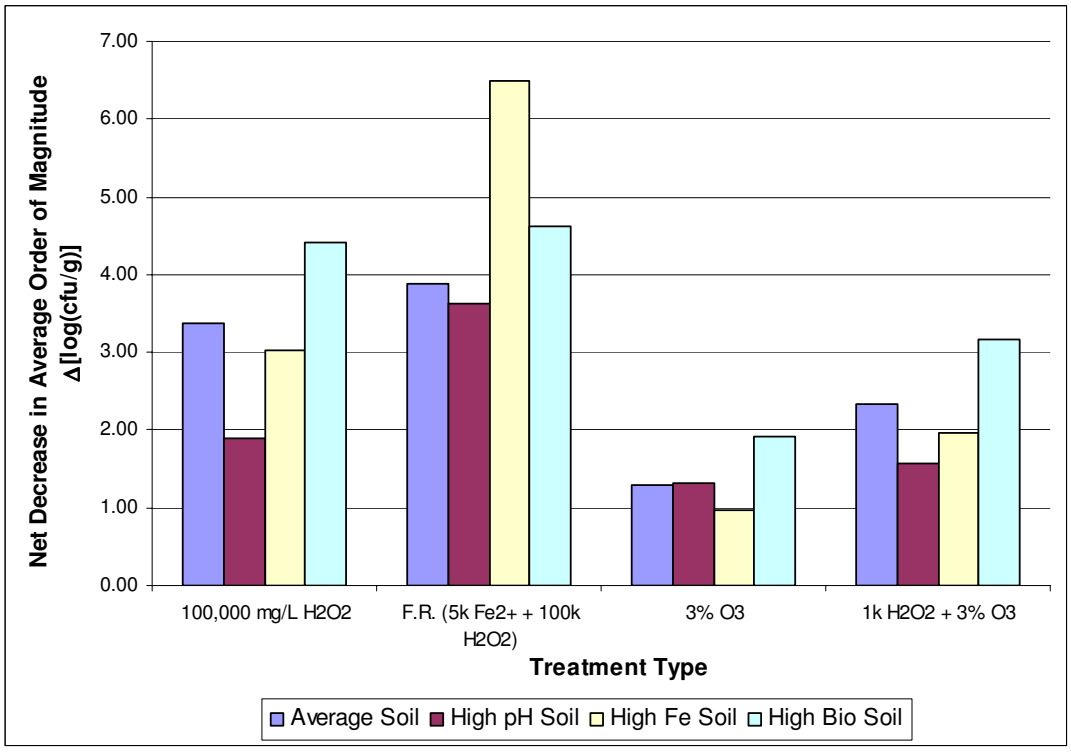

Figure 10.5: Net Decrease in Average Order of Magnitude for ISCO Treatments on Average, High pH, High Fe, and Biologically Stimulated Soils

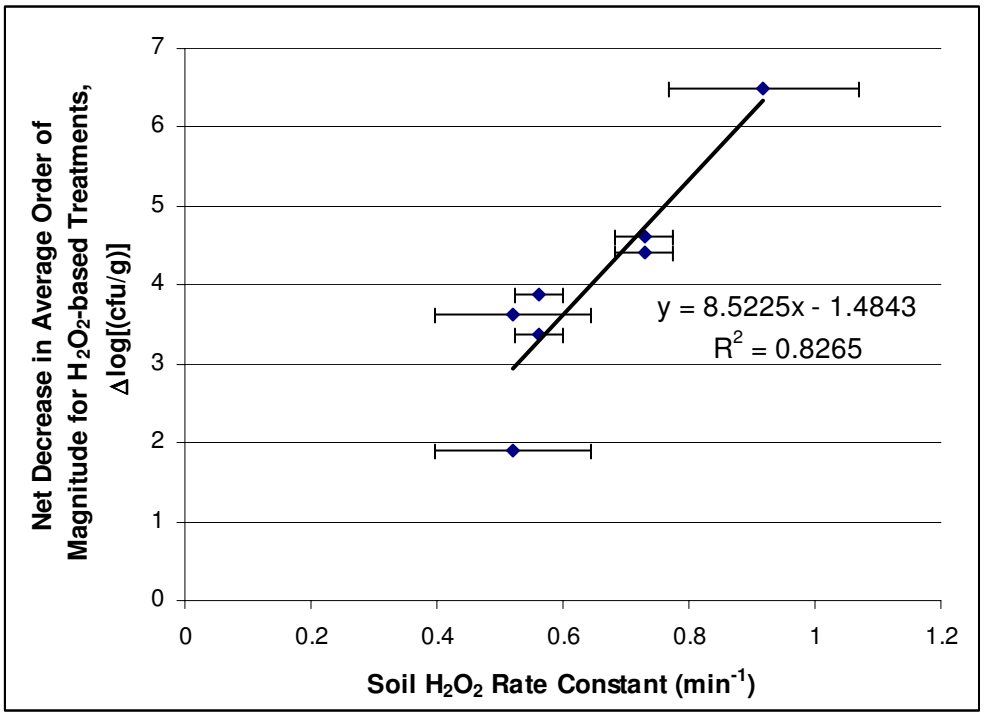

Figure 10.6: Soil H_2O_2 Kinetic Rate Constant versus Net Decrease in Soil Aerobes Correlation for H_2O_2-based treatments (Excluding High Fe – 100k H_2O_2 Treatment Data Point)

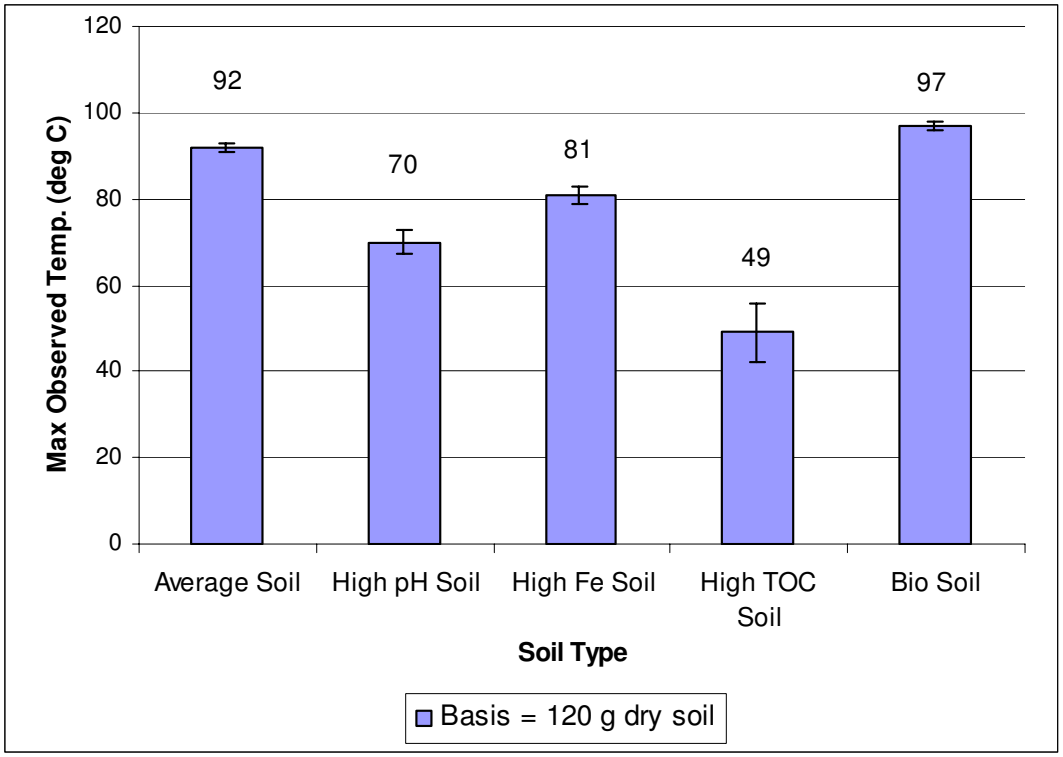

Figure 10.7: Maximum Observed Temperatures in Fenton's Reaction ISCO Treatment during Aerobic Heterotrophic Plate Count Studies

CHAPTER XI

IMPACT OF *IN SITU* CHEMICAL OXIDATION ON SOIL HYDRAULIC CONDUCTIVITY

Background

One very critical issue when dealing with the transport of ferrous iron, hydrogen peroxide, and other oxidizers into the soil matrix is soil hydraulic conductivity (i.e. permeability). The most important factor in ISCO success is being able to successfully transport the oxidizer from the surface storage tanks to the contaminant located within the subsurface (Amarante, 2000). Soil hydraulic conductivity values are highly dependent on the physical characteristics of the particular soil, and the nature of the soil environment will have a dramatic impact on the success of the ISCO treatment (LaGrega et al., 2001). Because of the relatively high permeability of sandy soils, Fenton's Reagent can often be applied successfully with few challenges (Amarante, 2000).

In addition to the initial hydraulic conductivity of the soil, *in situ* chemical oxidation has been shown to have an impact on the transport properties within the soil environment. During treatment, insoluble byproducts are produced via reaction with the hydrogen peroxide and hydroxyl radicals. These byproducts can serve as a hindrance to flow by blocking the channels available for flow of liquid reagents

(Amarante, 2000). Significant permeability changes have been observed due to the impact of particle release within the soil environment. When fine particles are mobilized within a soil environment, pore necks can become clogged and hinder transport within the soil matrix, thereby reducing the hydraulic conductivity (Blume et al., 2002).

Objective

Despite preliminary indications that ISCO impacts soil transport properties, no known literature was found to exist which experimentally quantified the impact of ISCO on soil hydraulic conductivity. Therefore, experiments were conducted to examine the impact of both H_2O_2-based and O_3-based ISCO process reagents on soil hydraulic conductivity. A series of column studies was developed that simulated application of oxidizers within natural soil environments and allowed for the determination of pre-treatment and post-treatment hydraulic conductivity values using Darcy's Law.

Methods and Materials

Column Supplies for H_2O_2-based ISCO Treatments

Clear PVC columns (12" length x 1" ID) were purchased from the U.S. Plastic Corp. and were used to evaluate changes in soil permeability during a simulation of an *in situ* chemical oxidation treatment via hydrogen peroxide and Fenton's Reagent. Figure 11.1 shows the complete setup of an individual soil column. A combination of

PVC and Swagelok fittings were used in column assembly. A stainless steel wire screen and a sample of TNS Advanced Technologies R080 geotextile material were applied to the base of the soil column. This setup provided a means to keep the soil sample stationary within the column while allowing liquids to pass freely, with negligible impact on flowrate. Rubber gaskets were used in the interior of the column, and Teflon tape was applied to all threads in an effort to prevent fluid leaks within the column.

In order to produce hydraulic gradients similar to field application, the pressure gradient was controlled by the application of a constant head pressure from inert nitrogen gas. A nitrogen tank and regulator were assembled, and a column manifold was created, allowing for as many six columns to be run simultaneously from the same nitrogen tank/regulator system. This allowed for multiple runs to occur under an identical operating pressure. The diagram of the column manifold is shown in Figure 11.2.

Column Assembly for H_2O_2-based ISCO Treatments

Prior to any soil addition, the brass fittings, wire screen, geotextile material, and gasket were applied to the lower end of the column (Figure 11.1). A constant packing procedure was developed in order to ensure that every column and every soil type was loaded in an equivalent manner. Soils were sieved using a No. 10 sieve to remove large random soil particles that might have significant effects on permeability readings. A hex-bolt (length = 10 & 3/8”; weight = 402 grams) was purchased from East Mississippi Lumber Company for use as a compaction hammer; the edges were

rounded such that the compaction hammer would drop smoothly through the 1” ID column. Gravity was used as the driving force behind the compaction hammer in order to prevent the human error involved in a manual force. A compaction hammer drop was defined to be the vertical release of the device from the point in which the base of the compaction hammer was directly even with the top of the 1” female adapter at the apex of the column. One inch of soil was added to the column, and five drops of the compaction hammer were then applied. This process was repeated for the second, third, and fourth inch additions of soil. Due to the soil packing procedure, the total length of soil column following these additions was less than four inches. A fifth addition of soil was added that brought the total length of the soil column to exactly four inches, and this was followed by ten drops of the compaction hammer. Distilled water was then added to the column such that the initial liquid level was six inches above the surface of the soil column. The upper portion of the column was then assembled and connected into the column manifold.

Column Operating Conditions for H_2O_2-based ISCO Treatments

All soil column experiments were run in the laboratory at room temperature (70°F). For every application of liquid, an initial volume of liquid (distilled water, iron solution, or hydrogen peroxide) was applied to the column such that the liquid height was six inches above the surface of the soil column. The pressure at the outlet of the column was atmospheric, and the nitrogen pressure regulator controlled the pressure in the interior of the column. A nitrogen pressure of 20 psig was applied to

all soil types except the High pH soil, which was run at a pressure of 40 psig due to the extremely low initial soil hydraulic conductivity.

Column Equilibration for H_2O_2-based ISCO Treatments

It was expected that a certain amount of water must be flushed through the soil column in order to saturate the soil column and achieve steady-state conditions. In addition to the column saturation requirements, a natural settling of soil particles was anticipated, which would be a cause for initial fluctuations in volumetric flow and therefore soil hydraulic conductivity calculations. Initial experiments sought to determine how much distilled water must be passed through a soil column of Average Soil in order to generate steady-state conditions. The initial six inches of distilled water were passed through the soil column. Once this run was completed, the nitrogen regulator was turned off, the top of the column was opened, and a second addition of distilled water was added to the column. The column was resealed and the inert nitrogen pressure was again applied. This process was repeated until the volumetric flow rate observed through the soil column converged to a stable value. The height of liquid within the column was recorded as a function of time during each run of distilled water, and the experiment was performed in duplicate.

Determination of Hydraulic Conductivity Changes due to H_2O_2-based ISCO

In order to determine the change in permeability due to oxidation, the initial permeability was determined prior to the oxidation of the soil by passing distilled water through the soil column. Following column assembly, an initial six inches of

distilled water was passed through the column, and the height of the liquid within the column was recorded as a function of time. When the net liquid height above the soil column approached zero, the nitrogen pressure was shut off. This procedure was repeated for a second and third application of distilled water. Liquid heights as a function of time were recorded within the column for each application of distilled water. Data from these DI-water applications enabled the calculation of the initial hydraulic conductivity of the soil column.

Both the application of hydrogen peroxide and Fenton's Reagent were analyzed for their impact on soil hydraulic conductivity. A 100,000 mg/L H_2O_2 solution was added to the column such that the initial liquid height was six inches above the apex of the soil column, in the exact same manner as the DI-water flushes. In total, two applications of peroxide were applied to the column, and liquid heights as a function of time were recorded within the column.

In order to assess the hydraulic conductivity effects of Fenton's Reagent, a similar procedure was used. Following the initial three applications of DI-water, the nitrogen pressure was shut off, and six inches of 5,000 mg/L Fe^{2+} solution was added to the column. The pressure was re-applied, and the first application of ferrous iron solution was passed through the column. Once the net height above the soil column apex approached zero, the column pressure was shut off, and a second application of ferrous iron was performed in the same manner as the first. After the second application of 5,000 mg/L Fe^{2+}, it was assumed that enough ferrous iron solution had been passed through the column to simulate a field application. Two subsequent

applications of 100,000 mg/L peroxide were then applied via the same peroxide application method previously described. Net liquid heights were recorded as a function of time for every application in all columns, and all experiments were run in triplicate.

Column Supplies and Assembly for O_3-based ISCO Treatments

The same PVC columns were used as was discussed in the hydraulic conductivity tests using hydrogen peroxide and Fenton's Reagent. The only difference in the construction of the column were that two ¼" threaded holes were bored into the side of the PVC column. One hole was centered 5" above the base of the column, and the other was centered 10" above the base of the column. Teflon tape was applied to two Swagelok brass fittings (¼" Female NPT x ¼" Tube), and these were affixed into each of the bored holes. The diagram of this column is shown in Figure 11.3. The column was loaded with soil and packed in the same manner as previously described in the experiments based on hydrogen peroxide and Fenton's Reagent. ¼" Copper tubing was used to connect the nitrogen regulator to the ball valve above the column.

Application of Ozone to Soil Column

Due to limitations of the applied pressure of the ozone generator output, ozone was introduced into soil columns in the liquid phase. However, due to the rapid auto-degradation of ozone, a process involving a constant recycle stream of ozonated DI-water was employed. The process flow diagram used in the application of ozone to

soil columns is shown in Figure 11.4. A tank of pressurized N_2 was used as the driving force behind liquid flow through the soil column in a similar manner as the H_2O_2 and Fenton's Reagent experiments.

A 1,000-mL Erlenmeyer flask was utilized as the recycle reactor to supply ozone to the system. A metering pump (Fluid Metering Inc., Model QG 50) was used to recycle a fresh solution of ozonated distilled-water from the recycle reactor to the interior of the column, ½" above the apex of the soil itself. A five-holed #10 silicone stopper was affixed to the Erlenmeyer flask as shown in Figure 11.4. Four of the holes were used as the recirculation inlet, recirculation outlet, ozone inlet, and ozone outlet respectively. A 50-mL plastic syringe was connected in series with the fifth hole to allow for both sampling and introduction of H_2O_2 and distilled water as needed. All of the tubing was ¼" rigid tygon tubing.

Startup Procedure for O_3-based ISCO Treatments

Following the complete setup of the soil column and equipment as shown in Figures 11.3 and 11.4, 800 mL of DI-water was added to the 1,000-mL Erlenmeyer flask (recycle reactor), and the solution was stirred using a magnetic stir bar and stir plate (#5 setting). For initial (pre-oxidation) test runs, the metering pump was initiated at its maximum (#10) setting, and liquid was allowed to reach a level 6" above the apex of the soil column. At this time, the ball valve controlling the N_2 pressure was opened to allow for a constant 20 psig N_2 head to be applied to the system. The ball valve on the recirculation exit stream was then adjusted to keep the

process at steady state, with the liquid level stabilized at 6" above the top of the soil column.

For ozone-based oxidative treatments, the DI-water application was followed up with either a treatment via ozone or a treatment via peroxone. The recycle reactor was emptied, and 800-mL of fresh DI-water was added to the flask. The solution was stirred using a magnetic stir bar and stir plate (#5 setting). For ozonation treatments, a gas stream of ozone (5.5 wt. % O_3) was then continuously applied to the recycle reactor at a rate of 2 scfh. After 10 minutes of ozonation, the metering pump was turned on, and the same procedure was followed as in the DI-water application. Ozonation of the recycle solution continued throughout the duration of the experiment. For peroxone treatments, a gas stream of ozone (5.5 wt. % O_3) was then continuously applied to the recycle reactor at a rate of 2 scfh. After 5 minutes of ozonation, a quantity of 30% (w/w) H_2O_2 stock solution was applied to the reactor such that the concentration of H_2O_2 within the flask was 1,000 mg/L. Following an additional 5 minutes of mixing, the metering pump was turned on, and the same startup procedure was followed as in the DI-water application.

Determination of Hydraulic Conductivity Changes due to O_3-based ISCO

In order to determine the change in permeability due to oxidation, the initial permeability was determined prior to the oxidation of the soil by passing distilled water through the soil column. Initially, 50-mL of DI-water was passed through the column in order to allow the soil in the columns to settle and reach steady state with respect to the hydraulic gradient. An additional 50-mL of DI-water was then passed

to generate the data allowing for the determination of the initial hydraulic conductivity. In the H_2O_2-based column experiments mentioned previously, liquid heights within the column were recorded as a function of time to calculate hydraulic conductivities. This method was not applicable to ozone-based treatments because the column height remained stabilized at six inches. To calculate the hydraulic conductivities in ozone-based experiments, the volume of liquid in the effluent of the column was recorded as a function of time.

Both the application of ozone and peroxone were analyzed for their impact on soil hydraulic conductivity. For treatment via ozone and peroxone, the column start-up procedures were followed as previously described. Once start-up had been completed, 50-mL of the ozone or peroxone-based liquid solution was allowed to pass through the soil column in the same manner as the DI-water. All experiments were run in duplicate.

Results and Discussion

Determination of Hydraulic Conductivity

For all experiments, Darcy's Law was used to calculated hydraulic conductivity values both before and after ISCO treatment. Darcy's Law (Equation 1) and its accompanying equation (Equation 2) for the calculation of the hydraulic gradient are shown as follows (La Grega et al., 2001):

$$q = k * i * A \tag{1}$$

$$i = \frac{h_1 - h_2}{l} \quad (2)$$

where,

q = volumetric flow rate, in^3/s

i = hydraulic gradient, in/in

k = hydraulic conductivity, in/s

A = inside cross-sectional area of column, in^2

h_1 = pressure acting on the soil column, in. H_2O

h_2 = pressure head at the column outlet, in. H_2O

l = length of soil column, in

While the formula for the calculation of hydraulic conductivity values remains the same for any soil column set-up, the method for determining appropriate values was handled differently for the H_2O_2 and Fenton's Reagent experiments as opposed to the O_3 and peroxone experiments. This was due to the fact that different column setups were applied to each scenario: a standard falling-head setup for H_2O_2 and Fenton's Reagent experiments versus a constant head setup for O_3 and peroxone systems. The only difference in calculations dealt with the how the volumetric flow rate (q) was determined.

For H_2O_2 and Fenton's Reagent experiments, net liquid heights were recorded as a function of time during these experimental runs. The interstitial liquid velocity (V_i) through the column was then calculated for each treatment via Equation 3, and the volumetric flow rate was then calculated using Equation 4:

$$V_i = \frac{\Delta y}{\Delta t_1} \quad (3)$$

$$q = V_i * A \quad (4)$$

where,

V_i = interstitial velocity, in/s

Δy = change in liquid column height, in

Δt_1 = length of time required for corresponding Δy, sec

A = inside cross-sectional area of column, in^2

Theoretically, the volumetric flow rate could have been calculated directly by measuring the total volume of the liquid effluent as a function of time. However, the calculation of V_i was preferred due to the potential for liquid volume loss due to evaporation. Volumetric flow rates were determined using Equation 4 after calculating the interstitial velocities.

For O_3 and peroxone experiments, net liquid heights did not change due to the recirculatory nature of the column setup. Since ozonated distilled water solution was continuously recharged into the column, the liquid height within the column remained constant. Therefore, the volumetric flow rate (q) was determined by measuring the amount of effluent exuded from the column in a given hour time period by using Equation 5:

$$q = \frac{\Delta V}{\Delta t_2} \quad (5)$$

where,

q = Volumetric flow rate, in^3/s

ΔV = Volume exuded from the column during measured period, in^3

Δt_2 = length of time corresponding with corresponding ΔV, sec

The hydraulic gradient was calculated using Equation 2. For the pressure head terms (h_1 & h_2), the pressure head due to the liquid column was neglected. The hydraulic gradient calculation becomes much more difficult if the pressure head acting on the soil column (h_1) is viewed to be changing with respect to time. This assumption is logical since a pressure of 10" H_2O is the equivalent of 0.36 psi. Since the N_2 pressure applied was either 20 psig or 40 psig, the pressure resulting from the column of liquid can be reasonably assumed to be negligible. Therefore, h_1 is simply the sum of the atmospheric pressure and the gauge pressure of nitrogen applied, and h_2 is the atmospheric pressure. Since this net pressure is simply the gauge pressure reading on the N_2 tank, the hydraulic gradient can then be calculated by dividing the N_2 gauge pressure (in. H_2O) by the length of the soil column (4 inches). After calculating the hydraulic gradient, Darcy's Law (Equation 1) was used to calculate the value of the hydraulic conductivities (k) for each soil treatment.

Column Equilibration

Darcy's Law hydraulic conductivity values were calculated for DI-water runs using the Average Soil to determine the time necessary for appropriate column equilibration. Results for the column equilibration experiment on the Average Soil type are shown in Figure 11.5. Columns showed a rapid decrease in permeability as the first 5" of water passed through the column. The hydraulic conductivity of the

soil decreased by a factor of almost five following the transport of 5" of DI-water through the soil column. However, once 7" of DI-water passed through the column, the net change of the calculated hydraulic conductivity of the Average Soil was negligible. As a precautionary measure, it was decided that future experiments would allow for three 6" applications of DI-water (18" total) to pass through all soil systems prior to application of further treatment cycles involving oxidizers. Results indicated that this equilibration period should provide for ample time for soil columns to achieve equilibrium as it relates to Darcy's Law. This result agreed with findings by Zappi et al. (1990) in their study of contaminated groundwater and soil-bentonite mixtures using rigid wall permeameters. They found that a minimum passage of two pore volumes of liquid was required for the hydraulic conductivity of a soil column to reach equilibrium and that a passage of three pore volumes was preferred.

Impact of H_2O_2 and Fenton's Reagent on the Hydraulic Conductivity of Sand

Soil columns were run using Ozonated Sand as an experimental control. Figure 11.6 displays two different data sets, treatment via hydrogen peroxide and treatment via Fenton's Reagent. The first data set (left half of Figure 11.6) shows the impact of H_2O_2 on the permeability of Ozonated Sand. Initially, the sand displayed a permeability of roughly 6×10^{-3} in/s, a relatively high permeability compared to most normal soils. The sand offered very little resistance to flow, and 6" of DI-water was passed in a time period varying between 6 and 8 seconds. Two applications of 100,000 mg/L H_2O_2 were applied to each sand column, and results showed that the H_2O_2 had a negligible impact on the permeability of the sand control. Hydrogen

peroxide additions took anywhere from 9 to 11 seconds, a permeability decrease that was deemed negligible after review of the data. The second data set (the right half of Figure 11.6) shows the impact of Fenton's Reagent on the permeability of Ozonated Sand. The net time required to flow 6" of DI-H_2O, 5,000 mg/L Fe^{2+}, and 100,000 mg/L H_2O_2 had values ranging between 6 and 10 seconds. While the average hydraulic conductivity was slightly lower once Fenton's Reaction was initiated via H_2O_2 application, the results do not suggest that permeability is dramatically impacted by the oxidation of sand columns. This result is also important because it infers minimal impacts on soil hydraulic conductivity as a result of Fe^{2+} oxidation physically blinding off of the sand.

In addition to determining oxidation impact on sand, these Ozonated Sand control columns served another important purpose. They confirmed that the physical column equipment was suitable for hydraulic conductivity analysis. Hydraulic conductivities of the soil were anticipated to be several orders of magnitude lower than the 10^{-3} in/s units range (LaGrega et al., 2001), and these results indicate that the valves, fittings, wire screen, and geotextile material did not cause a substantial effect on the hydraulic conductivities calculated within the column. Since liquid was allowed to pass through the sand column and column apparatus at a very fast rate, the impact of the column equipment on hydraulic conductivity could be assumed to be negligible.

Impact of H_2O_2 Addition and Fenton's Reagent on the Hydraulic Conductivity of Soils

Various oxidative treatments were applied to soil columns to determine the impact of H_2O_2 and Fenton's Reagent on the hydraulic conductivity of the various soil specimens. Figures 11.7, 11.8, 11.9, and 11.10 correspond to the hydraulic conductivity data determined for the Average Soil, High pH Soil, High Iron Soil, and High TOC Soil, respectively. Each figure contains data from two different treatment sets. The first treatment set (left half of the figure) corresponds to the impact of hydrogen peroxide treatment on the hydraulic conductivity of each soil. The second treatment set (right half of the figure) corresponds to the impact of a Fenton's Reagent treatment on the hydraulic conductivity of each soil. While some of the H_2O_2 reacted with the natural soil constituents, some of the H_2O_2 also reacted with the previously dosed ferrous iron ions to generate hydroxyl radicals via the Fenton's Reaction mechanism.

For the hydraulic conductivity data for the Average Soil (Figure 11.7), the initial hydraulic conductivity stabilized at approximately $7x10^{-6}$ in/s. During the first application of 100,000 mg/L hydrogen peroxide, the permeability was reduced to approximately $7x10^{-7}$ in/s, a full order of magnitude reduction. The second application of hydrogen peroxide yielded a further reduction in the hydraulic conductivity to a value of $4x10^{-7}$ in/s. For treatment of Average Soil via Fenton's Reagent, the application of 5,000 mg/L Fe^{2+} solution showed no significant impact on the soil's hydraulic conductivity, maintaining a level at approximately $7x10^{-6}$ in/s. However, once the soil was subjected to the hydrogen peroxide, dramatic decreases in

hydraulic conductivity were again observed, decreasing that soil property to $3x10^{-7}$ in/s.

Similar results were observed for the other three soil types. For the High pH Soil (Figure 11.8), treatment via hydrogen peroxide yielded a decrease in hydraulic conductivity from $8x10^{-8}$ in/s to $6x10^{-9}$ in/s. The application of 5,000 mg/L Fe^{2+} showed no signs of impacting hydraulic conductivity, while the initiation of Fenton's Reaction via 100,000 mg/L H_2O_2 decreased the hydraulic conductivity of the High pH Soil from $7x10^{-8}$ in/s to $1x10^{-8}$ in/s. For the High Iron Soil (Figure 11.9), treatment via hydrogen peroxide yielded a decrease in hydraulic conductivity from $3x10^{-5}$ in/s to $4x10^{-7}$ in/s. The application of Fe^{2+} solution proved to have a negligible impact on the flow rate through the column, as the hydraulic conductivity remained stable at approximately $4x10^{-5}$ in/s. However, when Fenton's Reagent was applied to the High Iron Soil, the hydraulic conductivity decreased to $3x10^{-6}$ in/s. For the High TOC Soil (Figure 11.10), treatment via 100,000 mg/L H_2O_2 decreased the hydraulic conductivity from $6x10^{-5}$ in/s to $6x10^{-7}$ in/s. As previously observed in other soil types, the 5,000 mg/L Fe^{2+} solution did not contribute to any reductions in soil permeability, but when Fenton's Reaction was initiated, soil hydraulic conductivity decreased from $4x10^{-5}$ in/s to $7x10^{-7}$ in/s.

In order to compare the impact of H_2O_2 and Fenton's Reagent oxidation among the different soils, hydraulic conductivity reductions were standardized based on the initial hydraulic conductivity for each individual soil. Hydraulic conductivity reduction factors (HCRF's) were defined according to Equation 6. The HCRF was

simply defined as the factor by which the initial hydraulic conductivity was reduced during soil treatment. HCRF values are located in Figure 11.11.

$$HCRF = \frac{k_i}{k_f} \tag{6}$$

where,

k_i = initial hydraulic conductivity (from DI-water Run 3), in/s

k_f = final hydraulic conductivity (from run 2 of treatment cycle), in/s

It is apparent from the data that the application of 5,000 mg/L Fe^{2+} had little effect on the hydraulic conductivity for any of the soil types since the HCRF values for all the ferrous iron treatments were approximately 1. The drastic changes in soil permeability always occurred following the addition of hydrogen peroxide.

The most dramatic reductions in permeability occurred during the H_2O_2 treatment of the High Iron Soil and both the H_2O_2 and Fenton's Reagent treatments of the High TOC Soil. One potential contributing factor in this result is the fact that the High Iron and High TOC Soils exhibited the greatest initial hydraulic conductivities. Because of these high initial permeabilities, it was ascertained that these soils initially had larger and more accessible flow channels. As insoluble oxidation by-products and fine particles clogged these large pores, the permeability reduction would be expected to be much greater than if the soils exhibited a much lower permeability initially. The High pH soil, having the lowest initial permeability, exhibited the least reduction in permeability due to oxidation. HCRF factors for High pH soil ranged from 6.5 to 12.3 following application of H_2O_2. An additional reason for this

observed result involves the known reaction of hydrogen peroxide with ferrous iron (via Fenton's Reaction) and TOC, creating insoluble byproducts that can block flow channels (Amarante, 2000; Blume et al., 2002; and ITRC, 2005). Figures 11.12 and 11.13 show the soil iron content versus the HCRF factor for the H_2O_2 and Fenton's Reagent treatments, respectively. Because both iron and TOC are hypothesized to be primary reactants with hydrogen peroxide, neither of these graphs generates a clear correlation since the High TOC Soil has low levels of iron, and the High Iron Soil has a low TOC content. Figures 11.14 and 11.15 show the soil TOC content versus the HCRF factor for the H_2O_2 and Fenton's Reagent treatments, respectively. While no evident correlation existed for the H_2O_2-only HCRF data, a positive linear correlation ($R^2 \sim 0.7$) was in fact observed for the Fenton's Reagent HCRF plot, further implicating TOC's impact on soil hydraulic conductivity reductions due to ISCO treatment via H_2O_2. In this case, all of the soil types were artificially dosed with excess ferrous iron prior to H_2O_2 application. This in essence adjusted the pre-treatment ferrous iron contents within each soil column to relatively constant levels, enabling for better comparison between the HCRF and TOC content without the impacts due to highly variable iron content.

An additional factor contributing to the observed hydraulic conductivity reductions is hypothesized to be due to the evolution of oxygen gas within the soil columns. Gas bubbles have been shown to potentially reduce the hydraulic conductivity of soil environments when they become entrapped within soil pores. Reynolds (1992) performed experiments to determine the effect of *in situ* methane

accumulation on the hydraulic conductivity of peat due to CH_4's production during anaerobic respiration. They found that methane bubbles entrapped within pores was a potential cause for significant decreases in the observed hydraulic conductivity. Therefore, oxygen produced during ISCO treatments of these soil columns could potentially be a contributing factor in the observed results of these ISCO column experiments.

It was also observed that the HCRF for Fenton's Reagent treatments appeared to be lower than the HCRF for a H_2O_2 treatment when compared with its corresponding soil. The hydrogen peroxide HCRF values for High pH Soil, High Iron Soil, and High TOC Soil were all much greater than their corresponding HCRF value for treatment via Fenton's Reagent. For the Average Soil, similar HCRF values were observed for both the H_2O_2 and the Fenton's treatment. It is suggested that this is due to the fact that less hydrogen peroxide is interacting with the natural soil constituents due to the competing Fenton's mechanism. The soil in the Fenton's treatment, having been artificially dosed with ferrous ions, will utilize much of the hydrogen peroxide for Fenton's Reaction, leaving less H_2O_2 to react with natural organic matter, thereby reducing the amount of insoluble by-products that would have been otherwise created within the soil matrix.

Ozone-based Constant Head Column Design Results

One of the key achievements in these experiments was the successful design and implementation of a constant head column setup that was used throughout testing. Two key problems existed that prevented the use of the column design

utilized during H_2O_2 and Fenton's Reagent experiments. Firstly, ozone is unstable in the liquid form due to its autodegradative nature. Therefore, an ozone solution can't simply be applied in place of the hydrogen peroxide solution since the ozone would have autodegraded prior to any contact with soil particles. Secondly, laboratory-scale ozone generators such as the Ozonology, Inc. generator used by the Mississippi State University E-Tech Laboratory do not generate ozone and pressures high enough to overcome the permeabilities observed in most soils. Therefore, ozone could not be simply forced through our existing soil column in the gas phase. However, a constant head column design using a modified recycle system (Figure 11.4) was successfully implemented in these experiments. This design enabled aqueous phase ozone to be continuously recycled into the column, thereby keeping the liquid-phase concentration of ozone within the column at a relatively constant level.

Impact of O_3 and Peroxone on the Hydraulic Conductivity of Soils

Various oxidative treatments were applied to soil columns to determine the impact of ozone and peroxone on the various soil types. Figures 11.16, 11.17, 11.18, 11.19, and 11.20 correspond to the hydraulic conductivity data determined for the Ozonated Sand Control, Average Soil, High pH Soil, High Iron Soil, and High TOC Soil, respectively. Each figure contains data from two different treatment sets. The first treatment set (left half of the figure) corresponds to the impact of ozone treatment on the hydraulic conductivity of each soil. The second treatment set (right half of the figure) corresponds to the impact of a peroxone treatment on the hydraulic conductivity of each soil.

The data in Figure 11.20 clearly indicated that the Ozonated Sand test control offered very little resistance to flow due to its high initial permeability that varied between $3x10^{-5}$ and $5x10^{-3}$ in/s. No significant impact in Ozonated Sand's hydraulic conductivity was observed due to treatment via ozone or peroxone. For ozone treatment of each of the four other soil types, no significant impact on soil hydraulic conductivity was observed during experiments. This was most likely due to the H_2O_2 vs. O_3 solubility issues as was previously discussed in Chapter X. While H_2O_2 is often applied at concentrations of up to 50%, O_3 is far less soluble in water than H_2O_2. The maximum solubility of ozone at ambient conditions is generally reported to be approximately 20 ppm (Heynes et al., 1999; Amarante, 2000; ITRC, 2005). Soils in these experiments were subjected to ozone treatments in which the O_3 was contained only in the aqueous phase; this prevented the treatment using high oxidizer concentrations as was obtainable in treatments which H_2O_2 was used.

Significant reductions in soil hydraulic conductivity were in fact observed due to peroxone treatment in all soil types except for the Ozonated Sand control. In the Average Soil (Figure 11.17), a peroxone treatment cycle reduced the soil hydraulic conductivity from $5.0x10^{-6}$ in/s to $9.3x10^{-7}$ in/s. The smallest reduction in hydraulic conductivity due to peroxone was observed in the High pH Soil (Figure 11.18); its permeability reduced from $9.4x10^{-8}$ in/s initially to only $7.7x10^{-8}$ in/s. Data clearly indicates that the addition of hydrogen peroxide into the treatment process had a significant impact on observed post-treatment soil hydraulic conductivity values.

Hydraulic conductivity reduction factors (HCRF's) were also calculated using Equation 6 for ozone-based ISCO treatments as was done for H_2O_2-based treatments. Figure 11.21 displays the calculated HCRF values for the ozone and peroxone ISCO treatments. Since ozonation was shown to have insignificantly impacted soil hydraulic conductivity, HCRF values for ozonation were all near 1.0. The greatest HCRF was observed in the treatment of the High TOC soil via peroxone; its hydraulic conductivity was reduced by a factor of almost 15. Figure 11.22 compares the HCRF results for H_2O_2 and Fenton's Reagent with the HCRF results for ozone and peroxone. The data clearly indicates that in all soil types, the application of either a 100,000 mg/L H_2O_2 or a 5,000 mg/L Fe^{2+}/100,000 mg/L H_2O_2 Fenton's Reagent treatment caused a much more drastic decrease in soil permeability than either treatment via ozone (5.5 wt. % gas phase O_3) or peroxone (5.5 wt. % gas phase O_3/1,000 mg/L H_2O_2). Since the effects of ozone-only treatment applications were insignificant on the permeability of all soil types, it is apparent that the HCRF is highly dependent on the amount of hydrogen peroxide applied to the system.

Summary of the Impact of ISCO on Soil Hydraulic Conductivity

It was observed that treatment via *in situ* chemical oxidation had the potential to dramatically impact the hydraulic conductivity within multiple soil environments. While treatment via ozone alone showed no significant impact on soil permeability, severe reductions in liquid flowrates were observed under a constant hydraulic gradient during initial contact with hydrogen peroxide, indicating that previously open flow channels had become sealed off by insoluble oxidation by-products and

fine particles. While most reductions in hydraulic conductivity due to H_2O_2 (100,000 mg/L) and Fenton's Reagent (5,000 mg/L Fe^{2+}/100,000 mg/L H_2O_2) were on the level of one order of magnitude, the High TOC soil was subjected to a massive permeability decrease of more than two orders of magnitude (HCRF ~ 105) due to oxidation via 100,000 mg/L H_2O_2.

Results from these experiments indicate that the addition of hydrogen peroxide into soil environments will result in significant changes in transport properties within the soil matrix. Certain flow paths within the soil will be blocked off, and subsequently rerouted to other areas within the matrix. This will have a dramatic impact on pollutant-H_2O_2 interaction within the subsurface. Secondly, the reduction in hydraulic conductivity must also be factored in when designing the pumping system necessary to transport process reagents into the subsurface since these pumping systems are sized based on an initial assessment of the site's permeability. The data from this research clearly indicates that the user can expect to see significant reductions in hydraulic conductivity, and this must be accounted for when calculating the necessary pumping power required to deliver the hydrogen peroxide into the targeted contaminant zone.

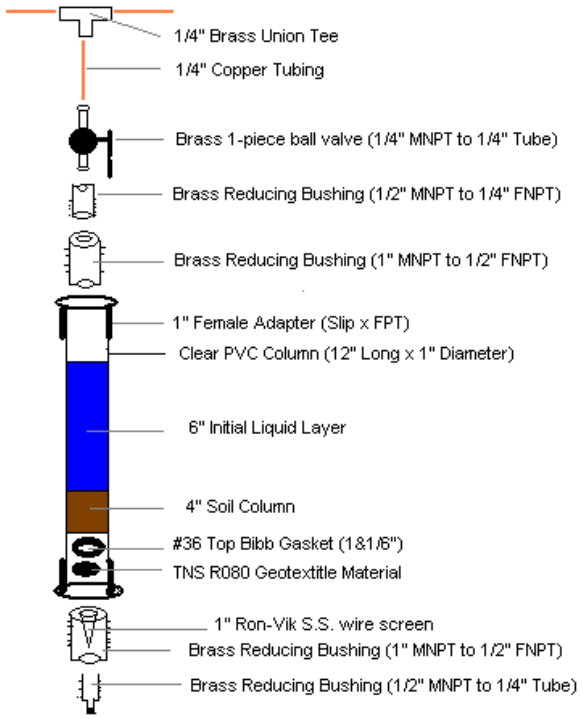

Figure 11.1: Diagram of Individual Column Assembly for H_2O_2 and Fenton's Reagent Applications

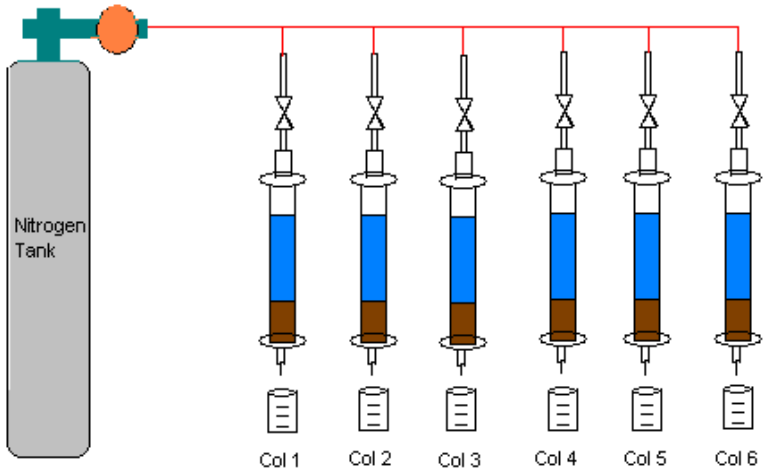

Figure 11.2: Diagram of Column Manifold for H_2O_2 and Fenton's Reagent Applications

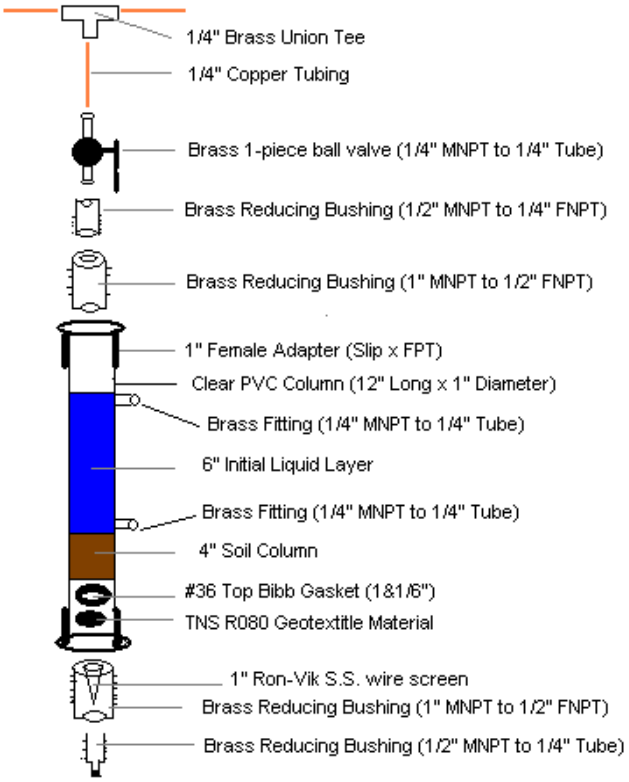

Figure 11.3: Diagram of Individual Column Assembly for O_3 and Peroxone Applications

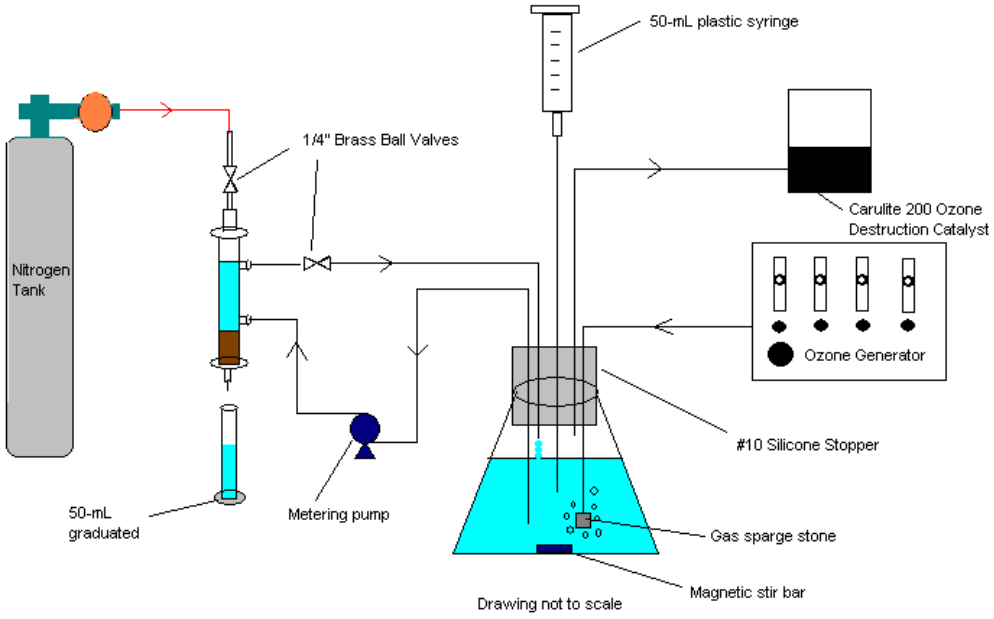

Figure 11.4: PFD for O_3-based ISCO of Soil Columns

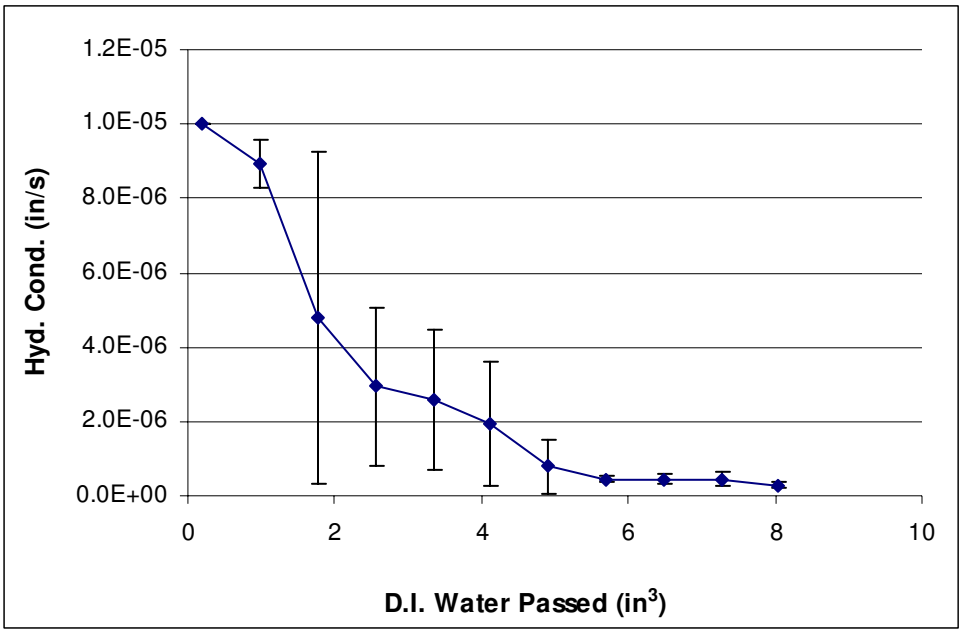

Figure 11.5: Column Equilibration Results for Average Soil Runs with DI-Water

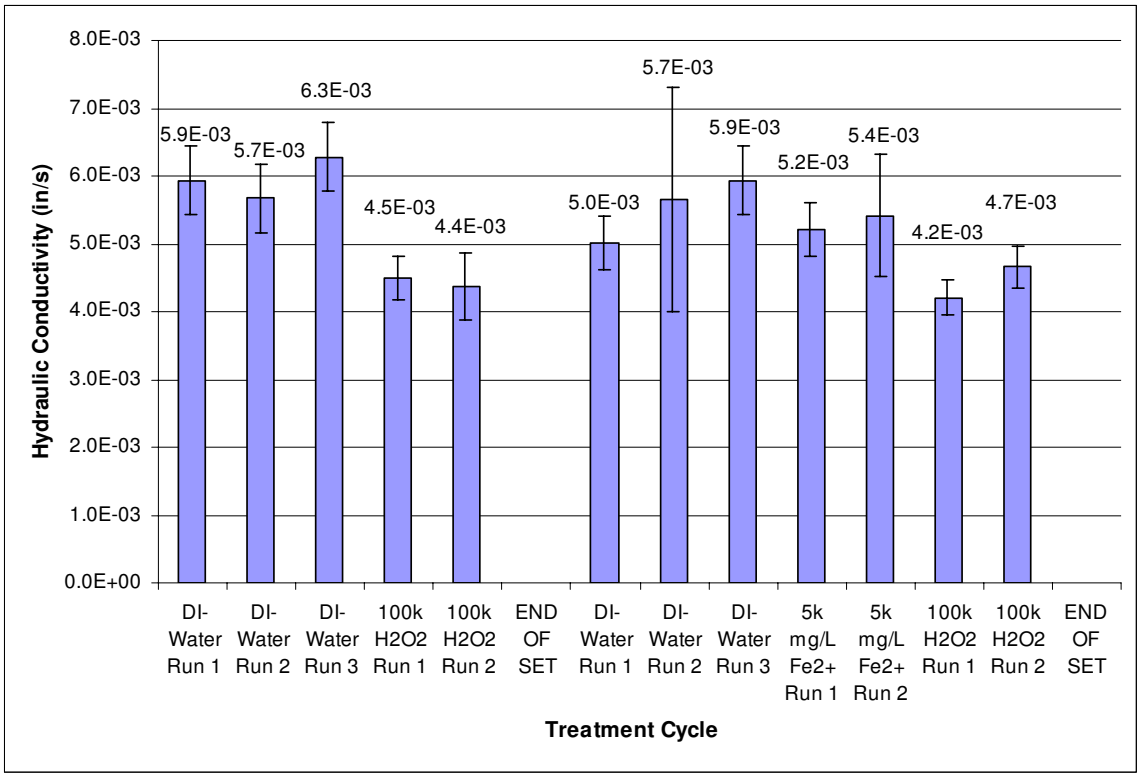

Figure 11.6: Impact of H_2O_2 and Fenton's Reagent on the Hydraulic Conductivity of Ozonated Sand (Control)

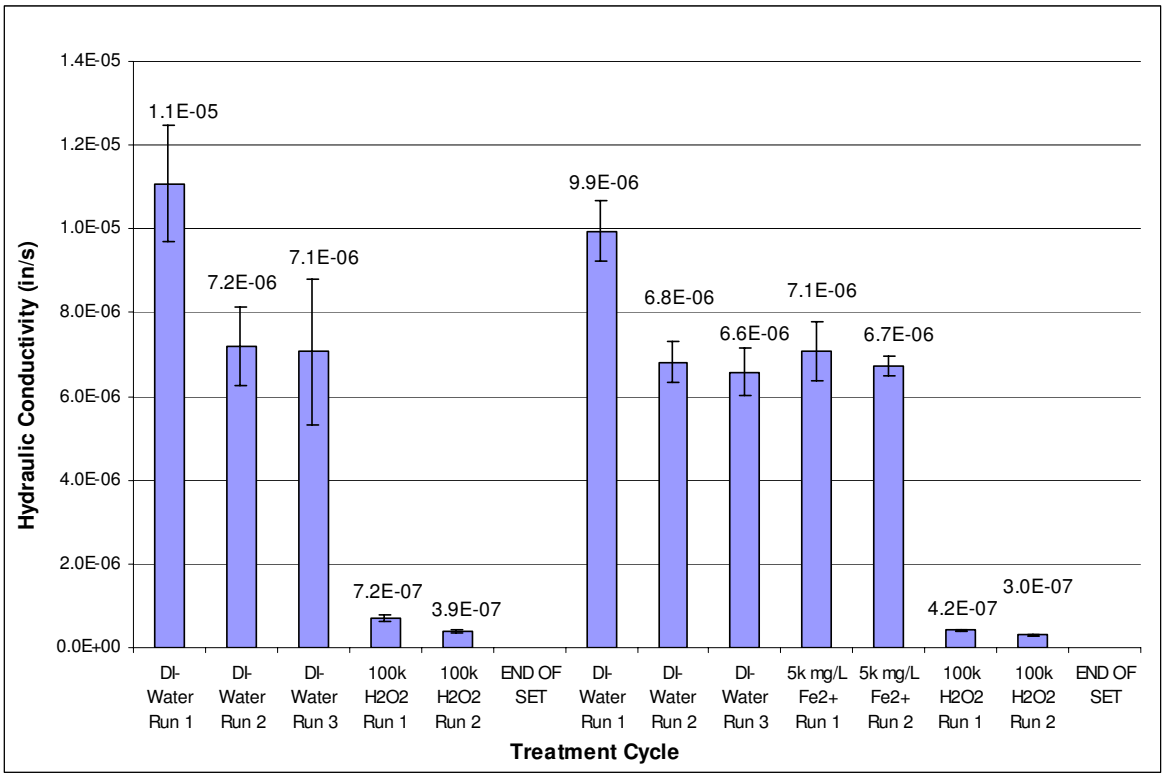

Figure 11.7: Impact of H_2O_2 and Fenton's Reagent on the Hydraulic Conductivity of Average Soil

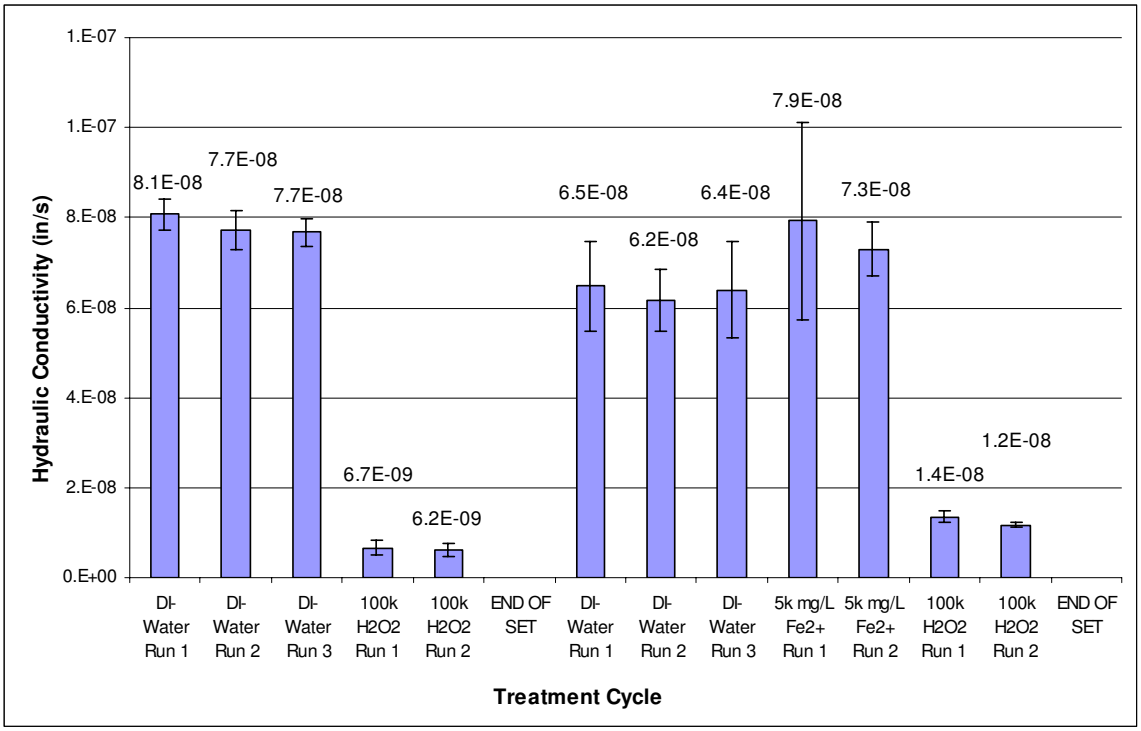

Figure 11.8: Impact of H_2O_2 and Fenton's Reagent on the Hydraulic Conductivity of High pH Soil

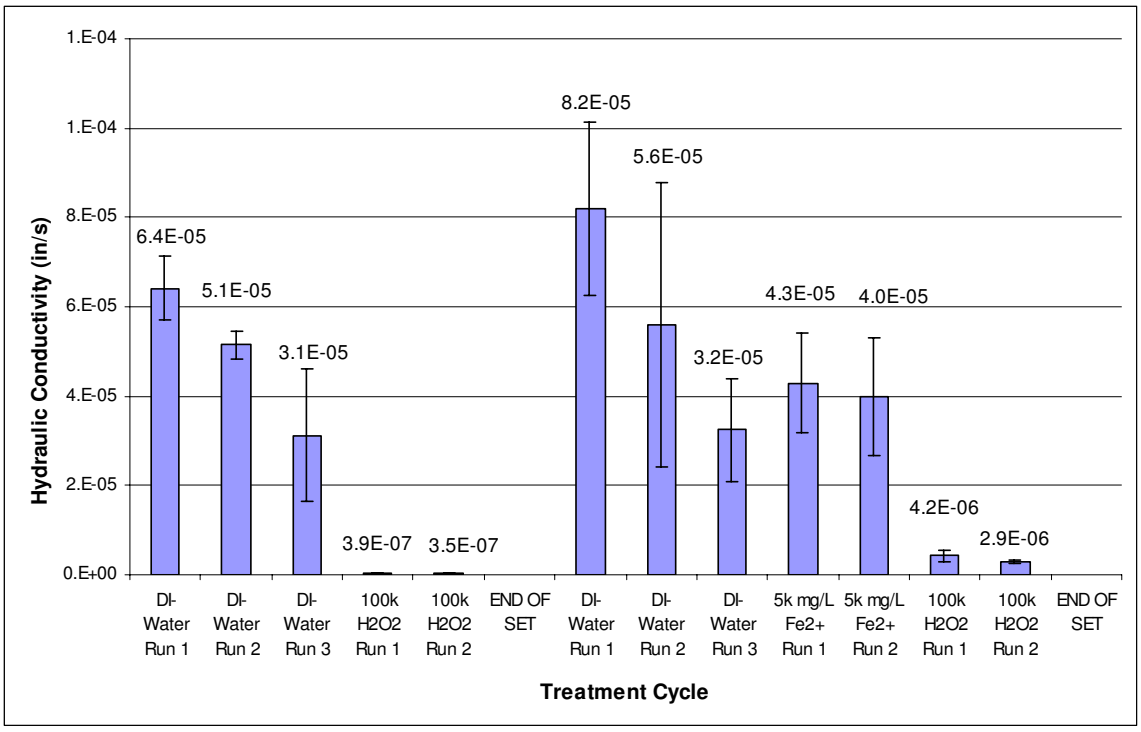

Figure 11.9: Impact of H_2O_2 and Fenton's Reagent on the Hydraulic Conductivity of High Fe Soil

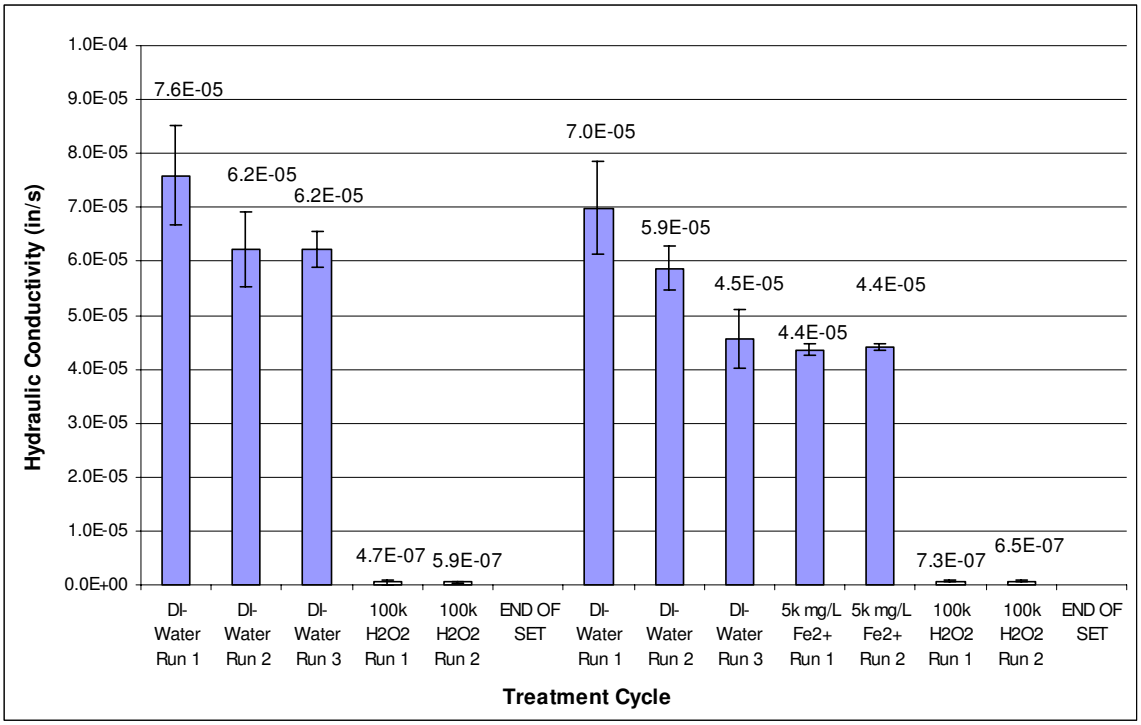

Figure 11.10: Impact of H_2O_2 and Fenton's Reagent on the Hydraulic Conductivity of High TOC Soil

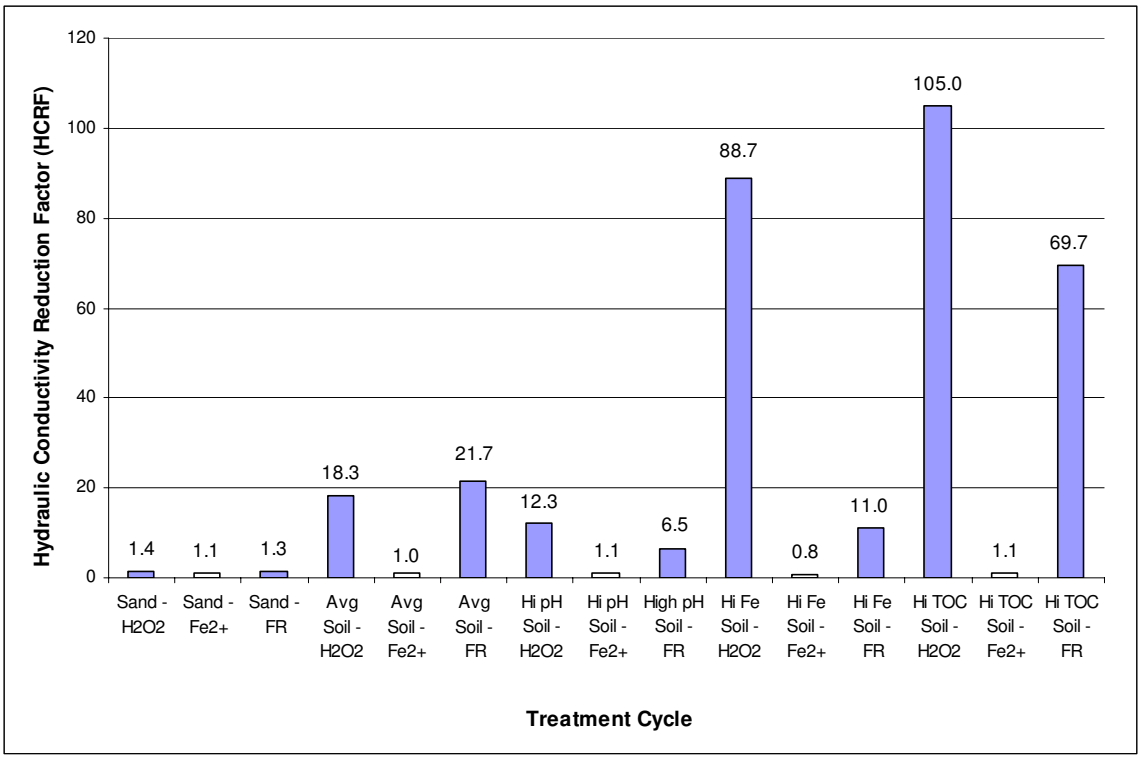

Figure 11.11: Hydraulic Conductivity Reduction Factors for H_2O_2 and Fenton's Reagent Treatments on Multiple Soil Types

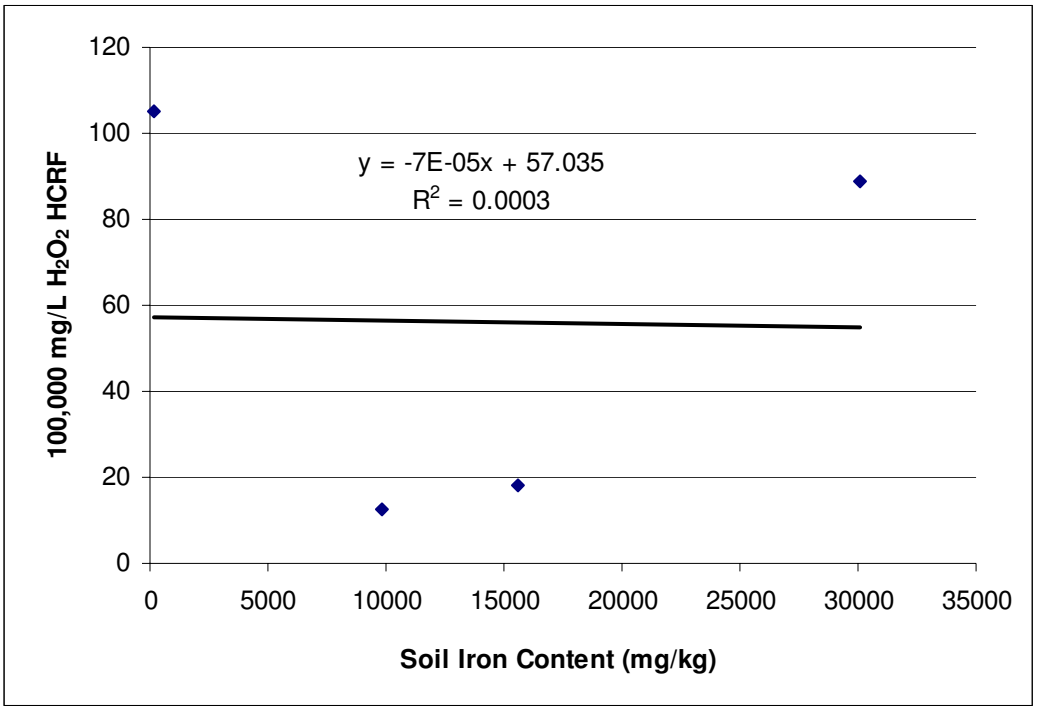

Figure 11.12: Hydraulic Conductivity Reduction Factors for H_2O_2 Treatment Versus Soil Iron Content

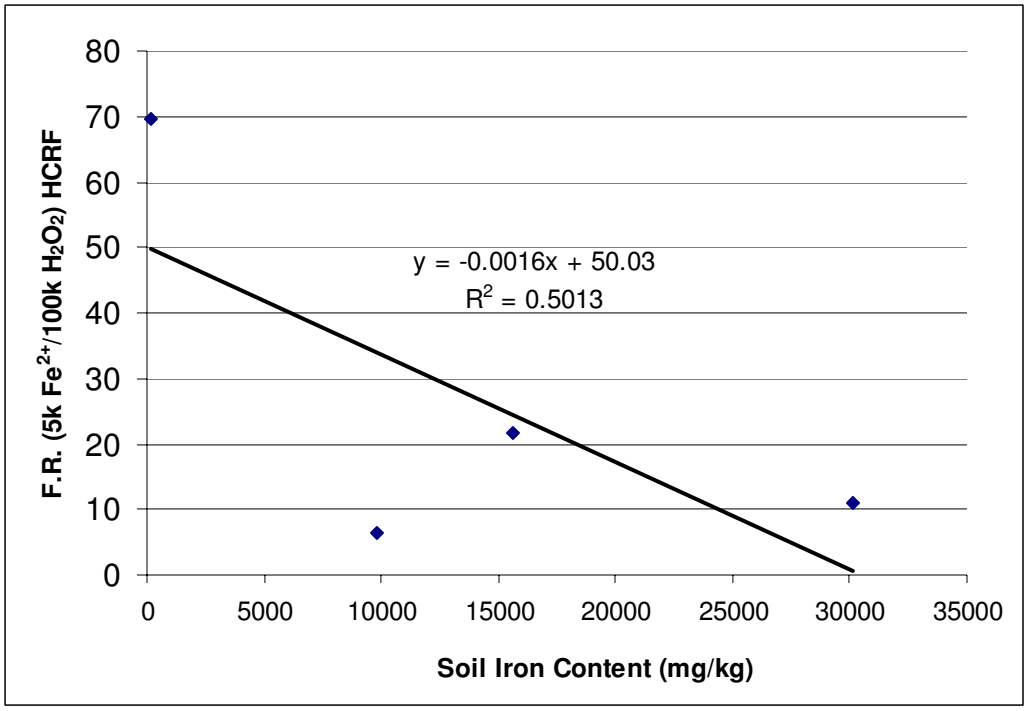

Figure 11.13: Hydraulic Conductivity Reduction Factors for Fenton's Reagent Treatment Versus Soil Iron Content

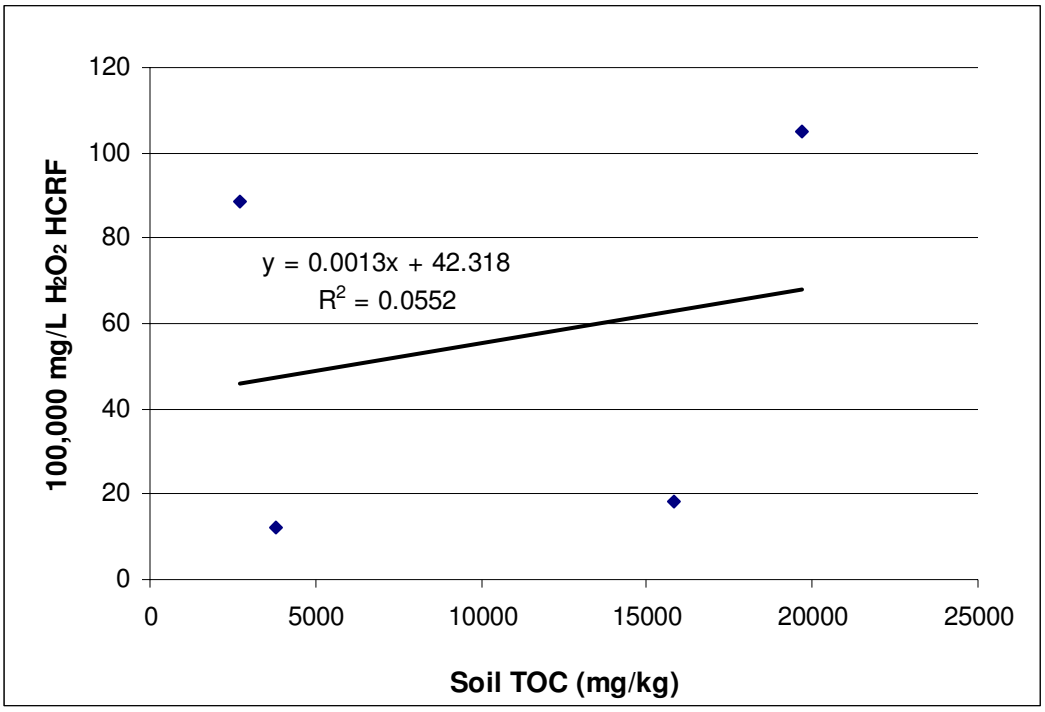

Figure 11.14: Hydraulic Conductivity Reduction Factors for H_2O_2 Treatment Versus Soil TOC Content

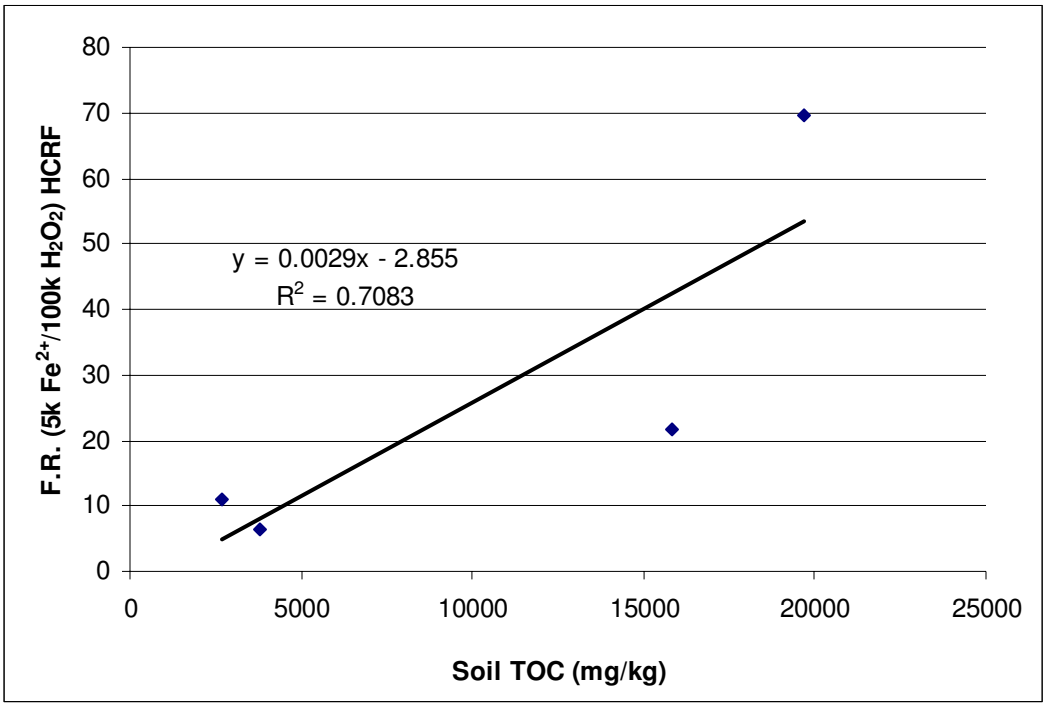

Figure 11.15: Hydraulic Conductivity Reduction Factors for Fenton's Reagent Treatment Versus Soil TOC Content

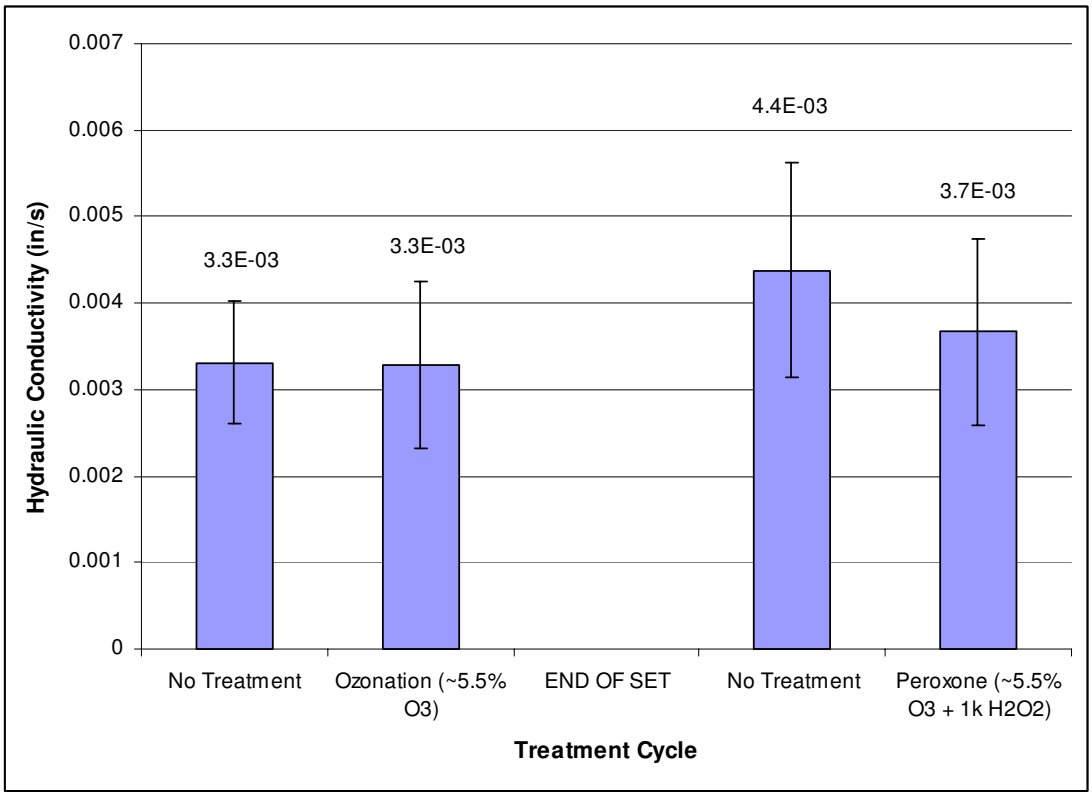

Figure 11.16: Impact of O_3 and Peroxone on the Hydraulic Conductivity of Ozonated Sand (Control)

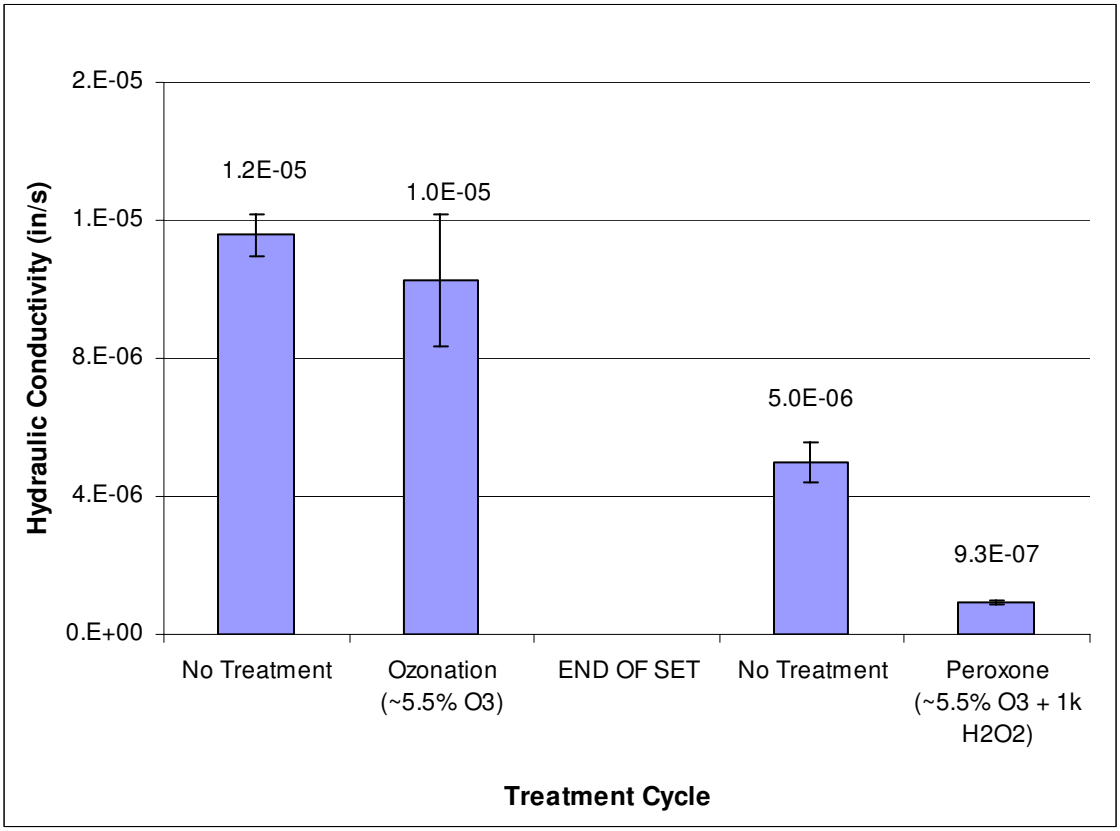

Figure 11.17: Impact of O_3 and Peroxone on the Hydraulic Conductivity of Average Soil

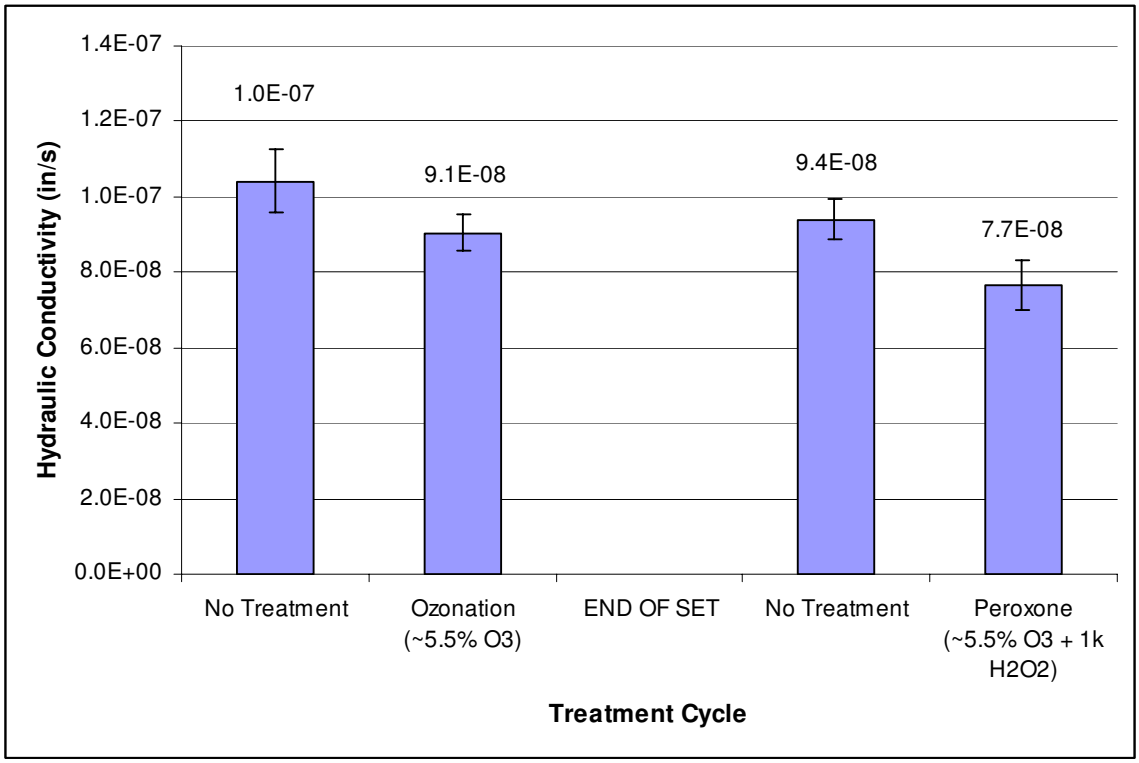

Figure 11.18: Impact of O_3 and Peroxone on the Hydraulic Conductivity of High pH Soil

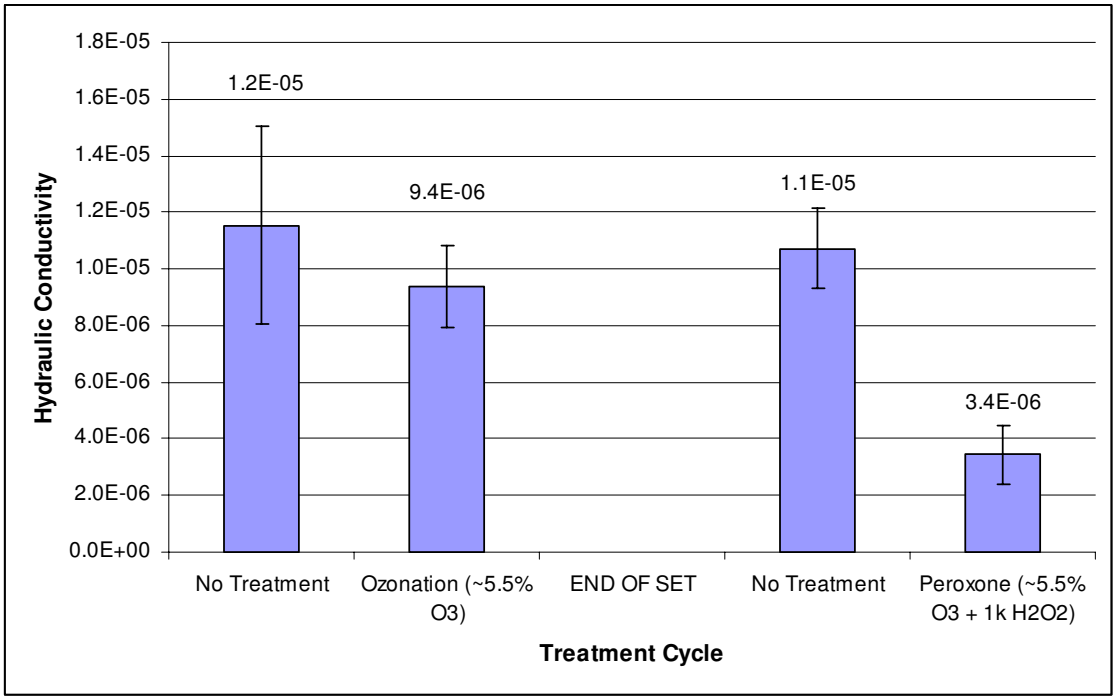

Figure 11.19: Impact of O_3 and Peroxone on the Hydraulic Conductivity of High Fe Soil

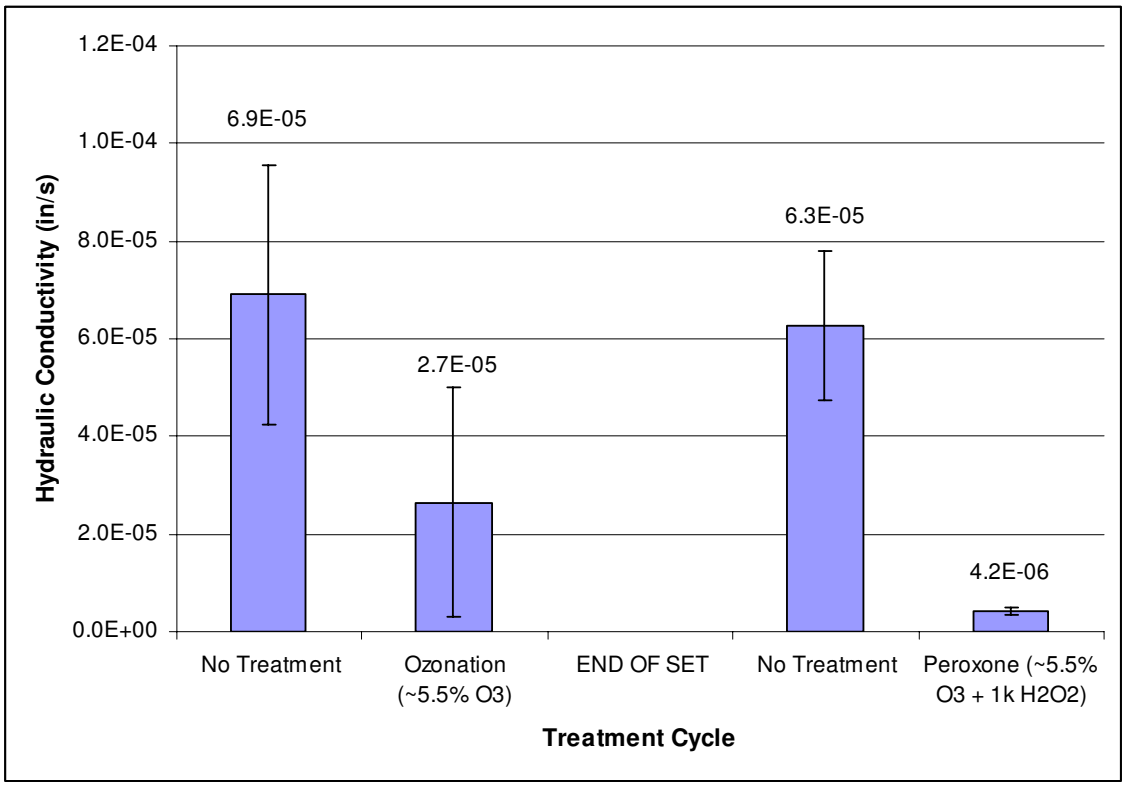

Figure 11.20: Impact of O_3 and Peroxone on the Hydraulic Conductivity of High TOC Soil

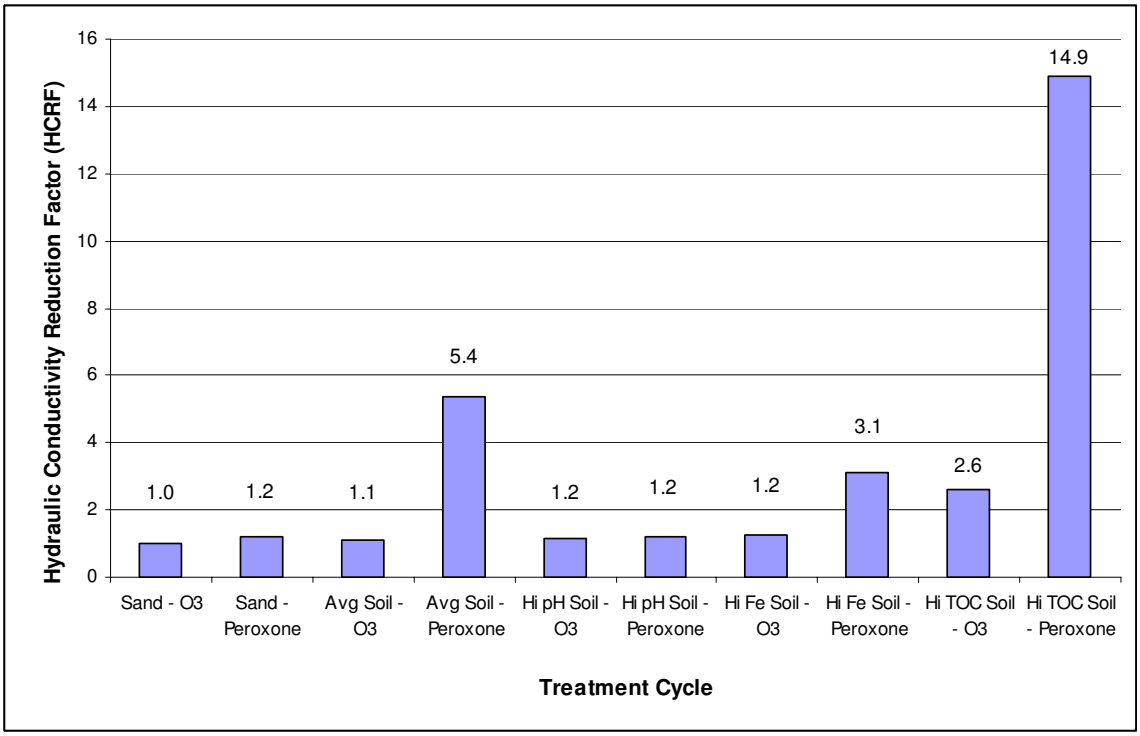

Figure 11.21: Hydraulic Conductivity Reduction Factors for O_3 and Peroxone Treatments on Multiple Soil Types

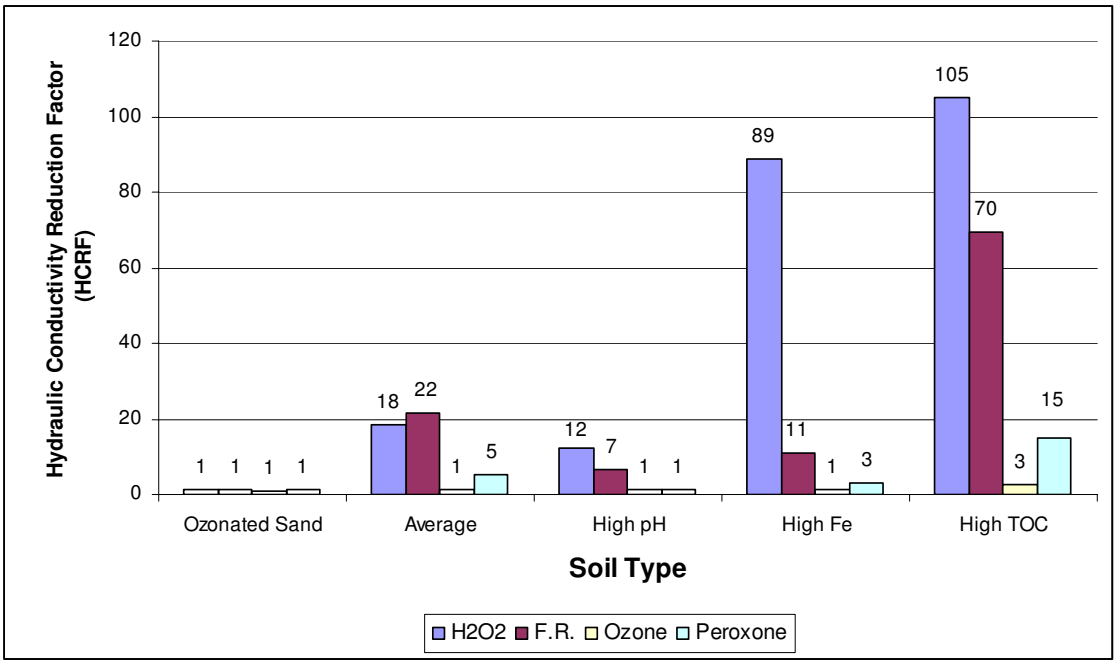

Figure 11.22: Hydraulic Conductivity Reduction Factors for ISCO Treatments on Multiple Soil Type

CHAPTER XII

IMPACT OF *IN SITU* CHEMICAL OXIDATION ON SOIL ORGANIC COMPOSITION

Background

In both surface soil and in subsoil layers, organic compounds make up an important part of soil colloidal fractions. This organic matter is generated from plant and animal debris which becomes intermixed within soils, and this debris can be physically and chemically altered by fungi and bacteria located within the soil matrix, a process known as humification (Gieseking, 1975). The chemical composition of humic substances can be defined by the elemental composition, the types of functional groups present, and the types of organic molecules making up the humic polymer structure. Carboxyl, phenolic hydroxyl, alcoholic hydroxyl, carbonyl, quinone, and methoxyl groups are all considered to be principal functional groups that make up soil humics. In addition to reaction with bacteria, soil humics are also subject to change via oxidative processes. These reactions can lead to the splitting of both carbon-carbon and carbon-hydrogen bonds within soil organic structures (Greenland and Hayes, 1978).

Objective

Because of literature's indication that soil organic compounds display the potential for oxidation reactions, it was desired to use nuclear magnetic resonance imaging technology to better identify the changes in soil organic structures due to applications of various oxidizers commonly used with *in situ* chemical oxidation.

Methods and Materials

Soil Treatment

A pre-treatment sample of the Average Soil was selected as the baseline sample. Additionally, the average soil was subjected to several treatments in 30% (w/w) slurries (120 g soil + 280 g liquid). The effect of air sparging was tested by subjecting the soil to nine hours of air sparging at 2 scfh. The effect of H_2O_2 was tested by subjecting the soil to three consecutive daily applications of 50,000 mg/L H_2O_2. The effect of ozone was tested by subjecting the soil to three consecutive daily applications of 5.5 wt. % O_3 (gas phase) at 2 scfh. The effect of peroxone was tested by subjecting the soil to three consecutive daily applications of 5.5 wt. % O_3 (gas phase) and 1,000 mg/L H_2O_2. The High TOC soil was tested in a similar fashion as the Average Soil. However, only pre-treatment, air sparging, and peroxone samples were tested.

Soil Washings

Fifty grams of appropriate soil samples were added to 250 mL polypropylene bottles. 200 mL of 10% hydrofluoric acid (HF) was added to each bottle, and the samples were shaken. Bottles were then centrifuged for 30 minutes at 2,000 rpm, and the supernatant was decanted and discarded. This process was repeated ten times at a rate of two HF washings per day. Soil samples were then washed with 200 mL of DI-H_2O ten times, following the same procedure as with the HF. This allowed for all the remaining HF to be removed.

Soil Extractions

Soil samples were then extracted overnight with 200 mL of 0.1 M NaOH. The extract was filtered using a 0.22 micron PVDF membrane and pressure filter. Each filtrate was saved in an individual stock bottle. This process was repeated four times for each sample, adding each filtrate to the appropriate filtrate stock bottle. The filtrate was refrigerated between extractions.

Ion Exchange

The filtrate from the prior procedure was then passed over a column of Amberlite IR-120(plus) ion-exchange resin (Aldrich, CAS 78922-04-0) to remove the sodium. A 1-liter burette was used as the column. The bottom was plugged with 2 inches of glass wool, and the column was filled with resin until it was two-thirds full.

Prior to the introduction of real samples, the resin was prepared for used. Initially, the resin was washed with 1 column volume of 10% HCl solution, followed

by 3 column volumes of DI-H_2O, followed by 3 column volumes of 0.1 M NaOH. This process was repeated ten times. Then, three additional volumes of 10% HCl were made, followed by 100 column volumes of DI-H_2O to ensure removal of all the HCl solution. The column was then ready for experimental use.

The filtrate stock samples were then passed through the column dropwise. The effluent of the column was collected in a new stock bottle for each respective sample. Following the ion exchange procedure, samples were freeze-dried. These freeze-dried samples were then analyzed by Dr. Andre Simpson at the University of Toronto at Scarborough using a Bruker 500 MHz ^{I}H-NMR with a liquid probe for both one and two dimensions.

Results and Discussion

NMR Analytical Results

NMR analysis was unable to be performed on the hydrogen peroxide treatment of the Average Soil. Figures 12.1, 12.2, and 12.3 show digital photographs of the Average Soil NaOH Extract for the initial, H_2O_2 treatment, and peroxone treatment, respectively. All of the NaOH extracts contained substantial quantities of recovered soil organics except for the H_2O_2 treatment (Figure 12.2). This extract from the hydrogen peroxide treatment was filtered and freeze-dried in the same manner as other samples, but an insufficient quantity of recovered organics was obtained, preventing NMR analysis on this sample. This almost complete absence of

extractable material indicates that hydrogen peroxide treatment degraded the natural organic matter very extensively.

Changes to the Average Soil's natural organic matter induced by ozone were much more subtle; relatively little change was induced by this treatment. Both the protein and carbohydrate signals remained unaltered in comparison to analysis of the controls. There did appear to be a slight relative increase in the aliphatic components after ozone treatment, consistent with the aliphatic material being highly unreactive with ozone (Westerhoff et al., 1999).

NMR data revealed evident differences in the composition of natural organic matter in the Average Soil treated with peroxone. The NMR spectra comparing the peroxone treatment with the DI-Water/Air-Sparge control are shown in Figure 12.4. The aliphatic and carbohydrate signals appeared relatively more intense after peroxone treatment whereas signals indicative of peptides, protein, and aromatic structures were significantly reduced. These results suggested that peroxone treatment degraded relatively labile protein and peptide structures, while leaving recalcitrant carbohydrate and aliphatic compounds intact.

The NMR data comparing the High TOC Soil peroxone treatment with the DI-Water/Air-Sparge control are shown in Figure 12.5. These results corresponded well with the changes observed in the NOM of the Average Soil due to peroxone treatment. Aliphatic and carbohydrate signals intensified, while protein, peptide, and aromatic signals lessened.

Summary

As a whole, these results indicate that soil NOM will be impacted by ISCO treatment via both hydrogen peroxide and ozone-based technologies. High quantities of hydrogen peroxide added to the soil offers the potential to extensively degrade soil organic structures to non-detectable levels. Results also indicated that aromatic, protein, and peptide structures will be converted to straight-chain aliphatic and carbohydrate structures following peroxone treatment. These results were consistent with the analysis of ozone-induced changes in natural organic matter structure by Westerhoff et al. (1999). They found that the ozonation of hydrophobic organic acids resulted in increased carboxyl and aliphatic organic structures and shifted products towards less hydrophobic compounds.

Carbohydrates play several important roles in soil environments. They are significant in soils for several various reasons, including (Stevenson, 1982):

- Ability to bind inorganic soil particles into stable aggregates
- Ability to form complexes with metal ions
- Ability to act as building blocks for humus synthesis

Therefore the build-up of carbohydrates will greatly impact both the physical and chemical interactions within soil environments. Additionally, the reduction of soil aromatics and increase in soil aliphatic components could also impact the soil environment. Gunasekara and Xing (2003) reported on the importance of aromatic and aliphatic organics in the sorption and desorption of naphthalene. Both their review of pertinent literature and their experimental results indicated that both of

these organic structures play key roles in the observed sorption capacities for naphthalene. These results indicate that changes in soil aromatic and aliphatic content could significantly impact adsorption properties within the soil matrix.

Figure 12.1: Photograph of Initial Average Soil NaOH Extract

Figure 12.2: Photograph of H_2O_2-Treated Average Soil NaOH Extract

Figure 12.3: Photograph of Peroxone-Treated Average Soil NaOH Extract

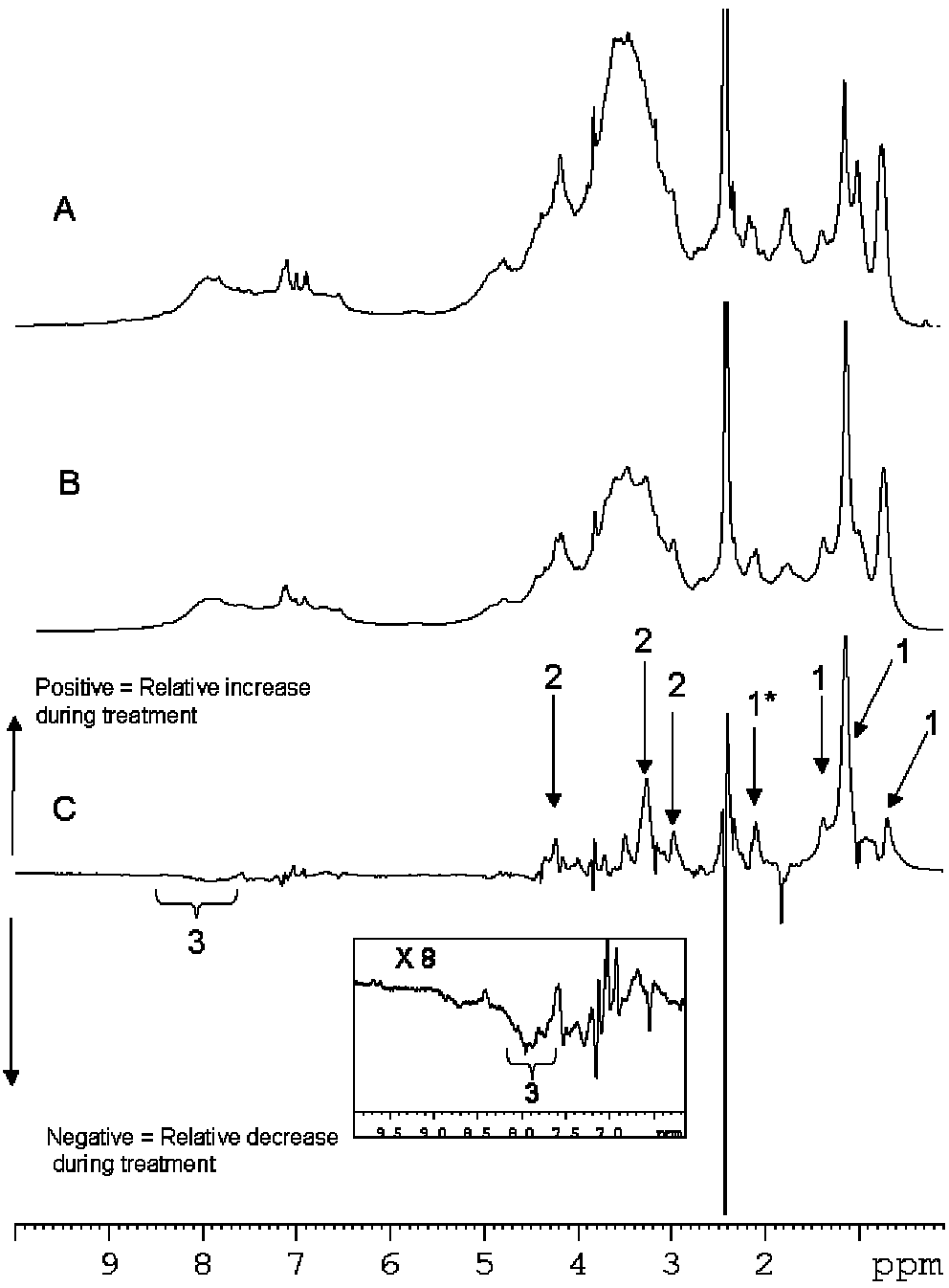

Figure 12.4: Impact of ISCO on Organics in Average Soil; A = ^{1}H NMR AVG water control, B = ^{1}H NMR AVG peroxone, C = difference spectrum. 1 = signals from aliphatic molecules, *aliphatic signals from aliphatic acids/esters. 2 = signals likely from carbohydrate, such as cellulose, 3 = amide protons, characteristic of proteins or peptides. Assignments have been confirmed by 2D NMR data not shown. Insert shows aromatic/amide region at x 8 multiplication.

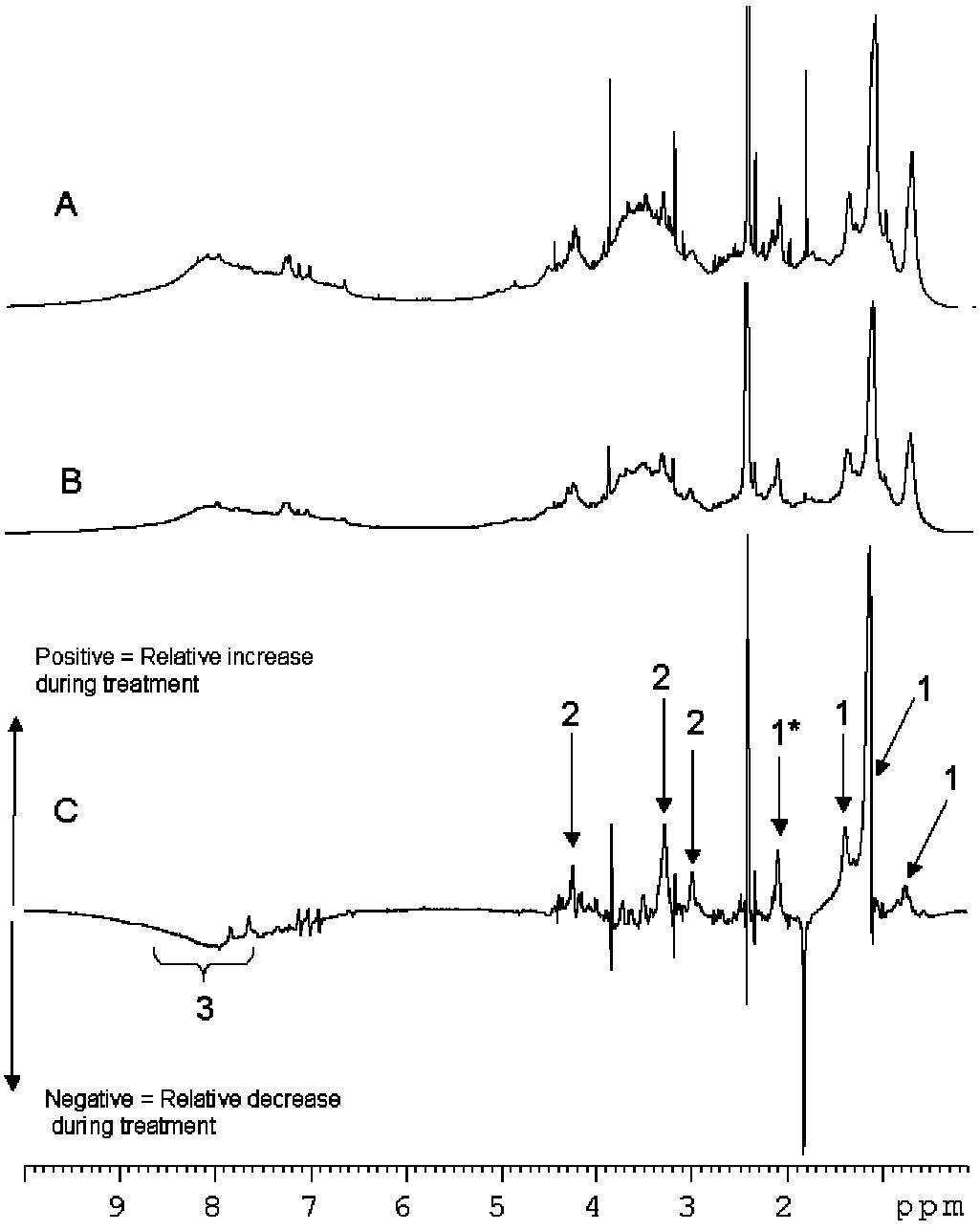

Figure 12.5: Impact of ISCO on Organics in High TOC Soil; A = ^{1}H NMR TOC water control, B = ^{1}H NMR TOC peroxone, C = difference spectrum. 1 = signals from aliphatic molecules, *aliphatic signals from aliphatic acids/esters. 2 = signals likely from carbohydrate, such as cellulose, 3 = amide protons, characteristic of proteins or peptides. Assignments have been confirmed by 2D NMR data not shown.

CHAPTER XIII

IMPACT OF *IN SITU* CHEMICAL OXIDATION ON SOIL ADSORPTION PROPERTIES

Background

It is hypothesized that ISCO will potentially impact soil-pollutant adsorption equilibria in the subsurface environment. It is readily known that oxidation of soils causes the degradation of organic carbon within the soil matrix. In the research of Freese et al. (1999), it was observed that the use of ozone and peroxide caused significant removals of organic matter from wastewater when applied in high enough concentrations. Similar results were also observed by Jung and Choi (2003) while examining the effects of ozonation on soil organic matter. They observed the formations of significant quantities of carboxylic acids following the oxidation of the soil organic matter via an ozonation treatment. Likewise, Westerhoff et al. (1999) observed a significant reduction in aromatic carbon content due to ozone-induced reactions. These findings indicate a potential impact to soil adsorption properties because of research experiments performed by Karickhoff (1984). He found that sorption processes in soils were highly dependent on the sorptive sites provided by natural organic matter, and that organic matter was the primary sorbing constituent in

sediments and soils. Kawahara et al. (1995) observed preliminary indications that PAH mobility within soils increased following remediation using Fenton's reagent.

Objective

Due to limitations in understanding the degree to which *in situ* chemical oxidation impacts the adsorption properties within the soil matrix, experiments using 2,4-Dichlorophenol were conducted in order to experimentally quantify the impact of ISCO on a variety of soil types.

Methods and Materials

Soil Treatments

Various treatments were performed on the different soils to determine the impact of oxidation on its adsorption properties. Tested soil treatments included pre-treatment, DI-H_2O/air-sparge, ferrous iron, Fenton's Reaction, ozone, and peroxone. Pre-treatment samples were tested by removing 100 grams of soil from the stock container and air-drying the samples for 2 weeks. To ensure that the changes in adsorption properties were due to the oxidation rather than mixing or centrifugation, a DI-H_2O/air-sparge treatment was conducted. 120 grams of dried soil and 280 g of DI-H_2O were added to a 1,000-mL Erlenmeyer flask. The slurry was mixed using a magnetic stir bar and stir plate on the #5 setting. Oxygen was sparged into the flask for three hours per day for three consecutive days at a flowrate of 2 scfh. The slurry

was then centrifuged at 2000 rpm for 30 minutes. The liquid was decanted, and the remaining soil was air-dried for 2 weeks.

For treatment via ferrous iron, 120 grams of dried soil and 280 g of 5,000 mg/L Fe^{2+} solution were added to a 1,000-mL Erlenmeyer flask. The flask was then shaken on an orbital shaker for 96 hours at 150 rpm to allow the ferrous iron to equilibrate with the soil slurry. Following the equilibration, the slurry was centrifuged for 30 minutes at 2000 rpm. The liquid was decanted, and the remaining soil was air-dried for 2 weeks.

For treatment via Fenton's Reaction, 120 grams of dried soil and 280 g of 5,000 mg/L Fe^{2+} solution were added to a 1,000-mL Erlenmeyer flask. The flask was then shaken on an orbital shaker for 24 hours at 150 rpm to allow the ferrous iron to equilibrate with the soil slurry. Following the equilibration, a quantity of 30% (w/w) stock H_2O_2 was added to the flask such that the concentration within the liquid was 50,000 mg/L. Following a 24-hour reaction, a second addition of H_2O_2 was made to regenerate the concentration of H_2O_2 within the flask to 50,000 mg/L. Following this second reaction period, a third application at 50,000 mg/L H_2O_2 was made. After a final 24-hour reaction period was allowed, the slurry was centrifuged for 30 minutes at 2000 rpm. The liquid was decanted, and the remaining soil was air-dried for 2 weeks.

For treatment via ozone, 120 grams of dried soil and 280 g of DI-H_2O were added to a 1,000-mL Erlenmeyer flask. The slurry was mixed using a magnetic stir bar and stir plate on the #5 setting. An ozone gas stream, at a concentration of 5.5

wt.% O_3 in the gas phase, was sparged into the flask for three hours per day for three consecutive days at a flowrate of 2 scfh. The slurry was then centrifuged at 2000 rpm for 30 minutes. The liquid was decanted, and the remaining soil was air-dried for 2 weeks.

For treatment via peroxone, 120 grams of dried soil and 280 g of DI-H_2O were added to a 1,000-mL Erlenmeyer flask. The slurry was mixed using a magnetic stir bar and stir plate on the #5 setting. An ozone gas stream, at a concentration of 5.5 wt.% O_3 in the gas phase, was sparged into the flask for three hours per day for three consecutive days at a flowrate of 2 scfh. Five minutes into each ozonation period, the slurry was spiked with a quantity of 30% (w/w) H_2O_2 such that the initial H_2O_2 concentration within the flask was 1,000 mg/L. The slurry was then centrifuged at 2000 rpm for 30 minutes. The liquid was decanted, and the remaining soil was air-dried for 2 weeks.

Test Adsorbate

2,4-Dichlorophenol (Aldrich, CAS: 120-83-2) was used as the test adsorbate in the experiments to determine the Freundlich adsorption isotherms. Stock solutions of 10, 50, 100, 250, and 500 mg/L DCP were created in the laboratory in 1-liter volumetric flasks by adding appropriate quantities of DCP and DI-H_2O. Solutions were then stirred on a hot plate for 15 minutes at 90°C to dissolve the DCP into solution. Solutions were then allowed to cool to room temperature.

Shake Vials

To determine the impact of oxidation on adsorption, 40-mL shake vial tests were utilized. For each specific soil and treatment (e.g. Ozonated High pH Soil), five shake vials were created by adding 5 grams of dried soil to each container. Then 20 grams of a specific DCP solution (10, 50, 100, 250, or 500 mg/L) were added to each shake vial. Fifteen 5mm glass beads were then added to each test vial in order to enhance the mixing process. The vials were then mixed for 24 hours at the maximum (#10) setting on a Burrell wrist action shaker (Model #75). Duplicate shake vial tests were performed on each specific soil treatment sample.

Separation of Solid/Liquid Phases

In order to calculate the Freundlich adsorption coefficients (K_d), the concentration of DCP within the liquid phase was required. Following the 24-hour shake period, the test vials were centrifuged for 60 minutes at 2000 rpm. Liquid samples were then decanted and filtered through a 0.20-micron glass fiber filter using a vacuum pump apparatus. Then, 2 mL of the resulting liquid was transferred into a standard HPLC vial and analyzed for the concentration of 2,4-Dichlorophenol.

Results and Discussion

Determination of the Freundlich Adsorption Coefficient

For each individual soil treatment type, a 5.0 g soil samples was added to each of five 40-mL shake vials. Each sample was subsequently dosed with 20.0 grams of a 10 mg/L, 50 mg/L, 100 mg/L, 250 mg/L, or a 500 mg/L solution of 2,4-DCP.

Following a 24-hour shake/equilibrium period, each of the five liquid phases was analyzed via HPLC to determine its respective concentration of 2,4-DCP (C_{DCP}). Once the concentration of 2,4-DCP in the liquid phases was analytically determined, mass balances were used to determine the concentration of 2,4-DCP that had adsorbed onto the soil. Equations 1-4 represent the mass balance equations used to obtain the concentration of 2,4-DCP in the soil partition after the 24-hour equilibration period (Q_{DCP}):

$$M_{DCP,total} = C_{DCP,initial} * V_L \quad (1)$$

$$M_{DCP,liquid} = C_{DCP} * V_L \quad (2)$$

$$M_{DCP,solid} = M_{DCP,total} - M_{DCP,liquid} \quad (3)$$

$$Q_{DCP} = \frac{M_{DCP,solid}}{M_{soil}} \quad (4)$$

where,

$M_{DCP,total}$ = Total mass of 2,4-DCP added to vial, mg

$C_{DCP,initial}$ = Initial concentration of 2,4-DCP solution, mg/L

V_L = Total volume of liquid solution added to vial, L

$M_{DCP,liquid}$ = Mass of 2,4-DCP in the liquid partition after 24 hrs, mg

C_{DCP} = Concentration of 2,4-DCP in the liquid partition after 24 hrs, mg/L

$M_{DCP,solid}$ = Mass of DCP adsorbed onto soil after 24 hrs, mg

M_{soil} = mass of dry soil in the shake vial, kg

Q_{DCP} = Conc. of 2,4-DCP in the soil partition after 24 hrs, mg DCP/kg dry soil

Once C_{DCP} and Q_{DCP} were successfully obtained for each of the five different DCP concentrations, adsorption isotherms could be plotted for each soil/treatment type. A direct comparison of the partitioning coefficients was made by utilizing a linear isotherm model, as reported by LaGrega et al. (2001) and represented by Equation 5:

$$Q_{DCP} = K_d * C_{DCP} \quad (5)$$

where,

Q_{DCP} = Conc. of 2,4-DCP in the soil partition after 24 hrs, mg DCP/kg dry soil

C_{DCP} = Concentration of 2,4-DCP in the liquid partition after 24 hrs, mg/L

K_d = Freundlich adsorption coefficient for particular soil/treatment, L/kg

This equation enabled the calculation of the Freundlich adsorption coefficients (K_d's) for each data set by plotting Q_{DCP} vs. C_{DCP}; K_d was then simply determined by calculating the slope of the line. Polymath 5.1 was used to mathematically determine the slope (K_d), the 95% confidence interval, and the R^2 value for the duplicate test runs on each soil/treatment type. Figure 13.1 shows a typical adsorption isotherm observed during experiments, this particular set representing the High TOC Soil prior to any treatment application.

Adsorption of 2,4-DCP onto the Ozonated Sand Control

The first experimental analyses using 2,4-Dichlorophenol were made by plotting the adsorption isotherm to determine the K_d of the Ozonated Sand test control. Because the Ozonated Sand had a non-detectable concentration of organic carbon, it was expected that minimal adsorptive capacity would be observed for the

Ozonated Sand sample. Table 13.1 shows the Polymath 5.1 results for K_d, 95 % confidence interval, and R^2 for all soils and treatment types. As was expected, the Ozonated Sand displayed a minimal capacity to adsorb 2,4-DCP as concluded by its low calculated K_d (0.06355 L/kg) and 95% confidence interval that contains a K_d value of zero. This result also proved the validity of the experimental methods in determining K_d's for other soil types. The low K_d indicated that no significant quantity of 2,4-DCP was lost during the shake period or the vacuum filtration step of the experimental procedure; this allowed for the assumption that any losses of 2,4-DCP during normal experimental procedures on other soil types would also be negligible.

Results of the Impact of ISCO on Soil Adsorption Properties

As was mentioned in the previous section, all of the Polymath 5.1 results for K_d, 95% confidence interval, and R^2 values for each of the soil/treatment types are shown in Table 13.1. Figures 13.2, 13.3, 13.4, and 13.5 show the results of the impact of ISCO to the Average Soil, High pH Soil, High Iron Soil, and High TOC Soil, respectively. For the Average Soil, the K_d was impacted by different ISCO treatments. While the DI-Water treatment application caused no significant change in the observed K_d, treatments via Fenton's Reaction, ozone, and peroxone did exhibit significant reductions in Freundlich adsorption coefficients. Treatment of the Average Soil using peroxone appeared to cause the most significant impact, reducing the K_d by over half, from 3.7 L/kg to 1.7 L/kg. This was most likely due to the

peroxone chemical oxidation technology being significantly more aggressive than other ISCO technologies (Hong et al., 1996).

The High pH Soil (Figure 13.3) offered very little adsorptive capacity for 2,4-DCP. Insignificant quantities of 2,4-DCP were observed to have adsorbed onto the soil partition, and this yielded K_d values which were very low for both the pre-treatment and post-treatment samples of High pH Soil. The negative values observed were most likely a function of the very poor R^2 values. Because insignificant adsorption occurred, data did not fit well with the linear model normally applied towards soil samples. The reason for the insignificant adsorption observed in the High pH soil was hypothesized to be due to results observed by Qui (1999) in his dissertation work. He found that at high pH values, the disassociation constant (K_a) of dichlorophenol was surpassed, and this resulted in the conversion of DCP into its ionic form of dichlorophenoxide anion. The conversion of the test adsorbate to a different chemical species most likely caused the observed changes in observed sorptive properties.

The High Iron Soil (Figure 13.4) displayed results that were somewhat similar to those results observed for the Average Soil. While a DI-Water/air sparge treatment showed no significant impact to the K_d as compared to pre-treatment soil samples, each of the three treatments via oxidation did significantly reduce the observed K_d. Again, treatment via peroxone appeared to cause the largest impact to a soil's adsorption properties, reducing K_d from 2.8 L/kg to 0.3 L/kg.

Much of the observed reductions in 2,4-DCP adsorption onto the Average Soil and High Iron Soil is hypothesized to be based on the changes in soils' natural organic matter (NOM) due to ISCO, results that were discussed in detail in Chapter XII. Those results indicated a relative increase in aliphatic compounds and a relative decrease in aromatic compounds contained within the soil matrix. Cabaniss et al. (2000) reported that the molecular weight of humic substances within soils played a key role in NOM properties such as adsorption. They illustrated that higher molecular weight components within soil environments offered increased adsorptive capacities. Xing (2001) expanded this thought in his discussion regarding the sorption of naphthalene and phenanthrene by soil humic acids by looking at both aliphatic and aromatic soil components. He found a positive correlation between a soil sample's aromaticity and the non-linearity of sorption isotherms. He concluded that hydrophobic organic compounds were strongly influenced by aromatic portions of soil organic matter. It is therefore hypothesized that the observed reductions in high-molecular weight soil aromatic compounds (Chapter XII observations) were playing a key role in the observed changes in K_d values due to ISCO.

The K_d's for the High TOC Soil (Figure 13.5) did not appear to be significantly altered no matter which treatment application was used. The 95% confidence intervals for each treatment type all share common values, indicating that the High TOC Soil was insignificantly altered by oxidation. This is most likely due to the overwhelming abundance of naturally occurring total organic carbon within the soil. Karickhoff (1984) discussed the high importance of organic matter as the

primary sorbing constituent. Because the High TOC Soil had a natural abundance of available sorption sites, applications of limited quantities of oxidizers were not enough to eliminate a significant quantity of all the available adsorptive sites, thus causing an insignificant impact to observed values of K_d.

Summary of the Impact of ISCO on Soil Adsorption Properties

Results indicated that in soil samples with relatively average levels of total organic carbon (e.g. Average Soil and High Iron Soil), observed values of the Freundlich adsorption coefficient (K_d) were significantly reduced following treatment via Fenton's reaction, ozone, and peroxone oxidation. This was hypothesized to be primarily a function of the degradation of the sorptive sites provided by the naturally occurring organic carbon. In the soil sample with a relatively high level of total organic carbon, the values of K_d were insignificantly impacted by all of the tested applications of chemical oxidizers. Results tended to agree with the observations of Kawahara (1995) when he observed the increased mobility of PAH's following application of Fenton's reagent.

For users of ISCO technologies, the impact of ISCO on soil adsorption properties is something that must be considered when seeking to remediate subsurface contaminants. Firstly, the release of contaminants from sorptive sites of the soil matrix could theoretically improve remediation efficiencies by making it easier for oxidizers to contact pollutants. Ravikumar and Gurol (1990) commented on the preference that pollutants be desorbed into the aqueous phase during remediation via ISCO as opposed to being actively adsorbed within the soil matrix.

Nelson and Brown (1994) also commented on the importance of ozone gas successfully reaching the contaminant of interest. As ozone dissolves into the groundwater, it is necessary that it come into direct contact with the contaminant that must be treated. Watts et al. (2002) discussed the necessary conditions for advanced oxidation using hydroxyl radicals. The hydroxyl radicals generated by Fenton's reaction are incapable of oxidizing organic pollutants that do not exist in the aqueous phase. Pollutants that are firmly interlaced within the soil matrix make it far more difficult to be treated via *in situ* chemical oxidation as compared to pollutants in the aqueous phase.

While a reduction in soil adsorption capacities can be beneficial in the respect that it makes pollutants more easily accessible by oxidizers, it also can present certain problems that ISCO users must be aware. Some contaminants, such as polycyclic aromatic hydrocarbons (PAH's), are hydrophobic and adsorb very strongly within the soil matrix (Saxe et al., 2000; Goi and Trapido, 2004). While this hydrophobic property makes it difficult to achieve optimal pollutant-oxidizer contact, the strong adsorption nature does provide one important advantage to ISCO users. Enell et al. (2004) performed experiments dealing with PAH leaching in soil columns. During a long-term study on this topic, Enell found that only a minor fraction (~0.3%) of the initial PAH mass was released from the column. Because of this property of PAH's, it significantly limits their mobility within the aquifer, minimizing the spread of PAH contamination over a larger area. However, upon applying ISCO remediation technologies to contaminated sites, users must be aware that soil adsorption properties

within the subsurface have the potential to significantly change, thereby changing the transport properties within the subsurface. In a remediation treatment of contaminated soil by Kawahara et al. (1995), PAH's became significantly more mobile following applications of Fenton's reaction. Users must therefore be aware of the potential for contaminants to further spread after ISCO applications, potentially increasing the boundaries of the contaminant zone that must be treated.

Table 13.1: Numerical Results for K_d, 95% Confidence Interval, and R^2 for Impact of ISCO on Soil Adsorption Experiments

Soil/Treatment	**K_d (L/kg)**	**95% C.I. (L/kg)**	**R^2**
Ozonated Sand/No Treatment	0.06355	0.1526	0.1034
Average Soil/No Treatment	3.731	1.1039	0.919
Average Soil/DI-Water	4.1509	2.034	0.846
Average Soil/Fenton's Reagent	1.9116	0.5236	0.8986
Average Soil/Ozone	1.5523	0.4276	0.9133
Average Soil/Peroxone	1.705	0.3137	0.9593
High pH Soil/No Treatment	-0.7161	0.171	0.946
High pH Soil/DI-Water	-0.02819	0.2809	0.0099
High pH Soil/Fenton's Reagent	-0.04846	0.3183	0.0152
High pH Soil/Ozone	-0.2902	0.1262	0.8407
High pH Soil/Peroxone	-0.2833	0.497	0.2488
High Fe Soil/No Treatment	2.8259	0.216	0.9927
High Fe Soil/DI-Water	2.323	0.4279	0.975
High Fe Soil/Fenton's Reagent	1.4874	0.6569	0.8365
High Fe Soil/Ozone	0.9314	0.32	0.8943
High Fe Soil/Peroxone	0.3202	0.1606	0.8844
High TOC Soil/No Treatment	10.781	0.4686	0.9976
High TOC Soil/DI-Water	9.1619	2.6237	0.8902
High TOC Soil/Fenton's Reagent	15.3935	4.3269	0.91
High TOC Soil/Ozone	9.3912	3.0818	0.8606
High TOC Soil/Peroxone	8.7287	3.5111	0.8316

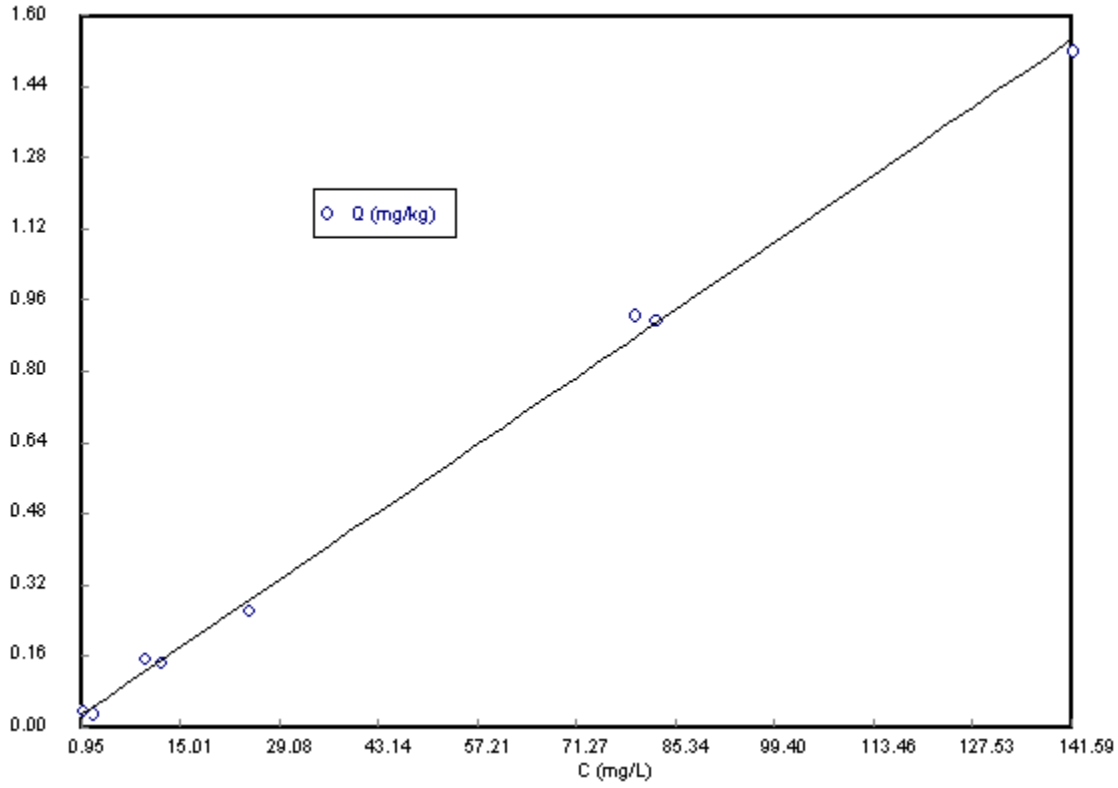

Figure 13.1: A Typical K_d Isotherm for Impact of ISCO on Soil Adsorption (High TOC Soil – No Treatment)

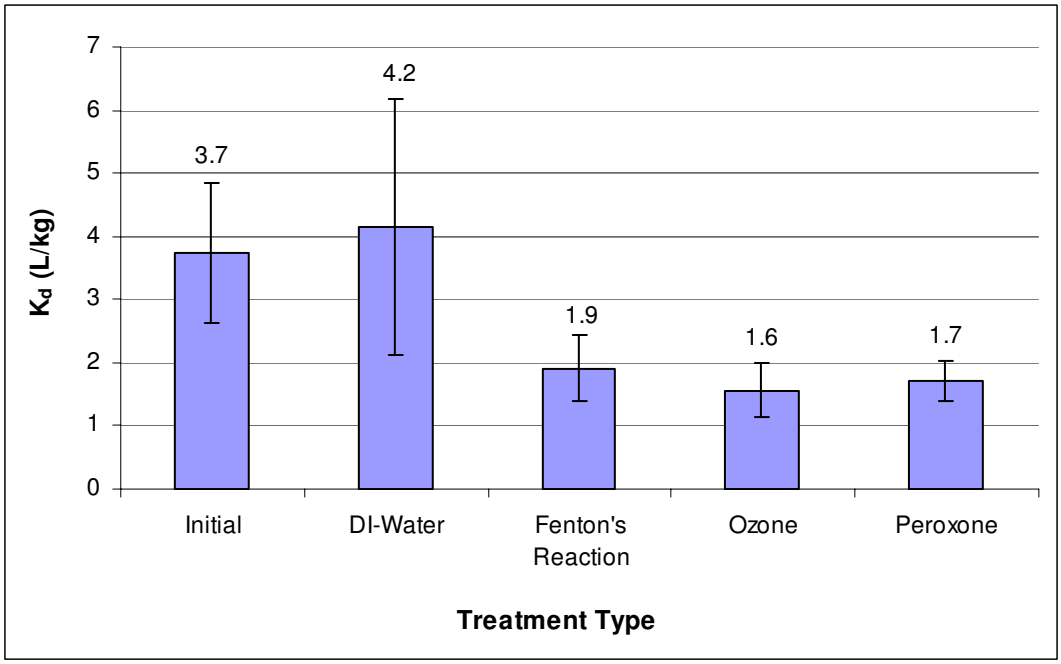

Figure 13.2: Impact of ISCO on the Adsorption Properties of Average Soil

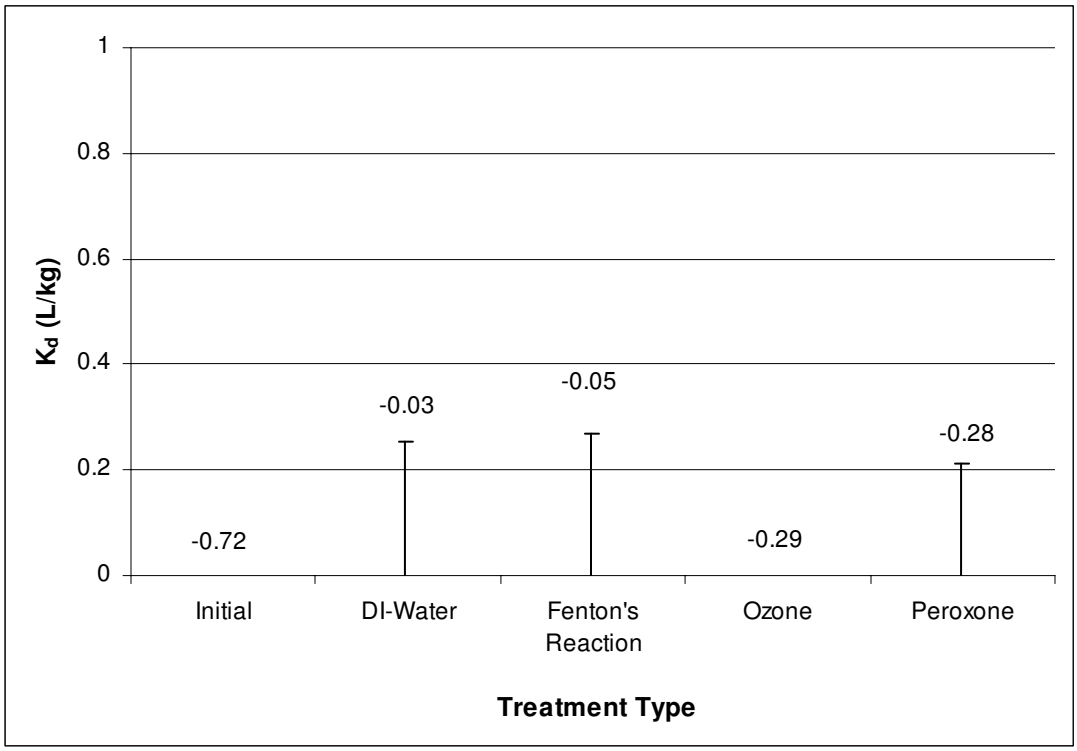

Figure 13.3: Impact of ISCO on the Adsorption Properties of High pH Soil

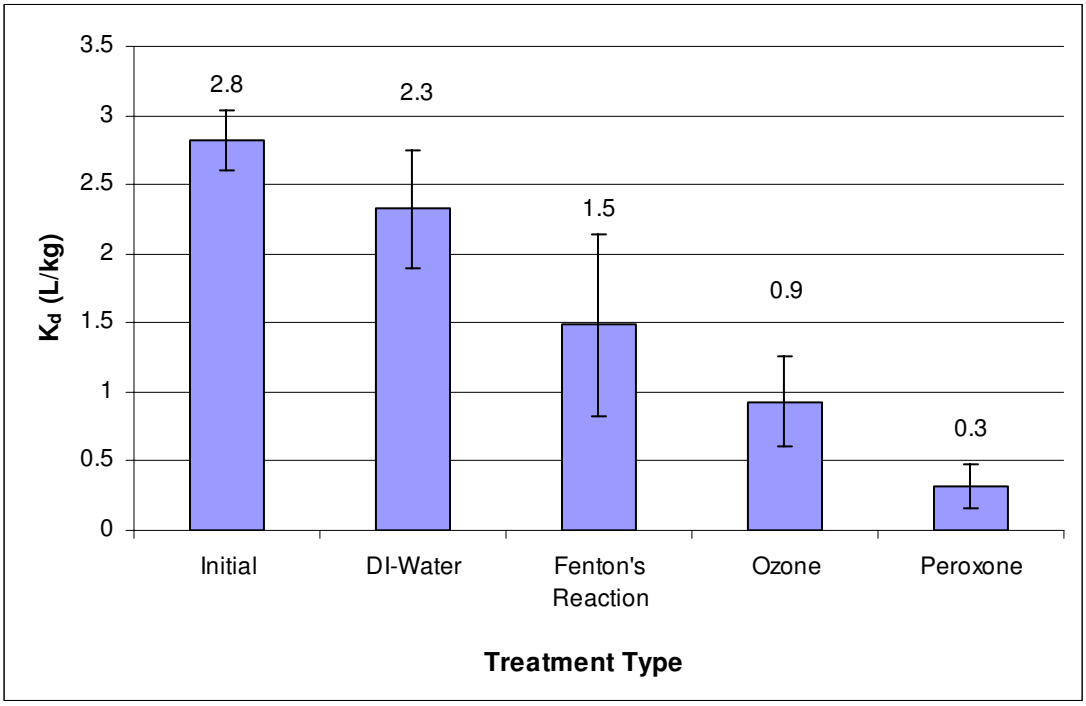

Figure 13.4: Impact of ISCO on the Adsorption Properties of High Iron Soil

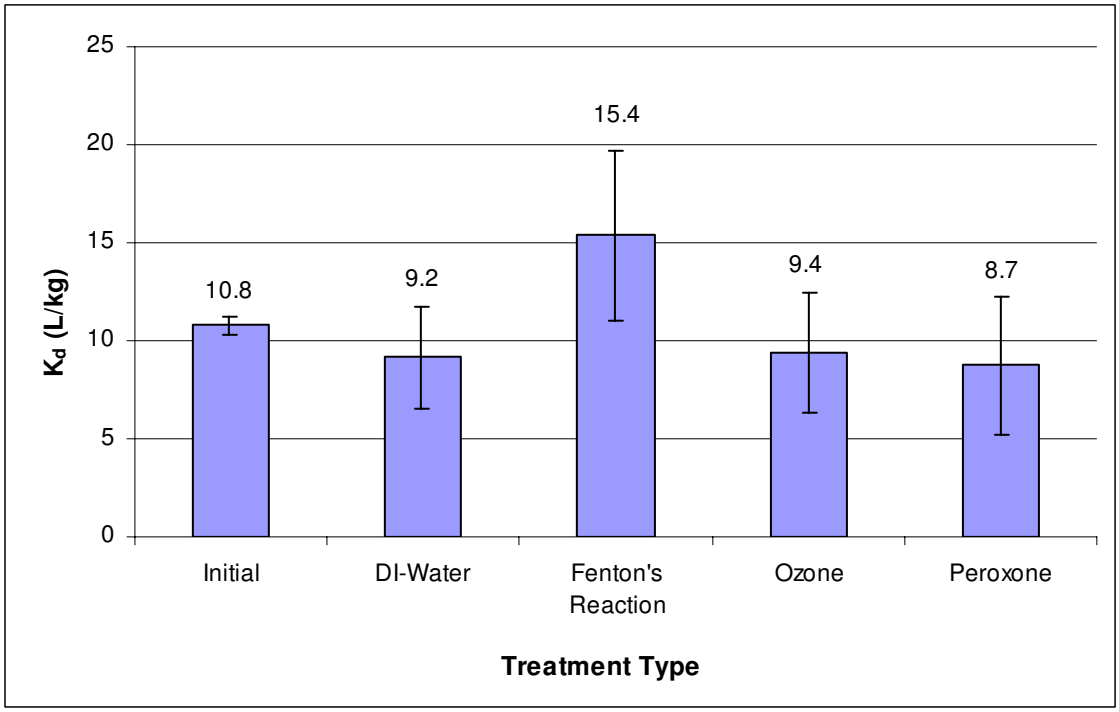

Figure 13.5: Impact of ISCO on the Adsorption Properties of High TOC Soil

CHAPTER XIV

FUTURE WORK

While the results of this research effort have shown conclusive evidence of key multi-level interactions between ISCO process reagents and multiple soil types, the following items indicate the potential for many further avenues of exploration related to this research:

- During experiments determining the total demand of hydrogen peroxide, it was observed that the hydrogen peroxide degradation rates decreased as the soil approached its total hydrogen peroxide demand. Therefore, it is proposed that experiments be run to determine H_2O_2 kinetic rate constants as a function of the amount of H_2O_2 added into the system.
- It is proposed that an expansion be made to the Langmuir-Hinshelwood Model that was used to further analyze the degradation kinetics of hydrogen peroxide. It is proposed that a soil poisoning constant, similar to the poisoning constant used for catalysts, be incorporated into the model to simulate the reduction in rate constant due to rate changes as the soil's total H_2O_2 demand is approached.

- It is proposed that a further expansion be made to the correlation comparing the total H_2O_2 demand of equilibrated water with its respective total H_2O_2 demand of the associated soil type. This expansion should not only include a multitude of other "clean" soil types but also incorporate the addition of contaminated soils and groundwater samples.
- It is proposed that further investigations be made into the soil buffering kinetics of acids and bases. Firstly, only one acid (H_3PO_4) and one base (NaOH) were explored during this research, and further testing on other acid and base types should be studied to determine the optimal acid and base that should be added to different soil types. Secondly, buffering kinetics were calculated based only of the adjustment of soil pH to 3.0 for additions of acid and 10.0 for additions of base. It is proposed that further analysis be made to determine soil buffering kinetics as a function of the level of pH adjustment.
- One potential factor in observed hydraulic conductivity reductions due to ISCO was hypothesized to be due to the evolution of oxygen gas that became entrapped within soil pores. Therefore, it is proposed that experiments be conducted which degas soil columns following ISCO treatments to determine the impact of entrapped O_2 bubbles on the observed hydraulic conductivity reduction factors.
- While the impact of oxidizers on soil hydraulic conductivities have been substantially discussed in this research, no work was done to determine the impact of acid and base additions on the hydraulic conductivity values. Therefore, it is

proposed that the existing column setup be used to determine the levels to which soil permeability is impacted by soil pH adjustments.

- Experiments using 2,4-Dichlorophenol were performed to determine the impact of ISCO on the adsorptive properties of multiple soil types. While 2,4-DCP was successfully used to calculate Freundlich adsorption isotherms, it is proposed that additional experiments be performed to determine impact of ISCO on the adsorption of both pentachlorophenol (PCP) and 2,4,6-Trinitrotoluene (TNT). Additionally, adsorption experiments only analyzed for the partitioning coefficient (K_d) and ignored potential changes in total adsorptive capacities. The determination of pre-treatment and post-treatment total adsorptive capacities would provide another tool to better understand ISCO's impact on contaminant adsorption.

CHAPTER XV

CONCLUSIONS

The results of this study provide a wealth of evidence that both *in situ* chemical oxidation (ISCO) process reagents and natural soil properties and characteristics are significantly impacted during the application of ISCO on different soil types. The following conclusions reflect the results obtained from experiments designed to elucidate key interactions and ensuing impacts.

Impact of Common Soil Constituents on Process Reagent Transport

- Hydroxide ions associated with high pH conditions and total microbial populations were determined to have the greatest impact on first-order H_2O_2 rate constants for equilibrated water; iron, total microbial populations, and soil particle size were shown to have the greatest impact on first-order H_2O_2 rate constants for soil slurries.
- The total organic carbon level had a significant impact on the total H_2O_2 demand of the equilibrated water, while total microbial populations had a significant impact on total H_2O_2 demand of the soil. Additionally, a linear, positive correlation was observed comparing the total H_2O_2 demand of the equilibrated water with the total H_2O_2 demand of its associated soil

type, giving ISCO practitioners a useful tool to estimate expected total hydrogen peroxide demands.

- Ozone utilization rates (OZUR's) and total O_3 demands of equilibrated water samples were highly dependent on the pH; OZUR's and total demands of soil slurries were highly dependent on both the pH of the soil slurry and the soil calcium content.
- The second-order buffering kinetics of H_3PO_4 was highly dependent on the initial soil pH, and the second-order buffering kinetics of NaOH was highly dependent on both the initial soil pH and the soil's total organic carbon content.
- As was observed in the soil buffering kinetic experiments, the initial soil pH played a key role in both the total H_3PO_4 and total NaOH demands, and the soil's TOC content also impacted the total NaOH demands observed.
- The Langmuir-Hinshelwood Model offered promising results in its ability to predict H_2O_2 degradation rates at multiple concentrations of H_2O_2. The model had more accuracy at the higher levels of H_2O_2 than at low levels of H_2O_2, possibly due to the differences in whether the soil reactive sites or the H_2O_2 was the limiting reagent during the reaction of hydrogen peroxide.

Investigation of Potential Personnel Safety Threats During Process Application

- Significant quantities of heat were produced during application of hydrogen peroxide into soil slurries due to the exothermic nature of Fenton's Reaction. Temperatures approached the boiling point of water in both the Average Soil and the Biologically Stimulated Soil. These results indicate a potential impact towards the many types of microbial populations that lose viability at high temperatures.
- Significant quantities of oxygen were produced during the application of hydrogen peroxide into soil slurries due to both the role of catalase-positive bacteria in promoting H_2O_2's degradation into oxygen gas and the O_2-producing reactions in the modified Fenton's Reaction mechanism. Oxygen concentrations in excess of 90% (v/v) were observed in batch reactors in which soil was treated with 100,000 mg/L of H_2O_2. This result indicates the potential for explosion risks during ISCO remediation due to increased oxygen levels.

Impact of Process Application on Soil Fabric Properties

- Results clearly indicated that treatment of different soil types by ISCO processes had a significant detrimental impact on aerobic soil bacteria populations due to both the reaction with oxidizers and the effects of increased temperature due to the exothermic nature of reactions. Microbial reductions were observed to decrease by as many as six orders of magnitude in some ISCO treatments. These results indicate

compatibility concerns for remediation strategies seeking to couple ISCO and bioremediation technologies.

- It was observed that treatment via ISCO had the potential to dramatically impact the hydraulic conductivity within multiple soil environments. While treatment via ozone alone showed no significant impact on soil permeability, severe reductions in liquid flowrates were observed under a constant hydraulic gradient during initial contact with hydrogen peroxide, indicating that previously open flow channels had become sealed off by insoluble oxidation by-products and fine particles. Therefore, the addition of hydrogen peroxide into soil environments will significantly alter transport properties within the subsurface during ISCO.
- ISCO treatment significantly altered the natural organic matter (NOM) of soils as indicated by NMR analyses. Hydrogen peroxide extensively degraded the NOM such that soil organics were irrecoverable post-treatment. Changes due to ozone-only treatments were much more subtle, and relatively little change was induced by this treatment. For treatment via peroxone, the aliphatic and carbohydrate signals appeared relatively more intense post-treatment whereas signals indicative of peptides, protein, and aromatic structures were significantly reduced.
- Results indicated that in soil samples with relatively average levels of total organic carbon (e.g. Average Soil and High Iron Soil), observed values of the Freundlich adsorption coefficient (K_d) were significantly reduced

following treatment via Fenton's Reaction, ozone, and peroxone oxidation. In the soil sample with a relatively high level of total organic carbon, the values of K_d were insignificantly impacted by all of the tested applications of chemical oxidizers. These results indicate the potential for increased desorption of contaminants from the soil phase during ISCO treatments.

REFERENCES

Acar, Y.B., and Zappi, M. "Infrastructural Needs in Waste Containment and Environmental Restoration." *Journal of Infrastructure Systems*. Vol. 1, No. 2 1995: 82-91.

ARS Technologies. "Liquid Atomization Injection of $KMnO_4$." Online posting. ARS Pneumatic Fracturing & Injection Field Services. 15 December 2005 <http://www.arstechnologies.com/chemical_oxidation.html>.

Acero, J.L. and von Gunten, U. "Influence of Carbonate on the Ozone/Hydrogen Peroxide Based Advanced Oxidation Process for Drinking Water Treatment." *Ozone: Science & Engineering*. Vol. 22, No. 3 2000: 305-328.

Adams, C.D. and Randtke, S.J. "Ozonation Byproducts of Atrazine in Synthetic and Natural Waters." *Environmental Science and Technology*. Vol. 26, No.11 1992: 2218-2227.

Amarante, David. "Applying In Situ Chemical Oxidation." *Pollution Engineering*. Vol. 32, No. 2 2000: 40-42.

Aronstein, B.N., Lawal, R.A., and Maka, A. "Chemical Degradation of Cyanides by Fenton's Reagent in Aqueous and Soil-containing Systems." *Environmental Toxicology and Chemistry*. Vol. 13, No. 11 1994: 1719-1726.

Baciocchi, R., Boni, M.R., and D'Aprile, L. Application of H_2O_2 Lifetime as an Indicator of TCE Fenton-like Oxidation in Soils. *Journal of Hazardous Materials*. Vol. 107, No. 3 2004: 97-102.

Bartoli, R., Philippy, R., Portal, J.M., and Gerard, B. "Poorly Ordered Hydrous Fe Oxides, Colloidal Dispersion and Soil Aggregation. I. Effect of Humic Macromolecules on Surface and Colloidal Properties of Fe (III) Polycations." *Journal of Soil Science*. Vol. 43 1992: 47-58.

Blume, T., Weisbrod, N., and Selker, J.S. "Permeability Changes in Layered Sediments: Impact of Particle Release." *Ground Water*. Vol. 40, No. 5 2002: 466-474.

Cabaniss, S.E., Zhou, Q., Maurice, P.A., Chin, Y-P., and Aiken, G.R. "A Log-normal Distribution Model for the Molecular Weight of Aquatic Fulvic Acids." *Environmental Science and Technology*. Vol. 34, No. 6 2000: 1103-1109.

Carmo, A.M., Lakhwinder, S.H., and Thompson, M.L. "Sorption of Hydrophobic Organic Compounds by Soil Materials: Application of Unit Equivalent Freundlich Coefficients." *Environmental Science and Technology*. Vol. 34 2000: 4363-4369.

Chandrakanth, M.S. and Amy, G.L. "Effects of Ozone on the Colloidal Stability and Aggregation of Particles Coated with Natural Organic Matter." *Environmental Science and Technology*. Vol. 30 1996: 431-443.

Chen, C.T., Tafuri, A.N., Rahman, M., and Foerst, M.B. "Chemical Oxidation Treatment of Petroleum Contaminated Soil using Fenton's Reagent." *Journal of Environmental Science and Health, Part A*. Vol. 33, No. 6 1998: 987-1008.

Chen, G., Hoag, G.E., Chedda, P., Nadim, F., Woody, B.A., and Dobbs, G.M. "The Mechanism and Applicability of In Situ Oxidation of Trichloroethylene with Fenton's Reagent." *Journal of Hazardous Materials*. Vol. 87, No. 1-3 2001: 171-186.

Chen, Y.H., Chang, C.Y., Chiu, C.Y., Huang, W.H., Yu, Y.H., Chiang, P.C., Ku, Y., and Chen, J.N. "Dynamic Model of Ozone Contacting Process with Oxygen Mass Transfer in Bubble Columns." *Journal of Environmental Engineering*. Vol. 128, No. 11 2002: 1036-1045.

Choi, H., Lim, H.-N., Kim, J., Hwang, T.-M., and Kang, J.-W. "Transport Characteristics of Gas Phase Ozone in Unsaturated Porous Media for In Situ Chemical Oxidation." *Journal of Contaminant Hydrology*. Vol. 57, No. 1-2 2002: 81-98.

Conrad, S.H., Glass, R.J., and Peplinski, W.J. "Bench-scale Visualization of DNAPL Remediation Processes in Analog Heterogeneous Aquifers: Surfactant Floods and In Situ Oxidation Using Permanganate." *Journal of Contaminant Hydrology*. Vol. 58 2002: 13-49.

Conyers, M.K., Helyar, K.R., and Poile, G.J. "pH Buffering: The Chemical Response of Acidic Soils to Added Alkali." *Soil Science*. Vol. 165, No. 7 2000: 560-566.

Daniel, D.E. and Choi, H. "Hydraulic Conductivity Evaluation of Vertical Barrier Walls." *Geo-Engineering for Underground Facilities*. 1999: 140-161.

Daniel, David E. "Note on Falling Headwater and Rising Tailwater Permeability Tests." *Geotechnical Testing Journal*. Vol. 12, No. 4 1989: 308-310.

Department of Energy. "Chapter 4 - Confined Space Entry." *OSH Technical Reference*. 1998.

Dieng, Ian Kennedy Tiang Kwong Dieng. "Chemical Oxidation Enhanced Bioremediation of Polycyclic Aromatic Hydrocarbon Contaminated Sediments." 2003. M.S. Thesis, Mississippi State University.

Dragun, J. and Chiasson, A. Elements in North American Soils. Greenbelt, MD: Hazardous Materials Control Resource Institute, 1991.

Elizardo, Kelly. "Fighting Pollution with Hydrogen Peroxide." *Pollution Engineering*. September, 1991: 106-109.

Elkins, J.G., Hassett, D.J., Stewart, P.S., Schweizer, H.P., and McDermott, T.R. Protective Role of Catalase in Pseudomonas aeruginosa Biofilm Resistance to Hydrogen Peroxide." *Applied and Environmental Microbiology*. Vol. 65, No. 10 1999: 4594-4600.

Elovitz, M.S. and von Gunten, U. "Hydroxyl Radical/Ozone Ratios During Ozonation Processes. II. The Effect of Temperature, pH, Alkalinity, and DOM Properties." *Ozone: Science and Engineering*. Vol. 22, No. 2 2000: 123-150.

Enell, A., Reichenberg, F., Warfvinge, P., and Ewald, G. "A Column Method for Determination of Leaching of Polycyclic Aromatic Hydrocarbons from Aged Contaminated Soil." *Chemosphere*. Vol. 54, No. 6 2004: 707-715.

Environmental Protection Agency. "In Situ Chemical Oxidation for Remediation of Contaminated Soil and Groundwater." *Ground Water Currents*. September, 2000: 1-6.

Fleming, Elizabeth. "Advanced Oxidation Processes for Remediation of Explosives Contaminated Soil." 2000. Ph.D. Dissertation, Louisiana State University.

Fogler, H.S. Elements of Chemical Reaction Engineering. 3rd Edition. Upper Saddle River, NJ: Prentice Hall, 1999.

Freese, S.D., Nozaic, D., Pryor, M.J., Trollip, D.L., and Smith, R.A. "Comparison of Ozone and Hydrogen Peroxide/Ozone for the Treatment of Eutrophic Waters." *Water Science and Technology*. Vol. 39, No. 10 1999: 325-328.

Freshour, A.R., Mawhinney, S., and Bhattacharyya, D. "Two-phase Ozonation of Hazardous Organics in Single and Multicomponent Systems." *Water Research*. Vol. 30, No. 9 1996: 1949-1958.

Frishe, T. and Hoper, H. "Soil Microbial Parameters and Luminescent Bacteria Assays as Indicators for In Situ Bioremediation of TNT-contaminated Soils." *Chemosphere*. Vol. 50 2003: 415-427.
Gieseking, J.E. Soil Components, Volume 1, Organic Components. New York: Springer-Verlag, 1975.

Glaze, W.H. and Kang, J.W. "Advanced Oxidation Processes. Description of a Kinetic Model for the Oxidation of Hazardous Materials in Aqueous Media with Ozone and Hydrogen Peroxide in a Semibatch Reactor." *Industrial Engineering Chemical Resource*. Vol. 28, No. 11 1989: 1573-1580.

Glaze, W.H. and Kang, J.-W. "Advanced oxidation processes. Test of a kinetic model for the oxidation of organic compounds with ozone and hydrogen peroxide in a semibatch reactor." *Industrial and Engineering Chemistry Research*. Vol. 28, No. 11 1989: 1580-1587.

Glaze, W.H., Beltran, F., Tuhkanen, T., and Kang, J.W. "Chemical Models of Advanced Oxidation Processes." *Water Pollution Research Journal of Canada*. Vol. 27, No. 1 1992: 23-42.

Goi, A. and Trapido, M. "Degradation of Polycyclic Aromatic Hydrocarbons in Soil: The Fenton Reagent Versus Ozonation." *Environmental Technology*. Vol. 25, No. 2 2004: 155-164.

Greenberg, R.S., Andrews, T., Kakarla, P.K., and Watts, R.J. "In Situ Fenton-like Oxidation of Volatile Organics: Laboratory, Pilot, and Full-scale Demonstrations." *Remediation*. Spring 1998: 29.

Greenland, D.J. and Hayes, M.H.B. The Chemistry of Soil Constituents. New York: John Wiley & Sons, 1978.

Gultekin, I. and Ince, N.H. "Degradation of Reactive Azo Dyes by UV/H_2O_2: Impact of Radical Scavengers." *Journal of Environmental Science and Health, Part A: Toxic/Hazardous Substances & Environmental Engineering*. Vol. A39, No. 4 2004: 1069-1081.

Gunasekara, A.S. and Xing, B. "Sorption and Desorption of Napthalene by Soil Organic Matter: Importance of Aromatic and Aliphatic Components." *Journal of Environmental Quality*. Vol. 32 2003: 240-246.

Gurol, M.D. and Singer, P.C. "Kinetics of Ozone Decomposition: A Dynamic Approach." *Environmental Science and Technology*. Vol. 16, No. 7 1982: 377-383.

Haselow, J.S., Siegrist, R.L., Crimi, M., and Jarosch, T. "Estimating the Total Oxidant Demand for In Situ Chemical Oxidation Design." *Remediation*. Vol. 13, No. 4 2003: 5-16.

Heister, S.D., Anderson, W.E., and Corpening, J.H. "A Model for Thermal Decomposition of Hydrogen Peroxide." *Proceedings of the American Institute of Aeronautics and Astronautics 40th Joint Propulsion Conference*. 2004: 1-18.

Hernandez, Rafael. "Integration of Zero-Valent Metals and Chemical Oxidation for the Destruction of 2,4,6-Trinitrotoluene within Aqueous Matrices." 2002. Ph.D. Dissertation, Mississippi State University.

Hernandez, R., Zappi, M., Colucci, J., and Jones, R. "Comparing the Performance of Various Advanced Oxidation Processes for Treatment of Acetone Contaminated Water." *Journal of Hazardous Materials*. Vol. 92, No. 1 2002: 33-50.

Heynes, M.M., Bearda, T., Mertens, P.W., Mertens, S., Cornelissen, I., and Meuris, M. "Cost-effective Cleaning and High Quality Thin-gate Oxides." *IBM Journal of Research and Development*. Vol. 43, No. 3 1999: 339-350.

Hoigne, J. and Bader, H. "Rate Constants of Reactions of Ozone with Organic and Inorganic Compounds in Water." *Water Resources*. Vol. 17 1983: 185-194.

Hong, A., Zappi, M.E., Kuo, C.H., and Hill, D. "Modeling Kinetics of Illuminated and Dark Advanced Oxidation Processes." *Journal of Environmental Engineering*. January, 1996: 58-62.

Hongmin, L., Zhiwei, L.., Xiaojiang, Y., and Wenfeng, S. "Kinetic Analysis of Photocatalytic Oxidation of Gas-phase Formaldehyde over Titanium Dioxide." *Chemosphere*. Vol. 60, No. 5 2005: 630-635.

Hwang, S., Batchelor, C.J., Davis, J.L., and MacMillan, D.K. "Sorption of 2,4,6-Trinitrotoluene to Natural Soils Before and After Hydrogen Peroxide Application." *Journal of Environmental Science and Health, Part A: Toxic/Hazardous Substances and Environmental Engineering*. Vol. 40, No. 3 2005: 581-592.

Interstate Technology & Regulatory Council (ITRC) In Situ Chemical Oxidation Team. Technical and Regulatory Guidance for In Situ Chemical Oxidation of Contaminated Soil and Groundwater. 2nd edition. Washington, D.C., 2005.

Jung, H. and Choi, H. "Effects of In Situ Ozonation on Structural Change of Soil Organic Matter." *Environmental Engineering Science*. Vol. 20, No. 4 2003: 289-299.

Kakarla, P.K., Andrews, T., Greenberg, R.S., and Zervas, D.S. "Modified Fenton's Processes for Effective In Situ Chemical Oxidation - Laboratory and Field Evaluation." *Remediation*. Vol. 12, No. 4 2002: 23-36.

Kakarla, P.K. and Watts, R.J. "Depth of Fenton-like Oxidation in Remediation of Surface Soils." *Journal of Environmental Engineering*. Vol. 123, No. 1 1997: 11-17.

Kaleli, H.A. and Islam, M.R. "Effect of Temperature on the Growth of Wastewater Bacteria." *Toxicological and Environmental Chemistry*. Vol. 59, No. 1-4 1997: 111-123.

Kanel, S.R., Neppolian, B., Choi, H., and Yang, J.-W. "Heterogeneous Catalytic Oxidation of Phenanthrene by Hydrogen Peroxide in Soil Slurry: Kinetics, Mechanism, and Implication." *Soil and Sediment Contamination*. Vol. 12, No. 1 2003: 101-117.

Karickhoff, S.W. "Organic Pollutant Sorption in Aquatic Systems." *Journal of Hydraulic Engineering*. Vol. 110, No. 6 1984: 707-735.

Kawahara, F., Davila, B., Al-Abed, S., Vesper, S., Ireland, J., and Rock, S. "Polynuclear Aromatic Hydrocarbon (PAH) Release from Soil During Treatment with Fenton's Reagent." *Chemosphere*. Vol. 31, No. 9 1995: 4131-4142.

Kobayashi, T., Shimizu, Y., and Urano, K. "Analysis of Adsorption Equilibrium of Volatile Chlorinated Organic Compounds to Dry Soil." *Journal of Hazardous Materials*. Vol. 108, No. 1-2 2004: 69-75.

Koch, B., Gramith, J.T., Dale, M.S., and Ferguson, D.W. "Control of 2-Methylisoborneol and Geosmin by Ozone and Peroxone: A Pilot Study." *Water Science and Technology*. Vol. 25, No. 2 1992: 291-298.

Kong, S.-H., Kwon, C.-I., and Kim, M.-H. "Ozone Kinetics and Diesel Decomposition by Ozonation in Groundwater." *Korean Journal of Chemical Engineering*. Vol. 20, No. 2 2003: 293-299.

Kotz, John and Treichel, Paul. Chemistry and Chemical Reactivity. 3rd Edition. Fort Worth, TX: Saunders College Publishing, 1996.

Ku, Y., Su, W.-J., and Shen, Y.-S. "Decomposition Kinetics of Ozone in Aqueous Solutions." *Industrial Engineering Chemistry Research*. Vol. 35 1996: 3369-3374.

Kuo, C.H., Li, K.Y., Wen, C.P., and Weeks, J.L. "Absorption and Decomposition of Ozone in Aqueous Solutions." *AIChE Symposium Series*. Vol. 73, No. 166 1977: 230-241.

Kuo, C.H. and Soong, H.S. "Oxidation of Benzene by Ozone in Aqueous Solutions." *The Chemical Engineering Journal*. Vol. 28 1984: 163-171.

Kuo, C.H., Zappi, M.E., and Chen, S.M. "Peroxone Oxidation of Toluene and 2,4,6-Trinitrotoluene." *Ozone: Science and Engineering*. Vol. 22, No. 5 2000: 519-534.

Kuo, C.H., Zhong, L., Zappi, M.E., and Hong, A.P. "Kinetics and Mechanism of the Reaction Between Ozone and Hydrogen Peroxide in Aqueous Solutions." *Canadian Journal of Chemical Engineering*. Vol. 77 1999: 473-482.

Kuo, C.H. and Chen, S.M. "Ozonation and Peroxone Oxidation of Toluene in Aqueous Solutions." *Industrial Engineering Chemical Research*. Vol. 35 1996: 3973-3983.

LaGrega, M.D., Buckingham, P.L., and Evans, J.C. Hazardous Waste Management. 2nd edition. Boston: McGraw Hill, 2001.

Langlais, B., Reckhow, D., and Brink, D. Ozone in Water Treatment. Chelsea, MI: Lewis Publishing, 1991.

Lee, W. and Batchelor, B. "Abiotic Reductive Dechlorination of Chlorinated Ethylenes by Iron-bearing Soil Minerals: 1. Pyrite and Magnetite." *Environmental Science and Technology*. Vol. 36, No. 23 2002: 5147-5154.

Leung, S.W. "Degradation of Perchloroethylene by Fenton's Reagent: Speciation and Pathway." *Journal of Environmental Quality*. Vol. 21 1992: 377-381.

Li, X.D.and Schwartz, F.W. "DNAPL Remediation with In Situ Chemical Oxidation Using Potassium Permanganate I. Mineralogy of Mn Oxide and its Dissolution in Organic Acids." *Journal of Contaminant Hydrology*. Vol. 68, No. 1-2 2004: 39-53.

Li, X.D.and Schwartz, F.W. "DNAPL Remediation with In Situ Chemical Oxidation Using Potassium Permanganate II. Increasing Removal Efficiency by Dissolving Mn Oxide Precipitates." *Journal of Contaminant Hydrology*. Vol. 68, No. 3-4 2004: 269-287.

Lim, H.N., Choi, H., Hwang, T.M., and Kang, J.W. "Characterization of Ozone Decomposition in a Soil Slurry: Kinetics and Mechanism." *Water Research*. Vol. 36, No. 1 2002: 219-229.

Louzao, M.J., Leiros, M.C., and Guitian, F. "Study of Buffering Systems in Soils from Galicia, N.W. Spain." *Water, Air, & Soil Pollution*. Vol. 49, No. 1-2 1990: 17-33.

Lowe, K.S., Gardner, F.G., and Siegrist, R.L. "Field Evaluation of In Situ Chemical Oxidation Through Vertical Well-to-Well Recirculation of $NaMnO_4$." *Ground Water Monitoring and Remediation*. Vol. 22, No. 1 2002: 106-115.

MacKinnon, L.K. and Thomson, N.R. "Laboratory-scale In Situ Chemical Oxidation of a Perchloroethylene Pool Using Permanganate." *Journal of Contaminant Hydrology*. Vol. 56, No. 1-2 2002: 49-74.

Magdoff, F.R. and Bartlett, R.J. "Soil pH Buffering Revisited." *Soil Science Society of American Journal*. Vol. 49 1985: 145-148.

Matula, J. and Pechova, M. "A Simplified Approach to Liming and its Evaluation." *Communications in Soil Science and Plant Analysis*. Vol. 33, No. 15-18 2002: 2989-3006.

Mesquita, M.E., Carranca, C., and Menino, M.R. "Influence of pH on Copper-Zinc Competitive Adsorption by a Sandy Soil." *Environmental Technology*. Vol. 23, No. 9 2002: 1043-1050.

Messerli, M.A., Amaral-Zettler, L.A., Zettler, E., Jung, S.K., Smith, P.J., and Sogin, M.L. "Life at Acidic pH Imposes an Increased Energetic Cost for a Eukaryotic Acidophile." *Journal of Experimental Biology*. Vol. 208 2005: 2569-2579.

Montville, T.J., Parris, N., and Conway, L.K. "Influence of pH on Organic Acid Production by Clostridium sporogenes in Test Tube and Fermentor Cultures." *Applied and Environmental Microbiology*. Vol. 49, No. 4 1985: 733-736.

Naval Air Station - Pensacola, FL. "Optimization of Remedial Action Operation to Treat Chlorinated Hydrocarbons in Groundwater." NAS Technical Report, Remedial Action Operation Optimization, 2002: 1-18.

Nelson, C. and Brown, R. "Adapting Ozonation for Soil and Groundwater Cleanup." *Chemical Engineering*. November, 1994: EE18-EE22.

Noll, M.R. "Building Bridges Between Field and Laboratory Studies in an Undergraduate Groundwater Course." *Journal of Geoscience Education*. Vol. 51, No. 2 2003: 231-236.

Prescott, L.M., Harley, J.P., and Klein, D.A. Microbiology. 5th Edition. McGraw Hill, 2001.

Qiu, Y. "Kinetic and Mass Transfer Studies of the Reactions Between Dichlorophenols and Ozone in Liquid-Liquid and Gas-Liquid Systems." 1999. Ph.D. Dissertation, Mississippi State University.

Qiu, Y., Zappi, M.E., Kuo, C.H., and Fleming, E.C. "Kinetics and Mechanistic Study of Ozonation of Three Dichlorophenols in Aqueous Solutions." *Journal of Environmental Engineering*. Vol. 125, No. 5 1999: 441-450.

Qiu, Y., Kuo, C.H., and Zappi, M.E. "Ozonation Kinetics of Six Dichlorophenol Isomers." *Ozone: Science and Engineering*. Vol. 24, No. 2 2002: 123-131.

Ravikumar, J.X. and Gurol, M.D. "In Situ Chemical Oxidation of Hazardous Compounds in Soil." *Proceedings of the Mid-Atlantic Industrial Waste Conference*. 1990: 57-65.

Reed, B.E., Lin, W., Matsumoto, M.R., and Jensen, J.N. "Physiochemical Processes." *Water Environment Research*. Vol. 69, No. 4 1997: 444-462.

Reynolds, W.D., Brown, D.A., Mathur, S.P., and Overend, R.P. "Effect of In-Situ Gas Accumulation on the Hydraulic Conductivity of Peat." *Soil Science*. Vol. 153, No. 5 1992: 397-408.

Saxe, J.K., Allen, H.E., and Nicol, G.R. "Fenton Oxidation of Polycyclic Aromatic Hydrocarbons After Surfactant-Enhanced Soil Washing." *Environmental Engineering Science*. Vol. 17, No. 4 2000: 233-244.

Schroth, M.H., Oostrom, M., Wietsma, T.W., and Istok, J.D. "In Situ Oxidation of Trichloroethene by Permanganate: Effects on Porous Medium Hydraulic Properties." *Journal of Contaminant Hydrology*. Vol. 50, No. 1-2 2001: 79-98.

Shawarbi, M.Y. Soil Chemistry. New York: John Wiley & Sons, 1952.

Siegrest, R.L., Urynowicz, O.R., West, O.R., Crimi, M.L., and Lowe, K.S. Guidance for In Situ Chemical Oxidation at Contaminated Sites: Technology Overview with a Focus on Permanganate Systems. 2001.

Siegrist, R.L., Urynowicz, M.A., Crimi, M.L., and Lowe, K.S. "Genesis and Effects of Particles Produced During In Situ Chemical Oxidation Using Permanganate." *Journal of Environmental Engineering*. Vol. 128, No. 11 2002: 1068-1079.

Slagle, Dan. "Ozonation an Attractive Option for Groundwater System." *Public Works*. Vol. 121, No. 13 1990: 45-46.

Sohi, S.P., Mahieu, N., Powlson, D.S., Madari, B., Smittenberg, R.H., and Gaunt, J.L. "Investigating the Chemical Characteristics of Soil Organic Matter Fractions Suitable for Modeling." *Soil Science Society of America Journal*. Vol. 69 2005: 1248-1255.

Sotelo, J.L., Beltran, F.J., Gonzalez, M., Dominguez, J. "Effect of High Salt Concentrations on Ozone Decomposition in Water." *Journal of Environmental Science and Health, Part A: Environmental Science and Engineering & Toxic and Hazardous Substance Control*. Vol. 24, No. 7 1989: 823-842.

Spain, J.C., Milligan, J.D., Downey, D.C., and Slaughter, J.K. "Excessive Bacterial Decomposition of H_2O_2 During Enhanced Biodegradation." *Ground Water*. Vol. 27, No. 2 1989: 163-167.

Spanggord, R.J., Yao, D., and Mill, T. "Kinetics of Aminodinitrotoluene Oxidations with Ozone and Hydroxyl Radical." *Environmental Science and Technology*. Vol. 34, No. 3 2000: 450-454.

Staehelin, J. and Hoigne, J. "Decomposition of Ozone in Water: Rate of Initiation by Hydroxide Ions and Hydrogen Peroxide." *Environmental Science and Technology*. Vol. 16 1982: 676-681.

Stevenson, F.J. Humus Chemistry. New York: John Wiley & Sons, 1982.

Struse, A.M., Siegrist, R.L., Dawson, H.E., and Urynowicz, M.A. "Diffusive Transport of Permanganate During In Situ Oxidation." *Journal of Environmental Engineering*. Vol. 128, No. 4 2002: 327-334.

Subramani, Arun. "Adsorption of Organic Pollutants onto Natural Adsorbants." 2002. M.S. Thesis, Mississippi State University.

Taconi, Katherine A. "Methanogenic Generation of Biogas from Synthesis-Gas Fermentation Wastewaters." 2004. Ph.D. Dissertation, Mississippi State University.

Teel, A.L., Warberg, C.R., Atkinson, D.A., and Watts, R.J. "Comparison of Mineral and Soluble Iron Fenton's Catalysts for the Treatment of Trichloroethylene." *Water Research*. Vol. 35, No. 4 2001: 977-984.

Teel, A.L. and Watts, R.J. "Degradation of Carbon Tetrachloride by Modified Fenton's Reagent." *Journal of Hazardous Materials*. Vol. 94, No. 2 2002: 179-189.

Thibodeaux, L. Chemodynamics: Environmental Movement of Chemicals in Air, Water, and Soil. New York: John Wiley & Sons, 1979.

Trapido, M.J. "Ozonation and AOP Treatment of Phenanthrene in Aqueous Solutions." *Ozone: Science and Engineering*. Vol. 16 1994: 475-485.

Trapido, M., Dello, A., Goi, A., and Munter, R. "Degradation of Nitroaromatics with the Fenton Reagent." *Proceedings of the Estonian Academy of Sciences, Chemistry*. Vol. 52, No. 1 2003: 38-47.

Tyre, B.W., Watts, R.J., and Miller, G.C. "Treatment of Four Biorefractory Contaminants in Soil Using Catalyzed Hydrogen Peroxide." *Journal of Environmental Quality*. Vol. 20 1991: 832-838.
U.S. Geological Survey. "National Geochemical Survey Database: U.S. Geological Survey." 2002. Reston, VA.

Van Craeynest, K., Dewulf, J., Vandeburie, S., and Van Langenhove, H. "Removal of Trichloroethylene from Waste Gases via the Peroxone Process." *New Research in Water and Wastewater*. Vol. 48, No. 3 2003: 65-72.

Vitolins, Andrew R.; Nelson, Bruce R.; Underhill, Scott A. "Fenton's Reagent-based In Situ Chemical Oxidation Treatment of Saturated and Unsaturated Soils at a Historic Railroad Site." *Soil and Sediment Contamination*. Vol. 12, No. 1 2003: 139-150.

Wang, W. and Zappi, M. "Using Chemical Priming as a Means of Enhancing the Performance of Biocells for Treating Petroleum Products Containing Recalcitrant Chemical Species." 2001. Technical Report, Mississippi Department of Transportation.

Watts, R.J., Udell, M.D., and Rauch, P.A. "Treatment of Pentachlorophenol-Contained Soils using Fenton's Reagent." *Hazardous Waste & Hazardous Materials*. Vol. 7, No. 4 1990: 335-345.

Watts, R.J., Bottenberg, B.C., Hess, T.F., Jensen, M.D., and Teel, A.L. "Role of Reductants in the Enhanced Desorption and Transformation of Chloroaliphatic Compounds by Modified Fenton's Reactions." *Environmental Science and Technology*. Vol. 33 1999: 3432-3437.

Watts, R.J., Foget, M.K., Kong, S.H., and Teel, A.L. "Hydrogen Peroxide Decomposition in Model Subsurface Systems." *Journal of Hazardous Materials*. Vol. 69, No. 2 1999: 229-243.

Watts, R.J. and Stanton, P.C. "Mineralization of Sorbed and NAPL-Phase Hexadecane by Catalyzed Hydrogen Peroxide." Water Research. Vol. 33, No. 6 1999: 1405-1414.

Watts, R.J., Udell, M.D., Kong, S., and Leung, S.W. "Fenton-Like Soil Remediation Catalyzed by Naturally Occurring Iron Minerals." *Environmental Engineering Science*. Vol. 16, No. 1 1999: 93-103.

Watts, R.J., Haller, D.R., Jones, A.P., and Teel, A.L. "Foundation for the Risk-based Treatment of Gasoline-Contaminated Soils Using Modified Fenton's Reactions." *Journal of Hazardous Materials*. Vol. 76, No. 1 2000: 73-89.

Watts, R.J., Stanton, P.C., Howsawkeng, J., and Teel, A.L. "Mineralization of a Sorbed Polycyclic Aromatic Hydrocarbon in Two Soils Using Catalyzed Hydrogen Peroxide." *Water Research*. Vol. 36, No. 17 2002: 4283-4292.

Watts, R.J., Sarasa, J., Loge, F.J., and Teel, A.L. "Oxidative and Reductive Pathways in Manganese-Catalyzed Fenton's Reactions." *Journal of Environmental Engineering*. Vol. 131, No. 1 2005: 158-164.

Westerhoff, P., Debroux, J., Aiken, G., and Amy, G. "Ozone-Induced Changes in Natural Organic Matter (NOM) Structure." *Ozone: Science and Engineering*. Vol. 21, No. 6 1999: 551-570.

Whiteside, C. and Hassan, H.M. "Induction and Inactivation of Catalase and Superoxide dismutase of Escherichia coli by Ozone." *Archives of Biochemistry and Biophysics*. Vol. 257, No. 2 1987: 464-471.

Xing, B. "Sorption of Naphthalene and Phenanthrene by Soil Humic Acids." *Environmental Pollution*. Vol. 111 2001: 303-309.

APPENDIX A

RAW DATA FOR H_2O_2 FATE

Table A.1: H_2O_2 Degradation in Ozonated Sand Equilibrated Water (No Autoclave)

Time (min)	$[H_2O_2]$ Run 1 (mg/L)	$[H_2O_2]$ Run 2 (mg/L)	$[H_2O_2]$ Run 3 (mg/L)
0	18.45	17.8	17.43333333
5	18.9	18.5	16.86666667
10	18.9	18.36666667	16.86666667
15	18.23333333	17.9	17.53333333
20	18.83333333	17.6	17.66666667
25	18.86666667	18.7	17.9

Table A.2: H_2O_2 Degradation in Ozonated Sand Equilibrated Water (With Autoclave)

Time (min)	$[H_2O_2]$ Run 1 (mg/L)	$[H_2O_2]$ Run 2 (mg/L)	$[H_2O_2]$ Run 3 (mg/L)
0	16.56666667	15.1	15.3
5	16.33333333	15.825	14.9
10	16.8	15.4	14.8
15	17.1	16.03333333	15.5
20	16.43333333	16	15.56666667
25	16.5	16.16666667	14.7

Table A.3: H_2O_2 Degradation in Average Soil Equilibrated Water (No Autoclave)

Time (min)	$[H_2O_2]$ Run 1 (mg/L)	$[H_2O_2]$ Run 2 (mg/L)	$[H_2O_2]$ Run 3 (mg/L)
0	13.45	12.4	14.3
5	12.25	11.76666667	13.6
10	12.7	11.95	14.53333333
15	12.15	11.4	13.73333333
20	12	11.35	13.35
25	11.4	11	13
30	10.95	10.3	12.7
35	10.9	10.55	X
40	10.7	10.4	X

Table A.4: H_2O_2 Degradation in Average Soil Equilibrated Water (With Autoclave)

Time (min)	$[H_2O_2]$ Run 1 (mg/L)	$[H_2O_2]$ Run 2 (mg/L)	$[H_2O_2]$ Run 3 (mg/L)
0	12.83333333	13.5	11
5	12.86666667	13.25	11
10	12.8	12.86666667	11.1
15	12.46666667	13	11.15
20	12.13333333	12.86666667	11.2
25	12.35	12.85	11.05

Table A.5: H_2O_2 Degradation in High pH Soil Equilibrated Water (No Autoclave)

Time (min)	$[H_2O_2]$ Run 1 (mg/L)	$[H_2O_2]$ Run 2 (mg/L)	$[H_2O_2]$ Run 3 (mg/L)
0	7.8	7.95	8.8
3	7.15	6.733333333	7.3
6	6.4	6.15	5.75
9	5.5	4.65	4.7
12	5.566666667	3.9	3.35
15	4.45	3.05	3.05
18	3.8	2.6	2.8
21	3	2.15	2.2
24	2.25	1.6	2.2
27	2.25	1.6	1.6
30	1.95	1.35	1.6
33	1.8	1.25	0

Table A.6: H_2O_2 Degradation in High pH Soil Equilibrated Water (With Autoclave)

Time (min)	$[H_2O_2]$ Run 1 (mg/L)	$[H_2O_2]$ Run 2 (mg/L)	$[H_2O_2]$ Run 3 (mg/L)
0	14.5	14.5	16.9
2	14.7	14.7	16.9
4	11.9	11.9	15.6
6	12.25	12.25	15.2
8	11.55	11.55	16.4
10	9.75	9.75	14.1
12	9.7	9.7	15
14	9.3	9.3	14.3
16	8.7	8.7	13.4
18	8.8	8.8	12.2
20	8.833333333	8.833333333	13.3
22	6.75	6.75	10.1

Table A.7: H_2O_2 Degradation in High Fe Soil Equilibrated Water (No Autoclave)

Time (min)	$[H_2O_2]$ Run 1 (mg/L)	$[H_2O_2]$ Run 2 (mg/L)	$[H_2O_2]$ Run 3 (mg/L)
0	11.3	12.3	12.15
5	11.2	11.45	13.43333333
10	11.4	11.2	11.95
15	11.45	10.75	11.65
20	11.95	11	11.45
25	11.6	10.2	12.1
30	11.3	11.45	12.26666667

Table A.8: H_2O_2 Degradation in High Fe Soil Equilibrated Water (With Autoclave)

Time (min)	$[H_2O_2]$ Run 1 (mg/L)	$[H_2O_2]$ Run 2 (mg/L)	$[H_2O_2]$ Run 3 (mg/L)
0	15.2	14.05	14.7
5	14.85	14	14.9
10	13.6	13.8	13.8
15	14.1	14.1	14.7
20	12.95	14.3	14.5
25	12.5	14.3	14.75
30	13.1	14.85	14.7

Table A.9: H_2O_2 Degradation in High TOC Soil Equilibrated Water (No Autoclave)

Time (min)	$[H_2O_2]$ Run 1 (mg/L)	$[H_2O_2]$ Run 2 (mg/L)	$[H_2O_2]$ Run 3 (mg/L)
0	14.8	13.9	14.5
5	14	13.5	14
10	13.6	13.2	13.8
15	13.3	13	13.4
20	12.9	12.9	12.7
25	12.5	12.6	12.6
30	12.1	12	12.3
35	11.9	11.5	14.5
40	11.6	11.1	14

Table A.10: H_2O_2 Degradation in High TOC Soil Equilibrated Water (With Autoclave)

Time (min)	$[H_2O_2]$ Run 1 (mg/L)	$[H_2O_2]$ Run 2 (mg/L)	$[H_2O_2]$ Run 3 (mg/L)
0	15	14.3	14.2
5	14.4	13.8	13.9
10	13.7	13.5	13.9
15	13.2	13.3	13.3
20	13	12.8	12.8
25	12.6	12.8	12.5
30	12.3	12.1	12.2
35	12	11.8	14.2
40	11.5	11.6	13.9

Table A.11: H_2O_2 Degradation in Biologically Stimulated Soil Equilibrated Water (No Autoclave)

Time (min)	$[H_2O_2]$ Run 1 (mg/L)	$[H_2O_2]$ Run 2 (mg/L)	$[H_2O_2]$ Run 3 (mg/L)
0	13.6	12.6	14.5
5	12.1	11.8	13.3
10	11.7	11.5	12.9
15	11.6	11.3	12.8
20	11.6	11.2	12.5
25	11.3	10.8	12.6
30	11	10.6	12.2
35	10.6	10.4	14.5
40	10.4	9.6	13.3

Table A.12: H_2O_2 Degradation in Biologically Stimulated Soil Equilibrated Water (With Autoclave)

Time (min)	$[H_2O_2]$ Run 1 (mg/L)	$[H_2O_2]$ Run 2 (mg/L)	$[H_2O_2]$ Run 3 (mg/L)
0	13	13.4	12
5	12.9	13.2	11.9
10	12.8	12.95	11.8
15	12.6	13	11.7
20	12.6	12.8	11.5
25	12.5	12.8	11.5
30	12.4	12.6	11.3
35	13	13.4	12
40	12.9	13.2	11.9

Table A.13: H_2O_2 Degradation in Ozonated Sand (No Autoclave)

Time (min)	$[H_2O_2]$ Run 1 (mg/L)	$[H_2O_2]$ Run 2 (mg/L)	$[H_2O_2]$ Run 3 (mg/L)
0	12.3	10.95	10.3
5	12.76666667	10.6	10.3
10	12.35	11.15	9.4
15	12.75	11.1	9.15
20	12.7	12.15	9.35
25	12.2	10.45	10.25
30	12	10.55	10.4

Table A.14: H_2O_2 Degradation in Ozonated Sand (With Autoclave)

Time (min)	$[H_2O_2]$ Run 1 (mg/L)	$[H_2O_2]$ Run 2 (mg/L)	$[H_2O_2]$ Run 3 (mg/L)
0	18.85	19.1	18.1
5	17.7	19.7	17.6
10	18.3	18.9	18.6
15	18.4	18.65	17.8
20	18.3	18.55	16.9
25	19.1	18.75	16.43333333
30	18	19	17.2

Table A.15: H_2O_2 Degradation in Average Soil (No Autoclave)

Time (min)	$[H_2O_2]$ Run 1 (mg/L)	$[H_2O_2]$ Run 2 (mg/L)	$[H_2O_2]$ Run 3 (mg/L)
0	17.95	16.55	15.7
2	5.95	6.95	6.25
4	1.65	2.25	2.3
6	0.1	0.65	0.7
8	0	0	0

Table A.16: H_2O_2 Degradation in Average Soil (With Autoclave)

Time (min)	$[H_2O_2]$ Run 1 (mg/L)	$[H_2O_2]$ Run 2 (mg/L)	$[H_2O_2]$ Run 3 (mg/L)
0	16.45	18.3	16.6
2	14.6	17.3	16.45
4	13.35	15.05	16.3
6	11.7	11.1	12.35
8	8.7	6.25	11.3
10	6.6	4.7	8.65
12	5.2	3.7	6.65
14	3.9	2.65	5.15
16	2.65	2.25	4.2
18	1.85	1.6	3.3
20	0.9	1.15	2.4

Table A.17: H_2O_2 Degradation in High pH Soil (No Autoclave)

Time (min)	$[H_2O_2]$ Run 1 (mg/L)	$[H_2O_2]$ Run 2 (mg/L)	$[H_2O_2]$ Run 3 (mg/L)
0	17.7	14.1	16.3
2	4.25	9.3	8.6
4	1.1	3.4	2.1
6	0.1	0.2	0.1
8	0	0	0

Table A.18: H_2O_2 Degradation in High pH Soil (With Autoclave)

Time (min)	$[H_2O_2]$ Run 1 (mg/L)	$[H_2O_2]$ Run 2 (mg/L)	$[H_2O_2]$ Run 3 (mg/L)
0	18.3	17.9	17.9
1	17.5	16.6	16.7
2	14	14	15.4
3	7.1	9.5	14.9
4	4.2	6.2	7.3
5	1.8	3.6	5.9
6	0.7	2.3	4.4
7	0	0	0

Table A.19: H_2O_2 Degradation in High Fe Soil (No Autoclave)

Time (min)	$[H_2O_2]$ Run 1 (mg/L)	$[H_2O_2]$ Run 2 (mg/L)	$[H_2O_2]$ Run 3 (mg/L)
0	16.7	15.8	13.1
1	6.5	4.3	6.7
2	2.5	1.8	2.8
3	1.3	0.5	0.2
4	0	0	0

Table A.20: H_2O_2 Degradation in High Fe Soil (With Autoclave)

Time (min)	$[H_2O_2]$ Run 1 (mg/L)	$[H_2O_2]$ Run 2 (mg/L)	$[H_2O_2]$ Run 3 (mg/L)
0	17.9	16.9	16.7
1	10.9	12.8	13.6
2	3.2	6.8	6.4
3	0.2	3.2	2.6
4	0	1.6	0.1
5	0	0	0

Table A.21: H_2O_2 Degradation in High TOC Soil (No Autoclave)

Time (min)	[H_2O_2] Run 1 (mg/L)	[H_2O_2] Run 2 (mg/L)	[H_2O_2] Run 3 (mg/L)
0	20.6	20.1	22.2
1	16.5	17.4	17.4
2	11.3	10.9	14.4
3.5	6	5.9	7.5
4.75	3.5	3	3.6
5.666666667	1	1.4	2.1
7	0.1	0.5	1
8.666666667	0	0.1	0.1
9	0	0	0

Table A.22: H_2O_2 Degradation in High TOC Soil (With Autoclave)

Time (min)	[H_2O_2] Run 1 (mg/L)	[H_2O_2] Run 2 (mg/L)	[H_2O_2] Run 3 (mg/L)
0	20.1	21.3	19.9
1	17.5	17.1	17.9
2	12.2	11	12.1
3.5	6.9	6.3	7.4
4.75	5	4	3.8
6	2	1.8	2.3
7.25	0.9	0.6	0.8
8.666666667	0.4	0.1	0.2
9	0	0	0

Table A.23: H_2O_2 Degradation in Biologically Stimulated Soil (No Autoclave)

Time (min)	[H_2O_2] Run 1 (mg/L)	[H_2O_2] Run 2 (mg/L)	[H_2O_2] Run 3 (mg/L)
0	19.8	18.9	19.4
2	5.5	6	5.8
4	1.2	2	1.8
6	0.2	0.2	0.3
8	0	0	0

Table A.24: H_2O_2 Degradation in Biologically Stimulated Soil (With Autoclave)

Time (min)	$[H_2O_2]$ Run 1 (mg/L)	$[H_2O_2]$ Run 2 (mg/L)	$[H_2O_2]$ Run 3 (mg/L)
0	17.6	18	17
2	15	16.4	16.3
4	13.6	15	16.1
6	12	10.9	11.9
8	8.5	6.4	11.8
10	7	4.9	8.4
12	5.8	3.6	6.5
14	3.5	3	5.1
16	2.2	2	4
18	1.6	1.6	3
20	1.3	1	2.2

Table A.25: H_2O_2 Total Equilibrated Water Demand Data

Equilibrated Water Sample	$[H_2O_2]_{initial}$ (mg/L)	$[H_2O_2]_{final}$ (mg/L)	Net H_2O_2 Equilibrated Water Demand (mg/L)
Ozonated Sand EW – Run 1	2500	2490	10
Ozonated Sand EW – Run 2	2600	2600	0
Average Soil EW – Run 1	2600	2500	100
Average Soil EW – Run 2	2600	2440	160
High pH Soil EW – Run 1	2600	2300	300
High pH Soil EW – Run 2	2600	2250	350
High Fe Soil EW – Run 1	2900	2500	400
High Fe Soil EW – Run 2	2600	2300	300
High TOC Soil EW – Run 1	2000	1300	700
High TOC Soil EW – Run 2	2500	1680	820
Biologically Stimulated Soil EW – Run 1	2600	2320	280
Biologically Stimulated Soil EW – Run 2	2600	2380	220

Table A.26: Soil Total H_2O_2 Demand Data

Soil	Vol. H_2O_2 30% Stock Added (mL)	Mass of H_2O_2 Added (g)	Final [H_2O_2] (mg/L)	Mass of H_2O_2 Remaining (mg)	Net Mass of H_2O_2 Consumed	H_2O_2 Demand (g H_2O_2/g soil)
Ozonated Sand 1	20	6.66	331000	6.62	0.04	0.02
Ozonated Sand 2	20	6.66	329000	6.58	0.08	0.04
Avg 1	150	49.95	170000	25.5	24.45	12.225
Avg 2	150	49.95	110000	16.5	33.45	16.725
pH 1	80	26.64	41000	3.28	23.36	11.68
pH 2	80	26.64	140000	11.2	15.44	7.72
Fe 1	130	43.29	7000	0.91	42.38	21.19
Fe 2	130	43.29	130	0.0169	43.2731	21.63655
TOC 1	80	26.64	310000	24.8	1.84	0.92
TOC 2	80	26.64	280000	22.4	4.24	2.12
Bio 1	200	66.6	113000	22.6	44	22
Bio 2	200	66.6	91000	18.2	48.4	24.2

APPENDIX B

RAW DATA FOR OZONE FATE

Table B.1: Fate of Ozone - Ozonated Sand Equilibrated Water (Run 1)

Time (min)	Weight % O_3 Gas Phase	Liquid Phase O_3 Conc. of Diluted Sample (ppm)	Actual Liquid Phase O_3 Conc. (ppm)
0	0	0	0.00
10	1.905	0.45	2.25
20	1.987	0.15	0.75
30	2.771	0.25	1.25
40	2.698	0.15	0.75
50	2.705	0.2	1.00
60	2.774	0.25	1.25
70	2.787	0.25	1.25
80	2.859	0.25	1.25
90	2.736	0.25	1.25
100	2.912	X	X

Table B.2: Fate of Ozone – Ozonated Sand Equilibrated Water (Run 2)

Time (min)	Weight % O_3 Gas Phase	Liquid Phase O_3 Conc. of Diluted Sample (ppm)	Actual Liquid Phase O_3 Conc. (ppm)
0	0	0.00	0.00
10	2.307	0.55	2.75
20	2.589	0.35	1.75
30	2.777	0.35	1.75
40	2.741	0.40	2.00
50	2.815	0.45	2.25
60	2.822	0.50	2.50
70	2.874	0.40	2.00
80	2.905	0.45	2.25
90	2.914	0.50	2.50
100	2.955	0.40	2.00
110	2.937	0.45	2.25
120	2.948	0.45	2.25

Table B.3: Fate of Ozone – Ozonated Sand Equilibrated Water (Run 3)

Time (min)	Weight % O_3 Gas Phase	Liquid Phase O_3 Conc. of Diluted Sample (ppm)	Actual Liquid Phase O_3 Conc. (ppm)
0	0	0.00	0.00
10	2.827	0.60	3.00
20	2.794	0.25	1.25
30	2.927	0.35	1.75
40	2.985	0.25	1.25
50	2.941	0.60	3.00
60	2.855	0.55	2.75
70	2.979	0.55	2.75
80	3.043	0.40	2.00
90	3.048	0.45	2.25
100	2.964	0.55	2.75
110	3.09	0.55	2.75
120	3.109	0.45	2.25

Table B.4: Fate of Ozone – Average Soil Equilibrated Water (Run 1)

Time (min)	Weight % O_3 Gas Phase	Liquid Phase O_3 Conc. of Diluted Sample (ppm)	Actual Liquid Phase O_3 Conc. (ppm)
0	0	0	0
10	Error	0.1	0.5
20	Error	0.17	0.85
30	2.268	0.25	1.25
40	2.292	0.25	1.25
50	2.443	0.05	0.25
60	2.392	0.18	0.9
70	2.496	0.15	0.75
80	2.542	0.05	0.25
90	2.404	0.13	0.65
100	2.412	0.075	0.375
110	2.474	0.1	0.5
120	2.498	0.25	1.25
150	2.509	X	X
200	2.918	X	X

Table B.5: Fate of Ozone – Average Soil Equilibrated Water (Run 2)

Time (min)	Weight % O_3 Gas Phase	Liquid Phase O_3 Conc. of Diluted Sample (ppm)	Actual Liquid Phase O_3 Conc. (ppm)
0	0	0.00	0.00
10	2.491	0.15	0.75
20	2.414	0.60	3.00
30	2.432	0.55	2.75
40	2.543	0.45	2.25
50	2.523	0.35	1.75
60	2.424	0.55	2.75
70	2.441	0.55	2.75
80	2.549	0.35	1.75
90	2.548	0.35	1.75
100	2.539	0.65	3.25
110	2.534	0.55	2.75
120	2.431	0.45	2.25
150	2.489	X	X
160	2.517	X	X
170	2.608	X	X
180	2.554	X	X
190	2.689	X	X
200	2.801	X	X
210	2.857	X	X
220	2.911	X	X

Table B.6: Fate of Ozone – Average Soil Equilibrated Water (Run 3)

Time (min)	Weight % O_3 Gas Phase	Liquid Phase O_3 Conc. of Diluted Sample (ppm)	Actual Liquid Phase O_3 Conc. (ppm)
0	0	0.00	0.00
10	2.422	0.50	2.50
20	2.41	0.35	1.75
30	2.396	0.20	1.00
40	2.431	0.35	1.75
50	2.525	0.30	1.50
60	2.526	0.35	1.75
70	2.535	0.55	2.75
80	2.459	0.45	2.25
90	2.591	0.45	2.25
100	2.631	0.50	2.50
110	2.58	X	X
120	2.597	X	X
150	2.608	X	X
160	2.615	X	X
170	2.807	X	X
180	2.925	X	X

Table B.7: Fate of Ozone – High pH Soil Equilibrated Water (Run 1)

Time (min)	Weight % O_3 Gas Phase	Liquid Phase O_3 Conc. of Diluted Sample (ppm)	Actual Liquid Phase O_3 Conc. (ppm)
0	0	0	0
10	2.203	0.075	0.375
20	2.302	0.075	0.375
30	2.315	0.1	0.5
40	2.333	0.1	0.5
50	2.248	0.15	0.75
60	2.335	0.1	0.5
70	2.299	0.15	0.75
80	2.252	0.1	0.5
90	2.111	0.15	0.75
100	2.187	0.15	0.75
110	2.294	0.1	0.5
120	2.251	0.15	0.75
150	2.214	X	X
200	2.305	X	X
250	2.348	X	X
260	2.507	X	X
270	2.689	X	X
280	2.805	X	X

Table B.8: Fate of Ozone – High pH Soil Equilibrated Water (Run 2)

Time (min)	Weight % O_3 Gas Phase	Liquid Phase O_3 Conc. of Diluted Sample (ppm)	Actual Liquid Phase O_3 Conc. (ppm)
0	0	0.00	0.00
10	2.333	0.10	0.50
20	2.358	0.10	0.50
30	2.312	0.08	0.38
40	2.318	0.15	0.75
50	2.297	0.15	0.75
60	2.309	0.15	0.75
70	2.317	0.10	0.50
80	2.385	0.15	0.75
90	2.401	0.10	0.50
100	2.398	0.10	0.50
110	2.368	0.10	0.50
120	2.451	0.15	0.75
150	2.467	X	X
200	2.681	X	X
250	2.745	X	X
260	2.812	X	X
270	2.923	X	X

Table B.9: Fate of Ozone – High pH Soil Equilibrated Water (Run 3)

Time (min)	Weight % O_3 Gas Phase	Liquid Phase O_3 Conc. of Diluted Sample (ppm)	Actual Liquid Phase O_3 Conc. (ppm)
0	0.000	0.00	0.00
10	2.048	0.075	0.38
20	2.005	0.10	0.50
30	2.004	0.15	0.75
40	1.926	0.10	0.50
50	2.027	0.15	0.75
60	1.988	0.10	0.50
70	2.041	0.15	0.75
80	2.023	0.10	0.50
90	2.141	0.15	0.75
100	2.117	X	X
150	2.205	X	X
200	2.113	X	X
250	2.254	X	X
260	2.267	X	X
270	2.398	X	X
280	2.475	X	X
290	2.607	X	X
300	2.855	X	X
310	2.934	X	X

Table B.10: Fate of Ozone – High Fe Soil Equilibrated Water (Run 1)

Time (min)	Weight % O_3 Gas Phase	Liquid Phase O_3 Conc. of Diluted Sample (ppm)	Actual Liquid Phase O_3 Conc. (ppm)
0	0	0.000	0
10	1.936	0.450	2.25
20	2.189	0.000	0
30	2.315	0.150	0.75
40	2.308	0.150	0.75
50	2.394	0.250	1.25
60	2.348	0.250	1.25
70	2.317	0.150	0.75
80	2.387	0.100	0.5
90	2.34	0.300	1.5
100	2.396	0.200	1
110	2.408	0.275	1.375
120	2.458	0.250	1.25
150	2.741	X	X
160	2.814	X	X
170	2.924	X	X

Table B.11: Fate of Ozone – High Fe Soil Equilibrated Water (Run 2)

Time (min)	Weight % O_3 Gas Phase	Liquid Phase O_3 Conc. of Diluted Sample (ppm)	Actual Liquid Phase O_3 Conc. (ppm)
0	0.000	0.00	0.00
10	2.358	0.17	0.85
20	2.296	0.12	0.60
30	2.189	0.15	0.75
40	2.283	0.15	0.75
50	2.303	0.22	1.10
60	2.642	0.20	1.00
70	2.83	0.15	0.75
80	2.962	0.15	0.75
90	2.724	0.20	1.00
100	2.674	0.20	1.00
110	2.579	0.20	1.00
120	2.691	0.35	1.75
150	2.618	X	X
160	2.697	X	X
170	2.655	X	X
180	2.789	X	X
190	2.891	X	X
200	2.933	X	X

Table B.12: Fate of Ozone – High Fe Soil Equilibrated Water (Run 3)

Time (min)	Weight % O_3 Gas Phase	Liquid Phase O_3 Conc. of Diluted Sample (ppm)	Actual Liquid Phase O_3 Conc. (ppm)
0	0.000	0.00	0.00
10	2.387	0.40	2.00
20	2.228	0.15	0.75
30	2.270	0.25	1.25
40	2.257	0.10	0.50
50	2.269	0.15	0.75
60	2.236	0.25	1.25
70	2.229	0.25	1.25
80	2.204	0.15	0.75
90	2.176	0.15	0.75
100	2.238	X	X
110	2.359	X	X
120	2.689	X	X
130	2.787	X	X
140	2.904	X	X

Table B.13: Fate of Ozone – High TOC Soil Equilibrated Water (Run 1)

Time (min)	Weight % O_3 Gas Phase	Liquid Phase O_3 Conc. of Diluted Sample (ppm)	Actual Liquid Phase O_3 Conc. (ppm)
0	0	0.000	0
10	2.058	0.450	2.25
20	2.412	0.000	0
30	2.385	0.200	1
40	2.354	0.250	1.25
50	2.389	0.150	0.75
60	2.371	0.200	1
70	2.399	0.200	1
80	2.405	0.150	0.75
90	2.318	0.300	1.5
100	2.356	0.250	1.25
110	2.343	0.250	1.25
120	2.398	0.200	1
150	2.458	X	X
200	2.489	X	X
250	2.813	X	X
300	2.925	X	X

Table B.14: Fate of Ozone – High TOC Soil Equilibrated Water (Run 2)

Time (min)	Weight % O_3 Gas Phase	Liquid Phase O_3 Conc. of Diluted Sample (ppm)	Actual Liquid Phase O_3 Conc. (ppm)
0	0.000	0.00	0.00
10	2.09	0.15	0.75
20	2.41	0.15	0.75
30	2.456	0.10	0.50
40	2.498	0.15	0.75
50	2.501	0.20	1.00
60	2.405	0.20	1.00
70	2.419	0.20	1.00
80	2.437	0.15	0.75
90	2.508	0.25	1.25
100	2.559	0.15	0.75
110	2.542	0.20	1.00
120	2.598	0.35	1.75
150	2.578	X	X
200	2.687	X	X
250	2.815	X	X
300	2.906	X	X

Table B.15: Fate of Ozone – High TOC Soil Equilibrated Water (Run 3)

Time (min)	Weight % O_3 Gas Phase	Liquid Phase O_3 Conc. of Diluted Sample (ppm)	Actual Liquid Phase O_3 Conc. (ppm)
0	0.000	0.00	0.00
10	2.289	0.30	1.50
20	2.345	0.25	1.25
30	2.311	0.25	1.25
40	2.324	0.20	1.00
50	2.387	0.25	1.25
60	2.319	0.30	1.50
70	2.345	0.20	1.00
80	2.405	0.15	0.75
90	2.411	0.25	1.25
100	2.391	X	X
150	2.405	X	X
200	2.789	X	X
250	2.922	X	X

Table B.16: Fate of Ozone – Ozonated Sand (Run 1)

Time (min)	Weight % O_3 (Gas Phase)
0	0.058
1	1.277
2	1.888
3	2.101
4	2.195
5	2.242
10	2.308
15	2.362
20	2.486
21	2.505
22	2.555
23	2.678
24	2.777
25	2.895
26	2.899
27	2.91
28	2.801
29	2.869
30	2.887
32	2.889
34	2.911
36	2.877
38	2.895
40	2.91
45	2.885
50	2.871
55	2.809
60	2.854
65	2.901
70	2.915
75	2.925
80	2.934
85	2.964
90	2.975
95	2.979
100	2.980
150	2.975
200	2.986
250	2.981

Table B.17: Fate of Ozone – Ozonated Sand (Run 2)

Time (min)	Weight % O_3 (Gas Phase)
0	0
1	1.713
3	1.925
10	2.401
15	2.692
20	2.845
25	2.799
30	2.859
35	2.813
40	2.901
45	2.868
50	2.919
55	2.894
60	2.916
65	2.935
70	2.921
75	2.959
80	2.971
85	2.985
90	2.979
95	2.99
100	X

Table B.18: Fate of Ozone – Ozonated Sand (Run 3)

Time (min)	Weight % O_3 (Gas Phase)
0	0
1	0.263
5	1.807
10	2.28
15	2.487
20	2.789
25	2.888
30	2.857
35	2.867
40	2.901
45	2.871
50	2.909
55	2.912
60	2.921
65	2.915
70	2.935
75	2.979
80	2.971
90	2.986

Table B.19: Fate of Ozone – Average Soil (Run 1)

Time (min)	Weight % O_3 (Gas Phase)
0	0.000
5	1.792
10	1.895
15	1.925
20	2.223
22	2.198
24	2.206
26	2.301
28	2.311
30	2.308
32	2.287
34	2.298
36	2.233
38	2.244
40	2.309
42	2.355
44	2.366
46	2.341
48	2.331
50	2.331
55	2.398
60	2.294
65	2.354
70	2.405
75	2.409
80	2.368
85	2.419
90	2.598
95	2.429
100	2.411
150	2.305
200	2.356
250	2.369
300	2.458
350	2.498
400	2.505
450	2.611
460	2.855
470	2.911
480	2.944
490	2.978

Table B.20: Fate of Ozone – Average Soil (Run 2)

Time (min)	Weight % O_3 (Gas Phase)
0	0.232
5	1.773
10	1.799
15	1.959
20	2.445
21	2.441
22	2.459
23	2.41
24	2.394
25	2.389
26	2.446
27	2.41
30	2.451
40	2.415
45	2.485
50	2.387
55	2.399
60	2.419
65	2.426
70	2.511
75	2.468
80	2.444
90	2.565
100	2.542
150	2.506
200	2.591
250	2.609
300	2.655
350	2.788
400	2.805
450	2.855
500	2.905
550	2.959

Table B.21: Fate of Ozone – Average Soil (Run 3)

Time (min)	Weight % O_3 (Gas Phase)
0	0
10	1.895
20	2.359
30	2.345
40	2.333
45	2.289
50	2.342
55	2.312
60	2.298
65	2.305
70	2.415
100	2.357
150	2.409
200	2.391
250	2.489
300	2.598
350	2.698
400	2.855
450	2.919
500	2.981

Table B.22: Fate of Ozone – High pH Soil (Run 1)

Time (min)	Weight % O_3 (Gas Phase)
0	0
1	0
3	0
5	0.001
10	1.889
20	1.772
30	1.925
40	1.671
45	1.652
50	1.755
55	1.742
60	1.848
70	1.788
80	1.791
90	1.824
100	1.745
110	1.657
120	1.727
130	1.825
140	1.819
150	1.799
200	1.815
250	1.809
300	1.799
350	1.839
400	1.829
450	1.839
500	1.805
550	2.089
600	2.459
650	2.905
700	2.955

Table B.23: Fate of Ozone – High pH Soil (Run 2)

Time (min)	Weight % O_3 (Gas Phase)
0	0
2	0
4	0
6	0.005
10	1.035
20	1.512
30	1.526
40	1.536
45	1.601
50	1.598
55	1.669
60	1.684
65	1.651
70	1.705
80	1.426
90	1.505
100	1.625
110	1.444
120	1.459
130	1.536
140	1.517
150	1.605
200	1.555
250	1.548
300	1.599
350	1.615
400	1.612
450	1.588
500	1.689
550	1.789
600	2.555
650	2.789
700	2.899
750	2.971
800	2.981

Table B.24: Fate of Ozone – High pH Soil (Run 3)

Time (min)	Weight % O_3 (Gas Phase)
0	0
2	0
4	0
6	0.135
10	1.122
20	1.335
30	1.399
40	1.445
45	1.398
50	1.418
55	1.429
60	1.438
70	1.399
100	1.387
150	1.459
200	1.441
250	1.509
300	1.511
350	1.485
400	1.601
450	1.587
500	1.496
550	1.542
600	1.598
650	1.899
700	2.118
750	2.389
800	2.777
850	2.951

Table B.25: Fate of Ozone – High Fe Soil (Run 1)

Time (min)	Weight % O_3 (Gas Phase)
0	0
1	1.502
2	2.005
5	2.401
10	2.617
15	2.618
25	2.494
35	2.655
40	2.715
45	2.706
50	2.719
55	2.685
60	2.705
70	2.603
80	2.555
100	2.645
120	2.605
150	2.689
200	2.745
250	2.731
300	2.89
350	2.918
400	2.95

Table B.26: Fate of Ozone – High Fe Soil (Run 2)

Time (min)	Weight % O_3 (Gas Phase)
0	0.000
1	0.000
2	0.000
5	2.465
10	2.524
15	2.709
40	2.777
45	2.761
55	2.685
60	2.710
90	2.683
100	2.636
150	2.711
200	2.744
250	2.692
300	2.664
350	2.814
400	2.905
450	2.923

Table B.27: Fate of Ozone – High Fe Soil (Run 3)

Time (min)	Weight % O_3 (Gas Phase)
0	0.000
1	0.100
5	2.549
13	2.567
20	2.580
30	2.598
40	2.587
45	2.564
50	2.591
55	2.619
60	2.623
100	2.610
150	2.689
200	2.668
250	2.709
300	2.811
350	2.905
400	2.941
450	2.952

Table B.28: Fate of Ozone – High TOC Soil (Run 1)

Time (min)	Weight % O_3 (Gas Phase)
0	0.000
5	1.985
10	2.412
15	2.513
20	2.541
40	2.502
45	2.528
50	2.531
55	2.524
60	2.518
70	2.601
100	2.598
150	2.789
200	2.810
250	2.915
300	2.950

Table B.29: Fate of Ozone – High TOC Soil (Run 2)

Time (min)	Weight % O_3 (Gas Phase)
0	0
5	1.645
10	2.098
15	2.456
20	2.485
30	2.598
40	2.574
45	2.588
50	2.512
55	2.532
60	2.506
65	2.569
70	2.465
90	2.441
100	2.459
150	2.568
200	2.548
250	2.785
300	2.895
350	2.911
400	2.923

Table B.30: Fate of Ozone – High TOC Soil (Run 3)

Time (min)	Weight % O_3 (Gas Phase)
0	0
5	1.556
10	2.298
15	2.601
20	2.654
25	2.632
30	2.512
40	2.606
45	2.698
50	2.634
55	2.648
60	2.612
70	2.663
100	2.701
150	2.694
200	2.752
250	2.887
300	2.909
350	2.915
400	2.945
450	2.956

Table B.31: Fate of Ozone – Biologically Stimulated Soil (Run 1)

Time (min)	Weight % O_3 (Gas Phase)
0	0.000
5	1.984
10	2.215
15	2.354
20	2.456
30	2.413
35	2.442
40	2.438
45	2.431
50	2.421
55	2.398
60	2.439
75	2.489
100	2.477
125	2.505
150	2.498
200	2.487
250	2.511
300	2.502
350	2.689
400	2.809
450	2.878
500	2.915
550	2.945

Table B.32: Fate of Ozone – Biologically Stimulated Soil (Run 2)

Time (min)	Weight % O_3 (Gas Phase)
0	0
5	1.459
10	2.325
15	2.365
20	2.412
30	2.31
40	2.298
45	2.309
50	2.335
55	2.367
60	2.311
65	2.304
70	2.455
75	2.411
100	2.266
150	2.409
200	2.551
250	2.605
300	2.418
350	2.396
400	2.409
450	2.437
500	2.678
550	2.845
600	2.919

Table B.33: Fate of Ozone – Biologically Stimulated Soil (Run 3)

Time (min)	Weight % O_3 (Gas Phase)
0	0
5	1.854
10	2.001
15	2.325
20	2.389
25	2.377
30	2.366
40	2.315
45	2.389
50	2.374
55	2.371
60	2.389
65	2.388
70	2.377
75	2.405
95	2.418
100	2.399
150	2.456
200	2.477
250	2.418
300	2.463
350	2.508
400	2.498
450	2.491
500	2.598
550	2.784
600	2.918
650	2.941

APPENDIX C

RAW DATA FOR SOIL pH BUFFERING

Table C.1: Ozonated Sand (Run 1) H_3PO_4 Buffering Raw Data

			1st Order	2nd Order	3rd Order
Time (min)	**pH**	**$[H_3O^+]$ (mmol/L)**	**$-\ln[H_3O^+]/[H_3O^+]_0$**	**$1/[H_3O^+] - 1/[H_3O^+]_0$**	**$1/2*[H_3O^+]^2 - 1/2*[H_3O^+]^2_0$**
0	3.01	0.977237221	0	0	0
1	3.02	0.954992586	0.023025851	0.023835556	0.024674824
2	3.05	0.891250938	0.092103404	0.098725462	0.105898432
3	3.06	0.87096359	0.115129255	0.124860629	0.135564095
4	3.08	0.831763771	0.161180957	0.178971442	0.199155611
5	3.08	0.831763771	0.161180957	0.178971442	0.199155611
6	3.09	0.812830516	0.184206807	0.206975779	0.23321635
8	3.09	0.812830516	0.184206807	0.206975779	0.23321635
40	3.05	0.891250938	0.092103404	0.098725462	0.105898432
98	3.04	0.912010839	0.069077553	0.073185204	0.077567943
173	3.08	0.831763771	0.161180957	0.178971442	0.199155611
923	3.09	0.812830516	0.184206807	0.206975779	0.23321635

Table C.2: Ozonated Sand (Run 2) H_3PO_4 Buffering Raw Data

			1st Order	2nd Order	3rd Order
Time (min)	**pH**	**$[H_3O^+]$ (mmol/L)**	**$-\ln[H_3O^+]/[H_3O^+]_0$**	**$1/[H_3O^+] - 1/[H_3O^+]_0$**	**$1/2*[H_3O^+]^2 - 1/2*[H_3O^+]^2_0$**
0	2.99	1.023292992	0	0	0
1	3	1	0.023025851	0.022762779	0.022503707
2	3	1	0.023025851	0.022762779	0.022503707
3	2.99	1.023292992	0	0	0
4	3	1	0.023025851	0.022762779	0.022503707
5	3.01	0.977237221	0.046051702	0.046055771	0.046067981
15	2.98	1.047128548	-0.023025851	-0.022244635	-0.021490873
60	3.03	0.933254301	0.092103404	0.094282084	0.096580518
150	3	1	0.023025851	0.022762779	0.022503707
650	2.99	1.023292992	0	0	0

Table C.3: Average Soil (Run 1) H_3PO_4 Buffering Raw Data

Time (min)	pH	$[H_3O^+]$ (mmol/L)	1st Order $-\ln[H_3O^+]/[H_3O^+]_0$	2nd Order $1/[H_3O^+] - 1/[H3O^+]_0$	3rd Order $1/2*[H_3O^+]^2 - 1/2*[H_3O^+]^2_0$
0	3	1	0	0	0
1	3.04	0.912010839	0.092103404	0.096478196	0.101132217
2	3.06	0.87096359	0.138155106	0.148153621	0.159128369
4	3.13	0.741310241	0.299336062	0.348962883	0.409850429
8	3.17	0.676082975	0.391439466	0.479108388	0.593880812
11	3.2	0.630957344	0.460517019	0.584893192	0.755943216
41	3.34	0.45708819	0.782878932	1.187761624	1.893150462
86	3.38	0.416869383	0.874982335	1.398832919	2.377199687
228	3.49	0.323593657	1.128266696	2.090295433	4.27496293
1278	3.89	0.128824955	2.049300733	6.762471166	29.6279793
1553	3.96	0.10964782	2.210481689	8.120108394	41.08818856
2373	4.08	0.083176377	2.4867919	11.02264435	71.77198854
2575	4.11	0.077624712	2.555869453	11.88249552	82.47934537
3093	4.13	0.074131024	2.601921155	12.48962883	90.48504293
3783	4.19	0.064565423	2.740076261	14.48816619	119.441646
4113	4.18	0.066069345	2.71705041	14.13561248	114.0433826

Table C.4: Average Soil (Run 2) H_3PO_4 Buffering Raw Data

Time (min)	pH	$[H_3O^+]$ (mmol/L)	1st Order $-\ln[H_3O^+]/[H_3O^+]_0$	2nd Order $1/[H_3O^+] - 1/[H3O^+]_0$	3rd Order $1/2*[H_3O^+]^2 - 1/2*[H_3O^+]^2_0$
0	3	1	0	0	0
1	3.02	0.954992586	0.046051702	0.047128548	0.048239098
2	3.03	0.933254301	0.069077553	0.071519305	0.074076811
3	3.06	0.87096359	0.138155106	0.148153621	0.159128369
4	3.08	0.831763771	0.184206807	0.202264435	0.222719885
5	3.11	0.776247117	0.25328436	0.288249552	0.329793454
6	3.13	0.741310241	0.299336062	0.348962883	0.409850429
7	3.14	0.72443596	0.322361913	0.380384265	0.452730359
8	3.16	0.691830971	0.368413615	0.445439771	0.544648065
9	3.17	0.676082975	0.391439466	0.479108388	0.593880812
10	3.18	0.660693448	0.414465317	0.513561248	0.645433826
11	3.19	0.645654229	0.437491168	0.548816619	0.69941646
12	3.2	0.630957344	0.460517019	0.584893192	0.755943216
13	3.21	0.616595002	0.48354287	0.621810097	0.815133996
14	3.22	0.602559586	0.50656872	0.659586907	0.877114352
15	3.23	0.588843655	0.529594571	0.698243652	0.942015752
28	3.34	0.45708819	0.782878932	1.187761624	1.893150462
36	3.37	0.426579519	0.851956484	1.344228815	2.247704369
54	3.41	0.389045145	0.944059888	1.570395783	2.80346724
88	3.46	0.34673685	1.059189143	1.884031503	3.658818856
124	3.51	0.309029543	1.174318397	2.235936569	4.73564274
149	3.53	0.295120923	1.220370099	2.388441561	5.240768107
184	3.55	0.281838293	1.266421801	2.548133892	5.794627059
474	3.82	0.151356125	1.888119776	5.60693448	21.32579161
1294	3.96	0.10964782	2.210481689	8.120108394	41.08818856
1495	4.05	0.089125094	2.417714348	10.22018454	62.44627059
2014	4.09	0.081283052	2.509817751	11.30268771	75.17806242
2704	4.19	0.064565423	2.740076261	14.48816619	119.441646
3034	4.16	0.069183097	2.670998708	13.45439771	103.9648065
4564	4.24	0.057543994	2.855205515	16.37800829	150.497586

Table C.5: High pH Soil (Run 1) H_3PO_4 Buffering Raw Data

Time (min)	pH	$[H_3O^+]$ (mmol/L)	1st Order $-\ln[H_3O^+]/[H_3O^+]_0$	2nd Order $1/[H_3O^+] - 1/[H3O^+]_0$	3rd Order $1/2*[H_3O^+]^2 - 1/2*[H_3O^+]^2_0$
0	2.98	1.047128548	0	0	0
1	3.02	0.954992586	0.092103404	0.092135962	0.092233678
2	3.04	0.912010839	0.138155106	0.14148561	0.145126798
3	3.07	0.851138038	0.207232658	0.219904969	0.234186713
4	3.09	0.812830516	0.25328436	0.275276185	0.300775205
5	3.11	0.776247117	0.299336062	0.333256966	0.373788034
6	3.13	0.741310241	0.345387764	0.393970297	0.45384501
7	3.15	0.707945784	0.391439466	0.457544959	0.541625738
8	3.17	0.676082975	0.437491168	0.524115802	0.637875392
9	3.18	0.660693448	0.460517019	0.558568662	0.689428407
10	3.2	0.630957344	0.50656872	0.629900606	0.799937796
11	3.21	0.616595002	0.529594571	0.666817511	0.859128576
12	3.23	0.588843655	0.575646273	0.743251066	0.986010332
13	3.24	0.575439937	0.598672124	0.782808243	1.053970441
14	3.25	0.562341325	0.621697975	0.823286824	1.12513341
15	3.26	0.549540874	0.644723826	0.864708273	1.199650188
16	3.27	0.537031796	0.667749677	0.907094551	1.277678833
20	3.3	0.501187234	0.73682723	1.040269729	1.534530433
23	3.33	0.467735141	0.805904783	1.182969503	1.829435528
27	3.36	0.436515832	0.874982335	1.335875067	2.168031882
31	3.39	0.407380278	0.944059888	1.49971633	2.556792511
37	3.42	0.380189396	1.013137441	1.675275406	3.003149435
47	3.47	0.338844156	1.128266696	1.996216641	3.89881253
73	3.56	0.27542287	1.335499354	2.675787962	6.135278273
95	3.61	0.245470892	1.450628609	3.118810192	7.841929118
126	3.66	0.218776162	1.565757863	3.61588931	9.990475235
159	3.72	0.190546072	1.703912969	4.293082016	13.3151381
207	3.79	0.16218101	1.865093925	5.210957433	18.5534644
257	3.82	0.151356125	1.934171478	5.651941894	21.36978619
407	3.97	0.107151931	2.279559242	8.377550422	43.09217408
617	4.11	0.077624712	2.601921155	11.92750293	82.52333995
1307	4.45	0.035481339	3.384800087	27.22883673	396.7081119
1637	4.5	0.031622777	3.499929341	30.66778402	499.5439946
3167	4.67	0.021379621	3.891368807	45.81852154	1093.424807
5777	4.85	0.014125375	4.305834124	69.83958585	2505.480163
7217	4.9	0.012589254	4.420963379	78.47783089	3154.330717

Table C.6: High pH Soil (Run 2) H_3PO_4 Buffering Raw Data

Time (min)	pH	$[H_3O^+]$ (mmol/L)	1st Order $-\ln[H_3O^+]/[H_3O^+]_0$	2nd Order $1/[H_3O^+] - 1/[H3O^+]_0$	3rd Order $1/2*[H_3O^+]^2 - 1/2*[H_3O^+]^2_0$
0	2.99	1.023292992	0.023025851	0.022244635	0.021490873
1	3.03	0.933254301	0.115129255	0.116526719	0.118071391
2	3.07	0.851138038	0.207232658	0.219904969	0.234186713
3	3.1	0.794328235	0.276310211	0.303932826	0.336441177
4	3.13	0.741310241	0.345387764	0.393970297	0.45384501
5	3.16	0.691830971	0.414465317	0.490447185	0.588642646
6	3.19	0.645654229	0.48354287	0.593824033	0.74341104
7	3.21	0.616595002	0.529594571	0.666817511	0.859128576
10	3.27	0.537031796	0.667749677	0.907094551	1.277678833
11	3.28	0.52480746	0.690775528	0.950468132	1.359384854
12	3.3	0.501187234	0.73682723	1.040269729	1.534530433
13	3.32	0.478630092	0.782878932	1.134303545	1.726573742
14	3.34	0.45708819	0.828930633	1.232769038	1.937145042
18	3.4	0.398107171	0.967085739	1.556893845	2.698781303
19	3.42	0.380189396	1.013137441	1.675275406	3.003149435
21	3.45	0.354813389	1.082214994	1.863390345	3.515635754
34	3.51	0.309029543	1.220370099	2.280943983	4.779637321
68	3.57	0.26915348	1.358525205	2.760359705	6.445915903
359	4.24	0.057543994	2.901257217	16.4230157	150.5415806
1199	4.48	0.033113112	3.453877639	29.24452462	455.5494143
1454	4.5	0.031622777	3.499929341	30.66778402	499.5439946
2669	4.71	0.019498446	3.983472211	50.33114581	1314.677991
2909	4.67	0.021379621	3.891368807	45.81852154	1093.424807
3124	4.74	0.018197009	4.052549764	53.9990948	1509.519855
3209	4.78	0.016595869	4.144653167	59.30096602	1814.934268
4139	4.8	0.015848932	4.190704869	62.14074186	1990.079847
9779	4.92	0.012022644	4.46701508	82.22138452	3458.698849

Table C.7: High Fe Soil (Run 1) H_3PO_4 Buffering Raw Data

Time (min)	pH	$[H_3O^+]$ (mmol/L)	1st Order $-\ln[H_3O^+]/[H_3O^+]_0$	2nd Order $1/[H_3O^+] - 1/[H3O^+]_0$	3rd Order $1/2*[H_3O^+]^2 - 1/2*[H_3O^+]^2_0$
0	3.01	0.977237221	0	0	0
2	3.03	0.933254301	0.046051702	0.048226313	0.050512537
3	3.06	0.87096359	0.115129255	0.124860629	0.135564095
4	3.08	0.831763771	0.161180957	0.178971442	0.199155611
5	3.1	0.794328235	0.207232658	0.23563242	0.268882322
6	3.11	0.776247117	0.230258509	0.264956559	0.30622918
7	3.13	0.741310241	0.276310211	0.32566989	0.386286155
8	3.14	0.72443596	0.299336062	0.357091272	0.429166085
9	3.15	0.707945784	0.322361913	0.389244552	0.474066883
10	3.16	0.691830971	0.345387764	0.422146778	0.521083791
11	3.17	0.676082975	0.368413615	0.455815396	0.570316538
12	3.18	0.660693448	0.391439466	0.490268256	0.621869552
13	3.18	0.660693448	0.391439466	0.490268256	0.621869552
14	3.19	0.645654229	0.414465317	0.525523627	0.675852185
22	3.23	0.588843655	0.50656872	0.67495066	0.918451478
45	3.29	0.512861384	0.644723826	0.926551607	1.377382708
57	3.32	0.478630092	0.713801379	1.066003139	1.659014887
77	3.33	0.467735141	0.73682723	1.114669097	1.761876674
125	3.4	0.398107171	0.898008186	1.488593439	2.631222448
177	3.47	0.338844156	1.059189143	1.927916234	3.831253676
327	3.6	0.251188643	1.358525205	2.957778713	7.400901688
537	3.81	0.154881662	1.842068074	5.433249298	20.3199049
1227	4.08	0.083176377	2.46376605	10.99935135	71.74842426
1557	4.13	0.074131024	2.578895304	12.46633583	90.46147866
3087	4.23	0.058884366	2.809153813	15.95914353	143.6780109
5757	4.55	0.028183829	3.545981043	34.45804593	628.9391416
7197	4.82	0.015135612	4.167679018	65.04605181	2182.055597
8637	4.81	0.015488166	4.144653167	63.54212991	2083.823353

Table C.8: High Fe Soil (Run 2) H_3PO_4 Buffering Raw Data

Time (min)	pH	$[H_3O^+]$ (mmol/L)	1st Order $-\ln[H_3O^+]/[H_3O^+]_0$	2nd Order $1/[H_3O^+] - 1/[H3O^+]_0$	3rd Order $1/2*[H_3O^+]^2 - 1/2*[H_3O^+]^2_0$
0	3	1	0	0	0
1	3.02	0.954992586	0.046051702	0.047128548	0.048239098
2	3.04	0.912010839	0.092103404	0.096478196	0.101132217
3	3.05	0.891250938	0.115129255	0.122018454	0.129462706
4	3.06	0.87096359	0.138155106	0.148153621	0.159128369
5	3.07	0.851138038	0.161180957	0.174897555	0.190192132
6	3.08	0.831763771	0.184206807	0.202264435	0.222719885
7	3.09	0.812830516	0.207232658	0.230268771	0.256780624
8	3.1	0.794328235	0.230258509	0.258925412	0.292446596
9	3.1	0.794328235	0.230258509	0.258925412	0.292446596
10	3.11	0.776247117	0.25328436	0.288249552	0.329793454
11	3.12	0.758577575	0.276310211	0.318256739	0.368900414
12	3.12	0.758577575	0.276310211	0.318256739	0.368900414
13	3.13	0.741310241	0.299336062	0.348962883	0.409850429
20	3.16	0.691830971	0.368413615	0.445439771	0.544648065
62	3.31	0.489778819	0.713801379	1.041737945	1.584346917
115	3.38	0.416869383	0.874982335	1.398832919	2.377199687
265	3.58	0.263026799	1.335499354	2.801893963	6.727198854
475	3.77	0.169824365	1.772990522	4.888436554	16.83684252
1165	4.12	0.075857758	2.578895304	12.18256739	86.39004144
1495	4.13	0.074131024	2.601921155	12.48962883	90.48504293
3025	4.21	0.0616595	2.786127963	15.21810097	131.0133996
5635	4.52	0.030199517	3.499929341	32.11311215	547.7390981
7075	4.74	0.018197009	4.006498062	53.95408739	1509.47586
8515	4.73	0.018620871	3.983472211	52.70317964	1441.515752

Table C.9: High TOC Soil (Run 1) H_3PO_4 Buffering Raw Data

Time (min)	pH	$[H_3O^+]$ (mmol/L)	1st Order $-\ln[H_3O^+]/[H_3O^+]_0$	2nd Order $1/[H_3O^+] - 1/[H3O^+]_0$	3rd Order $1/2*[H_3O^+]^2 - 1/2*[H_3O^+]^2_0$
0	3	1	0	0	0
1	3.02	0.954992586	0.046051702	0.047128548	0.048239098
2	3.04	0.912010839	0.092103404	0.096478196	0.101132217
3	3.06	0.87096359	0.138155106	0.148153621	0.159128369
4	3.08	0.831763771	0.184206807	0.202264435	0.222719885
5	3.09	0.812830516	0.207232658	0.230268771	0.256780624
6	3.1	0.794328235	0.230258509	0.258925412	0.292446596
7	3.11	0.776247117	0.25328436	0.288249552	0.329793454
8	3.12	0.758577575	0.276310211	0.318256739	0.368900414
9	3.13	0.741310241	0.299336062	0.348962883	0.409850429
10	3.13	0.741310241	0.299336062	0.348962883	0.409850429
11	3.14	0.72443596	0.322361913	0.380384265	0.452730359
13	3.15	0.707945784	0.345387764	0.412537545	0.497631157
14	3.16	0.691830971	0.368413615	0.445439771	0.544648065
15	3.16	0.691830971	0.368413615	0.445439771	0.544648065
16	3.17	0.676082975	0.391439466	0.479108388	0.593880812
17	3.17	0.676082975	0.391439466	0.479108388	0.593880812
20	3.18	0.660693448	0.414465317	0.513561248	0.645433826
36	3.23	0.588843655	0.529594571	0.698243652	0.942015752
58	3.27	0.537031796	0.621697975	0.862087137	1.233684252
826	3.54	0.28840315	1.24339595	2.467368505	5.511322173
1081	3.52	0.301995172	1.197344248	2.311311215	4.982390981
2296	3.67	0.213796209	1.542732012	3.677351413	10.43880812
2386	3.7	0.199526231	1.611809565	4.011872336	12.05943216
2749	3.71	0.19498446	1.634835416	4.12861384	12.65133996
3679	3.75	0.177827941	1.72693882	4.623413252	15.3113883
9319	3.91	0.123026877	2.095352435	7.128305162	32.5346724

Table C.10: High TOC Soil (Run 2) H_3PO_4 Buffering Raw Data

Time (min)	pH	$[H_3O^+]$ (mmol/L)	1st Order $-\ln[H_3O^+]/[H_3O^+]_0$	2nd Order $1/[H_3O^+] - 1/[H3O^+]_0$	3rd Order $1/2*[H_3O^+]^2 - 1/2*[H_3O^+]^2_0$
0	3	1	0	0	0
1	3.03	0.933254301	0.069077553	0.071519305	0.074076811
2	3.05	0.891250938	0.115129255	0.122018454	0.129462706
3	3.06	0.87096359	0.138155106	0.148153621	0.159128369
4	3.07	0.851138038	0.161180957	0.174897555	0.190192132
5	3.07	0.851138038	0.161180957	0.174897555	0.190192132
6	3.08	0.831763771	0.184206807	0.202264435	0.222719885
7	3.08	0.831763771	0.184206807	0.202264435	0.222719885
8	3.09	0.812830516	0.207232658	0.230268771	0.256780624
9	3.1	0.794328235	0.230258509	0.258925412	0.292446596
11	3.11	0.776247117	0.25328436	0.288249552	0.329793454
18	3.13	0.741310241	0.299336062	0.348962883	0.409850429
26	3.14	0.72443596	0.322361913	0.380384265	0.452730359
31	3.15	0.707945784	0.345387764	0.412537545	0.497631157
41	3.18	0.660693448	0.414465317	0.513561248	0.645433826
78	3.22	0.602559586	0.50656872	0.659586907	0.877114352
418	3.41	0.389045145	0.944059888	1.570395783	2.80346724
1128	3.54	0.28840315	1.24339595	2.467368505	5.511322173
1258	3.62	0.239883292	1.427602758	3.168693835	8.189004144
4256	3.75	0.177827941	1.72693882	4.623413252	15.3113883

Table C.11: Total H_3PO_4 Demand Raw Data

Soil Type	Mass of Dry Soil (g)	Total Moles H_3PO_4 Added (moles)	Total Mass H_3PO_4 Added (g)	Total Acid Demand (mol acid/g dry soil)	Total Acid Demand (g Acid/g dry soil)
Ozonated Sand 1	30	0.00125	0.1225	4.16667E-05	0.004083333
Ozonated Sand 2	30	0.00135	0.1323	0.000045	0.00441
Average Soil 1	30	0.00698	0.68404	0.000232667	0.022801333
Average Soil 2	30	0.0068	0.6664	0.000226667	0.022213333
High pH Soil 1	30	0.0356	3.4888	0.001186667	0.116293333
High pH Soil 2	30	0.0325	3.185	0.001083333	0.106166667
High Fe Soil 1	30	0.00552	0.54096	0.000184	0.018032
High Fe Soil 2	30	0.00521	0.51058	0.000173667	0.017019333
High TOC Soil 1	30	0.00466	0.45668	0.000155333	0.015222667
High TOC Soil 2	30	0.00456	0.44688	0.000152	0.014896

Table C.12: Ozonated Sand (Run 1) NaOH Buffering Raw Data

Time (min)	pH	pOH	$[OH^-]$ (mmol/L)	1st Order $-\ln[OH^-]/[OH^-]_0$	2nd Order $1/[OH^-] - 1/[OH^-]_0$	3rd Order $1/2*[OH^-]^2 - 1/2*[OH^-]^2_0$
0	10.01	3.99	0.102329299	0	0	0
15	10.02	3.98	0.104712855	-0.023025851	-0.222446349	-2.149087333
30	10	4	0.1	0.023025851	0.22762779	2.250370699
45	10.01	3.99	0.102329299	0	0	0
60	9.98	4.02	0.095499259	0.069077553	0.698913271	7.074280506
204	9.93	4.07	0.085113804	0.184206807	1.97660334	21.26958393
504	9.96	4.04	0.091201084	0.115129255	1.192409752	12.36359243
1824	9.92	4.08	0.083176377	0.207232658	2.250272137	24.52235924

Table C.13: Ozonated Sand (Run 2) NaOH Buffering Raw Data

Time (min)	pH	pOH	$[OH^-]$ (mmol/L)	1st Order $-\ln[OH^-]/[OH^-]_0$	2nd Order $1/[OH^-] - 1/[OH^-]_0$	3rd Order $1/2*[OH^-]^2 - 1/2*[OH^-]^2_0$
0	10	4	0.1	-0.023025851	0.22762779	2.250370699
10	9.97	4.03	0.09332543	0.092103404	0.942820843	9.658051774
20	9.99	4.01	0.097723722	0.046051702	0.460557713	4.606798101
30	10.01	3.99	0.102329299	0	0	0
40	9.98	4.02	0.095499259	0.069077553	0.698913271	7.074280506
50	9.99	4.01	0.097723722	0.046051702	0.460557713	4.606798101
60	9.99	4.01	0.097723722	0.046051702	0.460557713	4.606798101
100	9.97	4.03	0.09332543	0.092103404	0.942820843	9.658051774
1420	9.94	4.06	0.087096359	0.161180957	1.709164005	18.16320763
2680	9.96	4.04	0.091201084	0.115129255	1.192409752	12.36359243

Table C.14: Average Soil (Run 1) NaOH Buffering Raw Data

Time (min)	pH	pOH	$[OH^-]$ (mmol/L)	1st Order $-\ln[OH^-]/[OH^-]_0]$	2nd Order $1/[OH^-] - 1/[OH^-]_0$	3rd Order $1/2*[OH^-]^2 - 1/2*[OH^-]^2_0$
0	10	4	0.1	0	0	0
3	9.86	4.14	0.072443596	0.322361913	3.803842646	45.2730359
4	9.84	4.16	0.069183097	0.368413615	4.454397707	54.46480654
6	9.82	4.18	0.066069345	0.414465317	5.135612484	64.54338264
8	9.8	4.2	0.063095734	0.460517019	5.848931925	75.59432158
10	9.79	4.21	0.0616595	0.48354287	6.218100974	81.51339959
28	9.71	4.29	0.051286138	0.667749677	9.498445998	140.0946982
33	9.7	4.3	0.050118723	0.690775528	9.95262315	149.0535853
55	9.75	4.25	0.056234133	0.575646273	7.7827941	108.113883
98	9.74	4.26	0.054954087	0.598672124	8.197008586	115.5655607
313	9.56	4.44	0.036307805	1.013137441	17.54228703	329.2887875
973	9.4	4.6	0.025118864	1.381551056	29.81071706	742.4465962
1123	9.25	4.75	0.017782794	1.72693882	46.23413252	1531.13883
1288	9.29	4.71	0.019498446	1.634835416	41.2861384	1265.133996
1453	9.03	4.97	0.010715193	2.23350754	83.32543008	4304.81795
1753	8.75	5.25	0.005623413	2.878231366	167.827941	15761.3883
1948	8.6	5.4	0.003981072	3.22361913	241.1886432	31497.86722
2923	8.65	5.35	0.004466836	3.108489876	213.8721139	25009.36168
3343	8.61	5.39	0.004073803	3.200593279	235.4708916	30077.9793

Table C.15: Average Soil (Run 2) NaOH Buffering Raw Data

Time (min)	pH	pOH	$[OH^-]$ (mmol/L)	1st Order $-\ln[OH^-]/[OH^-]_0$	2nd Order $1/[OH^-] - 1/[OH^-]_0$	3rd Order $1/2*[OH^-]^2 - 1/2*[OH^-]^2_0$
0	10	4	0.1	0	0	0
1	9.96	4.04	0.091201084	0.092103404	0.964781961	10.11322173
2	9.92	4.08	0.083176377	0.184206807	2.022644346	22.27198854
3	9.87	4.13	0.074131024	0.299336062	3.489628826	40.98504293
5	9.83	4.17	0.067608298	0.391439466	4.791083882	59.3880812
8	9.8	4.2	0.063095734	0.460517019	5.848931925	75.59432158
48	9.68	4.32	0.047863009	0.73682723	10.89296131	168.2579161
263	9.44	4.56	0.027542287	1.289447652	26.30780548	609.1283693
923	9.25	4.75	0.017782794	1.72693882	46.23413252	1531.13883
1073	9.18	4.82	0.015135612	1.888119776	56.0693448	2132.579161
1238	9.23	4.77	0.016982437	1.772990522	48.88436554	1683.684252
1403	9.16	4.84	0.014454398	1.934171478	59.18309709	2343.150462
2303	8.87	5.13	0.007413102	2.601921155	124.8962883	9048.504293
2603	8.74	5.26	0.005495409	2.901257217	171.9700859	16506.55607
2798	8.73	5.27	0.005370318	2.924283068	176.2087137	17286.84252
3773	8.58	5.42	0.003801894	3.269670832	253.0267992	34541.54855
4193	8.57	5.43	0.003715352	3.292696683	259.1534804	36171.798
5903	8.3	5.7	0.001995262	3.914394658	491.1872336	125544.3216

Table C.16: High pH Soil (Run 1) NaOH Buffering Raw Data

Time (min)	pH	pOH	$[OH^-]$ (mmol/L)	1st Order $-\ln[OH^-]/[OH^-]_0$	2nd Order $1/[OH^-] - 1/[OH^-]_0$	3rd Order $1/2*[OH^-]^2 - 1/2*[OH^-]^2_0$
0	10	4	0.1	0	0	0
5	9.97	4.03	0.09332543	0.069077553	0.715193052	7.407681075
15	9.98	4.02	0.095499259	0.046051702	0.471285481	4.823909807
55	9.96	4.04	0.091201084	0.092103404	0.964781961	10.11322173
340	9.95	4.05	0.089125094	0.115129255	1.220184543	12.94627059
1000	9.7	4.3	0.050118723	0.690775528	9.95262315	149.0535853
1480	9.72	4.28	0.052480746	0.644723826	9.05460718	131.5390274
2500	9.58	4.42	0.03801894	0.967085739	16.30267992	295.9154855
2800	9.31	4.69	0.020417379	1.588783714	38.97788194	1149.41646
2995	9.23	4.77	0.016982437	1.772990522	48.88436554	1683.684252
3970	9.21	4.79	0.016218101	1.819042223	51.65950019	1850.946982
4390	9.21	4.79	0.016218101	1.819042223	51.65950019	1850.946982
8620	9.01	4.99	0.01023293	2.279559242	87.7237221	4724.96293

Table C.17: High pH Soil (Run 2) NaOH Buffering Raw Data

Time (min)	pH	pOH	$[OH^-]$ (mmol/L)	1st Order $-\ln[OH^-]/[OH^-]_0$	2nd Order $1/[OH^-] - 1/[OH^-]_0$	3rd Order $1/2*[OH^-]^2 - 1/2*[OH^-]^2_0$
0	10.04	3.96	0.10964782	0	0	0
40	10.01	3.99	0.102329299	0.069077553	0.652263816	6.161440746
325	9.98	4.02	0.095499259	0.138155106	1.351177087	13.23572125
985	9.81	4.19	0.064565423	0.529594571	6.368057796	78.3534574
1465	9.75	4.25	0.056234133	0.667749677	8.662685707	116.5256945
2365	9.6	4.4	0.039810717	1.013137441	15.99875592	273.8904837
2665	9.28	4.72	0.019054607	1.749964671	43.36063763	1335.526163
2860	9.14	4.86	0.013803843	2.072326584	63.32348761	2582.449113
3835	9.13	4.87	0.013489629	2.095352435	65.01091574	2706.116181
8065	8.97	5.03	0.009332543	2.46376605	98.03182213	5699.179919

Table C.18: High Fe Soil (Run 1) NaOH Buffering Raw Data

Time (min)	pH	pOH	$[OH^-]$ (mmol/L)	1st Order $-\ln[OH^-]/[OH^-]_0$	2nd Order $1/[OH^-] - 1/[OH^-]_0$	3rd Order $1/2*[OH^-]^2 - 1/2*[OH^-]^2_0$
0	10.02	3.98	0.104712855	0	0	0
1	9.99	4.01	0.097723722	0.069077553	0.683004063	6.755885435
2	9.95	4.05	0.089125094	0.161180957	1.670258683	17.34572862
3	9.93	4.07	0.085113804	0.207232658	2.199049689	23.41867126
4	9.9	4.1	0.079432823	0.276310211	3.039328258	33.64411766
5	9.89	4.11	0.077624712	0.299336062	3.332569657	37.3788034
6	9.88	4.12	0.075857758	0.322361913	3.632641525	41.28949947
7	9.87	4.13	0.074131024	0.345387764	3.939702966	45.38450096
8	9.86	4.14	0.072443596	0.368413615	4.253916786	49.67249393
9	9.85	4.15	0.070794578	0.391439466	4.575449586	54.16257378
10	9.84	4.16	0.069183097	0.414465317	4.904471847	58.86426457
11	9.83	4.17	0.067608298	0.437491168	5.241158021	63.78753923
12	9.82	4.18	0.066069345	0.460517019	5.585686624	68.94284067
13	9.81	4.19	0.064565423	0.48354287	5.938240329	74.34110398
15	9.8	4.2	0.063095734	0.50656872	6.299006064	79.99377961
16	9.79	4.21	0.0616595	0.529594571	6.668175113	85.91285763
17	9.78	4.22	0.060255959	0.552620422	7.045943214	92.1108932
18	9.77	4.23	0.058884366	0.575646273	7.432510664	98.60103319
19	9.76	4.24	0.057543994	0.598672124	7.828082427	105.3970441
20	9.76	4.24	0.057543994	0.598672124	7.828082427	105.3970441
22	9.74	4.26	0.054954087	0.644723826	8.647082726	119.9650188
24	9.74	4.26	0.054954087	0.644723826	8.647082726	119.9650188
27	9.73	4.27	0.05370318	0.667749677	9.070945506	127.7678833
30	9.71	4.29	0.051286138	0.713801379	9.948520137	144.4941562
33	9.71	4.29	0.051286138	0.713801379	9.948520137	144.4941562
35	9.7	4.3	0.050118723	0.73682723	10.40269729	153.4530433
38	9.69	4.31	0.048977882	0.759853081	10.86745359	162.8341498
42	9.68	4.32	0.047863009	0.782878932	11.34303545	172.6573742
46	9.67	4.33	0.046773514	0.805904783	11.82969503	182.9435528
51	9.66	4.34	0.045708819	0.828930633	12.32769038	193.7145042
62	9.64	4.36	0.043651583	0.874982335	13.35875067	216.8031882
67	9.62	4.38	0.041686938	0.921034037	14.43840333	242.1194267
162	9.48	4.52	0.030199517	1.24339595	23.56318629	502.6385561
327	9.3	4.7	0.019952623	1.657861267	40.5687975	1210.342674
1407	9.14	4.86	0.013803843	2.026274882	62.89367015	2578.436759
1707	8.85	5.15	0.007079458	2.694024559	131.7038286	9930.711033
1902	8.69	5.31	0.004897788	3.062438174	194.6238686	20797.86863
2877	8.76	5.24	0.005754399	2.901257217	164.230157	15054.15806
3297	8.89	5.11	0.007762471	2.601921155	119.2750293	8252.333995
5007	8.75	5.25	0.005623413	2.924283068	168.2780151	15765.78776
7527	8.7	5.3	0.005011872	3.039412323	189.9763056	19859.75799
11787	8.5	5.5	0.003162278	3.499929341	306.6778402	49954.39946

Table C.19: High Fe Soil (Run 2) NaOH Buffering Raw Data

Time (min)	pH	pOH	$[OH^-]$ (mmol/L)	1st Order $-\ln[OH^-]/[OH^-]_0$	2nd Order $1/[OH^-] - 1/[OH^-]_0$	3rd Order $1/2*[OH^-]^2 - 1/2*[OH^-]^2_0$
0	10	4	0.1	0	0	0
1	9.94	4.06	0.087096359	0.138155106	1.481536215	15.91283693
2	9.91	4.09	0.081283052	0.207232658	2.302687708	25.67806242
3	9.88	4.12	0.075857758	0.276310211	3.182567386	36.89004144
4	9.85	4.15	0.070794578	0.345387764	4.125375446	49.76311575
5	9.84	4.16	0.069183097	0.368413615	4.454397707	54.46480654
6	9.8	4.2	0.063095734	0.460517019	5.848931925	75.59432158
7	9.79	4.21	0.0616595	0.48354287	6.218100974	81.51339959
8	9.78	4.22	0.060255959	0.50656872	6.595869074	87.71143517
9	9.76	4.24	0.057543994	0.552620422	7.378008287	100.997586
10	9.74	4.26	0.054954087	0.598672124	8.197008586	115.5655607
11	9.73	4.27	0.05370318	0.621697975	8.620871367	123.3684252
12	9.72	4.28	0.052480746	0.644723826	9.05460718	131.5390274
13	9.71	4.29	0.051286138	0.667749677	9.498445998	140.0946982
14	9.7	4.3	0.050118723	0.690775528	9.95262315	149.0535853
15	9.69	4.31	0.048977882	0.713801379	10.41737945	158.4346917
16	9.68	4.32	0.047863009	0.73682723	10.89296131	168.2579161
17	9.67	4.33	0.046773514	0.759853081	11.3796209	178.5440948
18	9.66	4.34	0.045708819	0.782878932	11.87761624	189.3150462
19	9.66	4.34	0.045708819	0.782878932	11.87761624	189.3150462
20	9.66	4.34	0.045708819	0.782878932	11.87761624	189.3150462
21	9.65	4.35	0.044668359	0.805904783	12.38721139	200.5936168
22	9.64	4.36	0.043651583	0.828930633	12.90867653	212.4037301
23	9.63	4.37	0.042657952	0.851956484	13.44228815	224.7704369
24	9.62	4.38	0.041686938	0.874982335	13.98832919	237.7199687
25	9.62	4.38	0.041686938	0.874982335	13.98832919	237.7199687
26	9.62	4.38	0.041686938	0.874982335	13.98832919	237.7199687
27	9.61	4.39	0.040738028	0.898008186	14.54708916	251.279793
28	9.61	4.39	0.040738028	0.898008186	14.54708916	251.279793
29	9.6	4.4	0.039810717	0.921034037	15.11886432	265.4786722
30	9.6	4.4	0.039810717	0.921034037	15.11886432	265.4786722
31	9.59	4.41	0.038904514	0.944059888	15.70395783	280.346724
32	9.58	4.42	0.03801894	0.967085739	16.30267992	295.9154855
61	9.47	4.53	0.029512092	1.220370099	23.88441561	524.0768107
74	9.43	4.57	0.026915348	1.312473503	27.15352291	640.1921323
127	9.33	4.67	0.021379621	1.542732012	36.77351413	1043.880812
158	9.3	4.7	0.019952623	1.611809565	40.11872336	1205.943216
1178	9.17	4.83	0.014791084	1.911145627	57.60829754	2235.440948
1478	8.87	5.13	0.007413102	2.601921155	124.8962883	9048.504293
2648	8.88	5.12	0.007585776	2.578895304	121.8256739	8639.004144

Table C.20: High TOC Soil (Run 1) NaOH Buffering Raw Data

Time (min)	pH	pOH	$[OH^-]$ (mmol/L)	1st Order $-\ln[OH^-]/[OH^-]_0$	2nd Order $1/[OH^-] - 1/[OH^-]_0$	3rd Order $1/2*[OH^-]^2 - 1/2*[OH^-]^2_0$
0	10	4	0.1	0	0	0
1	9.92	4.08	0.083176377	0.184206807	2.022644346	22.27198854
2	9.89	4.11	0.077624712	0.25328436	2.882495517	32.97934537
3	9.84	4.16	0.069183097	0.368413615	4.454397707	54.46480654
4	9.81	4.19	0.064565423	0.437491168	5.488166189	69.94164595
5	9.79	4.21	0.0616595	0.48354287	6.218100974	81.51339959
6	9.78	4.22	0.060255959	0.50656872	6.595869074	87.71143517
7	9.77	4.23	0.058884366	0.529594571	6.982436525	94.20157516
8	9.74	4.26	0.054954087	0.598672124	8.197008586	115.5655607
9	9.72	4.28	0.052480746	0.644723826	9.05460718	131.5390274
10	9.71	4.29	0.051286138	0.667749677	9.498445998	140.0946982
11	9.7	4.3	0.050118723	0.690775528	9.95262315	149.0535853
12	9.69	4.31	0.048977882	0.713801379	10.41737945	158.4346917
13	9.68	4.32	0.047863009	0.73682723	10.89296131	168.2579161
14	9.67	4.33	0.046773514	0.759853081	11.3796209	178.5440948
15	9.66	4.34	0.045708819	0.782878932	11.87761624	189.3150462
16	9.65	4.35	0.044668359	0.805904783	12.38721139	200.5936168
17	9.64	4.36	0.043651583	0.828930633	12.90867653	212.4037301
18	9.63	4.37	0.042657952	0.851956484	13.44228815	224.7704369
19	9.62	4.38	0.041686938	0.874982335	13.98832919	237.7199687
20	9.6	4.4	0.039810717	0.921034037	15.11886432	265.4786722
21	9.6	4.4	0.039810717	0.921034037	15.11886432	265.4786722
22	9.59	4.41	0.038904514	0.944059888	15.70395783	280.346724
23	9.59	4.41	0.038904514	0.944059888	15.70395783	280.346724
24	9.58	4.42	0.03801894	0.967085739	16.30267992	295.9154855
25	9.57	4.43	0.037153523	0.99011159	16.91534804	312.21798
26	9.56	4.44	0.036307805	1.013137441	17.54228703	329.2887875
27	9.55	4.45	0.035481339	1.036163292	18.18382931	347.1641174
28	9.55	4.45	0.035481339	1.036163292	18.18382931	347.1641174
29	9.54	4.46	0.034673685	1.059189143	18.84031503	365.8818856
30	9.53	4.47	0.033884416	1.082214994	19.51209227	385.481795
31	9.52	4.48	0.033113112	1.105240845	20.1995172	406.0054197
35	9.5	4.5	0.031622777	1.151292546	21.6227766	450
270	8.79	5.21	0.00616595	2.786127963	152.1810097	13101.33996
1245	8.56	5.44	0.003630781	3.315722534	265.4228703	37878.87875
1665	8.59	5.41	0.003890451	3.246644981	247.0395783	32984.6724
3375	8.44	5.56	0.002754229	3.592032745	353.0780548	65862.83693
5895	8.13	5.87	0.001348963	4.305834124	731.3102413	274720.4369

Table C.21: High TOC Soil (Run 2) NaOH Buffering Raw Data

Time (min)	pH	pOH	$[OH^-]$ (mmol/L)	1st Order $-\ln[OH^-]/[OH^-]_0$	2nd Order $1/[OH^-] - 1/[OH^-]_0$	3rd Order $1/2*[OH^-]^2 - 1/2*[OH^-]^2_0$
0	10	4	0.1	0	0	0
1	9.92	4.08	0.083176377	0.184206807	2.022644346	22.27198854
2	9.86	4.14	0.072443596	0.322361913	3.803842646	45.2730359
3	9.81	4.19	0.064565423	0.437491168	5.488166189	69.94164595
4	9.78	4.22	0.060255959	0.50656872	6.595869074	87.71143517
5	9.74	4.26	0.054954087	0.598672124	8.197008586	115.5655607
6	9.73	4.27	0.05370318	0.621697975	8.620871367	123.3684252
7	9.71	4.29	0.051286138	0.667749677	9.498445998	140.0946982
8	9.69	4.31	0.048977882	0.713801379	10.41737945	158.4346917
9	9.67	4.33	0.046773514	0.759853081	11.3796209	178.5440948
10	9.65	4.35	0.044668359	0.805904783	12.38721139	200.5936168
11	9.64	4.36	0.043651583	0.828930633	12.90867653	212.4037301
12	9.63	4.37	0.042657952	0.851956484	13.44228815	224.7704369
13	9.61	4.39	0.040738028	0.898008186	14.54708916	251.279793
14	9.61	4.39	0.040738028	0.898008186	14.54708916	251.279793
15	9.6	4.4	0.039810717	0.921034037	15.11886432	265.4786722
16	9.58	4.42	0.03801894	0.967085739	16.30267992	295.9154855
17	9.56	4.44	0.036307805	1.013137441	17.54228703	329.2887875
18	9.55	4.45	0.035481339	1.036163292	18.18382931	347.1641174
19	9.54	4.46	0.034673685	1.059189143	18.84031503	365.8818856
20	9.54	4.46	0.034673685	1.059189143	18.84031503	365.8818856
21	9.53	4.47	0.033884416	1.082214994	19.51209227	385.481795
22	9.52	4.48	0.033113112	1.105240845	20.1995172	406.0054197
23	9.51	4.49	0.032359366	1.128266696	20.90295433	427.496293
24	9.5	4.5	0.031622777	1.151292546	21.6227766	450
25	9.49	4.51	0.030902954	1.174318397	22.35936569	473.564274
26	9.48	4.52	0.030199517	1.197344248	23.11311215	498.2390981
27	9.47	4.53	0.029512092	1.220370099	23.88441561	524.0768107
28	9.46	4.54	0.028840315	1.24339595	24.67368505	551.1322173
29	9.46	4.54	0.028840315	1.24339595	24.67368505	551.1322173
30	9.45	4.55	0.028183829	1.266421801	25.48133892	579.4627059
31	9.44	4.56	0.027542287	1.289447652	26.30780548	609.1283693
33	9.43	4.57	0.026915348	1.312473503	27.15352291	640.1921323
76	8.92	5.08	0.008317638	2.4867919	110.2264435	7177.198854
1051	8.69	5.31	0.004897788	3.016386472	194.1737945	20793.46917
1471	8.73	5.27	0.005370318	2.924283068	176.2087137	17286.84252
3121	8.59	5.41	0.003890451	3.246644981	247.0395783	32984.6724
5641	8.15	5.85	0.001412538	4.259782422	697.9457844	250543.6168
9901	7.93	6.07	0.000851138	4.766351142	1164.897555	690142.1323

Table C.22: Total NaOH Demand Raw Data

Soil Type	Mass of Dry Soil (g)	Total Moles NaOH Added (moles)	Total Mass NaOH Added (g)	Total Base Demand (g base/g dry soil)	Total Base Demand (g Base/g dry soil)
Ozonated Sand 1	30	0.00026	0.0104	8.66667E-06	0.000346667
Ozonated Sand 2	30	0.00029	0.0116	9.66667E-06	0.000386667
Average Soil 1	30	0.00705	0.282	0.000235	0.0094
Average Soil 2	30	0.0065	0.26	0.000216667	0.008666667
High pH Soil 1	30	0.0022	0.088	7.33333E-05	0.002933333
High pH Soil 2	30	0.00255	0.102	0.000085	0.0034
High Fe Soil 1	30	0.00355	0.142	0.000118333	0.004733333
High Fe Soil 2	30	0.0035	0.14	0.000116667	0.004666667
High TOC Soil 1	30	0.01255	0.502	0.000418333	0.016733333
High TOC Soil 2	30	0.0124	0.496	0.000413333	0.016533333

APPENDIX D

RAW DATA FOR OXYGEN PRODUCTION FROM H_2O_2

Table D.1: Ozonated Sand, 10,000 mg/L H_2O_2 Application (Run 1)

Time (min)	Total Pressure (psig)	Total Slurry Volume (mL)	Total Headspace Volume (mL)	Vol. % O_2	Vol. % N_2
Initial	0	60	440	20.99	78.03
1500	0.2	60	440	20.97	77.347

Table D.2: Ozonated Sand, 10,000 mg/L H_2O_2 Application (Run 2)

Time (min)	Total Pressure (psig)	Total Slurry Volume (mL)	Total Headspace Volume (mL)	Vol. % O_2	Vol. % N_2
Initial	0	60	440	20.99	78.03
1500	0.15	60	440	21.11	79.119

Table D.3: Average Soil, 10,000 mg/L H_2O_2 Application (Run 1)

Time (min)	Total Pressure (psig)	Total Slurry Volume (mL)	Total Headspace Volume (mL)	Vol. % O_2	Vol. % N_2
Initial	0	60	440	20.99	78.03
1500	1.8	60	440	31.78	68.222

Table D.4: Average Soil, 10,000 mg/L H_2O_2 Application (Run 2)

Time (min)	Total Pressure (psig)	Total Slurry Volume (mL)	Total Headspace Volume (mL)	Vol. % O_2	Vol. % N_2
Initial	0	60	440	20.99	78.03
1500	1.7	60	440	31.62	68.377

Table D.5: High pH Soil, 10,000 mg/L H_2O_2 Application (Run 1)

Time (min)	Total Pressure (psig)	Total Slurry Volume (mL)	Total Headspace Volume (mL)	Vol. % O_2	Vol. % N_2
Initial	0	60	440	20.99	78.03
1500	1.55	60	440	31.23	68.77

Table D.6: High pH Soil, 10,000 mg/L H_2O_2 Application (Run 2)

Time (min)	Total Pressure (psig)	Total Slurry Volume (mL)	Total Headspace Volume (mL)	Vol. % O_2	Vol. % N_2
Initial	0	60	440	20.99	78.03
1500	1.5	60	440	30.683	69.317

Table D.7: High Iron Soil, 10,000 mg/L H_2O_2 Application (Run 1)

Time (min)	Total Pressure (psig)	Total Slurry Volume (mL)	Total Headspace Volume (mL)	Vol. % O_2	Vol. % N_2
Initial	0	60	440	20.99	78.03
1500	1.75	60	440	31.497	68.5034

Table D.8: High Iron Soil, 10,000 mg/L H_2O_2 Application (Run 2)

Time (min)	Total Pressure (psig)	Total Slurry Volume (mL)	Total Headspace Volume (mL)	Vol. % O_2	Vol. % N_2
Initial	0	60	440	20.99	78.03
1500	1.7	60	440	31.267	68.7332

Table D.9: High TOC Soil, 10,000 mg/L H_2O_2 Application (Run 1)

Time (min)	Total Pressure (psig)	Total Slurry Volume (mL)	Total Headspace Volume (mL)	Vol. % O_2	Vol. % N_2
Initial	0	60	440	20.99	78.03
1500	1.7	60	440	31.201	68.7992

Table D.10: High TOC Soil, 10,000 mg/L H_2O_2 Application (Run 2)

Time (min)	Total Pressure (psig)	Total Slurry Volume (mL)	Total Headspace Volume (mL)	Vol. % O_2	Vol. % N_2
Initial	0	60	440	20.99	78.03
1500	1.4	60	440	31.373	68.6275

Table D.11: Biologically Stimulated Soil, 10,000 mg/L H_2O_2 Application (Run 1)

Time (min)	Total Pressure (psig)	Total Slurry Volume (mL)	Total Headspace Volume (mL)	Vol. % O_2	Vol. % N_2
Initial	0	60	440	20.99	78.03
1500	1.9	60	440	32.01	68.228

Table D.12: Biologically Stimulated Soil, 10,000 mg/L H_2O_2 Application (Run 2)

Time (min)	Total Pressure (psig)	Total Slurry Volume (mL)	Total Headspace Volume (mL)	Vol. % O_2	Vol. % N_2
Initial	0	60	440	20.99	78.03
1500	1.75	60	440	31.49	68.051

Table D.13: Ozonated Sand, 50,000 mg/L H_2O_2 Application (Run 1)

Time (min)	Total Pressure (psig)	Total Slurry Volume (mL)	Total Headspace Volume (mL)	Vol. % O_2	Vol. % N_2
Initial	0	60	440	20.99	78.03
350	0.2	60	440	21.297	76.66

Table D.14: Ozonated Sand, 50,000 mg/L H_2O_2 Application (Run 2)

Time (min)	Total Pressure (psig)	Total Slurry Volume (mL)	Total Headspace Volume (mL)	Vol. % O_2	Vol. % N_2
Initial	0	60	440	20.99	78.03
350	0.15	60	440	21.548	76.355

Table D.15: Average Soil, 50,000 mg/L H_2O_2 Application (Run 1)

Time (min)	Total Pressure (psig)	Total Slurry Volume (mL)	Total Headspace Volume (mL)	Vol. % O_2	Vol. % N_2
Initial	0	60	440	20.99	78.03
100	14.55	60	440	58.848	41.152
101*	0	60	440	57.859	42.141
360	2.85	60	440	66.067	33.53

Table D.16: Average Soil, 50,000 mg/L H_2O_2 Application (Run 2)

Time (min)	Total Pressure (psig)	Total Slurry Volume (mL)	Total Headspace Volume (mL)	Vol. % O_2	Vol. % N_2
Initial	0	60	440	20.99	78.03
70	14.45	60	440	60.196	39.804
75*	0	60	440	59.683	40.317
300	2.7	60	440	69.142	30.858

Table D.17: Average Soil, 50,000 mg/L H_2O_2 Application (Run 3)

Time (min)	Total Pressure (psig)	Total Slurry Volume (mL)	Total Headspace Volume (mL)	Vol. % O_2	Vol. % N_2
Initial	0	60	440	20.99	78.03
80	13	60	440	54.02	45.98
90*	0	60	440	58.886	41.114
350	3.5	60	440	70.421	29.579

Table D.18: High pH Soil, 50,000 mg/L H_2O_2 Application (Run 1)

Time (min)	Total Pressure (psig)	Total Slurry Volume (mL)	Total Headspace Volume (mL)	Vol. % O_2	Vol. % N_2
Initial	0	60	440	20.99	78.03
50	14.85	60	440	64.18	35.8194
55*	0	60	440	63.62	36.3832
150	2.45	60	440	68.21	31.7917

Table D.19: High pH Soil, 50,000 mg/L H_2O_2 Application (Run 2)

Time (min)	Total Pressure (psig)	Total Slurry Volume (mL)	Total Headspace Volume (mL)	Vol. % O_2	Vol. % N_2
Initial	0	60	440	20.99	78.03
55	15	60	440	62.86	37.1398
60*	0	60	440	62.69	37.3148
405	2.75	60	440	70	29.9957

Table D.20: High pH Soil, 50,000 mg/L H_2O_2 Application (Run 3)

Time (min)	Total Pressure (psig)	Total Slurry Volume (mL)	Total Headspace Volume (mL)	Vol. % O_2	Vol. % N_2
Initial	0	60	440	20.99	78.03
65	14.8	60	440	63.75	36.2501
70*	0	60	440	62.29	37.7144
1000	2.4	60	440	68.3	31.704

Table D.21: High Iron Soil, 50,000 mg/L H_2O_2 Application (Run 1)

Time (min)	Total Pressure (psig)	Total Slurry Volume (mL)	Total Headspace Volume (mL)	Vol. % O_2	Vol. % N_2
Initial	0	Initial	0	20.99	78.03
5	13.5	5	13.5	61.608	38.392
	0		0	61.608	38.392
180	4.15	180	4.15	71.411	28.589

Table 22: High Iron Soil, 50,000 mg/L H_2O_2 Application (Run 2)

Time (min)	Total Pressure (psig)	Total Slurry Volume (mL)	Total Headspace Volume (mL)	Vol. % O_2	Vol. % N_2
Initial	0	60	Initial	20.99	78.03
4	12.2	60	4	60.643	39.357
	0	60		60.643	39.357
5.9	5.9	60	5.9	72.791	27.209

Table D.23: High Iron Soil, 50,000 mg/L H_2O_2 Application (Run 3)

Time (min)	Total Pressure (psig)	Total Slurry Volume (mL)	Total Headspace Volume (mL)	Vol. % O_2	Vol. % N_2
Initial	0	60	440	20.99	78.03
5	13.2	60	440	60.947	39.053
	0	60	440	60.947	39.053
45	4.65	60	440	71.299	28.701

Table D.24: High TOC Soil, 50,000 mg/L H_2O_2 Application (Run 1)

Time (min)	Total Pressure (psig)	Total Slurry Volume (mL)	Total Headspace Volume (mL)	Vol. % O_2	Vol. % N_2
Initial	0	60	440	20.99	78.03
170	13.9	60	440	62.77	37.235
175*	0.1	60	440	58.52	41.481
1200	4.2	60	440	69.48	30.518

Table D.25: High TOC Soil, 50,000 mg/L H_2O_2 Application (Run 2)

Time (min)	Total Pressure (psig)	Total Slurry Volume (mL)	Total Headspace Volume (mL)	Vol. % O_2	Vol. % N_2
Initial	0	60	440	20.99	78.03
80	13.15	60	440	60.28	39.72
85*	0	60	440	59.44	40.557
380	4.65	60	440	71.02	28.977

Table D.26: High TOC Soil, 50,000 mg/L H_2O_2 Application (Run 3)

Time (min)	Total Pressure (psig)	Total Slurry Volume (mL)	Total Headspace Volume (mL)	Vol. % O_2	Vol. % N_2
Initial	0	60	440	20.99	78.03
150	14.85	60	440	63.41	36.586
160*	0	60	440	61.28	38.724
420	2.85	60	440	68.55	31.449

Table D.27: Biologically Stimulated Soil, 50,000 mg/L H_2O_2 Application (Run 1)

Time (min)	Total Pressure (psig)	Total Slurry Volume (mL)	Total Headspace Volume (mL)	Vol. % O_2	Vol. % N_2
Initial	0	60	440	20.99	78.03
150	16.15	60	440	71.604	28.339

Table D.28: Biologically Stimulated Soil, 50,000 mg/L H_2O_2 Application (Run 2)

Time (min)	Total Pressure (psig)	Total Slurry Volume (mL)	Total Headspace Volume (mL)	Vol. % O_2	Vol. % N_2
Initial	0	60	440	20.99	78.03
350	15.9	60	440	72.938	27.863

Table D.29: Biologically Stimulated Soil, 50,000 mg/L H_2O_2 Application (Run 3)

Time (min)	Total Pressure (psig)	Total Slurry Volume (mL)	Total Headspace Volume (mL)	Vol. % O_2	Vol. % N_2
Initial	0	60	440	20.99	78.03
350	16.1	60	440	71.223	27.535

Table D.30: Ozonated Sand, 100,000 mg/L H_2O_2 Application (Run 1)

Time (min)	Total Pressure (psig)	Total Slurry Volume (mL)	Total Headspace Volume (mL)	Vol. % O_2	Vol. % N_2
Initial	0	60	440	20.99	78.03
1500	0.5	60	440	23.186724	76.663864

Table D.31: Ozonated Sand, 100,000 mg/L H_2O_2 Application (Run 2)

Time (min)	Total Pressure (psig)	Total Slurry Volume (mL)	Total Headspace Volume (mL)	Vol. % O_2	Vol. % N_2
Initial	0	60	440	20.99	78.03
1500	0.5	60	440	24.110613	74.967959

Table D.32: Ozonated Sand, 100,000 mg/L H_2O_2 Application (Run 3)

Time (min)	Total Pressure (psig)	Total Slurry Volume (mL)	Total Headspace Volume (mL)	Vol. % O_2	Vol. % N_2
Initial	0	60	440	20.99	78.03
1500	0.5	60	440	23.459909	74.650212

Table D.33: Average Soil, 100,000 mg/L H_2O_2 Application (Run 1)

Time (min)	Total Pressure (psig)	Total Slurry Volume (mL)	Total Headspace Volume (mL)	Vol. % O_2	Vol. % N_2
Initial	0	60	440	20.99	78.03
10	13.65	60	440	49.951532	50.048468
	0	60	440	49.951532	50.048468
130	12.5	60	440	84.248859	15.751141
	0	60	440	84.248859	15.751141
1400	10.9	60	440	89.796597	8.6108985

Table D.34: Average Soil, 100,000 mg/L H_2O_2 Application (Run 2)

Time (min)	Total Pressure (psig)	Total Slurry Volume (mL)	Total Headspace Volume (mL)	Vol. % O_2	Vol. % N_2
Initial	0	60	440	20.99	78.03
11	14.4	60	440	54.589384	45.410616
	0	60	440	54.589384	45.410616
170	11.65	60	440	83.138934	16.731285
	0	60	440	83.138934	16.731285
1500	7.55	60	440	87.461523	10.803391

Table D.35: Average Soil, 100,000 mg/L H_2O_2 Application (Run 3)

Time (min)	Total Pressure (psig)	Total Slurry Volume (mL)	Total Headspace Volume (mL)	Vol. % O_2	Vol. % N_2
Initial	0	60	440	20.99	78.03
10	15	60	440	53.83892	46.16108
	0	60	440	53.83892	46.16108
185	13.4	60	440	85.259737	14.740263
	0	60	440	85.259737	14.740263
1600	4.45	60	440	88.124696	10.253115

Table D.36: High pH Soil, 100,000 mg/L H_2O_2 Application (Run 1)

Time (min)	Total Pressure (psig)	Total Slurry Volume (mL)	Total Headspace Volume (mL)	Vol. % O_2	Vol. % N_2
Initial	0	60	440	20.99	78.03
15	13.3	60	440	60.293	39.707
60	13.6	60	440	83.56	16.44
0	0	60	440	83.56	16.44
165	10.5	60	440	87.548	12.452
450	3.95	60	440	89.763	10.148

Table D.37: High pH Soil, 100,000 mg/L H_2O_2 Application (Run 2)

Time (min)	Total Pressure (psig)	Total Slurry Volume (mL)	Total Headspace Volume (mL)	Vol. % O_2	Vol. % N_2
Initial	0	60	440	20.99	78.03
25	12.6	60	440	59.974	40.026
125	14.9	60	440	80.937	19.063
0	0	60	440	80.937	19.063
400	6.95	60	440	86.685	13.315

Table D.38: High pH Soil, 100,000 mg/L H_2O_2 Application (Run 3)

Time (min)	Total Pressure (psig)	Total Slurry Volume (mL)	Total Headspace Volume (mL)	Vol. % O_2	Vol. % N_2
Initial	0	60	440	20.99	78.03
25	14.4	60	440	61.841	38.159
120	15	60	440	81.184	18.816
0	0	60	440	81.184	18.816
400	8.85	60	440	88.102	11.898

Table D.39: High Iron Soil, 100,000 mg/L H_2O_2 Application (Run 1)

Time (min)	Total Pressure (psig)	Total Slurry Volume (mL)	Total Headspace Volume (mL)	Vol. % O_2	Vol. % N_2
Initial	0	60	440	20.99	78.03
2	14.7	60	440	63.3605	36.64
	0	60	440	63.3605	36.64
3	14	60	440	79.7571	20.243
	0	60	440	79.7571	20.243
1000	6.15	60	440	87.3672	12.633

Table D.40: High Iron Soil, 100,000 mg/L H_2O_2 Application (Run 2)

Time (min)	Total Pressure (psig)	Total Slurry Volume (mL)	Total Headspace Volume (mL)	Vol. % O_2	Vol. % N_2
Initial	0	60	440	20.99	78.03
2	14.7	60	440	62.2752	37.725
	0	60	440	62.2752	37.725
3	14	60	440	81.1874	18.813
	0	60	440	81.1874	18.813
1000	7.6	60	440	88.7363	11.264

Table D.41: High Iron Soil, 100,000 mg/L H_2O_2 Application (Run 3)

Time (min)	Total Pressure (psig)	Total Slurry Volume (mL)	Total Headspace Volume (mL)	Vol. % O_2	Vol. % N_2
Initial	0	60	440	20.99	78.03
2	13.9	60	440	61.1022	38.898
	0	60	440	61.1022	38.898
3	13.5	60	440	81.9849	18.015
	0	60	440	81.9849	18.015
95	4.45	60	440	87.2286	12.771

Table D.42: High TOC Soil, 100,000 mg/L H_2O_2 Application (Run 1)

Time (min)	Total Pressure (psig)	Total Slurry Volume (mL)	Total Headspace Volume (mL)	Vol. % O_2	Vol. % N_2
Initial	0	60	440	21	78.03
440	13.85	60	440	61.2	38.81
0	0	60	440	61.2	38.81
1400	3.65	60	440	66	32.1

Table D.43: High TOC Soil, 100,000 mg/L H_2O_2 Application (Run 2)

Time (min)	Total Pressure (psig)	Total Slurry Volume (mL)	Total Headspace Volume (mL)	Vol. % O_2	Vol. % N_2
Initial	0	60	440	21	78.03
160	12.65	60	440	59.3	40.66
0	0	60	440	59.3	40.66
1000	6.6	60	440	68.7	28.96

Table D.44: High TOC Soil, 100,000 mg/L H_2O_2 Application (Run 3)

Time (min)	Total Pressure (psig)	Total Slurry Volume (mL)	Total Headspace Volume (mL)	Vol. % O_2	Vol. % N_2
Initial	0	60	440	21	78.03
160	12.5	60	440	60.3	39.68
0	0	60	440	60.3	39.68
1000	6.5	60	440	70	28.17

Table D.45: Biologically Stimulated Soil, 100,000 mg/L H_2O_2 Application (Run 1)

Time (min)	Total Pressure (psig)	Total Slurry Volume (mL)	Total Headspace Volume (mL)	Vol. % O_2	Vol. % N_2
Initial	0	60	440	20.99	78.03
8	13.8	60	440	49.342496	50.43618
	0	60	440	49.342496	50.43618
130	12.4	60	440	84.660359	15.249475
	0	60	440	84.660359	15.249475
1500	10.75	60	440	90.420253	8.6948524

Table D.46: Biologically Stimulated Soil, 100,000 mg/L H_2O_2 Application (Run 2)

Time (min)	Total Pressure (psig)	Total Slurry Volume (mL)	Total Headspace Volume (mL)	Vol. % O_2	Vol. % N_2
Initial	0	60	440	20.99	78.03
8	14.5	60	440	54.944355	44.627621
	0	60	440	54.944355	44.627621
180	11.8	60	440	83.573597	16.712107
	0	60	440	83.573597	16.712107
1500	7.7	60	440	87.271949	10.918764

Table D.47: Biologically Stimulated Soil, 100,000 mg/L H_2O_2 Application (Run 3)

Time (min)	Total Pressure (psig)	Total Slurry Volume (mL)	Total Headspace Volume (mL)	Vol. % O_2	Vol. % N_2
Initial	0	60	440	20.99	78.03
7	15	60	440	53.870854	45.842164
	0	60	440	53.870854	45.842164
175	13.3	60	440	85.981591	14.665502
	0	60	440	85.981591	14.665502
1500	4.5	60	440	88.098647	10.136576

Table D.48: Ozonated Sand, Fenton's Reagent (100,000 mg/L H_2O_2/5,000 mg/L Fe^{2+}) Application (Run 1)

Time (min)	Total Pressure (psig)	Total Slurry Volume (mL)	Total Headspace Volume (mL)	Vol. % O_2	Vol. % N_2
Initial	0	60	440	20.99	78.03
2	14.5	60	440	63.187	36.813
	0	60	440	63.187	36.813
155	3.85	60	440	71.576	28.232

Table D.49: Ozonated Sand, Fenton's Reagent (100,000 mg/L H_2O_2/5,000 mg/L Fe^{2+}) Application (Run 2)

Time (min)	Total Pressure (psig)	Total Slurry Volume (mL)	Total Headspace Volume (mL)	Vol. % O_2	Vol. % N_2
Initial	0	60	440	20.99	78.03
2	14.7	60	440	63.301	36.699
	0	60	440	63.301	36.699
115	4.55	60	440	72.701	27.299

Table D.50: Ozonated Sand, Fenton's Reagent (100,000 mg/L H_2O_2/5,000 mg/L Fe^{2+}) Application (Run 3)

Time (min)	Total Pressure (psig)	Total Slurry Volume (mL)	Total Headspace Volume (mL)	Vol. % O_2	Vol. % N_2
Initial	0	60	440	20.99	78.03
2	15	60	440	64.566	35.434
	0	60	440	64.566	35.434
85	2.75	60	440	71.485	28.277

Table D.51: Average Soil, Fenton's Reagent (100,000 mg/L H_2O_2/5,000 mg/L Fe^{2+}) Application (Run 1)

Time (min)	Total Pressure (psig)	Total Slurry Volume (mL)	Total Headspace Volume (mL)	Vol. % O_2	Vol. % N_2
Initial	0	60	440	20.99	78.03
1.5	15	60	440	58.876	41.12
	0	60	440	58.876	41.12
1000	2.6	60	440	74.515	24.31

Table D.52: Average Soil, Fenton's Reagent (100,000 mg/L H_2O_2/5,000 mg/L Fe^{2+}) Application (Run 2)

Time (min)	Total Pressure (psig)	Total Slurry Volume (mL)	Total Headspace Volume (mL)	Vol. % O_2	Vol. % N_2
Initial	0	60	440	20.99	78.03
2	13.6	60	440	57.05	42.95
	0	60	440	57.05	42.95
115	4.75	60	440	72.532	26.75

Table D.53: Average Soil, Fenton's Reagent (100,000 mg/L H_2O_2/5,000 mg/L Fe^{2+}) Application (Run 3)

Time (min)	Total Pressure (psig)	Total Slurry Volume (mL)	Total Headspace Volume (mL)	Vol. % O_2	Vol. % N_2
Initial	0	60	440	20.99	78.03
2.5	15	60	440	61.575	38.42
	0	60	440	61.575	38.42
190	2.65	60	440	71.68	27.08

Table D.54: High pH Soil, Fenton's Reagent (100,000 mg/L H_2O_2/5,000 mg/L Fe^{2+}) Application (Run 1)

Time (min)	Total Pressure (psig)	Total Slurry Volume (mL)	Total Headspace Volume (mL)	Vol. % O_2	Vol. % N_2
Initial	0	60	440	20.99	78.03
15	12.75	60	440	57.90236	38.5255
	0	60	440	57.90236	38.5255
360	6.85	60	440	71.40149	25.3163
1300	7	60	440	71.66891	25.0082

Table D.55: High pH Soil, Fenton's Reagent (100,000 mg/L H_2O_2/5,000 mg/L Fe^{2+}) Application (Run 2)

Time (min)	Total Pressure (psig)	Total Slurry Volume (mL)	Total Headspace Volume (mL)	Vol. % O_2	Vol. % N_2
Initial	0	60	440	20.99	78.03
11	14.2	60	440	62.08294	35.4752
	0	60	440	62.08294	35.4752
250	5.3	60	440	69.69955	26.4437

Table D.56: High pH Soil, Fenton's Reagent (100,000 mg/L H_2O_2/5,000 mg/L Fe^{2+}) Application (Run 3)

Time (min)	Total Pressure (psig)	Total Slurry Volume (mL)	Total Headspace Volume (mL)	Vol. % O_2	Vol. % N_2
Initial	0	60	440	20.99	78.03
3.5	12.9	60	440	61.13032	37.1589
	0	60	440	61.13032	37.1589
215	6.25	60	440	71.15335	24.9504

Table D.57: High Iron Soil, Fenton's Reagent (100,000 mg/L H_2O_2/5,000 mg/L Fe^{2+}) Application (Run 1)

Time (min)	Total Pressure (psig)	Total Slurry Volume (mL)	Total Headspace Volume (mL)	Vol. % O_2	Vol. % N_2
Initial	0	60	440	20.99	78.03
1.5	13.3	60	440	62.298	37.702
	0	60	440	62.298	37.702
180	5.85	60	440	74.434	25.566

Table D.58: High Iron Soil, Fenton's Reagent (100,000 mg/L H_2O_2/5,000 mg/L Fe^{2+}) Application (Run 2)

Time (min)	Total Pressure (psig)	Total Slurry Volume (mL)	Total Headspace Volume (mL)	Vol. % O_2	Vol. % N_2
Initial	0	60	440	20.99	78.03
2.5	14.7	60	440	63.653	36.347
	0	60	440	63.653	36.347
1000	3.8	60	440	71.795	28.205

Table D.59: High Iron Soil, Fenton's Reagent (100,000 mg/L H_2O_2/5,000 mg/L Fe^{2+}) Application (Run 3)

Time (min)	Total Pressure (psig)	Total Slurry Volume (mL)	Total Headspace Volume (mL)	Vol. % O_2	Vol. % N_2
Initial	0	60	440	20.99	78.03
2.5	15	60	440	65.883	34.117
	0	60	440	65.883	34.117
135	4.1	60	440	73.785	26.215

Table D.60: High TOC Soil, Fenton's Reagent (100,000 mg/L H_2O_2/5,000 mg/L Fe^{2+}) Application (Run 1)

Time (min)	Total Pressure (psig)	Total Slurry Volume (mL)	Total Headspace Volume (mL)	Vol. % O_2	Vol. % N_2
Initial	0	60	440	20.99	78.03
2.5	14.5	60	440	53.74	46.26
	0	60	440	53.74	46.26
360	3.2	60	440	78.043	20.906
1200	3.2	60	440	78.176	20.5018

Table D.61: High TOC Soil, Fenton's Reagent (100,000 mg/L H_2O_2/5,000 mg/L Fe^{2+}) Application (Run 2)

Time (min)	Total Pressure (psig)	Total Slurry Volume (mL)	Total Headspace Volume (mL)	Vol. % O_2	Vol. % N_2
Initial	0	60	440	20.99	78.03
2	12	60	440	49.091	50.9093
	0	60	440	49.091	50.9093
225	4.15	60	440	77.031	21.5569

Table D.62: High TOC Soil, Fenton's Reagent (100,000 mg/L H_2O_2/5,000 mg/L Fe^{2+}) Application (Run 3)

Time (min)	Total Pressure (psig)	Total Slurry Volume (mL)	Total Headspace Volume (mL)	Vol. % O_2	Vol. % N_2
Initial	0	60	440	20.99	78.03
2	14.9	60	440	60.686	39.314
	0	60	440	60.686	39.314
23	2.4	60	440	75.933	23.9133

Table D.63: Biologically Stimulated Soil, Fenton's Reagent (100,000 mg/L H_2O_2/5,000 mg/L Fe^{2+}) Application (Run 1)

Time (min)	Total Pressure (psig)	Total Slurry Volume (mL)	Total Headspace Volume (mL)	Vol. % O_2	Vol. % N_2
Initial	0	60	440	20.99	78.03
2	15	60	440	58.218	40.4
	0	60	440	58.218	40.4
1000	2.6	60	440	75.002	24.14

Table D.64: Biologically Stimulated Soil, Fenton's Reagent (100,000 mg/L H_2O_2/5,000 mg/L Fe^{2+}) Application (Run 2)

Time (min)	Total Pressure (psig)	Total Slurry Volume (mL)	Total Headspace Volume (mL)	Vol. % O_2	Vol. % N_2
Initial	0	60	440	20.99	78.03
3	13.9	60	440	57.657	42.83
	0	60	440	57.657	42.83
115	4.75	60	440	77.198	22.02

Table D.65: Biologically Stimulated Soil, Fenton's Reagent (100,000 mg/L H_2O_2/5,000 mg/L Fe^{2+}) Application (Run 3)

Time (min)	**Total Pressure (psig)**	**Total Slurry Volume (mL)**	**Total Headspace Volume (mL)**	**Vol. % O_2**	**Vol. % N_2**
Initial	0	60	440	20.99	78.03
3	14.9	60	440	61.666	38.05
	0	60	440	61.666	38.05
190	2.55	60	440	71.567	26.87

APPENDIX E

RAW DATA FOR IMPACT OF ISCO ON SOIL AEROBES

Table E.1: Constants for Impact of ISCO to Microbial Populations

Mass of Dry Soil	120	g
Mass of Solution	280	g
Volume of Solution	280	mL
Slurry Weight Percent	30	%

Table E.2: Impact of ISCO on Average Soil, 1A

Treatment	1A # of Colonies	1A Dilution Factor	1A CFU/mL solution	1A CFU/g dry soil	1A log CFU/g dry soil
No Treatment	289	1.00E+04	2.89E+06	6.74E+06	6.83
500 mg/L Fe^{2+}	259	1.00E+04	2.59E+06	6.04E+06	6.78
5,000 mg/L Fe^{2+}	159	1.00E+04	1.59E+06	3.71E+06	6.57
100,000 mg/L H_2O_2	65	1.00E+01	6.50E+02	1.52E+03	3.18
Fenton's Reaction (5,000 mg/L Fe^{2+} + 100,000 mg/L H_2O_2)	49	1.00E+01	4.90E+02	1.14E+03	3.06
Fenton's Reaction (500 mg/L Fe^{2+} + 10,000 mg/L H_2O_2)	255	1.0E+02	2.55E+04	5.95E+04	4.77
1% O_3	39	1.00E+04	3.90E+05	9.10E+05	5.96
3% O_3	255	1.00E+03	2.55E+05	5.95E+05	5.77
Peroxone (1,000 mg/L H_2O_2 + 3% O_3)	198	1.0E+02	1.98E+04	4.62E+04	4.66
Peroxone (10,000 mg/L H_2O_2 + 1% O_3)	31	1.0E+02	3.10E+03	7.23E+03	3.86

Table E.3: Impact of ISCO on Average Soil, 1B

Treatment	1B # of Colonies	1B Dilution Factor	1B CFU/mL solution	1B CFU/g dry soil	1B log CFU/g dry soil
No Treatment	101	1.0E+05	1.01E+07	2.36E+07	7.37
500 mg/L Fe^{2+}	198	1.00E+04	1.98E+06	4.62E+06	6.66
5,000 mg/L Fe^{2+}	287	1.00E+04	2.87E+06	6.70E+06	6.83
100,000 mg/L H_2O_2	36	1.0E+02	3.60E+03	8.40E+03	3.92
Fenton's Reaction (5,000 mg/L Fe^{2+} + 100,000 mg/L H_2O_2)	61	1.00E+01	6.10E+02	1.42E+03	3.15
Fenton's Reaction (500 mg/L Fe^{2+} + 10,000 mg/L H_2O_2)	145	1.0E+02	1.45E+04	3.38E+04	4.53
1% O_3	122	1.0E+05	1.22E+07	2.85E+07	7.45
3% O_3	189	1.00E+03	1.89E+05	4.41E+05	5.64
Peroxone (1,000 mg/L H_2O_2 + 3% O_3)	45	1.0E+02	4.50E+03	1.05E+04	4.02
Peroxone (10,000 mg/L H_2O_2 + 1% O_3)	45	1.0E+02	4.50E+03	1.05E+04	4.02

Table E.4: Impact of ISCO on Average Soil, 1C

Treatment	1C # of Colonies	1C Dilution Factor	1C CFU/mL solution	1C CFU/g dry soil	1C log CFU/g dry soil
No Treatment	258	1.00E+04	2.58E+06	6.02E+06	6.78
500 mg/L Fe^{2+}	65	1.0E+05	6.50E+06	1.52E+07	7.18
5,000 mg/L Fe^{2+}	42	1.0E+05	4.20E+06	9.80E+06	6.99
100,000 mg/L H_2O_2	165	1.00E+01	1.65E+03	3.85E+03	3.59
Fenton's Reaction (5,000 mg/L Fe^{2+} + 100,000 mg/L H_2O_2)	31	1.00E+01	3.10E+02	7.23E+02	2.86
Fenton's Reaction (500 mg/L Fe^{2+} + 10,000 mg/L H_2O_2)	198	1.0E+02	1.98E+04	4.62E+04	4.66
1% O_3	55	1.0E+05	5.50E+06	1.28E+07	7.11
3% O_3	119	1.00E+03	1.19E+05	2.78E+05	5.44
Peroxone (1,000 mg/L H_2O_2 + 3% O_3)	49	1.0E+02	4.50E+03	1.05E+04	4.02
Peroxone (10,000 mg/L H_2O_2 + 1% O_3)	155	1.00E+01	1.55E+03	3.62E+03	3.56

Table E.5: Impact of ISCO on Average Soil, 2A

Treatment	2A # of Colonies	2A Dilution Factor	2A CFU/mL solution	2A CFU/g dry soil	2A log CFU/g dry soil
No Treatment	213	1.00E+04	2.13E+06	4.97E+06	6.70
500 mg/L Fe^{2+}	98	1.00E+04	9.80E+05	2.29E+06	6.36
5,000 mg/L Fe^{2+}	41	1.0E+05	4.20E+06	9.80E+06	6.99
100,000 mg/L H_2O_2	49	1.0E+02	4.90E+03	1.14E+04	4.06
Fenton's Reaction (5,000 mg/L Fe^{2+} + 100,000 mg/L H_2O_2)	49	1.00E+01	4.90E+02	1.14E+03	3.06
Fenton's Reaction (500 mg/L Fe^{2+} + 10,000 mg/L H_2O_2)	68	1.0E+02	6.80E+03	1.59E+04	4.20
1% O_3	39	1.0E+05	3.90E+06	9.10E+06	6.96
3% O_3	158	1.00E+03	1.58E+05	3.69E+05	5.57
Peroxone (1,000 mg/L H_2O_2 + 3% O_3)	300	1.0E+02	3.00E+04	7.00E+04	4.85
Peroxone (10,000 mg/L H_2O_2 + 1% O_3)	57	1.0E+02	5.70E+03	1.33E+04	4.12

Table E.6: Impact of ISCO on Average Soil, 2B

Treatment	2B # of Colonies	2B Dilution Factor	2B CFU/mL solution	2B CFU/g dry soil	2B log CFU/g dry soil
No Treatment	78	1.0E+05	7.80E+06	1.82E+07	7.26
500 mg/L Fe^{2+}	116	1.00E+04	1.16E+06	2.71E+06	6.43
5,000 mg/L Fe^{2+}	45	1.0E+06	4.50E+07	1.05E+08	8.02
100,000 mg/L H_2O_2	67	1.00E+01	6.70E+02	1.56E+03	3.19
Fenton's Reaction (5,000 mg/L Fe^{2+} + 100,000 mg/L H_2O_2)	106	1.00E+01	1.06E+03	2.47E+03	3.39
Fenton's Reaction (500 mg/L Fe^{2+} + 10,000 mg/L H_2O_2)	55	1.0E+02	5.50E+03	1.28E+04	4.11
1% O_3	58	1.0E+05	5.80E+06	1.35E+07	7.13
3% O_3	245	1.00E+03	2.45E+05	5.72E+05	5.76
Peroxone (1,000 mg/L H_2O_2 + 3% O_3)	255	1.0E+02	2.55E+04	5.95E+04	4.77
Peroxone (10,000 mg/L H_2O_2 + 1% O_3)	215	1.00E+01	2.15E+03	5.02E+03	3.70

Table E.7: Impact of ISCO on Average Soil, 2C

Treatment	2C # of Colonies	2C Dilution Factor	2C CFU/mL solution	2C CFU/g dry soil	2C log CFU/g dry soil
No Treatment	33	1.0E+05	3.30E+06	7.70E+06	6.89
500 mg/L Fe^{2+}	39	1.0E+05	3.90E+06	9.10E+06	6.96
5,000 mg/L Fe^{2+}	99	1.00E+04	9.90E+05	2.31E+06	6.36
100,000 mg/L H_2O_2	169	1.00E+01	1.69E+03	3.94E+03	3.60
Fenton's Reaction (5,000 mg/L Fe^{2+} + 100,000 mg/L H_2O_2)	39	1.00E+01	3.90E+02	9.10E+02	2.96
Fenton's Reaction (500 mg/L Fe^{2+} + 10,000 mg/L H_2O_2)	166	1.0E+02	1.66E+04	3.87E+04	4.59
1% O_3	41	1.0E+05	4.10E+06	9.57E+06	6.98
3% O_3	300	1.00E+03	3.00E+05	7.00E+05	5.85
Peroxone (1,000 mg/L H_2O_2 + 3% O_3)	274	1.0E+02	2.74E+04	6.39E+04	4.81
Peroxone (10,000 mg/L H_2O_2 + 1% O_3)	33	1.0E+02	3.30E+03	7.70E+03	3.89

Table E.8: Impact of ISCO on High pH Soil, 1A

Treatment	1A # of Colonies	1A Dilution Factor	1A CFU/mL solution	1A CFU/g dry soil	1A log CFU/g dry soil
No Treatment	128	1.0E+04	1.28E+06	2.99E+06	6.48
500 mg/L Fe^{2+}	50	1.00E+04	5.00E+05	1.17E+06	6.07
5,000 mg/L Fe^{2+}	39	1.0E+04	3.90E+05	9.10E+05	5.96
100,000 mg/L H_2O_2	297	1.0E+02	2.97E+04	6.93E+04	4.84
Fenton's Reaction (5,000 mg/L Fe^{2+} + 100,000 mg/L H_2O_2)	41	1.00E+01	4.10E+02	9.57E+02	2.98
Fenton's Reaction (500 mg/L Fe^{2+} + 10,000 mg/L H_2O_2)	139	1.0E+03	1.39E+05	3.24E+05	5.51
1% O_3	175	1.0E+03	1.75E+05	4.08E+05	5.61
3% O_3	123	1.0E+03	1.23E+05	2.87E+05	5.46
Peroxone (1,000 mg/L H_2O_2 + 3% O_3)	35	1.0E+02	3.50E+03	8.17E+03	3.91
Peroxone (10,000 mg/L H_2O_2 + 1% O_3)	98	1.0E+03	9.80E+04	2.29E+05	5.36

Table E.9: Impact of ISCO on High pH Soil, 1B

Treatment	1B # of Colonies	1B Dilution Factor	1B CFU/mL solution	1B CFU/g dry soil	1B log CFU/g dry soil
No Treatment	73	1.0E+04	7.30E+05	1.70E+06	6.23
500 mg/L Fe^{2+}	70	1.00E+04	7.00E+05	1.63E+06	6.21
5,000 mg/L Fe^{2+}	237	1.00E+03	2.37E+05	5.53E+05	5.74
100,000 mg/L H_2O_2	245	1.0E+02	2.45E+04	5.72E+04	4.76
Fenton's Reaction (5,000 mg/L Fe^{2+} + 100,000 mg/L H_2O_2)	65	1.00E+01	6.50E+02	1.52E+03	3.18
Fenton's Reaction (500 mg/L Fe^{2+} + 10,000 mg/L H_2O_2)	191	1.0E+03	1.91E+05	4.46E+05	5.65
1% O_3	53	1.0E+04	5.30E+05	1.24E+06	6.09
3% O_3	47	1.0E+03	4.70E+04	1.10E+05	5.04
Peroxone (1,000 mg/L H_2O_2 + 3% O_3)	149	1.0E+03	1.49E+05	3.48E+05	5.54
Peroxone (10,000 mg/L H_2O_2 + 1% O_3)	92	1.0E+03	9.20E+04	2.15E+05	5.33

Table E.10: Impact of ISCO on High pH Soil, 1C

Treatment	1C # of Colonies	1C Dilution Factor	1C CFU/mL solution	1C CFU/g dry soil	1C log CFU/g dry soil
No Treatment	33	1.0E+05	3.30E+06	7.70E+06	6.89
500 mg/L Fe^{2+}	46	1.00E+04	4.60E+05	1.07E+06	6.03
5,000 mg/L Fe^{2+}	54	1.0E+04	5.40E+05	1.26E+06	6.10
100,000 mg/L H_2O_2	143	1.0E+02	1.43E+04	3.34E+04	4.52
Fenton's Reaction (5,000 mg/L Fe^{2+} + 100,000 mg/L H_2O_2)	51	1.00E+01	5.10E+02	1.19E+03	3.08
Fenton's Reaction (500 mg/L Fe^{2+} + 10,000 mg/L H_2O_2)	135	1.0E+03	1.35E+05	3.15E+05	5.50
1% O_3	141	1.0E+03	1.41E+05	3.29E+05	5.52
3% O_3	149	1.0E+03	1.49E+05	3.48E+05	5.54
Peroxone (1,000 mg/L H_2O_2 + 3% O_3)	57	1.0E+03	5.70E+04	1.33E+05	5.12
Peroxone (10,000 mg/L H_2O_2 + 1% O_3)	216	1.0E+03	2.16E+05	5.04E+05	5.70

Table E.11: Impact of ISCO on High pH Soil, 2A

Treatment	2A # of Colonies	2A Dilution Factor	2A CFU/mL solution	2A CFU/g dry soil	2A log CFU/g dry soil
No Treatment	129	1.0E+04	1.29E+06	3.01E+06	6.48
500 mg/L Fe^{2+}	56	1.00E+04	5.60E+05	1.31E+06	6.12
5,000 mg/L Fe^{2+}	58	1.0E+04	5.80E+05	1.35E+06	6.13
100,000 mg/L H_2O_2	261	1.0E+02	2.61E+04	6.09E+04	4.78
Fenton's Reaction (5,000 mg/L Fe^{2+} + 100,000 mg/L H_2O_2)	46	1.00E+01	4.60E+02	1.07E+03	3.03
Fenton's Reaction (500 mg/L Fe^{2+} + 10,000 mg/L H_2O_2)	155	1.0E+03	1.55E+05	3.62E+05	5.56
1% O_3	162	1.0E+03	1.62E+05	3.78E+05	5.58
3% O_3	92	1.0E+03	9.20E+04	2.15E+05	5.33
Peroxone (1,000 mg/L H_2O_2 + 3% O_3)	184	1.0E+03	1.84E+05	4.29E+05	5.63
Peroxone (10,000 mg/L H_2O_2 + 1% O_3)	233	1.0E+03	2.33E+05	5.44E+05	5.74

Table E.12: Impact of ISCO on High pH Soil, 2B

Treatment	2B # of Colonies	2B Dilution Factor	2B CFU/mL solution	2B CFU/g dry soil	2B log CFU/g dry soil
No Treatment	174	1.0E+04	1.74E+06	4.06E+06	6.61
500 mg/L Fe^{2+}	85	1.00E+04	8.50E+05	1.98E+06	6.30
5,000 mg/L Fe^{2+}	59	1.0E+04	5.90E+05	1.38E+06	6.14
100,000 mg/L H_2O_2	31	1.0E+03	3.10E+04	7.23E+04	4.86
Fenton's Reaction (5,000 mg/L Fe^{2+} + 100,000 mg/L H_2O_2)	39	1.00E+01	3.90E+02	9.10E+02	2.96
Fenton's Reaction (500 mg/L Fe^{2+} + 10,000 mg/L H_2O_2)	195	1.0E+03	1.95E+05	4.55E+05	5.66
1% O_3	148	1.0E+03	1.48E+05	3.45E+05	5.54
3% O_3	299	1.00E+02	2.99E+04	6.98E+04	4.84
Peroxone (1,000 mg/L H_2O_2 + 3% O_3)	237	1.0E+03	2.37E+05	5.53E+05	5.74
Peroxone (10,000 mg/L H_2O_2 + 1% O_3)	140	1.0E+03	1.40E+05	3.27E+05	5.51

Table E.13: Impact of ISCO on High pH Soil, 2C

Treatment	2C # of Colonies	2C Dilution Factor	2C CFU/mL solution	2C CFU/g dry soil	2C log CFU/g dry soil
No Treatment	51	1.0E+05	5.10E+06	1.19E+07	7.08
500 mg/L Fe^{2+}	74	1.00E+04	7.40E+05	1.73E+06	6.24
5,000 mg/L Fe^{2+}	125	1.00E+03	1.25E+05	2.92E+05	5.46
100,000 mg/L H_2O_2	161	1.0E+02	1.61E+04	3.76E+04	4.57
Fenton's Reaction (5,000 mg/L Fe^{2+} + 100,000 mg/L H_2O_2)	29	1.00E+01	2.90E+02	6.77E+02	2.83
Fenton's Reaction (500 mg/L Fe^{2+} + 10,000 mg/L H_2O_2)	111	1.0E+03	1.11E+05	2.59E+05	5.41
1% O_3	268	1.0E+03	2.68E+05	6.25E+05	5.80
3% O_3	199	1.0E+03	1.99E+05	4.64E+05	5.67
Peroxone (1,000 mg/L H_2O_2 + 3% O_3)	242	1.0E+03	2.42E+05	5.65E+05	5.75
Peroxone (10,000 mg/L H_2O_2 + 1% O_3)	161	1.0E+03	1.61E+05	3.76E+05	5.57

Table E.14: Impact of ISCO on High Fe Soil, 1A

Treatment	1A # of Colonies	1A Dilution Factor	1A CFU/mL solution	1A CFU/g dry soil	1A log CFU/g dry soil
No Treatment	191	1.00E+04	1.91E+06	4.46E+06	6.65
500 mg/L Fe^{2+}	92	1.00E+03	9.20E+04	2.15E+05	5.33
5,000 mg/L Fe^{2+}	60	1.00E+03	6.00E+04	1.40E+05	5.15
100,000 mg/L H_2O_2	45	1.00E+01	4.50E+02	1.05E+03	3.02
Fenton's Reaction (5,000 mg/L Fe^{2+} + 100,000 mg/L H_2O_2)	0	1.00E+01	0.00E+00	0.00E+00	#NUM!
Fenton's Reaction (500 mg/L Fe^{2+} + 10,000 mg/L H_2O_2)	55	1.0E+02	5.50E+03	1.28E+04	4.11
1% O_3	133	1.0E+04	1.33E+06	3.10E+06	6.49
3% O_3	146	1.0E+03	1.46E+05	3.41E+05	5.53
Peroxone (1,000 mg/L H_2O_2 + 3% O_3)	196	1.0E+02	1.96E+04	4.57E+04	4.66
Peroxone (10,000 mg/L H_2O_2 + 1% O_3)	211	1.0E+02	2.11E+04	4.92E+04	4.69

Table E.15: Impact of ISCO on High Fe Soil, 1B

Treatment	1B # of Colonies	1B Dilution Factor	1B CFU/mL solution	1B CFU/g dry soil	1B log CFU/g dry soil
No Treatment	49	1.00E+04	4.90E+05	1.14E+06	6.06
500 mg/L Fe^{2+}	98	1.00E+03	9.80E+04	2.29E+05	5.36
5,000 mg/L Fe^{2+}	53	1.00E+03	5.30E+04	1.24E+05	5.09
100,000 mg/L H_2O_2	58	1.00E+01	5.80E+02	1.35E+03	3.13
Fenton's Reaction (5,000 mg/L Fe^{2+} + 100,000 mg/L H_2O_2)	0	1.00E+01	0.00E+00	0.00E+00	#NUM!
Fenton's Reaction (500 mg/L Fe^{2+} + 10,000 mg/L H_2O_2)	256	1.00E+01	2.56E+03	5.97E+03	3.78
1% O_3	101	1.0E+04	1.01E+06	2.36E+06	6.37
3% O_3	108	1.0E+03	1.08E+05	2.52E+05	5.40
Peroxone (1,000 mg/L H_2O_2 + 3% O_3)	107	1.0E+02	1.07E+04	2.50E+04	4.40
Peroxone (10,000 mg/L H_2O_2 + 1% O_3)	295	1.00E+01	2.95E+03	6.88E+03	3.84

Table E.16: Impact of ISCO on High Fe Soil, 1C

Treatment	1C # of Colonies	1C Dilution Factor	1C CFU/mL solution	1C CFU/g dry soil	1C log CFU/g dry soil
No Treatment	167	1.00E+04	1.67E+06	3.90E+06	6.59
500 mg/L Fe^{2+}	153	1.00E+03	1.53E+05	3.57E+05	5.55
5,000 mg/L Fe^{2+}	35	1.0E+04	3.50E+05	8.17E+05	5.91
100,000 mg/L H_2O_2	47	1.00E+01	4.70E+02	1.10E+03	3.04
Fenton's Reaction (5,000 mg/L Fe^{2+} + 100,000 mg/L H_2O_2)	0	1.00E+01	0.00E+00	0.00E+00	#NUM!
Fenton's Reaction (500 mg/L Fe^{2+} + 10,000 mg/L H_2O_2)	98	1.00E+01	9.80E+02	2.29E+03	3.36
1% O_3	115	1.0E+04	1.15E+06	2.68E+06	6.43
3% O_3	132	1.0E+03	1.32E+05	3.08E+05	5.49
Peroxone (1,000 mg/L H_2O_2 + 3% O_3)	171	1.0E+02	1.71E+04	3.99E+04	4.60
Peroxone (10,000 mg/L H_2O_2 + 1% O_3)	101	1.0E+02	1.01E+04	2.36E+04	4.37

Table E.17: Impact of ISCO on High Fe Soil, 2A

Treatment	2A # of Colonies	2A Dilution Factor	2A CFU/mL solution	2A CFU/g dry soil	2A log CFU/g dry soil
No Treatment	252	1.00E+04	2.52E+06	5.88E+06	6.77
500 mg/L Fe^{2+}	45	1.00E+03	4.50E+04	1.05E+05	5.02
5,000 mg/L Fe^{2+}	43	1.00E+03	4.30E+04	1.00E+05	5.00
100,000 mg/L H_2O_2	73	1.0E+02	7.30E+03	1.70E+04	4.23
Fenton's Reaction (5,000 mg/L Fe^{2+} + 100,000 mg/L H_2O_2)	0	1.00E+01	0.00E+00	0.00E+00	#NUM!
Fenton's Reaction (500 mg/L Fe^{2+} + 10,000 mg/L H_2O_2)	41	1.0E+02	4.10E+03	9.57E+03	3.98
1% O_3	52	1.0E+04	5.20E+05	1.21E+06	6.08
3% O_3	235	1.0E+03	2.35E+05	5.48E+05	5.74
Peroxone (1,000 mg/L H_2O_2 + 3% O_3)	136	1.0E+02	1.36E+04	3.17E+04	4.50
Peroxone (10,000 mg/L H_2O_2 + 1% O_3)	39	1.0E+02	3.90E+03	9.10E+03	3.96

Table E.18: Impact of ISCO on High Fe Soil, 2B

Treatment	2B # of Colonies	2B Dilution Factor	2B CFU/mL solution	2B CFU/g dry soil	2B log CFU/g dry soil
No Treatment	46	1.00E+04	4.60E+05	1.07E+06	6.03
500 mg/L Fe^{2+}	36	1.00E+03	3.60E+04	8.40E+04	4.92
5,000 mg/L Fe^{2+}	35	1.0E+04	3.50E+05	8.17E+05	5.91
100,000 mg/L H_2O_2	43	1.0E+02	4.30E+03	1.00E+04	4.00
Fenton's Reaction (5,000 mg/L Fe^{2+} + 100,000 mg/L H_2O_2)	0	1.00E+01	0.00E+00	0.00E+00	#NUM!
Fenton's Reaction (500 mg/L Fe^{2+} + 10,000 mg/L H_2O_2)	57	1.0E+02	5.70E+03	1.33E+04	4.12
1% O_3	71	1.0E+04	7.10E+05	1.66E+06	6.22
3% O_3	151	1.0E+03	1.51E+05	3.52E+05	5.55
Peroxone (1,000 mg/L H_2O_2 + 3% O_3)	99	1.0E+02	9.90E+03	2.31E+04	4.36
Peroxone (10,000 mg/L H_2O_2 + 1% O_3)	87	1.0E+02	8.70E+03	2.03E+04	4.31

Table E.19: Impact of ISCO on High Fe Soil, 2C

Treatment	2C # of Colonies	2C Dilution Factor	2C CFU/mL solution	2C CFU/g dry soil	2C log CFU/g dry soil
No Treatment	35	1.0E+05	3.50E+06	8.17E+06	6.91
500 mg/L Fe^{2+}	40	1.00E+03	4.00E+04	9.33E+04	4.97
5,000 mg/L Fe^{2+}	49	1.0E+04	4.90E+05	1.14E+06	6.06
100,000 mg/L H_2O_2	121	1.00E+01	1.21E+03	2.82E+03	3.45
Fenton's Reaction (5,000 mg/L Fe^{2+} + 100,000 mg/L H_2O_2)	0	1.00E+01	0.00E+00	0.00E+00	#NUM!
Fenton's Reaction (500 mg/L Fe^{2+} + 10,000 mg/L H_2O_2)	254	1.00E+01	2.54E+03	5.93E+03	3.77
1% O_3	73	1.0E+04	7.30E+05	1.70E+06	6.23
3% O_3	115	1.0E+03	1.15E+05	2.68E+05	5.43
Peroxone (1,000 mg/L H_2O_2 + 3% O_3)	189	1.0E+02	1.89E+04	4.41E+04	4.64
Peroxone (10,000 mg/L H_2O_2 + 1% O_3)	208	1.00E+01	2.08E+03	4.85E+03	3.69

Table E.20: Impact of ISCO on Biologically Stimulated Soil, 1A

Treatment	1A # of Colonies	1A Dilution Factor	1A CFU/mL solution	1A CFU/g dry soil	1A log CFU/g dry soil
No Treatment	276	1.0E+06	2.76E+08	6.44E+08	8.81
500 mg/L Fe^{2+}	254	1.0E+05	2.54E+07	5.93E+07	7.77
5,000 mg/L Fe^{2+}	62	1.0E+06	6.20E+07	1.45E+08	8.16
100,000 mg/L H_2O_2	121	1.00E+01	1.21E+03	2.82E+03	3.45
Fenton's Reaction (5,000 mg/L Fe^{2+} + 100,000 mg/L H_2O_2)	68	1.00E+01	6.80E+02	1.59E+03	3.20
Fenton's Reaction (500 mg/L Fe^{2+} + 10,000 mg/L H_2O_2)	168	1.0E+03	1.68E+05	3.92E+05	5.59
1% O_3	39	1.0E+05	3.90E+06	9.10E+06	6.96
3% O_3	49	1.0E+04	4.90E+05	1.14E+06	6.06
Peroxone (1,000 mg/L H_2O_2 + 3% O_3)	120	1.0E+02	1.20E+04	2.80E+04	4.45
Peroxone (10,000 mg/L H_2O_2 + 1% O_3)	198	1.00E+01	1.98E+03	4.62E+03	3.66

Table E.21: Impact of ISCO on Biologically Stimulated Soil, 1B

Treatment	1B # of Colonies	1B Dilution Factor	1B CFU/mL solution	1B CFU/g dry soil	1B log CFU/g dry soil
No Treatment	289	1.0E+05	2.89E+07	6.74E+07	7.83
500 mg/L Fe^{2+}	198	1.0E+05	1.98E+07	4.62E+07	7.66
5,000 mg/L Fe^{2+}	300	1.0E+05	3.00E+07	7.00E+07	7.85
100,000 mg/L H_2O_2	36	1.00E+01	3.60E+02	8.40E+02	2.92
Fenton's Reaction (5,000 mg/L Fe^{2+} + 100,000 mg/L H_2O_2)	32	1.00E+01	3.20E+02	7.47E+02	2.87
Fenton's Reaction (500 mg/L Fe^{2+} + 10,000 mg/L H_2O_2)	300	1.0E+02	3.00E+04	7.00E+04	4.85
1% O_3	268	1.0E+05	2.68E+07	6.25E+07	7.80
3% O_3	259	1.00E+03	2.59E+05	6.04E+05	5.78
Peroxone (1,000 mg/L H_2O_2 + 3% O_3)	39	1.0E+03	3.90E+04	9.10E+04	4.96
Peroxone (10,000 mg/L H_2O_2 + 1% O_3)	68	1.0E+02	6.80E+03	1.59E+04	4.20

Table E.22: Impact of ISCO on Biologically Stimulated Soil, 1C

Treatment	1C # of Colonies	1C Dilution Factor	1C CFU/mL solution	1C CFU/g dry soil	1C log CFU/g dry soil
No Treatment	300	1.0E+05	3.00E+07	7.00E+07	7.85
500 mg/L Fe^{2+}	45	1.0E+06	4.50E+07	1.05E+08	8.02
5,000 mg/L Fe^{2+}	265	1.0E+05	2.65E+07	6.18E+07	7.79
100,000 mg/L H_2O_2	59	1.00E+01	5.90E+02	1.38E+03	3.14
Fenton's Reaction (5,000 mg/L Fe^{2+} + 100,000 mg/L H_2O_2)	51	1.00E+01	5.10E+02	1.19E+03	3.08
Fenton's Reaction (500 mg/L Fe^{2+} + 10,000 mg/L H_2O_2)	45	1.0E+03	4.50E+04	1.05E+05	5.02
1% O_3	65	1.0E+05	6.50E+06	1.52E+07	7.18
3% O_3	291	1.00E+03	2.91E+05	6.79E+05	5.83
Peroxone (1,000 mg/L H_2O_2 + 3% O_3)	259	1.0E+02	2.59E+04	6.04E+04	4.78
Peroxone (10,000 mg/L H_2O_2 + 1% O_3)	33	1.0E+02	3.30E+03	7.70E+03	3.89

Table E.23: Impact of ISCO on Biologically Stimulated Soil, 2A

Treatment	2A # of Colonies	2A Dilution Factor	2A CFU/mL solution	2A CFU/g dry soil	2A log CFU/g dry soil
No Treatment	198	1.0E+05	1.98E+07	4.62E+07	7.66
500 mg/L Fe^{2+}	102	1.0E+05	1.02E+07	2.38E+07	7.38
5,000 mg/L Fe^{2+}	98	1.0E+05	9.80E+06	2.29E+07	7.36
100,000 mg/L H_2O_2	109	1.0E+02	1.09E+04	2.54E+04	4.41
Fenton's Reaction (5,000 mg/L Fe^{2+} + 100,000 mg/L H_2O_2)	44	1.0E+02	4.40E+03	1.03E+04	4.01
Fenton's Reaction (500 mg/L Fe^{2+} + 10,000 mg/L H_2O_2)	259	1.0E+02	2.59E+04	6.04E+04	4.78
1% O_3	58	1.0E+05	5.80E+06	1.35E+07	7.13
3% O_3	81	1.0E+04	8.10E+05	1.89E+06	6.28
Peroxone (1,000 mg/L H_2O_2 + 3% O_3)	212	1.0E+02	2.12E+04	4.95E+04	4.69
Peroxone (10,000 mg/L H_2O_2 + 1% O_3)	222	1.00E+01	2.22E+03	5.18E+03	3.71

Table E.24: Impact of ISCO on Biologically Stimulated Soil, 2B

Treatment	2B # of Colonies	2B Dilution Factor	2B CFU/mL solution	2B CFU/g dry soil	2B log CFU/g dry soil
No Treatment	215	1.0E+05	2.15E+07	5.02E+07	7.70
500 mg/L Fe^{2+}	66	1.0E+05	6.60E+06	1.54E+07	7.19
5,000 mg/L Fe^{2+}	60	1.0E+05	6.00E+06	1.40E+07	7.15
100,000 mg/L H_2O_2	39	1.0E+02	3.90E+03	9.10E+03	3.96
Fenton's Reaction (5,000 mg/L Fe^{2+} + 100,000 mg/L H_2O_2)	187	1.00E+01	1.87E+03	4.36E+03	3.64
Fenton's Reaction (500 mg/L Fe^{2+} + 10,000 mg/L H_2O_2)	281	1.00E+01	2.81E+03	6.56E+03	3.82
1% O_3	32	1.0E+06	3.20E+07	7.47E+07	7.87
3% O_3	111	1.0E+04	1.11E+06	2.59E+06	6.41
Peroxone (1,000 mg/L H_2O_2 + 3% O_3)	41	1.0E+03	4.10E+04	9.57E+04	4.98
Peroxone (10,000 mg/L H_2O_2 + 1% O_3)	190	1.00E+01	1.90E+03	4.43E+03	3.65

Table E.25: Impact of ISCO on Biologically Stimulated Soil, 2C

Treatment	2C # of Colonies	2C Dilution Factor	2C CFU/mL solution	2C CFU/g dry soil	2C log CFU/g dry soil
No Treatment	266	1.0E+05	2.66E+07	6.21E+07	7.79
500 mg/L Fe^{2+}	32	1.0E+06	3.20E+07	7.47E+07	7.87
5,000 mg/L Fe^{2+}	244	1.0E+05	2.44E+07	5.69E+07	7.76
100,000 mg/L H_2O_2	96	1.00E+01	9.60E+02	2.24E+03	3.35
Fenton's Reaction (5,000 mg/L Fe^{2+} + 100,000 mg/L H_2O_2)	55	1.00E+01	5.50E+02	1.28E+03	3.11
Fenton's Reaction (500 mg/L Fe^{2+} + 10,000 mg/L H_2O_2)	177	1.0E+02	1.77E+04	4.13E+04	4.62
1% O_3	190	1.0E+05	1.90E+07	4.43E+07	7.65
3% O_3	255	1.00E+03	2.55E+05	5.95E+05	5.77
Peroxone (1,000 mg/L H_2O_2 + 3% O_3)	300	1.0E+02	3.00E+04	7.00E+04	4.85
Peroxone (10,000 mg/L H_2O_2 + 1% O_3)	266	1.00E+01	2.66E+03	6.21E+03	3.79

APPENDIX F

RAW DATA FOR IMPACT OF ISCO ON SOIL HYDRAULIC CONDUCTIVITY

Table F.1: Ozonated Sand, Data Set 1, DI-Water Treatment

N_2 Pressure	20	psi
Initial H_2O Head	6	in.
Soil Column	4	in.
Hydraulic Gradient	138.4	in/in
Diameter of column	1	in
Cross Sectional Area	0.7853975	in^2

Column	Run 1 Time (min)	Liquid Through (in)	Flow Rate (in^3/s)	Hydraulic Conductivity (in/s)
1	0.116666667	6	0.673197857	0.006193229
2	0.13	6	0.589048125	0.005419075
3	0.12	6	0.673197857	0.006193229
		Average Hydraulic Conductivity (in/s) =		**0.005935178**
		Standard Deviation		**0.000446958**
		95% Confidence		**0.000505771**

Column	Run 2 Time (min)	Liquid Through (in)	Flow Rate (in^3/s)	Hydraulic Conductivity (in/s)
1	0.13	6	0.589048125	0.005419075
2	0.13	6	0.589048125	0.005419075
3	0.116666667	6	0.673197857	0.006193229
		Average Hydraulic Conductivity (in/s) =		**0.005677126**
		Standard Deviation		**0.000446958**
		95% Confidence		**0.000505771**

Column	Run 3 Time (min)	Liquid Through (in)	Flow Rate (in^3/s)	Hydraulic Conductivity (in/s)
1	0.10	6	0.7853975	0.007225434
2	0.12	6	0.673197857	0.006193229
3	0.13	6	0.589048125	0.005419075
		Average Hydraulic Conductivity (in/s) =		**0.006279246**
		Standard Deviation		**0.000906246**
		95% Confidence		**0.001025494**

Table F.2: Ozonated Sand, Data Set 1, 100,000 mg/L H_2O_2 Treatment

N_2 Pressure	20	psi
Initial H_2O Head	6	in.
Soil Column	4	in.
Hydraulic Gradient	138.4	in/in
Diameter of column	1	in
Cross Sectional Area	0.7853975	in^2

Column	Run 1 Time (min)	Liquid Through (in)	Flow Rate (in^3/s)	Hydraulic Conductivity (in/s)
1	0.166666667	6	0.4712385	0.00433526
2	0.17	6	0.4712385	0.00433526
3	0.15	6	0.523598333	0.004816956
		Average Hydraulic Conductivity (in/s) =		**0.004495825**
		Standard Deviation		**0.000278107**
		95% Confidence		**0.000314702**

Column	Run 2 Time (min)	Liquid Through (in)	Flow Rate (in^3/s)	Hydraulic Conductivity (in/s)
1	0.17	6	0.4712385	0.00433526
2	0.18	6	0.428398636	0.003941146
3	0.15	6	0.523598333	0.004816956
		Average Hydraulic Conductivity (in/s) =		**0.004364454**
		Standard Deviation		**0.000438634**
		95% Confidence		**0.000496352**

Table F.3: Ozonated Sand, Data Set 2, DI-Water Treatment

N_2 Pressure	20	psi
Initial H_2O Head	6	in.
Soil Column	4	in.
Hydraulic Gradient	138.4	in/in
Diameter of column	1	in
Cross Sectional Area	0.7853975	in^2

Column	Run 1 Time (min)	Liquid Through (in)	Flow Rate (in^3/s)	Hydraulic Conductivity (in/s)
1	0.133333333	6	0.589048125	0.005419075
2	0.15	6	0.523598333	0.004816956
3	0.15	6	0.523598333	0.004816956

Average Hydraulic Conductivity (in/s) =	**0.005017662**
Standard Deviation	**0.000347634**
95% Confidence	**0.000393377**

Column	Run 2 Time (min)	Liquid Through (in)	Flow Rate (in^3/s)	Hydraulic Conductivity (in/s)
1	0.17	6	0.4712385	0.00433526
2	0.10	6	0.7853975	0.007225434
3	0.133333333	6	0.589048125	0.005419075

Average Hydraulic Conductivity (in/s) =	**0.005659923**
Standard Deviation	**0.001460062**
95% Confidence	**0.001652184**

Column	Run 3 Time (min)	Liquid Through (in)	Flow Rate (in^3/s)	Hydraulic Conductivity (in/s)
1	0.12	6	0.673197857	0.006193229
2	0.12	6	0.673197857	0.006193229
3	0.133333333	6	0.589048125	0.005419075

Average Hydraulic Conductivity (in/s) =	**0.005935178**
Standard Deviation	**0.000446958**
95% Confidence	**0.000505771**

Table F.4: Ozonated Sand, Data Set 2, F.R. (5,000 mg/L Fe^{2+} Addition)

N_2 Pressure	20	psi
Initial H_2O Head	6	in.
Soil Column	4	in.
Hydraulic Gradient	138.4	in/in
Diameter of column	1	in
Cross Sectional Area	0.7853975	in^2

Column	Run 1 Time (min)	Liquid Through (in)	Flow Rate (in^3/s)	Hydraulic Conductivity (in/s)
1	0.15	6	0.523598333	0.004816956
2	0.13	6	0.589048125	0.005419075
3	0.13	6	0.589048125	0.005419075

Average Hydraulic Conductivity (in/s) =	**0.005218369**
Standard Deviation	**0.000347634**
95% Confidence	**0.000393377**

Column	Run 2 Time (min)	Liquid Through (in)	Flow Rate (in^3/s)	Hydraulic Conductivity (in/s)
1	0.12	6	0.673197857	0.006193229
2	0.12	6	0.673197857	0.006193229
3	0.15	6	0.523598333	0.004816956

Average Hydraulic Conductivity (in/s) =	**0.005419075**
Standard Deviation	**0.000794592**
95% Confidence	**0.000899148**

Table F.5: Ozonated Sand, Data Set 2, F.R. (100,000 mg/L H_2O_2 Addition)

Column	Run 1 Time (min)	Liquid Through (in)	Flow Rate (in^3/s)	Hydraulic Conductivity (in/s)
1	0.166666667	6	0.4712385	0.00433526
2	0.166666667	6	0.4712385	0.00433526
3	0.18	6	0.428398636	0.003941146
		Average Hydraulic Conductivity (in/s) =		**0.004203889**
		Standard Deviation		**0.000227542**
		95% Confidence		**0.000257483**

Column	Run 2 Time (min)	Liquid Through (in)	Flow Rate (in^3/s)	Hydraulic Conductivity (in/s)
1	0.15	6	0.523598333	0.004816956
2	0	6	0.4712385	0.00433526
3	0.15	6	0.523598333	0.004816956
		Average Hydraulic Conductivity (in/s) =		**0.00465639**
		Standard Deviation		**0.000278107**
		95% Confidence		**0.000314702**

Table F.6: Ozonated Sand, Data Set 3, Ozone Treatment

N_2 Pressure	20	psi
Initial H_2O Head	6	in.
Soil Column	4	in.
Hydraulic Gradient	138.4	in/in
Diameter of column	1	in
Cross Sectional Area	0.7853975	in^2

No Treatment

Column	Run Time (min)	Volume Collected (mL)	Volume Collected (in^3)	Flow Rate (in3/s)	Hydraulic Conductivity (in/s)
1	0.116666667	50	3.051187205	0.435883886	0.004010008
2	0.15	50	3.051187205	0.339020801	0.003118895
3	0.166666667	50	3.051187205	0.30511872	0.002807005

Average Hydraulic Conductivity (in/s) =	**0.003311969**
Standard Deviation	**0.000624309**
95% Confidence	**0.000706458**

Ozonation

Column	Run Time (min)	Volume Collected (mL)	Volume Collected (in^3)	Flow Rate (in3/s)	Hydraulic Conductivity (in/s)
1	0.2	50	3.051187205	0.2542656	0.002339171
2	0.133333333	50	3.051187205	0.381398401	0.003508757
3	0.116666667	50	3.051187205	0.435883886	0.004010008

Average Hydraulic Conductivity (in/s) =	**0.003285979**
Standard Deviation	**0.000857407**
95% Confidence	**0.000970228**

Table F.7: Ozonated Sand, Data Set 4, Peroxone Treatment

N_2 Pressure	20	psi
Initial H_2O Head	6	in.
Soil Column	4	in.
Hydraulic Gradient	138.4	in/in
Diameter of column	1	in
Cross Sectional Area	0.7853975	in^2

Column	Run Time (min)	Volume Collected (mL)	Volume Collected (in^3)	Flow Rate (in3/s)	Hydraulic Conductivity (in/s)
1	0.083333333	50	3.051187205	0.610237441	0.005614011
2	0.116666667	50	3.051187205	0.435883886	0.004010008
3	0.133333333	50	3.051187205	0.381398401	0.003508757

Average Hydraulic Conductivity (in/s) =	**0.004377592**
Standard Deviation	**0.00109971**
95% Confidence	**0.001244414**

Column	Run Time (min)	Volume Collected (mL)	Volume Collected (in^3)	Flow Rate (in3/s)	Hydraulic Conductivity (in/s)
1	0.166666667	50	3.051187205	0.30511872	0.002807005
2	0.133333333	50	3.051187205	0.381398401	0.003508757
3	0.1	50	3.051187205	0.508531201	0.004678342

Average Hydraulic Conductivity (in/s) =	**0.003664702**
Standard Deviation	**0.000945365**
95% Confidence	**0.00106976**

Table F.8: Average Soil, Data Set 1, DI-Water Treatment

N_2 Pressure	20	psi
Initial H_2O Head	6	in.
Soil Column	4	in.
Hydraulic Gradient	138.4	in/in
Diameter of column	1	in
Cross Sectional Area	0.7853975	in^2

Column	Run 1 Time (min)	Liquid Through (in)	Flow Rate (in^3/s)	Hydraulic Conductivity (in/s)
1	74.33333333	6	0.001056589	9.72031E-06
2	63.42	6	0.001238472	1.13936E-05
3	59.50	6	0.001319996	1.21436E-05

Average Hydraulic Conductivity (in/s) =	**1.10858E-05**
Standard Deviation	**1.2406E-06**
95% Confidence	**1.40385E-06**

Column	Run 2 Time (min)	Liquid Through (in)	Flow Rate (in^3/s)	Hydraulic Conductivity (in/s)
1	111.00	6	0.000707565	6.5094E-06
2	104.00	6	0.00075519	6.94753E-06
3	89	6	0.000882469	8.11846E-06

Average Hydraulic Conductivity (in/s) =	**7.1918E-06**
Standard Deviation	**8.31879E-07**
95% Confidence	**9.41342E-07**

Column	Run 3 Time (min)	Liquid Through (in)	Flow Rate (in^3/s)	Hydraulic Conductivity (in/s)
1	111.00	6	0.000707565	6.5094E-06
2	123.00	6	0.000638535	5.87434E-06
3	82.00	6	0.000957802	8.8115E-06

Average Hydraulic Conductivity (in/s) =	**7.06508E-06**
Standard Deviation	**1.54542E-06**
95% Confidence	**1.74877E-06**

Table F.9: Average Soil, Data Set 1, 100,000 mg/L H_2O_2 Treatment

N_2 Pressure	20 psi
Initial H_2O Head	6 in.
Soil Column	4 in.
Hydraulic Gradient	138.4 in/in
Diameter of column	1 in
Cross Sectional Area	0.7853975 in^2

Column	Run 1 Time (min)	Liquid Through (in)	Flow Rate (in^3/s)	Hydraulic Conductivity (in/s)
1	1130	6	6.95042E-05	6.39419E-07
2	990.00	6	7.93331E-05	7.29842E-07
3	930.00	6	8.44513E-05	7.76928E-07

Average Hydraulic Conductivity (in/s) =	**7.15396E-07**
Standard Deviation	**6.98836E-08**
95% Confidence	**7.90792E-08**

Column	Run 2 Time (min)	Liquid Through (in)	Flow Rate (in^3/s)	Hydraulic Conductivity (in/s)
1	1805.00	5.25	3.80733E-05	3.50263E-07
2	1455.00	5.125	4.61072E-05	4.24174E-07
3	1805.00	5.75	4.16993E-05	3.83622E-07

Average Hydraulic Conductivity (in/s) =	**3.8602E-07**
Standard Deviation	**3.70133E-08**
95% Confidence	**4.18837E-08**

Table F.10: Average Soil, Data Set 2, DI-Water Treatment

N_2 Pressure	20	psi
Initial H_2O Head	6	in.
Soil Column	4	in.
Hydraulic Gradient	138.4	in/in
Diameter of column	1	in
Cross Sectional Area	0.7853975	in^2

Column	Run 1 Time (min)	Liquid Through (in)	Flow Rate (in^3/s)	Hydraulic Conductivity (in/s)
1	78	6	0.00100692	9.26338E-06
2	72.00	6	0.00109083	1.00353E-05
3	68.50	6	0.001146566	1.05481E-05

Average Hydraulic Conductivity (in/s) =	**9.94893E-06**
Standard Deviation	**6.46694E-07**
95% Confidence	**7.31789E-07**

Column	Run 2 Time (min)	Liquid Through (in)	Flow Rate (in^3/s)	Hydraulic Conductivity (in/s)
1	107.50	6	0.000730602	6.72133E-06
2	112.00	6	0.000701248	6.45128E-06
3	99	6	0.000793331	7.29842E-06

Average Hydraulic Conductivity (in/s) =	**6.82368E-06**
Standard Deviation	**4.32743E-07**
95% Confidence	**4.89685E-07**

Column	Run 3 Time (min)	Liquid Through (in)	Flow Rate (in^3/s)	Hydraulic Conductivity (in/s)
1	119.00	6	0.000659998	6.07179E-06
2	109.00	6	0.000720548	6.62884E-06
3	102.5	6	0.000766241	7.0492E-06

Average Hydraulic Conductivity (in/s) =	**6.58328E-06**
Standard Deviation	**4.90295E-07**
95% Confidence	**5.54811E-07**

Table F.11: Average Soil, Data Set 2, F.R. (5,000 mg/L Fe^{2+} Addition)

N_2 Pressure	20	psi
Initial H_2O Head	6	in.
Soil Column	4	in.
Hydraulic Gradient	138.4	in/in
Diameter of column	1	in
Cross Sectional Area	0.7853975	in^2

Column	Run 1 Time (min)	Liquid Through (in)	Flow Rate (in^3/s)	Hydraulic Conductivity (in/s)
1	93	6	0.000844513	7.76928E-06
2	110.00	6	0.000713998	6.56858E-06
3	105.00	6	0.000747998	6.88137E-06
		Average Hydraulic Conductivity (in/s) =		**7.07307E-06**
		Standard Deviation		**6.22888E-07**
		95% Confidence		**7.0485E-07**

Column	Run 2 Time (min)	Liquid Through (in)	Flow Rate (in^3/s)	Hydraulic Conductivity (in/s)
1	94.00	6	0.000835529	7.68663E-06
2	92.00	6	0.000853693	7.85373E-06
3	100	6	0.000785398	7.22543E-06
		Average Hydraulic Conductivity (in/s) =		**6.72497E-06**
		Standard Deviation		**2.21175E-07**
		95% Confidence		**2.50279E-07**

Table F.12: Average Soil, Data Set 2, F.R. (100,000 mg/L H_2O_2 Addition)

Column	Run 1 Time (min)	Liquid Through (in)	Flow Rate (in^3/s)	Hydraulic Conductivity (in/s)
1	1115	3.75	4.40245E-05	4.05013E-07
2	1115	3.75	4.40245E-05	4.05013E-07
3	1165.00	4.25	4.77531E-05	4.39315E-07
		Average Hydraulic Conductivity (in/s) =		**4.16447E-07**
		Standard Deviation		**1.9804E-08**
		95% Confidence		**2.24099E-08**

Column	Run 2 Time (min)	Liquid Through (in)	Flow Rate (in^3/s)	Hydraulic Conductivity (in/s)
1	1525	3.75	3.21884E-05	2.96124E-07
2	1433	3.75	3.4255E-05	3.15136E-07
3	1705.00	4.25	3.26289E-05	3.00177E-07
		Average Hydraulic Conductivity (in/s) =		**3.03812E-07**
		Standard Deviation		**1.00136E-08**
		95% Confidence		**1.13312E-08**

Table F.13: Average Soil, Data Set 3, Ozone Treatment

N_2 Pressure	20	psi
Initial H_2O Head	6	in.
Soil Column	4	in.
Hydraulic Gradient	138.4	in/in
Diameter of column	1	in
Cross Sectional Area	0.7853975	in^2

No Treatment

Column	Run Time (min)	Volume Collected (mL)	Volume Collected (in^3)	Flow Rate (in3/s)	Hydraulic Conductivity (in/s)
1	35	50	3.051187205	0.001452946	1.33667E-05
2	47	50	3.051187205	0.001081981	9.95392E-06
3	41	50	3.051187205	0.00124032	1.14106E-05

Average Hydraulic Conductivity (in/s) =	**1.15771E-05**
Standard Deviation	**1.71247E-06**
95% Confidence	**1.9378E-06**

Ozonation

Column	Run Time (min)	Volume Collected (mL)	Volume Collected (in^3)	Flow Rate (in3/s)	Hydraulic Conductivity (in/s)
1	45.5	50	3.051187205	0.001117651	1.02821E-05
2	42	50	3.051187205	0.001210789	1.11389E-05
3	50	50	3.051187205	0.001017062	9.35668E-06

Average Hydraulic Conductivity (in/s) =	**1.02592E-05**
Standard Deviation	**8.91333E-07**
95% Confidence	**1.00862E-06**

Table F.14: Average Soil, Data Set 4, Peroxone Treatment

N_2 Pressure	20	psi
Initial H_2O Head	6	in.
Soil Column	4	in.
Hydraulic Gradient	138.4	in/in
Diameter of column	1	in
Cross Sectional Area	0.7853975	in^2

Column	Run Time (min)	Volume Collected (mL)	Volume Collected (in^3)	Flow Rate (in3/s)	Hydraulic Conductivity (in/s)
1	94	50	3.051187205	0.000540991	4.97696E-06
2	105	50	3.051187205	0.000484315	4.45556E-06
3	85	50	3.051187205	0.000598272	5.50393E-06
			Average Hydraulic Conductivity (in/s) =		**4.97882E-06**
			Standard Deviation		**5.24186E-07**
			95% Confidence		**5.93161E-07**

Column	Run Time (min)	Volume Collected (mL)	Volume Collected (in^3)	Flow Rate (in3/s)	Hydraulic Conductivity (in/s)
1	500	50	3.051187205	0.000101706	9.35668E-07
2	485	50	3.051187205	0.000104852	9.64607E-07
3	525	50	3.051187205	9.68631E-05	8.91113E-07
			Average Hydraulic Conductivity (in/s) =		**9.30463E-07**
			Standard Deviation		**3.70224E-08**
			95% Confidence		**4.1894E-08**

Table F.15: High pH Soil, Data Set 1, DI-Water Treatment

N_2 Pressure	40	psi
Initial H_2O Head	6	in.
Soil Column	4	in.
Hydraulic Gradient	276.8	in/in
Diameter of column	1	in
Cross Sectional Area	0.7853975	in^2

Column	Run 1 Time (min)	Liquid Through (in)	Flow Rate (in^3/s)	Hydraulic Conductivity (in/s)
1	4650	6	1.68903E-05	7.76928E-08
2	4309.00	6	1.82269E-05	8.38412E-08
3	4490.00	6	1.74921E-05	8.04614E-08
		Average Hydraulic Conductivity (in/s) =		**8.06651E-08**
		Standard Deviation		**3.07924E-09**
		95% Confidence		**3.48442E-09**

Column	Run 2 Time (min)	Liquid Through (in)	Flow Rate (in^3/s)	Hydraulic Conductivity (in/s)
1	4725.00	6	1.66222E-05	7.64596E-08
2	4440.00	6	1.76891E-05	8.13675E-08
3	4900	6	1.60285E-05	7.37289E-08
		Average Hydraulic Conductivity (in/s) =		**7.71853E-08**
		Standard Deviation		**3.87066E-09**
		95% Confidence		**4.37998E-09**

Column	Run 3 Time (min)	Liquid Through (in)	Flow Rate (in^3/s)	Hydraulic Conductivity (in/s)
1	4745.00	6	1.65521E-05	7.61373E-08
2	4525.00	6	1.73569E-05	7.9839E-08
3	4850.00	6	1.61938E-05	7.4489E-08
		Average Hydraulic Conductivity (in/s) =		**7.68218E-08**
		Standard Deviation		**2.73991E-09**
		95% Confidence		**3.10044E-09**

Table F.16: High pH Soil, Data Set 1, 100,000 mg/L H_2O_2 Treatment

N_2 Pressure	40 psi
Initial H_2O Head	6 in.
Soil Column	4 in.
Hydraulic Gradient	276.8 in/in
Diameter of column	1 in
Cross Sectional Area	0.7853975 in^2

Column	Run 1 Time (min)	Liquid Through (in)	Flow Rate (in^3/s)	Hydraulic Conductivity (in/s)
1	48000.00	6	1.63624E-06	7.52649E-09
2	70500.00	6	1.11404E-06	5.12442E-09
3	48500	6	1.61938E-06	7.4489E-09
		Average Hydraulic Conductivity (in/s) =		**6.69994E-09**
		Standard Deviation		**1.36499E-09**
		95% Confidence		**1.5446E-09**

Column	Run 2 Time (min)	Liquid Through (in)	Flow Rate (in^3/s)	Hydraulic Conductivity (in/s)
1	49900.00	6	1.57394E-06	7.23991E-09
2	73800.00	6	1.06422E-06	4.89528E-09
3	55300.00	6	1.42025E-06	6.53294E-09
		Average Hydraulic Conductivity (in/s) =		**6.22271E-09**
		Standard Deviation		**1.20271E-09**
		95% Confidence		**1.36097E-09**

Table F.17: High pH Soil, Data Set 2, DI-Water Treatment

N_2 Pressure	40	psi
Initial H_2O Head	6	in.
Soil Column	4	in.
Hydraulic Gradient	276.8	in/in
Diameter of column	1	in
Cross Sectional Area	0.7853975	in^2

Column	Run 1 Time (min)	Liquid Through (in)	Flow Rate (in^3/s)	Hydraulic Conductivity (in/s)
1	5500	6	1.428E-05	6.56858E-08
2	4950.00	6	1.58666E-05	7.29842E-08
3	6500.00	6	1.2083E-05	5.55803E-08
		Average Hydraulic Conductivity (in/s) =		**6.47501E-08**
		Standard Deviation		**8.73961E-09**
		95% Confidence		**9.88961E-09**

Column	Run 2 Time (min)	Liquid Through (in)	Flow Rate (in^3/s)	Hydraulic Conductivity (in/s)
1	5750.00	6	1.36591E-05	6.28299E-08
2	5400.00	6	1.45444E-05	6.69022E-08
3	6550	6	1.19908E-05	5.5156E-08
		Average Hydraulic Conductivity (in/s) =		**6.16293E-08**
		Standard Deviation		**5.96441E-09**
		95% Confidence		**6.74923E-09**

Column	Run 3 Time (min)	Liquid Through (in)	Flow Rate (in^3/s)	Hydraulic Conductivity (in/s)
1	5700.00	6	1.37789E-05	6.3381E-08
2	4900.00	6	1.60285E-05	7.37289E-08
3	6600	6	1.19E-05	5.47381E-08
		Average Hydraulic Conductivity (in/s) =		**6.39493E-08**
		Standard Deviation		**9.50814E-09**
		95% Confidence		**1.07593E-08**

Table F.18: High pH Soil, Data Set 2, F.R. (5,000 mg/L Fe^{2+} Treatment)

N_2 Pressure	20	psi
Initial H_2O Head	6	in.
Soil Column	4	in.
Hydraulic Gradient	138.4	in/in
Diameter of column	1	in
Cross Sectional Area	0.7853975	in^2

Column	Run 1 Time (min)	Liquid Through (in)	Flow Rate (in^3/s)	Hydraulic Conductivity (in/s)
1	5300	6	1.48188E-05	6.81645E-08
2	5300.00	6	1.48188E-05	6.81645E-08
3	3550.00	6	2.21239E-05	1.01767E-07
		Average Hydraulic Conductivity (in/s) =		**7.93652E-08**
		Standard Deviation		**1.94002E-08**
		95% Confidence		**2.1953E-08**

Column	Run 2Time (min)	Liquid Through (in)	Flow Rate (in^3/s)	Hydraulic Conductivity (in/s)
1	5130.00	6	1.53099E-05	7.04233E-08
2	5200.00	6	1.51038E-05	6.94753E-08
3	4575	6	1.71672E-05	7.89665E-08
		Average Hydraulic Conductivity (in/s) =		**7.2955E-08**
		Standard Deviation		**5.22759E-09**
		95% Confidence		**5.91547E-09**

Table F.19: High pH Soil, Data Set 2, F.R. (100,000 mg/L H_2O_2 Treatment)

Column	Run 1 Time (min)	Liquid Through (in)	Flow Rate (in^3/s)	Hydraulic Conductivity (in/s)
1	58000.00	6	1.35413E-06	1.24576E-08
2	49500.00	6	1.58666E-06	1.45968E-08
3	52700	6	1.49032E-06	1.37105E-08
		Average Hydraulic Conductivity (in/s) =		**1.35883E-08**
		Standard Deviation		**1.07482E-09**
		95% Confidence		**1.21625E-09**

Column	Run 2 Time (min)	Liquid Through (in)	Flow Rate (in^3/s)	Hydraulic Conductivity (in/s)
1	65000	6	1.2083E-06	1.11161E-08
2	60000	6	1.309E-06	1.20424E-08
3	59500.00	6	1.32E-06	1.21436E-08
		Average Hydraulic Conductivity (in/s) =		**1.17673E-08**
		Standard Deviation		**5.66299E-10**
		95% Confidence		**6.40816E-10**

Table F.20: High pH Soil, Data Set 3, Ozone Treatment

N_2 Pressure	20	psi
Initial H_2O Head	6	in.
Soil Column	4	in.
Hydraulic Gradient	138.4	in/in
Diameter of column	1	in
Cross Sectional Area	0.7853975	in^2

No Treatment

Column	Run Time (min)	Volume Collected (mL)	Volume Collected (in^3)	Flow Rate (in3/s)	Hydraulic Conductivity (in/s)
1	830	10	0.610237441	1.22538E-05	1.12731E-07
2	930	10	0.610237441	1.09362E-05	1.0061E-07
3	945	10	0.610237441	1.07626E-05	9.90125E-08
			Average Hydraulic Conductivity (in/s) =		**1.04118E-07**
			Standard Deviation		**7.50205E-09**
			95% Confidence		**8.4892E-09**

Ozonation

Column	Run Time (min)	Volume Collected (mL)	Volume Collected (in^3)	Flow Rate (in3/s)	Hydraulic Conductivity (in/s)
1	1030	10	0.610237441	9.87439E-06	9.08416E-08
2	990	10	0.610237441	1.02734E-05	9.4512E-08
3	1085	10	0.610237441	9.37385E-06	8.62367E-08
			Average Hydraulic Conductivity (in/s) =		**9.05301E-08**
			Standard Deviation		**4.14641E-09**
			95% Confidence		**4.69201E-09**

Table F.21: High pH Soil, Data Set 4, Peroxone Treatment

N_2 Pressure	20	psi
Initial H_2O Head	6	in.
Soil Column	4	in.
Hydraulic Gradient	138.4	in/in
Diameter of column	1	in
Cross Sectional Area	0.7853975	in^2

No Treatment

Column	Run Time (min)	Volume Collected (mL)	Volume Collected (in^3)	Flow Rate (in3/s)	Hydraulic Conductivity (in/s)
1	950	10	0.610237441	1.07059E-05	9.84914E-08
2	1050	10	0.610237441	9.68631E-06	8.91113E-08
3	995	10	0.610237441	1.02217E-05	9.4037E-08

Average Hydraulic Conductivity (in/s) =	**9.38799E-08**
Standard Deviation	**4.69204E-09**
95% Confidence	**5.30944E-09**

Peroxone

Column	Run Time (min)	Volume Collected (mL)	Volume Collected (in^3)	Flow Rate (in3/s)	Hydraulic Conductivity (in/s)
1	1245	10	0.610237441	8.16918E-06	7.51541E-08
2	1300	10	0.610237441	7.82356E-06	7.19745E-08
3	1125	10	0.610237441	9.04055E-06	8.31705E-08

Average Hydraulic Conductivity (in/s) =	**7.67664E-08**
Standard Deviation	**5.76952E-09**
95% Confidence	**6.5287E-09**

Table F.22: High Iron Soil, Data Set 1, DI-Water Treatment

N_2 Pressure	20	psi
Initial H_2O Head	6	in.
Soil Column	4	in.
Hydraulic Gradient	138.4	in/in
Diameter of column	1	in
Cross Sectional Area	0.7853975	in^2

Column	Run 1 Time (min)	Liquid Through (in)	Flow Rate (in^3/s)	Hydraulic Conductivity (in/s)
1	10.25	6	0.007662415	7.0492E-05
2	12.50	6	0.00628318	5.78035E-05
3	11.25	6	0.006981311	6.42261E-05
		Average Hydraulic Conductivity (in/s) =		**6.41739E-05**
		Standard Deviation		**6.34444E-06**
		95% Confidence		**7.17928E-06**

Column	Run 2 Time (min)	Liquid Through (in)	Flow Rate (in^3/s)	Hydraulic Conductivity (in/s)
1	13.50	6	0.005817759	5.35217E-05
2	13.75	6	0.005711982	5.25486E-05
3	15	6	0.005235983	4.81696E-05
		Average Hydraulic Conductivity (in/s) =		**5.14133E-05**
		Standard Deviation		**2.85099E-06**
		95% Confidence		**3.22614E-06**

Column	Run 3 Time (min)	Liquid Through (in)	Flow Rate (in^3/s)	Hydraulic Conductivity (in/s)
1	19.25	6	0.004079987	3.75347E-05
2	18.00	6	0.004363319	4.01413E-05
3	45.00	6	0.001745328	1.60565E-05
		Average Hydraulic Conductivity (in/s) =		**3.12442E-05**
		Standard Deviation		**1.32173E-05**
		95% Confidence		**1.49565E-05**

Table F.23: High Iron Soil, Data Set 1, 100,000 mg/L H_2O_2 Treatment

N_2 Pressure	20 psi
Initial H_2O Head	6 in.
Soil Column	4 in.
Hydraulic Gradient	138.4 in/in
Diameter of column	1 in
Cross Sectional Area	0.7853975 in^2

Column	Run 1 Time (min)	Liquid Through (in)	Flow Rate (in^3/s)	Hydraulic Conductivity (in/s)
1	1700.00	6	4.61999E-05	4.25026E-07
2	1475.00	6	5.32473E-05	4.8986E-07
3	2750	6	2.85599E-05	2.62743E-07

Average Hydraulic Conductivity (in/s) =	**3.92543E-07**
Standard Deviation	**1.16991E-07**
95% Confidence	**1.32385E-07**

Column	Run 2 Time (min)	Liquid Through (in)	Flow Rate (in^3/s)	Hydraulic Conductivity (in/s)
1	1975.00	6	3.9767E-05	3.65845E-07
2	1750.00	6	4.48799E-05	4.12882E-07
3	2600.00	6	3.02076E-05	2.77901E-07

Average Hydraulic Conductivity (in/s) =	**3.52209E-07**
Standard Deviation	**6.85156E-08**
95% Confidence	**7.75312E-08**

Table F.24: High Iron Soil, Data Set 2, DI-Water Treatment

N_2 Pressure	20	psi
Initial H_2O Head	6	in.
Soil Column	4	in.
Hydraulic Gradient	138.4	in/in
Diameter of column	1	in
Cross Sectional Area	0.7853975	in^2

Column	Run 1 Time (min)	Liquid Through (in)	Flow Rate (in^3/s)	Hydraulic Conductivity (in/s)
1	7.25	6	0.010833069	9.96612E-05
2	11.00	6	0.007139977	6.56858E-05
3	9.00	6	0.008726639	8.02826E-05
		Average Hydraulic Conductivity (in/s) =		**8.18765E-05**
		Standard Deviation		**1.70437E-05**
		95% Confidence		**1.92864E-05**

Column	Run 2 Time (min)	Liquid Through (in)	Flow Rate (in^3/s)	Hydraulic Conductivity (in/s)
1	8.50	6	0.009239971	8.50051E-05
2	13.50	6	0.005817759	5.35217E-05
3	25	6	0.00314159	2.89017E-05
		Average Hydraulic Conductivity (in/s) =		**5.58095E-05**
		Standard Deviation		**2.81216E-05**
		95% Confidence		**3.18219E-05**

Column	Run 3 Time (min)	Liquid Through (in)	Flow Rate (in^3/s)	Hydraulic Conductivity (in/s)
1	19.25	6	0.004079987	3.75347E-05
2	18.50	6	0.004245392	3.90564E-05
3	35	6	0.002243993	2.06441E-05
		Average Hydraulic Conductivity (in/s) =		**3.24117E-05**
		Standard Deviation		**1.02194E-05**
		95% Confidence		**1.15642E-05**

Table F.25: High Iron Soil, Data Set 2, F.R. (5,000 mg/L Fe^{2+} Treatment)

N_2 Pressure	20	psi
Initial H_2O Head	6	in.
Soil Column	4	in.
Hydraulic Gradient	138.4	in/in
Diameter of column	1	in
Cross Sectional Area	0.7853975	in^2

Column	Run 1 Time (min)	Liquid Through (in)	Flow Rate (in^3/s)	Hydraulic Conductivity (in/s)
1	14.75	6	0.00532472 9	4.8986E-05
2	22.75	6	0.00345229 7	3.17601E-05
3	15.00	6	0.00523598 3	4.81696E-05
		Average Hydraulic Conductivity (in/s) =		**4.29719E-05**
		Standard Deviation		**9.71824E-06**
		95% Confidence		**1.0997E-05**

Column	Run 2 Time (min)	Liquid Through (in)	Flow Rate (in^3/s)	Hydraulic Conductivity (in/s)
1	16.75	6	0.00468894	4.31369E-05
2	22.75	6	0.00345229 7	3.17601E-05
3	20	6	0.00392698 8	3.61272E-05
		Average Hydraulic Conductivity (in/s) =		**3.99649E-05**
		Standard Deviation		**1.16032E-05**
		95% Confidence		**1.313E-05**

Table F.26: High Iron Soil, Data Set 2, F.R. (100,000 mg/L H_2O_2 Treatment)

Column	Run 1 Time (min)	Liquid Through (in)	Flow Rate (in^3/s)	Hydraulic Conductivity (in/s)
1	220	6	0.000356999	3.28429E-06
2	185	6	0.000424539	3.90564E-06
3	130.00	6	0.000604152	5.55803E-06
		Average Hydraulic Conductivity (in/s) =		**4.24932E-06**
		Standard Deviation		**1.17518E-06**
		95% Confidence		**1.32982E-06**

Column	Run 2 Time (min)	Liquid Through (in)	Flow Rate (in^3/s)	Hydraulic Conductivity (in/s)
1	260	6	0.000302076	2.77901E-06
2	225	6	0.000349066	3.2113E-06
3	255.00	6	0.000307999	2.8335E-06
		Average Hydraulic Conductivity (in/s) =		**2.94127E-06**
		Standard Deviation		**2.35435E-07**
		95% Confidence		**2.66415E-07**

Table F.27: High Iron Soil, Data Set 3, Ozone Treatment

N_2 Pressure	20	psi
Initial H_2O Head	6	in.
Soil Col.	4	in.
Hydraulic Gradient	138.4	in/in
Diam.	1	in
Cross Sect. Area	0.7853975	in^2

No Treatment

Column	Run Time (min)	Volume Collected (mL)	Volume Collected (in^3)	Flow Rate (in3/s)	Hydraulic Conductivity (in/s)
1	31	50	3.051187205	0.001640423	1.50914E-05
2	50	50	3.051187205	0.001017062	9.35668E-06
3	46	50	3.051187205	0.001105503	1.01703E-05

Average Hydraulic Conductivity (in/s) =	**1.15395E-05**
Standard Deviation	**3.10287E-06**
95% Confidence	**3.51115E-06**

Ozone

N_2 Pressure	15	psi
Initial H_2O Head	6	in.
Soil Column	4	in.
Hydraulic Gradient	103.8	in/in
Diameter of column	1	in
Cross Sectional Area	0.7853975	in^2

Column	Run Time (min)	Volume Collected (mL)	Volume Collected (in^3)	Flow Rate (in3/s)	Hydraulic Conductivity (in/s)
1	44	50	3.051187205	0.001155753	1.06326E-05
2	58	50	3.051187205	0.000876778	8.06611E-06
3	50	50	3.051187205	0.001017062	9.35668E-06

Average Hydraulic Conductivity (in/s) =	**9.3518E-06**
Standard Deviation	**1.28325E-06**
95% Confidence	**1.45211E-06**

Table F.28: High Iron Soil, Data Set 4, Peroxone Treatment

N_2 Pressure	20	psi
Initial H_2O Head	6	in.
Soil Col.	4	in.
Hydraulic Gradient	138.4	in/in
Diam.	1	in
Cross Sect. Area	0.7853975	in^2

No Treatment

Column	Run Time (min)	Volume Collected (mL)	Volume Collected (in^3)	Flow Rate (in3/s)	Hydraulic Conductivity (in/s)
1	38.5	50	3.051187205	0.00132086	1.21515E-05
2	45.5	50	3.051187205	0.001117651	1.02821E-05
3	48	50	3.051187205	0.00105944	9.74655E-06
			Average Hydraulic Conductivity (in/s) =		**1.07267E-05**
			Standard Deviation		**1.26265E-06**
			95% Confidence		**1.42879E-06**

Peroxone

N_2 Pressure	20	psi
Initial H_2O Head	6	in.
Soil Column	4	in.
Hydraulic Gradient	138.4	in/in
Diameter of column	1	in
Cross Sectional Area	0.7853975	in^2

Column	Run Time (min)	Volume Collected (mL)	Volume Collected (in^3)	Flow Rate (in3/s)	Hydraulic Conductivity (in/s)
1	188	50	3.051187205	0.000270495	2.48848E-06
2	107	50	3.051187205	0.000475263	4.37228E-06
3	136	50	3.051187205	0.00037392	3.43996E-06
			Average Hydraulic Conductivity (in/s) =		**3.43357E-06**
			Standard Deviation		**9.41918E-07**
			95% Confidence		**1.06586E-06**

Table F.29: High TOC Soil, Data Set 1, DI-Water Treatment

N_2 Pressure	20	psi
Initial H_2O Head	6	in.
Soil Column	4	in.
Hydraulic Gradient	138.4	in/in
Diameter of column	1	in
Cross Sectional Area	0.7853975	in^2

Column	Run 1 Time (min)	Liquid Through (in)	Flow Rate (in^3/s)	Hydraulic Conductivity (in/s)
1	9.75	6	0.008055359	7.4107E-05
2	10.50	6	0.007479976	6.88137E-05
3	8.50	6	0.009239971	8.50051E-05
		Average Hydraulic Conductivity (in/s) =		**7.59753E-05**
		Standard Deviation		**8.25582E-06**
		95% Confidence		**9.34216E-06**

Column	Run 2 Time (min)	Liquid Through (in)	Flow Rate (in^3/s)	Hydraulic Conductivity (in/s)
1	11.75	6	0.006684234	6.14931E-05
2	12.75	6	0.00615998	5.66701E-05
3	10.5	6	0.007479976	6.88137E-05
		Average Hydraulic Conductivity (in/s) =		**6.23256E-05**
		Standard Deviation		**6.11445E-06**
		95% Confidence		**6.91902E-06**

Column	Run 3 Time (min)	Liquid Through (in)	Flow Rate (in^3/s)	Hydraulic Conductivity (in/s)
1	15.50	6	0.005067081	4.66157E-05
2	14.50	6	0.005416534	4.98306E-05
3	13.75	6	0.005711982	5.25486E-05
		Average Hydraulic Conductivity (in/s) =		**4.9665E-05**
		Standard Deviation		**2.96992E-06**
		95% Confidence		**3.36072E-06**

Table F.30: High TOC Soil, Data Set 1, 100,000 mg/L H_2O_2 Treatment

N_2 Pressure	20	psi
Initial H_2O Head	6	in.
Soil Column	4	in.
Hydraulic Gradient	138.4	in/in
Diameter of column	1	in
Cross Sectional Area	0.7853975	in^2

Column	Run 1 Time (min)	Liquid Through (in)	Flow Rate (in^3/s)	Hydraulic Conductivity (in/s)
1	1230.00	6	6.38535E-05	5.87434E-07
2	11500.00	6	6.82954E-06	6.28299E-08
3	950	6	8.26734E-05	7.60572E-07

Average Hydraulic Conductivity (in/s) =	**4.70278E-07**
Standard Deviation	**3.63325E-07**
95% Confidence	**4.11133E-07**

Column	Run 2 Time (min)	Liquid Through (in)	Flow Rate (in^3/s)	Hydraulic Conductivity (in/s)
1	1530.00	6	5.13332E-05	4.72251E-07
2	1250.00	6	6.28318E-05	5.78035E-07
3	990.00	6	7.93331E-05	7.29842E-07

Average Hydraulic Conductivity (in/s) =	**5.93376E-07**
Standard Deviation	**1.29479E-07**
95% Confidence	**1.46517E-07**

Table F.31: High TOC Soil, Data Set 2, DI-Water Treatment

N_2 Pressure	20	psi
Initial H_2O Head	6	in.
Soil Column	4	in.
Hydraulic Gradient	138.4	in/in
Diameter of column	1	in
Cross Sectional Area	0.7853975	in^2

Column	Run 1 Time (min)	Liquid Through (in)	Flow Rate (in^3/s)	Hydraulic Conductivity (in/s)
1	9.25	6	0.008490784	7.81128E-05
2	10.50	6	0.007479976	6.88137E-05
3	11.50	6	0.006829543	6.28299E-05
		Average Hydraulic Conductivity (in/s) =		**6.99188E-05**
		Standard Deviation		**7.70117E-06**
		95% Confidence		**8.71453E-06**

Column	Run 2 Time (min)	Liquid Through (in)	Flow Rate (in^3/s)	Hydraulic Conductivity (in/s)
1	13.25	6	0.005927528	5.45316E-05
2	11.75	6	0.006684234	6.14931E-05
3	12	6	0.006544979	6.02119E-05
		Average Hydraulic Conductivity (in/s) =		**5.87455E-05**
		Standard Deviation		**3.70518E-06**
		95% Confidence		**4.19272E-06**

Column	Run 3 Time (min)	Liquid Through (in)	Flow Rate (in^3/s)	Hydraulic Conductivity (in/s)
1	14.25	6	0.005511561	5.07048E-05
2	17.50	6	0.004487986	4.12882E-05
3	16.25	6	0.004833215	4.44642E-05
		Average Hydraulic Conductivity (in/s) =		**4.54857E-05**
		Standard Deviation		**4.79069E-06**
		95% Confidence		**5.42108E-06**

Table F.32: High TOC Soil, Data Set 2, F.R. (5,000 mg/L Fe^{2+} Treatment)

N_2 Pressure	20	psi
Initial H_2O Head	6	in.
Soil Column	4	in.
Hydraulic Gradient	138.4	in/in
Diameter of column	1	in
Cross Sectional Area	0.7853975	in^2

Column	Run Time (min)	Liquid Through (in)	Flow Rate (in^3/s)	Hydraulic Conductivity (in/s)
1	17	6	0.004619985	4.25026E-05
2	16.50	6	0.004759985	4.37905E-05
3	16.25	6	0.004833215	4.44642E-05

Average Hydraulic Conductivity (in/s) =	**4.35858E-05**
Standard Deviation	**9.96728E-07**
95% Confidence	**1.12788E-06**

Column	Run Time (min)	Liquid Through (in)	Flow Rate (in^3/s)	Hydraulic Conductivity (in/s)
1	16.50	6	0.004759985	4.37905E-05
2	18.75	6	0.004188787	3.85356E-05
3	17	6	0.004619985	4.25026E-05

Average Hydraulic Conductivity (in/s) =	**4.41274E-05**
Standard Deviation	**4.76378E-07**
95% Confidence	**5.39062E-07**

Table F.33: High TOC Soil, Data Set 2, F.R. (100,000 mg/L H_2O_2 Treatment)

Column	Run Time (min)	Liquid Through (in)	Flow Rate (in^3/s)	Hydraulic Conductivity (in/s)
1	1150	6	6.82954E-05	6.28299E-07
2	975	6	8.05536E-05	7.4107E-07
3	895.00	6	8.77539E-05	8.07311E-07
		Average Hydraulic Conductivity (in/s) =		**7.2556E-07**
		Standard Deviation		**9.05085E-08**
		95% Confidence		**1.02418E-07**

Column	Run Time (min)	Liquid Through (in)	Flow Rate (in^3/s)	Hydraulic Conductivity (in/s)
1	1300	6	6.04152E-05	5.55803E-07
2	950	6	8.26734E-05	7.60572E-07
3	1125.00	6	6.98131E-05	6.42261E-07
		Average Hydraulic Conductivity (in/s) =		**6.52878E-07**
		Standard Deviation		**1.02797E-07**
		95% Confidence		**1.16323E-07**

Table F.34: High TOC Soil, Data Set 3, Ozone Treatment

N_2 Pressure	20	psi
Initial H_2O Head	6	in.
Soil Column	4	in.
Hydraulic Gradient	138.4	in/in
Diameter of column	1	in
Cross Sectional Area	0.7853975	in^2

No Treatment

Column	Run Time (min)	Volume Collected (mL)	Volume Collected (in^3)	Flow Rate (in3/s)	Hydraulic Conductivity (in/s)
1	7	50	3.051187205	0.007264731	6.68335E-05
2	5	50	3.051187205	0.010170624	9.35668E-05
3	10	50	3.051187205	0.005085312	4.67834E-05

Average Hydraulic Conductivity (in/s) =	**6.90612E-05**
Standard Deviation	**2.34711E-05**
95% Confidence	**2.65596E-05**

Ozonation

Column	Run Time (min)	Volume Collected (mL)	Volume Collected (in^3)	Flow Rate (in3/s)	Hydraulic Conductivity (in/s)
1	10	50	3.051187205	0.005085312	4.67834E-05
2	6	50	3.051187205	0.00847552	7.79724E-05
3	12	50	3.051187205	0.00423776	3.89862E-05

Average Hydraulic Conductivity (in/s) =	**5.45807E-05**
Standard Deviation	**2.06296E-05**
95% Confidence	**2.33441E-05**

Table F.35: High TOC Soil, Data Set 4, Peroxone Treatment

No Treatment

Column	Run Time (min)	Volume Collected (mL)	Volume Collected (in^3)	Flow Rate (in3/s)	Hydraulic Conductivity (in/s)
1	8	50	3.051187205	0.00635664	5.84793E-05
2	6	50	3.051187205	0.00847552	7.79724E-05
3	9	50	3.051187205	0.005650347	5.19816E-05
			Average Hydraulic Conductivity (in/s) =		**6.28111E-05**
			Standard Deviation		**1.3526E-05**
			95% Confidence		**1.53058E-05**

Peroxone

Column	Run Time (min)	Volume Collected (mL)	Volume Collected (in^3)	Flow Rate (in3/s)	Hydraulic Conductivity (in/s)
1	110	50	3.051187205	0.000462301	4.25304E-06
2	135	50	3.051187205	0.00037669	3.46544E-06
3	95	50	3.051187205	0.000535296	4.92457E-06
			Average Hydraulic Conductivity (in/s) =		**4.21435E-06**
			Standard Deviation		**7.30335E-07**
			95% Confidence		**8.26435E-07**

APPENDIX G

RAW DATA FOR IMPACT OF ISCO ON SOIL ADSORPTION

Table G.1: Ozonated Sand, No Treatment

C_{DCP} (mg/L)	Q_{DCP} (mg/kg)
9.232193368	0.009785857
44.37839462	0.017584113
84.03586849	0.005207409
297.1000316	0.059215975
481.3753424	0.103701715
9.588190085	0.00836187
46.84308437	0.007725354
93.55935565	0.031531227
261.004245	0.080759963
553.9489985	-0.025720091

Table G.2: Average Soil, No Treatment

C_{DCP} (mg/L)	Q_{DCP} (mg/kg)
11.65628562	-0.003276025
22.38111698	0.106370627
32.75701655	0.233514947
171.5653568	0.561354674
4.00271438	0.02733826
24.67195995	0.097207255
45.90319574	0.18093023
144.6128779	0.66916459

Table G.3: Average Soil, DI Water Treatment

C_{DCP} (mg/L)	Q_{DCP} (mg/kg)
14.32980893	-0.010604605
26.07657434	0.127882066
40.87294271	0.273730378
139.4689337	0.620029873
1.612639527	0.040264072
11.60218713	0.185779614
32.09447505	0.308844249

Table G.4: Average Soil, Fenton's Reagent Treatment

C_{DCP} (mg/L)	Q_{DCP} (mg/kg)
6.230702561	0.02179182
27.92631801	0.120483091
62.92040246	0.185540539
169.4004279	0.500303896
350.9774733	0.78616601
3.695260998	0.019995804
17.53677702	0.095676566
39.75743786	0.190848603
132.4191247	0.495254266
349.1736738	0.608747583

Table G.5: Average Soil, Ozone Treatment

C_{DCP} (mg/L)	Q_{DCP} (mg/kg)
11.72216382	-0.003539538
44.08242756	0.019565384
78.25400272	0.051527002
366.5696695	0.624295329
4.611936967	0.02490137
17.59623178	0.125510167
54.80775035	0.145312011
200.858751	0.444181097
387.1240049	0.542077987

Table G.6: Average Soil, Peroxone Treatment

C_{DCP} (mg/L)	Q_{DCP} (mg/kg)
4.327699934	0.026038318
22.86954498	0.104416915
48.70081359	0.169739758
194.7686841	0.468541365
365.1719199	0.629886327
2.396520026	0.033763037
11.90567663	0.148272388
40.6603649	0.201901553
345.4362797	0.708828888

Table G.7: High pH Soil, No Treatment

C_{DCP} (mg/L)	Q_{DCP} (mg/kg)
10.51157617	0.001302813
55.2669025	-0.025172515
100.08	-0.035776987
361.2425167	-0.197353966
9.729220617	0.004432235
54.79069182	-0.023267673
109.9734668	-0.075350854
388.8285285	-0.307698013

Table G.8: High pH Soil, DI-Water Treatment

C_{DCP} (mg/L)	Q_{DCP} (mg/kg)
7.24415824	0.014372485
41.23753116	0.03094497
110.3230798	-0.076749306
311.1452333	0.003035168
8.904872292	0.007729628
42.95523694	0.024074147
99.24284227	-0.032428356
309.604166	0.009199438

Table G.9: High pH Soil, Fenton's Reagent Treatment

C_{DCP} (mg/L)	Q_{DCP} (mg/kg)
7.964477019	0.011491209
35.7433819	0.052921567
80.12598129	0.044039088
330.3593024	-0.073821108
537.2067337	-0.058252928
6.742130663	0.016380595
32.520142	0.065814527
76.26014449	0.059502435
258.703779	0.212800985
497.2623379	0.101524655

Table G.10: High pH Soil, Ozone Treatment

C_{DCP} (mg/L)	Q_{DCP} (mg/kg)
8.645380171	0.008767597
42.92569512	0.024192314
89.1912783	0.0077779
315.8539866	-0.015799845
561.7975591	-0.15661623
7.491909061	0.013381481
38.06107529	0.043650793
95.50375242	-0.017471997

Table G.11: High pH Soil, Peroxone Treatment

C_{DCP} (mg/L)	Q_{DCP} (mg/kg)
7.736473736	0.012403223
37.07601255	0.047591044
134.4276183	-0.173167461
314.9293661	-0.012101363
8.869744583	0.007870139
36.13695864	0.05134726
97.6950036	-0.026237002
335.8464319	-0.095769626

Table G.12: High Iron Soil, No Treatment

C_{DCP} (mg/L)	Q_{DCP} (mg/kg)
1.582280368	0.037019996
21.91455791	0.108236863
54.55500138	0.146323007
183.2384831	0.514662169
1.563173342	0.037096424
21.46226245	0.110046045
49.122416	0.168053349
171.8953308	0.560034778
301.1929115	0.885802361

Table G.13: High Iron Soil, DI-Water Treatment

C_{DCP} (mg/L)	Q_{DCP} (mg/kg)
5.299758372	0.025515597
28.06497735	0.119928454
61.44476843	0.191443075
5.879948129	0.046898298
29.07491694	0.108525981
64.95777594	0.145937546
166.4940874	0.42097481

Table G.14: High Iron Soil, Fenton's Reagent Treatment

C_{DCP} (mg/L)	Q_{DCP} (mg/kg)
8.421254432	0.0096641
37.47734129	0.045985729
61.30595393	0.119319197
216.9026546	0.380005483
5.326718976	0.013469972
21.01823454	0.081750736
35.54083873	0.207715
186.8678431	0.277459392

Table G.15: High Iron Soil, Ozone Treatment

C_{DCP} (mg/L)	Q_{DCP} (mg/kg)
7.70743828	0.003947095
23.85906796	0.070387402
54.26991662	0.132798688
200.9293517	0.221213358
5.051066973	0.01457258
25.48309422	0.063891297
62.07270247	0.101587545
204.1594386	0.20829301

Table G.16: High Iron Soil, Peroxone Treatment

C_{DCP} (mg/L)	Q_{DCP} (mg/kg)
10.10936704	0.002911649
43.66621687	0.021230227
9.687132633	0.0079661
39.96771939	0.036024217
77.15539445	0.055921435
287.163077	0.098963793

Table G.17: High TOC Soil, No Treatment

C_{DCP} (mg/L)	Q_{DCP} (mg/kg)
2.397149376	0.03376052
12.16317039	0.147242413
24.54596921	0.266359136
79.45609146	0.929791736
141.5945773	1.524195697
0.946212738	0.039564267
9.854159882	0.156478455
24.53612317	0.26639852
82.44231033	0.91784686

Table G.18: High TOC Soil, DI-Water Treatment

C_{DCP} (mg/L)	Q_{DCP} (mg/kg)
1.847599803	0.027386449
11.32163263	0.120537143
13.75125072	0.294873352
73.75520887	0.729909929
137.7101489	1.454601683
2.520737032	0.0246939
4.423849967	0.148128274
8.995356533	0.313896929
31.49765045	0.898940163
148.2771145	1.412333821

Table G.19: High TOC Soil, Fenton's Reagent Treatment

C_{DCP} (mg/L)	Q_{DCP} (mg/kg)
-0.361214708	0.036221707
3.97831845	0.1499104
5.571864084	0.327590898
26.12263684	0.920440217
0.116655614	0.034310226
2.124271832	0.157326586
6.564804005	0.323619139
37.6220961	0.87444238
101.0263391	1.601336922

Table G.20: High TOC Soil, Ozone Treatment

C_{DCP} (mg/L)	Q_{DCP} (mg/kg)
2.347969796	0.037322751
8.985716678	0.196245496
16.70054892	0.370419953
45.82990341	0.994585995
155.7212141	1.406318228
0.269502955	0.045636619
3.86776067	0.21671732
13.23586507	0.384278689
47.72583093	0.987002284
127.544631	1.519024561

Table G.21: High TOC Soil, Peroxone Treatment

C_{DCP} (mg/L)	Q_{DCP} (mg/kg)
0.062511819	0.046464583
2.16544025	0.223526602
8.207690085	0.404391389
38.20729671	1.025076421
0.410040053	0.04507447
4.133519041	0.215654287
19.53219269	0.359093378
83.17823949	0.84519265
147.7736882	1.438108332